

Diss. ETH No. 15206

**SPECIFIC OXYFUNCTIONALIZATION OF PSEUDOCUMENE BY  
MULTISTEP BIOCATALYSIS – MECHANISM AND SCALE UP**

A dissertation submitted to the

SWISS FEDERAL INSTITUTE OF TECHNOLOGY ZURICH

for the degree of

Doctor of Natural Sciences

presented by

BRUNO ALBERT BÜHLER

Dipl. Nat. Sci., Swiss Federal Institute of Technology Zurich, Switzerland

born December 26, 1973

Citizen of Homburg, TG (CH)

Accepted on the recommendation of

Prof. Dr. Bernard Witholt, examiner

Dr. Andreas Schmid, co-examiner

PD Dr. Bernhard Hauer, co-examiner

Prof. Dr. Erick M. Carreira, co-examiner

Zurich, 2003

## ACKNOWLEDGMENTS

First of all, I would like to thank the promoters of my thesis: Prof. Dr. Bernard Witholt and Dr. Andreas Schmid, who enabled me to carry out this work at the IBT. Thanks a lot for always motivating me, for the helpful and interesting discussions, and for teaching me all the smaller and bigger “details” needed to make good science. Andreas, I thank you for always showing me the positive sides, when my critical attitude tended to end up in frustration, and for your excellent supervision.

I am most grateful to PD Dr. Bernhard Hauer and Prof. Dr. Erick M. Carreira for being in the committee acting as coreferees.

Furthermore, I would like to thank Bernhard Hauer, Thomas Zelinski, and Tilo Habicher from BASF for the good collaboration, their input in this project, and the good atmosphere during the project meetings including the nice dinners in the surroundings of Ludwigshafen. Adrie Straathof is gratefully acknowledged for his kind and competent collaboration and help during his sabbatical at the IBT. Thanks for excellent scientific input and helpful discussions also go to Birgit, Frank, Jan, Jin Byung, Kuno, Peter R., Sven, Wouter, and Zhi.

For great technical assistance and teaching or helping me at various stages of the work, I am most thankful to Hans-Jürgen and Martina. Of course, I also thank the diploma students Irene and Pascal for their great contribution to this work.

An especially big “thank you” I would like to address to Helena, who brilliantly mastered all administrative concerns. You always had an open door and a solution for all kind of organizational but also personal problems, not underestimating her impact on the social life creating a good atmosphere at the IBT. Thanks also to Petra and Rahel for perfectly managing the ordering stuff, to Helen and Monika for the clean up of glassware and coffee cups, to Collette for her excellent IT support, and to Peter Koller for repairing and tuning all kind of equipment.

### III

My profound gratitude goes to my long term (all female) lab mates Barbara, Karin, Martina, and in former times Yvonne for being great colleagues and friends. I greatly appreciated the always funny atmosphere and your tolerance towards my chaotic behavior in terms of marking all the lab space with bottles and flasks and especially of creating a big mess on my desk and bench.

I always will remember the nice evenings in the bistro, the parties and aperos in the aquarium, the skiing days, and other social events in connection with the IBT. Thanks to all the people who have contributed to the nice atmosphere at the Höneggerberg but also at other places in and around Zurich, especially to Barbara, Daniel, Georgios, Guy, Helena, Jochen, Karin, Martina, and Peter R.. Three people have become special friends and more during my PhD time at the IBT, Frank, Katja, and Kuno; I thank you very much not only for your scientific but especially for your personal assistance, the interesting and intensive discussions, and the nice and funny time, we had, have, and surely will have in the future. Furthermore, I would like to thank my friends from outside the institute, who always supported me personally or just by accompanying me for a beer.

Finally and very greatly, I thank my Mum and Dad as well as my sister and her family for their moral support, helping me through all my ups and downs.

This work was financially supported by the BASF corporation.

# CONTENTS

<b>Summary</b>	<b>VI</b>
<b>Zusammenfassung</b>	<b>VII</b>
<b>1. Introduction</b>	<b>1</b>
1.1. General Introduction	2
1.2. Biocatalysis in the Chemical Industry	3
1.2.1. Impact of Enzymes as Catalysts in the Chemical Industry	3
1.2.2. Bioprocesses and the Environment	4
1.2.3. Commercialized Applications of Enzymes in the Chemical Industry	4
1.2.4. Industrial Enzyme Applications in the Exploratory Phase	8
1.2.5. Potential of Biocatalysis and Future Perspectives	11
1.3. Oxyfunctionalization of Hydrocarbons	13
1.3.1. Bacterial Hydrocarbon Degradation; Potential for Applications in Organic Synthesis	13
1.3.2. Oxyfunctionalization of $sp^3$ -Hybridized Carbons	16
1.3.2.1. Heme Dependent Oxygenases	19
1.3.2.2. Nonheme Iron Oxygenases	21
1.4. Application of Oxygenases	28
1.4.1. Biocatalyst Selection	28
1.4.2. Intrinsic Oxygenase Properties	29
1.4.2.1. Specific Activity	29
1.4.2.2. Uncoupling	31
1.4.2.3. Multiple Oxidation	31
1.4.3. Physiological Aspects – Biocatalyst Stability	33
1.4.3.1. Product Degradation	33
1.4.3.2. Recombinant Biocatalysis	33
1.4.3.3. Cofactor Recycling in Whole cells	34
1.4.3.4. Toxicity of Substrates and Products	35
1.4.4. Bioprocess Engineering Aspects	37
1.4.4.1. In Situ Product Removal	37
1.4.4.2. Solid Phase Extraction	37

1.4.4.3. Two-Liquid Phase Concept	38
1.4.4.4. Oxygen Transfer and Explosion Hazard	45
1.4.5. Perspectives of Biocatalytic Oxyfunctionalization	46
1.5. Scope of this Thesis	47
<b>2. Xylene Monooxygenase Catalyzes the Multistep Oxygenation of Toluene and Pseudocumene to Corresponding Alcohols, Aldehydes and Acids in <i>Escherichia coli</i> JM101</b>	<b>49</b>
<b>3. Characterization and Application of Xylene Monooxygenase for Multistep Biocatalysis</b>	<b>75</b>
<b>4. Use of the Two-Liquid Phase Concept to Exploit Kinetically Controlled Multistep Biocatalysis</b>	<b>101</b>
<b>5. Chemical Biotechnology for the Specific Oxyfunctionalization of Hydrocarbons on a Technical Scale</b>	<b>131</b>
<b>6. Modeling and Simulation of a Whole-Cell Multistep Biooxidation Process in a Two-Liquid Phase System</b>	<b>151</b>
<b>7. Conclusions and Outlook</b>	<b>197</b>
<b>8. References</b>	<b>205</b>
<b>Curriculum Vitae</b>	<b>229</b>

## SUMMARY

Oxygenases catalyze, among other interesting reactions, highly selective hydrocarbon oxyfunctionalizations, which are important in industrial organic synthesis but difficult to achieve by chemical means. Many enzymatic oxygenations have been described, but few of these have been scaled up to a commercial level, due to the complexity of oxygenase-based biocatalysts and demanding process implementation. The topic of this thesis was the specific oxyfunctionalization of xylenes by the use of xylene monooxygenase (XMO) from *Pseudomonas putida* mt-2. Recombinant *Escherichia coli* expressing the XMO genes *xylM* and *xylA* were found to catalyze the multistep oxidation of xylenes to corresponding alcohols, aldehydes, and acids. For all steps, the incorporation of molecular oxygen was verified. Kinetic analyzes to characterize this multistep oxygenation allowed to determine the kinetic parameters for the individual oxygenation steps. Furthermore, we found that the substrates toluene and pseudocumene and the corresponding alcohols inhibit aldehyde oxidation and that elevated toluene and pseudocumene concentrations also weakly inhibit alcohol oxidation.

As an example for a technically demanding biooxidation, we exploited this complex multistep reaction for the production of 3,4-dimethylbenzaldehyde from pseudocumene. For this purpose, we combined recombinant whole-cell catalysis in an aqueous-organic two-liquid phase system with fed-batch cultivation in an optimized medium. A system with bis(2-ethylhexyl)phthalate as organic carrier solvent allowed the production of 3,4-dimethylbenzaldehyde as the predominant product. Process optimization, scale up, and suitable downstream processing enabled the production of 484 ml 97% pure 3,4-dimethylbenzaldehyde on a 30-L scale. A productivity of  $31 \text{ g L}^{-1} \text{ day}^{-1}$  and a product concentration of  $37 \text{ g L}^{-1}$  in the organic phase were achieved. The higher biocatalyst activity at the expense of cell growth as a consequence of a pH increase pointed to a pH-influenced competition for NADH between XMO and the respiratory chain. A mathematical model including a pH-dependent metabolic inhibition of the NADH-consuming bioconversions allowed consistent simulation of experimental biotransformations performed at varying conditions. Moreover, bioconversion kinetics and process simulation based on this model indicated efficient substrate-cell transfer and the occurrence of direct substrate uptake from organic phase droplets.

This work describes the characterization of a complex oxygenase-based biocatalyst and its implementation into a process on a technical scale, thus illustrating the general feasibility of industrial biocatalytic oxyfunctionalization.

## ZUSAMMENFASSUNG

Oxygenasen katalysieren eine Vielzahl interessanter Reaktionen, darunter hoch spezifische Oxyfunktionalisierungen von Kohlenwasserstoffen. Solche, für die chemische Industrie relevante Reaktionen sind jedoch mit organisch chemischen Methoden schwierig durchführbar. Viele enzymatische Oxygenierungen wurden beschrieben, aber wenige davon sind kommerzialisiert. Dies liegt an der Komplexität solcher Biokatalysatoren und an der anspruchsvollen Prozessführung. Thema der vorliegenden Forschungsarbeit war die spezifische Oxyfunktionalisierung von Xylolen mit der Xylolmonooxygenase (XMO) aus *Pseudomonas putida* mt-2. Rekombinante *Escherichia coli*, die die XMO-gene *xylM* und *xylA* exprimieren, ermöglichten die Mehrstufenoxidation von Xylolen zu den entsprechenden Alkoholen, Aldehyden und Säuren. Bei allen Reaktionsschritten wurde der Einbau von Luftsauerstoff nachgewiesen. Die Kinetik dieser Mehrstufenoxygenierung wurde analysiert, was die Bestimmung der kinetischen Parameter erlaubte. Zudem wurde gefunden, dass die Substrate Toluol und Pseudocumol und deren Alkohole die Aldehydoxidierung inhibieren, und dass erhöhte Xylolkonzentrationen auch die Alkoholoxidierung inhibieren.

Wir nutzten diese komplexe Mehrstufenreaktion für die Produktion von 3,4-Dimethylbenzaldehyd aus Pseudocumol, ein Beispiel für eine technisch anspruchsvolle Biooxidation. Dabei kombinierten wir rekombinante Ganzzellkatalyse in einer Emulsion mit Fed-Batch-Kultivierung in einem optimierten Medium. Ein System mit Bis(2-ethylhexyl)phthalsäure als organischer Phase erlaubte die Produktion von 3,4-Dimethylbenzaldehyd als Hauptprodukt. Prozessoptimierung, Scale-up und eine geeignete Produktaufarbeitung ermöglichten die Herstellung von 484 ml 3,4-Dimethylbenzaldehyd (97% rein) im 30-L Massstab. Dabei wurden eine Produktivität von  $31 \text{ g L}^{-1} \text{ d}^{-1}$  und eine Produktkonzentration in der organischen Phase von  $37 \text{ g L}^{-1}$  erreicht. Erhöhte spezifische Biokatalysatoraktivität auf Kosten des Zellwachstums als Folge einer pH-Erhöhung deutete an, dass XMO und die Atmungskette um NADH konkurrieren. Ein mathematisches Modell, das eine pH-abhängige Inhibition der NADH-verbrauchenden Reaktionen einschliesst, erlaubte eine gute Korrelation zwischen Simulationen und Experimenten. Prozesssimulationen basierend auf diesem Modell wiesen ausserdem auf effizienten Substrat-Zell-Transport sowie direkte Substrataufnahme aus der organischen Phase hin.

Diese Arbeit beschreibt die Charakterisierung eines komplexen oxygenase-basierten Biokatalysators und dessen Anwendung in technischem Massstab, was die industrielle Eignung der biokatalytischen Oxyfunktionalisierung veranschaulicht.





# CHAPTER 1

## INTRODUCTION

### **Bruno Bühler**

Chapter 1.2 partly as published by A. Schmid, F. Hollmann, J. B. Park, and B. Bühler in *Current Opinion in Biotechnology*, 2002, 13:359-366.

## 1.1. GENERAL INTRODUCTION

There are several reasons that make enzymes valuable catalysts interesting for applications in organic synthesis: a highly selective operation in complex reaction mixtures, their chemo-, regio-, and enantioselectivity, the prevalent absence of side reactions leading to simpler separation processes and higher yields, and savings in energy and waste treatment costs owing to mild reaction conditions. However, biological systems also have limitations, as does any other highly specialized catalyst. One drawback arises from the high selectivity of enzymes, which may effect the requirement for many special enzymes to cover the diversity of chemical reactions desired in organic chemistry. In future however, such requirements may be accomplished by the large pool of enzymes in nature, their increasing commercial availability, and progresses in biocatalyst design. Other critical issues - especially encountered in applications of oxidoreductases - include, e.g., poor water-solubilities and high toxicities of substrates and products, low biocatalyst stability, especially when membrane associated enzymes are used, and the need for cofactor regeneration. Biocatalyst engineering as well as biochemical reaction engineering have provided solutions to a number of such problems.

This thesis deals with different aspects of biocatalyst design and characterization as well as of biochemical reaction engineering. The goal was to develop a biocatalyst and a process suitable for the production of aromatic aldehydes - ingredients in flavors and fragrances and interesting building blocks in organic synthesis - from cheap substrates such as xylenes. Specific aspects addressed in this work include the characterization of a microbial degradation pathway with a focus on the application of part of it for the regiospecific multistep oxidation of xylenes to corresponding benzaldehydes, recombinant whole-cell biocatalysis on the basis of *Escherichia coli*, biocatalyst activity and stability, in vivo cofactor regeneration, and the handling of toxic and scarcely water-soluble substrates and products. The objectives of this introduction are to give an overview over the present status and future directions of biocatalysis in the chemical industry, to highlight the potential of biocatalysis for oxyfunctionalization of hydrocarbons, to provide an insight into the mechanism of oxygenase catalysis, and to summarize possible solutions to problems encountered in the application of oxygenases.

## **1.2. BIOCATALYSIS IN THE CHEMICAL INDUSTRY**

The chemical industry, one of the biggest economic sectors worldwide, is highly developed, but introduction of new technologies continues, including biocatalysis. This allows access to new market segments and products in analytical but even more in synthetic applications. Recent reviews on biocatalysis focus on different topics like enzyme classes (Liese, et al., 2000; Wandrey, et al., 2000), specific features of biocatalysts (Zaks, 2001), optimization of biocatalysts (Burton, et al., 2002), and selected aspects of bioprocesses (Panke and Wubbolts, 2002). Representative processes of BASF, DSM, and Lonza have been discussed with respect to technological and economical perspectives of industrial enzyme applications (Schmid, et al., 2001). Rasor and Voss reviewed enzyme catalyzed processes in the pharmaceutical industry describing reactions and conditions in detail (Rasor and Voss, 2001).

In the following, recent industrial processes based on enzyme catalysis are highlighted, the role of sustainability is discussed, and an overview on research and development activities with industrial relevance is given. Of the increasing number of commercialized processes (Straathof, et al., 2002), representative examples are presented. Applications of enzymes in the analytical field and for small-scale lead compound preparation and derivatization in the pharmaceutical industry are not considered.

### **1.2.1. IMPACT OF ENZYMES AS CATALYSTS IN THE CHEMICAL INDUSTRY**

Enzyme applications, which are in different development stages, are found mainly in the organics, drugs, and cleaners market segments. Rapid developments are expected in the polymer field (e.g. 1,3 propanediol) culminating in applications in all segments, excluding only bulk products with prices below 1 \$/kg (Thayer, 2001). Today, the market of basic, intermediate, fine, and speciality chemicals and polymers made by bioprocesses accounts already for 2% of the chemical market, or \$25 billion in revenue, excluding revenues from chemicals like ethanol made by traditional fermentation (Bachmann, et al., 2000).

### 1.2.2. BIOPROCESSES AND THE ENVIRONMENT

The sustainability of a process relates to energy and raw material use, waste production, process stability/safety, and product quality. These factors often translate into a reduction of production costs and then contribute to improved competitiveness, especially in highly regulated countries. In a recent report, the OECD illustrates this with various examples and case studies (Griffiths, 2001).

Process improvements such as increase in yield and reductions in raw material demand, emissions, and waste result in process cost savings and can give bioprocesses advantages over traditional chemical routes. This was shown by Ciba (UK) for the synthesis of acrylic acid on pilot-scale using nitrilase. Budel Zink (NL) are using sulphate reducing bacteria to treat 30 m<sup>3</sup> wash tower acid per hour and recover 8.5 tons/d of ZnS, an impressive application in the industry sector of inorganics. Today, bioprocesses based on genetically modified organisms (GMOs) are economically feasible, thanks to internationally harmonized guidelines as in the European Union. A successful example is the setup of a new plant (on stream since early 2001) for the enzymatic production of 7-aminocephalosporanic acid (7-ACA) by Biochemie in Frankfurt. The bioprocess uses no toxic raw materials, operates under mild reaction conditions, and produces significantly less waste. Another example is the one-step manufacture of riboflavin from glucose by Hoffmann La-Roche (in Grenzach, Germany) using a mutant of *Bacillus subtilis*. Thanks to a reduction of 50% of production costs and fast approval through legislation, a new plant with a capacity of 2000 tons/yr started production in May 2000. Sustainability is achieved via the reduction of emissions by 33 and 50% (volatile organic compounds and waste water, respectively). In this case, an existing process was replaced based on new research findings.

### 1.2.3. COMMERCIALIZED APPLICATIONS OF ENZYMES IN THE CHEMICAL INDUSTRY

Today, key reactions in bioprocesses running on production scale are mostly hydrolytic, or the processes are based on fermentations of cheap starting materials like glucose (Table 1.1). Mechanistic exceptions are the hydroxylations of trimethylaminobutyrate and heteroaromatic compounds by Lonza, using oxygen derived from water (Lonza, 2003). DSM is using ammonia lyase for the production of L-aspartic acid and is implementing a process for the

Table 1.1: Commercialized bioprocesses.\*

Company	Strategy	Product(s)	Substrate(s)	Catalyst(s)	Remarks	References
Avecia (ICI)	Kinetic resolution	( <i>S</i> )-2-Chloropropionic acid	Racemic 2-chloropropionic acid	Whole cells, ( <i>S</i> )-specific dehalogenase	Knock out of ( <i>R</i> )-specific dehalogenase, Scale: several 1000 tons/yr	(Griffiths, 2001)
BASF	Fermentation	L-Lysine	Glucose	<i>Corynebacterium glutamicum</i>	Scale: > 100 tons/yr	(Dingler, et al., 1996; BASF, 2003)
		( <i>R</i> )-Isobutyl lactate	Glucose	Microorganism	Precursor for ( <i>S</i> )-chloropropionic acid, Scale: several 100 tons/yr	
	Kinetic resolution	Enantiopure alcohols	Racemic alcohols	Lipases	Enantiospecific acylation, ChiPros™, Scale: several 100 tons/yr	(BASF, 2003)
		Chiral amines	Racemic <i>sec</i> -amines	Lipases	Enantiospecific acylation, ChiPros™, Scale: up to 1000 tons/yr	
	Dynamic resolution	e.g. ( <i>R</i> )-mandelic acid	Racemic cyanohydrins	Nitrilase	Racemization via preequilibrium, ChiPros™, Scale: several tons/yr	(BASF, 2003)
		( <i>R</i> )-2-(4'-Hydroxyphenoxy)propionic acid	( <i>R</i> )-2-Phenoxypropionic acid	Whole cells, oxidase	Broad substrate range of the biocatalyst	(Dingler, et al., 1996)
Chirotech (Dow)	Kinetic resolution	Various $\alpha$ -amino acids	Lactams, N-protected racemic $\alpha$ -amino acid esters	Lactamases	Complementary stereoisomers via complementary lactamases, Scale: kg to tons/yr	(Nishi, et al., 1990; Collins, et al., 1997; Smith, et al., 2001)
		Various D-amino acids	Racemic N-acylated amino acids	D-aminoacylase		
		Various L-amino acids	Racemic N-Acetyl amino acids	N-Acetyl-L-amino acid amidohydrolase (aminoacylase)	Immobilized enzyme in packed-bed reactor, Scale: up to several kg on demand	
		4-Endo-hydroxy-2-oxabicyclo[3.3.0]oct-7-en-3-one	4-Hydroxy-2-oxabicyclo[3.3.0]oct-7-en-3-one butyrate ester	Triacylglycerol acylhydrolase	Scale: up to multi-kg on demand	
	Dynamic resolution	Various ( <i>S</i> )-ester amides	Racemic aralactones	Immobilized triacylglycerol acylhydrolase (triacylglycerol lipase)	The reaction is performed in organic media, spontaneous racemization of the substrate	(Turner, et al., 1995)

Table 1.1 continued.

Company	Strategy	Product(s)	Substrate(s)	Catalyst(s)	Remarks	References
Degussa	Fermentation	L-Threonine	Glucose	Whole cells	REXIM (subsidiary in France), Scale: multi 1000 tons/yr	(Bommarius, et al., 2001; Drauz, et al., 2002)
	Dynamic resolution	Enantiopure L-amino acids	Racemic N-acetyl amino acids	L-Acylases	In vitro in an EMR, chemical or enzymatic racemization, Scale: 100 tons/yr, D-acylase process under preparation	
		Enantiopure D-amino acids	Racemic hydantoins	Hydantoinases, decarbamylases, Racemase	In vivo process, 3 enzymes cloned in <i>E. coli</i> . Process for L-amino acids under development	
	Enantioselective production	L- <i>tert</i> -Leucine	Trimethyl pyruvic acid	Leucine-dehydrogenase	NADH-regeneration with formate dehydrogenase in an EMR, Scale: tons/yr	
DSM	Kinetic resolution	(2 <i>R</i> ,3 <i>S</i> )-3-( <i>p</i> -methoxy phenyl)glycidyl methyl ester	Racemic trans-3-( <i>p</i> -methoxy phenyl)glycidyl methyl ester	Lipase	Intermediate in the synthesis of Diltiazem, Scale: several 100 tons/yr	(Kaptein, et al., 2001; Wolf, et al., 2001; DSM, 2002a)
		Enantiopure L-amino acids	Racemic amino acid derivatives	Amidases, esterases, proteases	Scale: Few to several 100 tons/yr	
	Dynamic resolution	Enantiopure D-amino acids	Racemic hydantoins	Hydantoinase, decarbamylase	Spontaneous racemization, Scale: up to several 1000 tons/yr ( <i>p</i> -hydroxy phenylglycine)	(DSM, 2002a)
	Enantioselective synthesis	L-Aspartic acid	Fumaric acid	Ammonia lyase	Scale: 1000 tons/yr	(Schulze, et al., 1998; DSM, 2002a)
		Aspartame	N-Protected L-aspartic acid, D/L-phenylalanine methyl ester	Thermolysine	Selective coupling, Scale: 1000 tons/yr	
		Enantiopure cyanohydrins	Aldehydes	Hydroxynitrile lyase (HNL)	Implementation phase	
	Enzymatic hydrolysis / synthesis	6-APA, 7-ADCA	Penicillin G/V	Penicillin acylase	Scale: 1000 tons/yr	(Bruggink, 1996; Bruggink, et al., 1998; van de Sandt and de Vroom, 2000; Schroen, et al., 2001; Youshko, et al., 2001; DSM, 2002b)
		$\beta$ -Lactam antibiotics	7-ADCA or 6-APA and acid derivatives	Acylases	Enzymatic coupling in aqueous solution, Scale: Few to several 100 tons/yr	

Table 1.1 continued.

Company	Strategy	Product(s)	Substrate(s)	Catalyst(s)	Remarks	References
Lonza	Hydrolysis	Niacinamide	Nicotinonitrile	Immobilized whole cells, nitrile hydratase	Scale > 3000 tons/yr	(Lonza, 2003)
	Hydrolysis	2-Pyridinamide, pyrazinamide	Corresponding nitriles	Whole cells, nitrile hydratase	Synthons	(Eichhorn, et al., 1997; Lonza, 2003)
	Kinetic resolution	(S)-Pipelicolic acid, (R)- and (S)-piperazinic acid	Corresponding racemic amides	Whole cells, (R)- and (S)-amidases	Substrates derived chemically from products of previous entry	(Eichhorn, et al., 1997; Lonza, 2003)
	Oxidation	(S)-2-Phenyl-propionic acid	Racemic-2-phenylpropionitrile	Whole cells, nitrile hydratase, amidase	2 enzymes in one microorganism	(Lonza, 2003)
	Oxidation	L-Camitine	4-Trimethylamino butyrate	Whole cells, desaturase and hydratase	Large scale	(Kiener, 1992; Petersen and Kiener, 1999; Lonza, 2003)
		Ring-hydroxylated pyridine and pyrazine derivatives	Pyridine and pyrazine derivatives	Whole cells, various nitrilases and dehydrogenases	e.g. 6-hydroxynicotinic acid, 5-hydroxypyrazinic acid, 6-hydroxy-(S)-nicotine, scale: up to a few tons/yr	
		5-Methylpyrazine-2-carboxylic acid	2,5-Dimethylpyrazine	Whole cells, xylene degradation pathway	Heteroaromatic acids are not metabolized further, Scale: several tons/yr	
Novartis	Aminooxidation and hydrolysis	7-ACA	Cephalosporin C	D-Amino acid oxidase and glutaryl amidase		(Griffiths, 2001)
Roche	Fermentation	Riboflavin	Glucose	Genetically engineered <i>Bacillus subtilis</i>	Scale: 2000 tons/yr	(Griffiths, 2001)

\* Abbreviations: 6-APA, 6-aminopenicillanic acid; 7-ACA, 7-aminocephalosporanic acid; 7-ADCA, 7-aminodesacetoxycephalosporanic acid; EMR, enzyme-membrane reactor.

enantioselective production of cyanohydrins (DSM, 2002a). A series of processes operate on the multihundred or thousand tons per year scale, which illustrates the technological feasibility and increasing acceptance of biocatalysis for industrial organic synthesis (Table 1.1).

A representative review on the activities of Degussa Fine Chemicals in the field of amino acid production (Drauz, et al., 2002) shows the broad technology basis used, ranging from chemical resolution via kinetic resolution with acylases and hydantoinases, which were in part successfully engineered to invert enantioselectivity (Arnold, et al., 2000), to oxidoreductions for *L-tert*-leucine production and selective addition reactions using *L*-aspartase. Reaction conditions for bioprocesses are often determined by highly interdependent parameters. Thus, mathematical description is one important basis for optimization. Practical process development and control necessitates simple models based on a limited number of constants. Such a model based on only 5 constants was presented for the synthesis of cephalexin. The model could be used to optimize reaction conditions and identify high starting material concentrations as necessary to increase yields (Schroen, et al., 2001).

A frequently underestimated point is the importance of integrated process development as a main factor for success of industrial biocatalysis. Avecia (a former part of ICI) stated that the 'key determining factor is not the identification of an appropriate enzyme but the speed of scale up' (Griffiths, 2001). Another important point for Avecia was the close collaboration with academic institutions, which contributed to the successful development of a process for the production of (*S*)-chloropropionic acid (2000 tons/yr). Close networking with external collaborators is rather common for European chemical industries and often allows the implementation of new technologies (Table 1.2).

#### **1.2.4. INDUSTRIAL ENZYME APPLICATIONS IN THE EXPLORATORY PHASE**

Selected developments are highlighted in Table 1.2. New reactions evaluated in industry now include epoxidations (Panke, et al., 2002) and C-C bond formations (Fessner and Helaine, 2001), processes often limited in productivity by product inhibition. Due to the need for high product concentrations in commercial processes, *in situ* extraction techniques, as discussed in section 1.4.4 of the introduction, are now applied on the pilot-scale (Held, et al., 1999a; Held, 2000; Panke, et al., 2002).



**Table 1.2: Examples of current catalyst and process development work.**

Areas	Strategy	Examples	References
Advances in catalyst development	Directed evolution (Arnold, 2001; Taylor, et al., 2001)	Error prone PCR, saturation mutagenesis, gene/family shuffling, staggered extension, mutator strains	(May, et al., 2000; Drauz, et al., 2002)
	Metabolic engineering	Peroxidase with 110-fold increased thermostability and 3-fold increased resistance against H <sub>2</sub> O <sub>2</sub>	(Cherry, et al., 1999)
	Bioinformatics	Molecular breeding of strains Proteome analysis using 2D PAGE	(Peters-Wendisch, et al., 2001) (Hermann, et al., 2000; Hermann, et al., 2001)
Screening for new biocatalyst	Transcriptome analysis using DNA microarray	2D PAGE analysis of the <i>C. glutamicum</i> proteome	(Lee, et al., 2001)
Exploitation of microbial adaptation	High-throughput screening	Study of gene expression and regulation in <i>Bacillus subtilis</i> for riboflavin production	(Wahler and Reymond, 2001b; a)
Two-phase systems	Selection following various cultivation procedures	Development of enzyme assays based on fluorogenic substrates and on fluorescent product sensors	(Zelder and Hauer, 2000)
<i>In vitro</i> redox reactions including regeneration techniques	Emulsion process, <i>in situ</i> product extraction	Production of enantiopure styrene epoxide. Solubility and toxicity limitations are overcome by employing a two-liquid phase system	(Panke, et al., 2002)
	Electrochemical NADH regeneration	Electroenzymatic hydroxylations including Cp*Rh(bpy)-mediated NADH regeneration	(Hollmann, et al., 2001)
	Direct enzyme regeneration	Zn-driven, Co(sep)-mediated, P450 catalyzed ω-hydroxylation	(Schwaneberg, et al., 2000)
		Formate driven, Cp*Rh(bpy)-mediated, styrene monooxygenase catalyzed asymmetric epoxidation of (substituted) styrenes	(Hollmann, et al., 2003)

\*Abbreviations: 2D PAGE, two-dimensional polyacrylamide gel electrophoresis; Co(sep), cobalt(III)-sepulchrate; Cp\*Rh(bpy), pentamethyl-cyclopentadienyl-rhodium-bipyridine.

Synthetic applications of isolated oxygenases have to be based on efficient cofactor regeneration techniques. In addition to enzymatic recycling systems, electrons can also be derived from Zn, mediated by cobalt(III)-sepulchrates, as in the case of Cytochrome P450 BM3 monooxygenase (Schwaneberg, et al., 2000; Urlacher and Schmid, 2002), from the cathode, mediated by pentamethylcyclopentadienyl-rhodium-bipyridine, as shown for hydroxybiphenyl 3-monooxygenase (Hollmann, et al., 2001), or from cheap sources of reduction equivalents like formate using the same mediator, as illustrated for the asymmetric synthesis of chiral epoxides by the FAD-dependent oxygenase component of styrene monooxygenase (Hollmann, et al., 2003).

Catalysts can efficiently be engineered on the enzyme level by directed evolution. The activity of hydantoinase, used for the production of L-methionine by Degussa, was increased fivefold with inversion of the enantioselectivity using random mutagenesis and saturation mutagenesis (May, et al., 2000). A detailed analysis of cellular metabolism can be the entry point for catalyst improvements at the whole-cell level. Roche used a *Bacillus subtilis* gene chip for the analysis of gene expression and regulation, which allowed the detection of differential expression of vitamin-regulated genes including the identification of potentially important new transcripts (Lee, et al., 2001). In *Corynebacterium glutamicum*, phosphoenolpyruvate carboxylase and pyruvate carboxylase (PCx) both contribute to lysine production via oxaloacetate. Carbon flux analysis based on <sup>13</sup>C-NMR analysis revealed PCx to be rate limiting for the overall flux through the anaplerotic reaction sequences. Overexpression of the PCx gene resulted in 50% higher lysine accumulation in a lysine production strain and a 150% increase in the production of the threonine precursor homoserine in a threonine production strain (Peters-Wendisch, et al., 2001). Descriptions of traditional methods for whole-cell catalyst improvements are very rare. Recently, Zelder and Hauer (Zelder and Hauer, 2000) reviewed the application of environmentally directed mutations for biocatalyst and process improvement. The authors pointed out that microbial adaptation still plays an important role in the selection of improved strains for biotechnological processes and the maintenance and selection of production strains. Sequencing of genomes of established and optimized production strains will bring new possibilities for catalyst improvement based on a more detailed understanding of regulatory systems and key enzymes in metabolism. Thus, the sequencing of the *Corynebacterium glutamicum* genome by Integrated Genomics and BASF is expected to enable optimization of the current lysine process in Kunsan, Korea (100 000 tons/yr).

### 1.2.5. POTENTIAL OF BIOCATALYSIS AND FUTURE PERSPECTIVES

Today, applications of enzymes in the chemical industry are already well established and, given the current developments, the number of biocatalytic processes will continue to increase rapidly.

Widespread application of enzymes in the chemical industry will also depend on the possibility to couple enzymatic with chemical steps. Chemo-enzymatic reaction sequences profit from the high technical development level of both chemical and enzymatic reactions. DSM uses well established amidase catalysis to produce enantiopure C $\alpha$ -tetrasubstituted  $\alpha$ -amino acids containing terminal double bonds reacting to cyclic oligopeptides by Grubbs olefin metathesis (Table 1.1) (Kaptein, et al., 2001). Lonza uses a sequence of nitrile hydratase catalysis, chemical hydrogenation, and amidase catalyzed reactions to obtain enantiopure pipercolic and piperazine carboxylic acids from aromatic nitrile precursors (Lonza, 2003). Making biocatalysis compatible with chemical multistep synthesis is one of the important future challenges for this new technology.

Nature but also strain collections harbor a large pool of still unused but industrially interesting enzymes. The diversity of natural compounds suggests the existence of a, yet undiscovered, potential of functional group biocatalysis (Parales, et al., 2002; Hou, et al., 2003). Beside selective enrichments and isolation of desired enzymes, the identification of new reactions can be based on high throughput approaches, which need efficient assays for detecting desired activities. Robust activity assays are also an important requirement for the practical application of powerful enzyme engineering techniques [reviewed recently by Arnold (Arnold, 2001) and Hilvert and colleagues (Taylor, et al., 2001)]. Examples are assays using new fluorogenic and chromogenic substrates and applications of pH and pM indicator methods (Table 1.2) (Wahler and Reymond, 2001b; a). The characterization and application of new enzymes catalyzing reactions with commercial potential will significantly broaden the spectrum of industrial biocatalysis.

Enzyme-catalyzed reactions yet hardly applied in but of special interest for the chemical industry include carbon-carbon bond formation and the application of oxidoreductases, especially the introduction of molecular oxygen into (unfunctionalized) hydrocarbons by oxygenases under mild reaction conditions. An interesting C-C bond formation reaction was reported for the preparation of (*R*)-phenylacetylcarbinol by carbonylation of pyruvate and benzaldehyde using various pyruvate decarboxylases (Rosche, et al., 2001). Continuous

production of (*R*)-phenylacetylcarbinol from acetaldehyde and benzaldehyde could be achieved using a mutant of pyruvate decarboxylase from *Zymomonas mobilis* in an enzyme membrane reactor (EMR) with space-time yields of 81 g L<sup>-1</sup> d<sup>-1</sup> (Goetz, et al., 2001). This thesis and the subsequent part of the introduction deal with the specific enzymatic oxyfunctionalization of hydrocarbons.

### 1.3. OXYFUNCTIONALIZATION OF HYDROCARBONS

Biocatalytic oxyfunctionalization of hydrocarbons is of special interest in organic synthesis because readily available petrochemicals can be transformed to functionalized building blocks in a highly regio- and enantioselective way by the insertion of oxygen from molecular oxygen into hydrocarbons under mild conditions. Chemical oxyfunctionalization of hydrocarbons via carbonylation or oxygen addition usually requires the use of expensive and hazardous reactants and catalysts and often yields product mixtures complicating product isolation (Fujiyama, et al., 1983; Fujiyama and Matsumoto, 1984; Carelli, et al., 1999; Thomas, et al., 1999; Hartmann and Ernst, 2000; Thomas, et al., 2001). Due to the high potential of microbial degradation pathways of aromatic and aliphatic hydrocarbons for environmental (Shannon and Unterman, 1993; Guieysse, et al., 2001) and preparative applications (Witholt, et al., 1990; Schmid, et al., 2001), biocatalytic oxygenation reactions gained a lot of scientific interest during the last decades.

#### 1.3.1. BACTERIAL HYDROCARBON DEGRADATION; POTENTIAL FOR APPLICATIONS IN ORGANIC SYNTHESIS

The catabolic sequences employed by microbes for the aerobic degradation of hydrocarbons as well as xenobiotics often can be separated into two parts. Here, we refer to these two parts as upper and lower pathway, following the nomenclature of the TOL degradation pathway (Ramos and Timmis, 1987). The genes of the TOL pathway are located on the catabolic plasmid pWW0 of *Pseudomonas putida* mt-2 (Burlage, et al., 1989; Ramos, et al., 1997; Greated, et al., 2002). This plasmid harbors upper and lower (*meta* cleavage) pathway genes on two separate operons, the upper operon and the *meta* operon, encoding enzymes involved in the degradation of toluene and xylenes by these organisms (Fig. 1.1) (Franklin, et al., 1981; Harayama, et al., 1984; Abril, et al., 1989; Harayama, et al., 1989; Harayama and Reikik, 1990).

A general comparison of the major pathways for catabolism of, e.g., aromatic compounds in bacteria, as toluene degradation by *P. putida* mt-2 (Fig. 1.1), reveals that upper pathways include diverse enzymes but that the compounds are transformed to a limited number of central intermediates (Gibson and Subramanian, 1984). Upper pathways are usually initiated by an oxygenase-catalyzed chemo-, regio-, and stereospecific hydroxylation of the

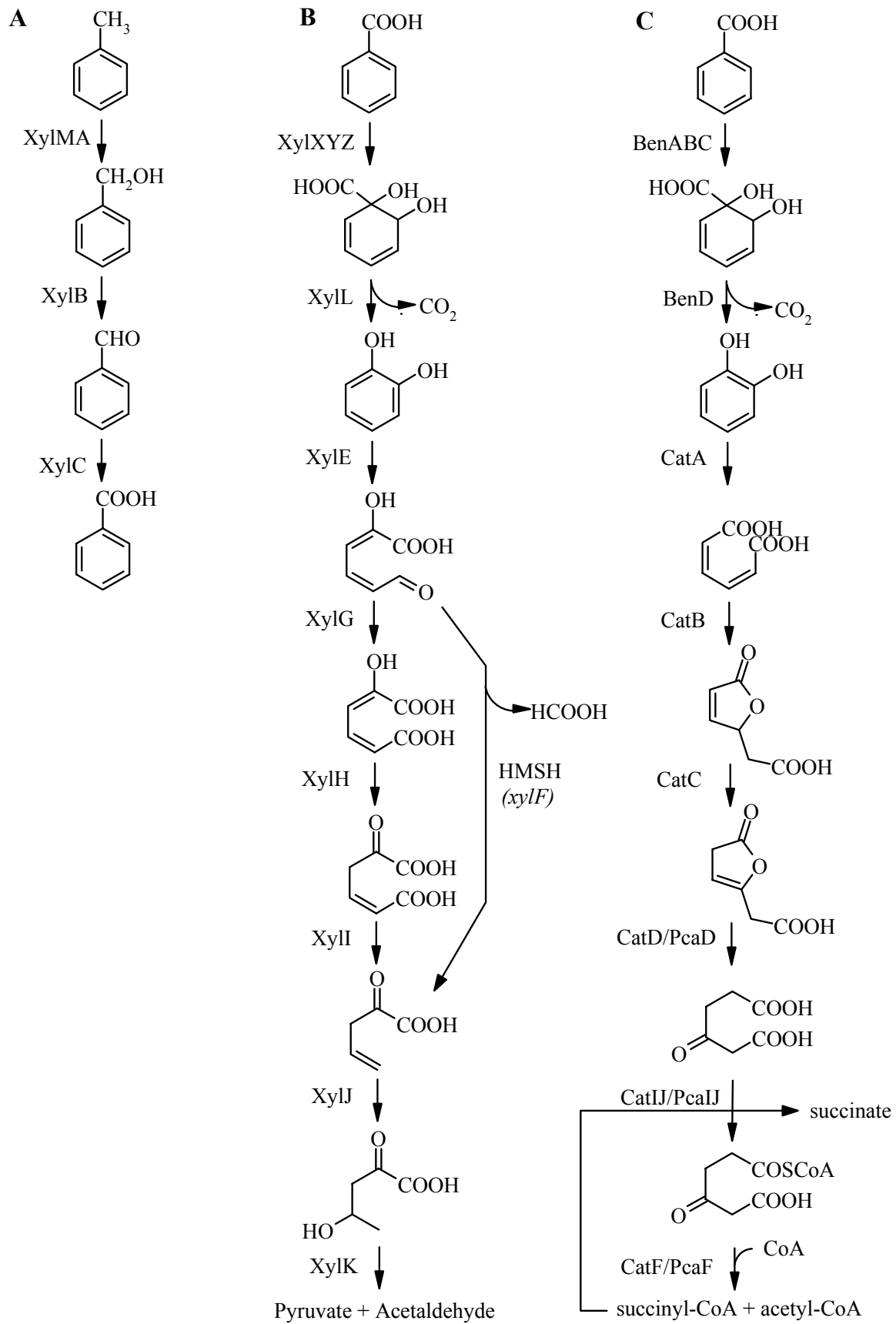


**Figure 1.1. Degradation of toluene by *P. putida* mt-2.** The upper TOL pathway (A) and the *meta*-cleavage pathway (B) both are encoded on the catabolic plasmid pWW0. The *ortho*-cleavage pathway (C) is encoded on the chromosome. XylMA, xylene monooxygenase; XylB, benzyl alcohol dehydrogenase, XylC, benzaldehyde dehydrogenase; XylXYZ, toluate 1,2-dioxygenase; XylL, *cis*-1,2-dihydroxycyclohexa-3,5-diene-1-carboxylate dehydrogenase; XylE, catechol 2,3-dioxygenase; XylF, 2-hydroxymuconic semialdehyde hydrolase; XylH, 4-oxalocrotonate tautomerase; XylI, 4-oxalocrotonate decarboxylase; XylJ, 2-hydroxypent-2,4-dienoate hydratase; XylK, 4-hydroxy-2-oxovalerate aldolase; BenABC, benzoate 1,2-dioxygenase; BenD, benzoate *cis*-dihydrodiol dehydrogenase; CatA, catechol 1,2-dioxygenase; CatB, muconate cycloisomerase; CatC, muconolactone delta-isomerase; CatD/PcaD, 3-oxoadipate enol-lactonase; CatIJ/PcaIJ, 3-oxoadipate:succinyl-CoA transferase; CatF/PcaF, 3-oxoadipyl-CoA thiolase.

hydrocarbons, a reaction for which often no organic chemical counterpart is known (Harayama, et al., 1992; Faber, 2000). Thereby and by the action of additional enzymes such as dehydrogenases, hydrocarbons are modified up to a stage at which one of the central metabolites of microbial degradation has been formed. The most abundant central metabolites in the degradation of aromatics include catechol, protocatechuate, homoprotocatechuate, gentisate, and homogentisate (Dagley, 1986; Harayama and Timmis, 1987). These oxyfunctionalized metabolites are channeled into one of two possible lower pathways, either a *meta* cleavage-type pathway or an *ortho* cleavage-type pathway (Harayama and Reikik, 1989; van der Meer, et al., 1992). Both types of pathways lead to intermediates of central metabolic routes such as the Krebs cycle and involve ring-cleaving dioxygenases. In the case of *P. putida* mt-2, both lower pathways exist. Whereas the enzymes of the *meta* cleavage pathway are encoded on the catabolic TOL plasmid, the *ortho* cleavage pathway is encoded on the chromosome (Franklin, et al., 1981; van der Meer, et al., 1992).

This generalized scheme of catabolic pathways for aromatic compounds emphasizes the so called "metabolic funnel" as it is found for many other degradation pathways. It suggests that microorganisms have extended their substrate range by developing highly diverse upper pathways, which allow the transformation of initial substrates into one of the central metabolites. Thus, the variability of the upper pathways contributes to a great extent to the flexibility of the microbial machinery for degrading xenobiotic compounds and delivers a versatile toolbox for oxyfunctionalization in organic synthesis. Such oxygenations interesting for industrial applications include hydroxylations of alkyl-, allyl-, or benzyl carbons (C-H activation at  $sp^3$ -hybridized carbon atoms), vinyl group and aromatic (di)oxygenations (oxygenation of  $sp^2$ -hybridized carbon atoms), Bayer-Villiger oxidations, and heteroatom oxygenations (Fig. 1.2).

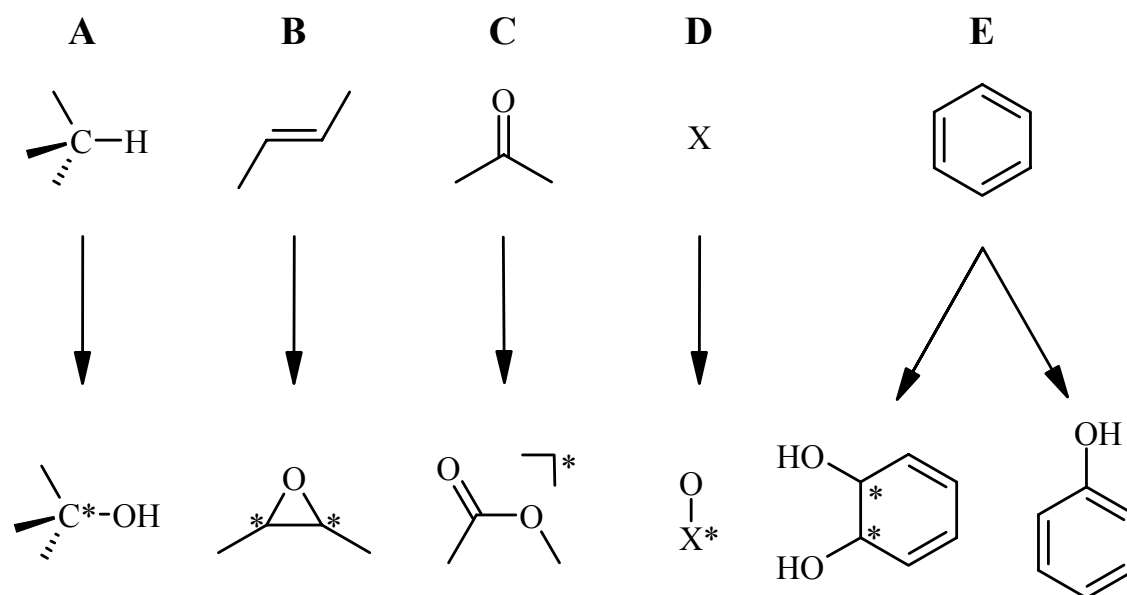


**Figure 1.2. Some examples of oxygenase-catalyzed biotransformations.** A, C-H activation at  $sp^3$ -hybridized carbon atoms; B, vinyl group epoxidation; C, Bayer-Villiger oxidation; D, heteroatom oxygenation; E, aromatic di- and monooxygenation. \*, potential introduction of a chiral center.

A number of excellent reviews with a comprehensive coverage of the literature on biooxidations have appeared in journals and books summarizing present and possible future applications of oxygenases (Holland, 1992; 1998; Flitsch, et al., 1999; Holland, 1999; May, 1999; Azerad, 2000; Grogan and Holland, 2000; Holland, 2000; Holland and Weber, 2000; Flitsch, et al., 2002; Li, et al., 2002). The remaining part of the introduction concentrates mainly on oxygenases, which introduce oxygen into C-H bonds of  $sp^3$ -hybridized carbons, whereas other types of biocatalytic oxyfunctionalization are only marginally considered.

### 1.3.2. OXYFUNCTIONALIZATION OF $sp^3$ -HYBRIDIZED CARBONS

Figure 1.3 shows a simplified tree of oxidoreductase classes with a focus on enzymes capable to oxyfunctionalize  $sp^3$ -hybridized carbon atoms. This tree will lead through the present section of the introduction, which concentrates on mechanistic aspects of C-H activation. Considering the first level in the tree, such reactions are mainly catalyzed by oxygenases and peroxidases. However, also oxidases and dehydrogenases have been reported to catalyze the hydroxylation of benzylic and allylic C-H bonds.



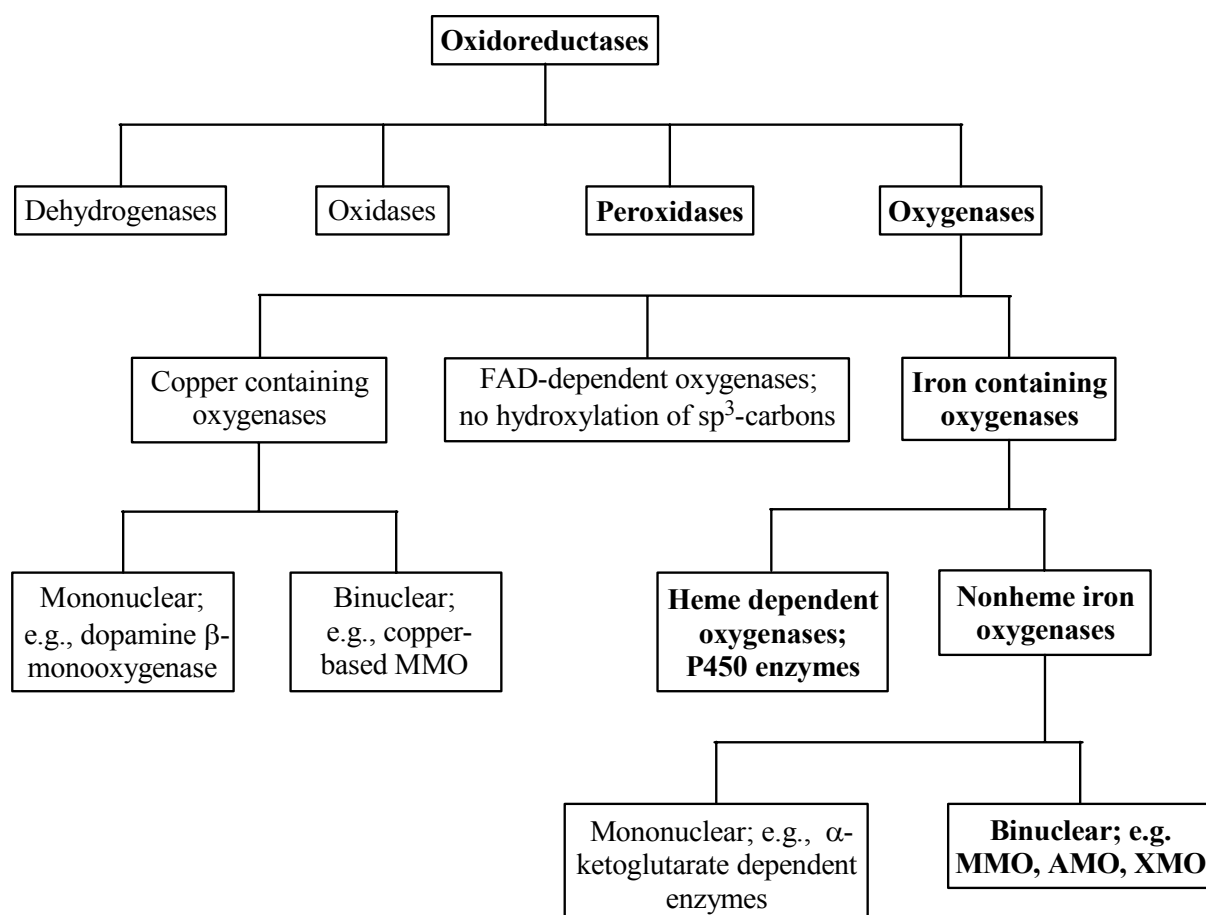


**Figure 1.3. Simplified tree of oxidoreductase classes with a focus on enzymes capable of  $sp^3$ -carbon oxyfunctionalization.** MMO, methane monooxygenase; AMO, alkane monooxygenase; XMO, xylene monooxygenase. The most prominent enzyme classes with respect to  $sp^3$ -carbon oxyfunctionalization are shown in bold.

Thereby, dehydrogenases use water as oxygen donor. Examples are 4-cresol dehydrogenase found in *Pseudomonas putida* strains or denitrifying bacteria (Hopper, et al., 1985; Bossert, et al., 1989) and ethylbenzene dehydrogenase of *Azoarcus*-like strains initiating, interestingly, an anaerobic catabolic pathway (Johnson, et al., 2001; Kniemeyer and Heider, 2001; Rabus, et al., 2002). 4-cresol dehydrogenase requires azurin or nitrate as physiological electron acceptors, whereas the natural electron acceptor of ethylbenzene dehydrogenase is not known yet.

Oxidases couple the one-, two-, or four-electron oxidation of substrates to the two- or four-electron reduction of dioxygen to hydrogen peroxide or water. Since oxygen from molecular oxygen is not introduced into the substrate, hydroxylations are not typical for oxidases.

However, vanillyl-alcohol oxidase from *Penicillium simplicissimum*, for instance, catalyzes both the benzylic desaturation and the benzylic hydroxylation of *para*-alkylphenols depending on the nature of the aliphatic side chain (van den Heuvel, et al., 2001a; van den Heuvel, et al., 2001b). The mechanisms include *para*-quinone methides as common intermediates and differ in whether water attacks the methide or not. Thus, the introduced oxygen atom is derived from water as in the case of dehydrogenases.

Peroxidases use hydrogen peroxide or organic peroxides as oxygen donor and produce one molecule of water (or alcohol in the case of organic peroxide driven peroxidations) as a co-product. They catalyze a large variety of reactions including allylic and benzylic hydroxylations, but no aliphatic hydroxylations have been reported, yet (van Deurzen, et al., 1997b; Adam, et al., 1999; van Rantwijk and Sheldon, 2000). An advantage of peroxidases is that they need no regeneration of cofactors such as NAD(P)H, as is the case for, e.g., monooxygenases or dehydrogenases. However, a major shortcoming is the low operational stability of peroxidases, generally resulting from peroxide induced deactivation (van de Velde, et al., 2001). An example is the facile oxidative deterioration of the porphyrin ring in heme-dependent peroxidases such as the frequently used chloroperoxidase (van Deurzen, et al., 1997a; van de Velde, et al., 2000).

Oxygenases derive the oxygen atom introduced into the C-H bonds from molecular oxygen, produce, in the case of monooxygenases, one molecule of water as a co-product, and can be found in almost all kinds of living cells, ranging from bacterial to mammalian. Beside the initiation of hydrocarbon degradation in bacteria (as described above), physiological roles of oxygenases comprise detoxification, e.g., in mammalian liver cells, and the biosynthesis of secondary metabolites, hormones, signaling molecules, and many other compounds. Due to the flexibility needed for the degradation and detoxification of hydrocarbons and xenobiotics, oxygenases catalyze an even larger variety of oxyfunctionalizations than peroxidases, also including aliphatic hydroxylations. As shown in Figure 1.3, the main classes of oxygenases are FAD-, copper-, and iron-dependent. FAD-dependent oxygenases are known to catalyze epoxidations, aromatic oxygenations, Bayer-Villiger oxidations, and heteroatom oxygenations, but no oxyfunctionalizations of  $sp^3$ -hybridized carbons. In contrast, copper containing oxygenases such as the mononuclear dopamine  $\beta$ -monooxygenase and the binuclear copper based methane monooxygenase catalyze the hydroxylation of C-H bonds (Klinman, 1996; Solomon, et al., 1996; Wimalasena and Alliston, 1999). However, the most abundant and best-studied oxygenases catalyzing C-H oxyfunctionalizations are iron containing enzymes, on which we concentrate in the following. Iron containing oxygenases

can be divided in two categories: heme monooxygenases and nonheme iron oxygenases (Fig. 1.3).

### 1.3.2.1. HEME DEPENDENT OXYGENASES

Heme monooxygenases harbor a protoporphyrin IX tetrapyrrole system containing one catalytic iron nucleus; the resulting prosthetic group is designated a heme group. The iron is coordinated by four nitrogen atoms, one from each pyrrole ring, and has two coordination sites left. The ligands occupying these coordination sites and the surrounding protein structure that defines the electronic and steric environment of the heme group convey the typical catalytic spectrum to the enzymes.

Such heme monooxygenases usually belong to the class of cytochrome P450s. Cytochrome P450 monooxygenases catalyze diverse reactions ranging from participation in the biosynthesis of hormones in animals and secondary metabolites in plants to the biodegradation of xenobiotic compounds. Furthermore, P450 enzymes ensure detoxification of exogenous compounds by rendering these mostly lipophilic compounds water-soluble, thus facilitating their excretion. Because of this essential function, mammalian cytochrome P450 monooxygenases have been thoroughly studied in the context of drug metabolism (Coon, et al., 1980; Guengerich, 1987; Ortiz de Montellano, 1995). Increasing attention is given to microbial P450 monooxygenases and in particular to their application for biotransformations (Schneider, et al., 1998; Schneider, et al., 1999; Urlacher and Schmid, 2002). Bacterial cytochrome P450s tend to be soluble whereas the eucaryotic enzymes tend to be membrane associated (Sono, et al., 1996).

The majority of the cytochrome P450 systems reported to date are multicomponent enzymes with additional proteins for transport of reducing equivalents from NAD(P)H to the terminal cytochrome P450 component. Typical electron transfer chains of class I P450 systems (bacterial or from mammalian adrenal mitochondria) consist of a ferredoxin reductase and a ferredoxin, whereas class II P450 systems (mammalian hepatic drug-metabolizing isoforms) include a flavin containing P450 reductase. An exception is cytochrome P450 BM-3 of *Bacillus megaterium* which consists of a single polypeptide with a P450 domain and an electron transport domain of the microsomal type (class II) (Ravichandran, et al., 1993; Munro, et al., 2002). The fusion-based efficiency of the electron transfer in cytochrome P450 BM-3 provides this enzyme with the highest catalytic activity known for P450 monooxygenases ( $\sim 285 \text{ s}^{-1}$  NADPH oxidation activity with arachidonate) (Noble, et al., 1999).

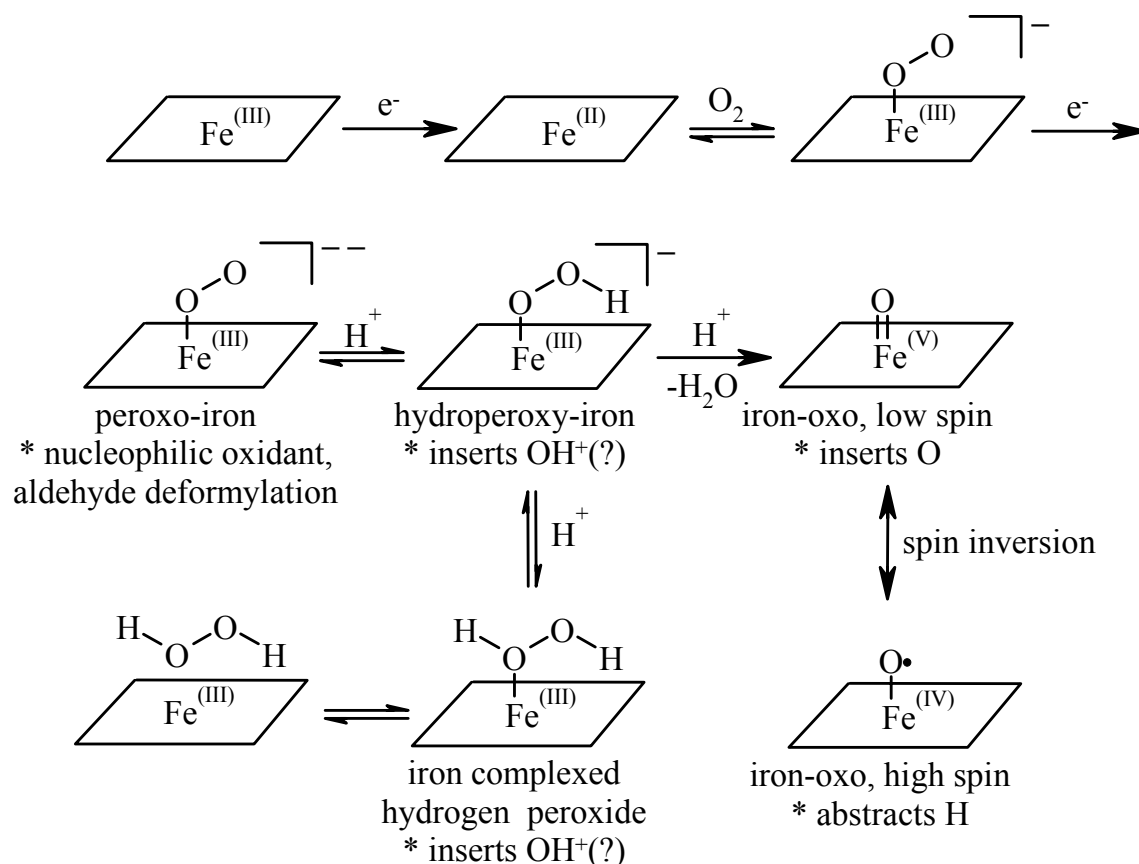


**Figure 1.4. Intermediate species formed in P450 reactions.** The parallelogram represents heme. \*, proposed roles of iron-oxygen intermediates as oxidants. Adapted from Newcomb et al. (2003).

A number of crystal structures of microbial cytochrome P450s are now available (Poulos and Raag, 1992; Ravichandran, et al., 1993; Yano, et al., 2000; Yano, et al., 2003). The first X-ray structure for P450 was that of cytochrome P450<sub>cam</sub> (Poulos and Raag, 1992), which was isolated from *P. putida* and catalyzes the 5-*exo* hydroxylation of its natural substrate D-camphor to 5-*exo* hydroxycamphor. The P450<sub>cam</sub> enzyme has served as a model system for general studies of cytochrome P450 enzymes in terms of structure, function, and mechanism (Poulos and Raag, 1992; Schlichting, et al., 2000). The heme group of P450 monooxygenases is directly involved in the oxidation process by activating molecular oxygen. Up to the present, the catalytic cycle, by which cytochrome P450-mediated hydroxylation occurs, is intensively studied (Ortiz de Montellano, 1995; Schlichting, et al., 2000; Newcomb, et al., 2003). Figure 1.4 shows the various intermediate species formed in P450 reactions.

The resting iron(III) enzyme binds substrate reversibly resulting in a lowering of the reduction potential of iron. An electron is transferred from NAD(P)H via the electron transfer chain to P450 to give an iron(II) species. Reversible binding of oxygen then occurs to give the superoxide-iron complex. A second reduction reaction gives the peroxo-iron species where oxygen is in the formal oxidation state of hydrogen peroxide. Protonation of the peroxo-iron species on the distal oxygen gives the hydroperoxo-iron intermediate. A second protonation on the distal oxygen and water abstraction results in the iron-oxo species, considered as the consensus oxidizing species 10 years ago. Alternatively, protonation of the hydroperoxo-iron species on the proximal oxygen gives iron-complexed hydrogen peroxide, which can dissociate. This dissociation is reversible, and P450 enzymes can be shunted with hydrogen peroxide to give an active oxidant.

However, the exact mechanistic details of oxygen insertion into the C-H bond are still the subject of intense discussion. Recent mechanistic studies, as reviewed by Newcomb et al. (2003), indicate that the cytochrome P450-catalyzed hydroxylation reaction is complex, involving multiple mechanisms and oxidants. In addition to the iron-oxo species, the existence of another electrophilic oxidant, either the hydroperoxo-iron species or iron-complexed hydrogen peroxide, seems apparent (Fig. 1.4). This other electrophilic oxidant appears to react by insertion of  $\text{OH}^+$  into the C-H bond to give the protonated alcohol (Vaz, et al., 1998; Newcomb, et al., 2000). Furthermore, the iron-oxo species is proposed to react through different spin states, a high-spin quartet state and a low-spin doublet state (Fig. 1.4) (Oligaro, et al., 2000; de Visser, et al., 2001). The reactions via both states start in a similar manner that has the appearance of a hydrogen abstraction reaction. After reaching the transition states for the abstraction, however, the energetics of the two pathways diverge. The reaction on the low-spin ensemble proceeds through a radical-like species that collapses with no or a low barrier to give the alcohol product; that is, the reaction is effectively an insertion. The reaction on the high-spin ensemble has a considerable barrier to collapse. Thus, this pathway gives a true radical intermediate and resembles the rebound mechanism (Groves and Han, 1995; Filatov, et al., 1999).

### **1.3.2.2. NONHEME IRON OXYGENASES**

Nonheme iron oxygenases participate in a range of reactions as broad as found for heme containing oxygenases but are generally much less well understood. However, the understanding of the biological significance and chemical properties of nonheme iron oxygenases has increased dramatically in recent years (Ryle and Hausinger, 2002). This

enzyme category can be divided into two groups, mononuclear nonheme iron enzymes and binuclear nonheme iron enzymes (Fig. 1.3).

The former group mainly catalyzes dioxygenations and lipoxygenations, but also hydroxylations (Solomon, et al., 2000). As an example, pterin-dependent hydroxylases catalyze aromatic oxygenations. Here, we focus on monooxygenases catalyzing oxyfunctionalizations of  $sp^3$ -hybridized carbon atoms. Such an activity can also be found among mononuclear nonheme iron oxygenases, namely in the group of  $\alpha$ -ketoglutarate dependent iron enzymes. Most of these enzymes are hydroxylases and catalyze the coupled reaction of hydroxylation of a (unactivated) C-H bond in a substrate and oxidative decarboxylation of the co-substrate  $\alpha$ -ketoglutarate, leading to succinate and  $CO_2$ . Thus, these enzymes are actually dioxygenases. Recent progress in understanding of structure and function of such  $\alpha$ -ketoglutarate dependent dioxygenases has been reviewed (Schofield and Zhang, 1999; Prescott and Lloyd, 2000). These enzymes are present in animals, plants, and microorganisms, catalyze C-H bond oxygenations primarily in large and highly functionalized molecules, and thus are important for medicine and agriculture. Some  $\alpha$ -ketoglutarate dependent dioxygenases are used in the synthesis of pharmaceutical compounds.

Among the known reactions catalyzed by oxygen dependent binuclear nonheme iron enzymes, usually containing a bridged diiron center in the active site, are hydrocarbon monooxygenations, fatty acid desaturations, and ribonucleotide reduction (Wallar and Lipscomb, 1996; Solomon, et al., 2000). With respect to hydrocarbon oxyfunctionalization, methane monooxygenase (MMO) is the best-studied nonheme diiron monooxygenase.

**Methane monooxygenases** catalyze the NADH dependent insertion of one atom of  $O_2$  into the exceptionally stable C-H bond of methane to form methanol, the first step in the degradation of methane by methanotrophs such as *Methylosinus trichosporium* and *Methylococcus capsulatus*. The soluble MMOs typically have a broad substrate spectrum including saturated and unsaturated, linear, branched, and cyclic hydrocarbons up to about  $C_8$ , as well as aromatic, heterocyclic, and chlorinated compounds (Higgins, et al., 1980; Merkx, et al., 2001). The MMO system consists of three protein components (Fox, et al., 1989), a hydroxylase (MMOH) containing a carboxylate- and hydroxo-bridged diiron cluster in the active site, a reductase (MMOR) channeling electrons from NADH to MMOH, and a small effector protein termed component B (MMOB) with several roles in MMO catalysis, of which one involves the enhancement of the electron transfer from MMOR to MMOH (Merkx, et al., 2001; Wallar and Lipscomb, 2001).

The first crystal structure for the hydroxylase component was reported by Rosenzweig et al. (Rosenzweig, et al., 1993) for *M. capsulatus* MMOH, followed by the crystal structure of MMOH from *M. trichosporium* OB3b (Elango, et al., 1997). Furthermore, *M. capsulatus* MMOH has successfully been crystallized in different crystal forms, oxidation states, and in the presence of various substrates and products. Together with spectroscopic studies, this allowed detailed analyses of structural changes during the catalytic cycle (Merkx, et al., 2001). Four glutamate and two histidine residues coordinate the diiron centers of MMOHs. The remainder of the coordination sites is occupied by solvent-derived ligands. Very similar structures occur in other enzymes using a carboxylate-bridged diiron center to activate dioxygen such as ribonucleotide reductase and soluble stearoyl-ACP  $\Delta^9$  desaturase (Nordlund, et al., 1990; Lindqvist, et al., 1996; Lombardi, et al., 2000).

The current understanding of the MMO catalytic cycle is shown in Figure 1.5 (Wallar and Lipscomb, 1996; Brazeau, et al., 2001). The cycle starts with the NADH coupled reduction of the diferric [Fe(III)Fe(III)] form to the diferrous [Fe(II)Fe(II)] form of MMOH involving the components MMOR and MMOB. Oxygen appears to react in two steps with reduced MMOH. First, a putative Michaelis complex (compound O) is formed. In compound O, the oxygen is proposed to bind to the enzyme but not to the dinuclear iron center. Then a terminal superoxo or a bridging peroxo complex with the diiron cluster (compound P\*) is formed (Lee and Lipscomb, 1999; Brazeau and Lipscomb, 2000). P\* decays to compound P which has been shown to have a diferric cluster by Mössbauer spectroscopy (Shu, et al., 1997). In addition, Mössbauer and other spectroscopic studies have suggested that P is a diferric peroxy species and both the P formation and decay reactions were demonstrated to require a proton, suggesting that P may be a hydroperoxo adduct, as shown in Figure 1.5 (Lee and Lipscomb, 1999). P spontaneously converts to Q, which has been shown to react with methane to yield methanol (Lee, et al., 1993). Q was proposed to contain a bis  $\mu$ -oxo Fe(IV)<sub>2</sub> cluster in which the two single atom oxygen bridges form a so-called “diamond core” (Shu, et al., 1997). Q is electronically equivalent to the iron-oxo intermediate that is thought to be one of the reactive species in cytochrome P450 (see Fig. 1.4) (Newcomb, et al., 2003). After the reaction of Q with the substrate via a putative intermediate R, product bound compound T is formed, and, with the release of the product, the resting diferric state of MMOH is regenerated in the rate-limiting step of the cycle (Lee, et al., 1993).

There is currently significant debate regarding the mechanism of the substrate oxidation by Q (Ryle and Hausinger, 2002). The most definitive studies were those examining MMO-catalyzed oxidation of norcarane, of which the products derived from radical and cationic

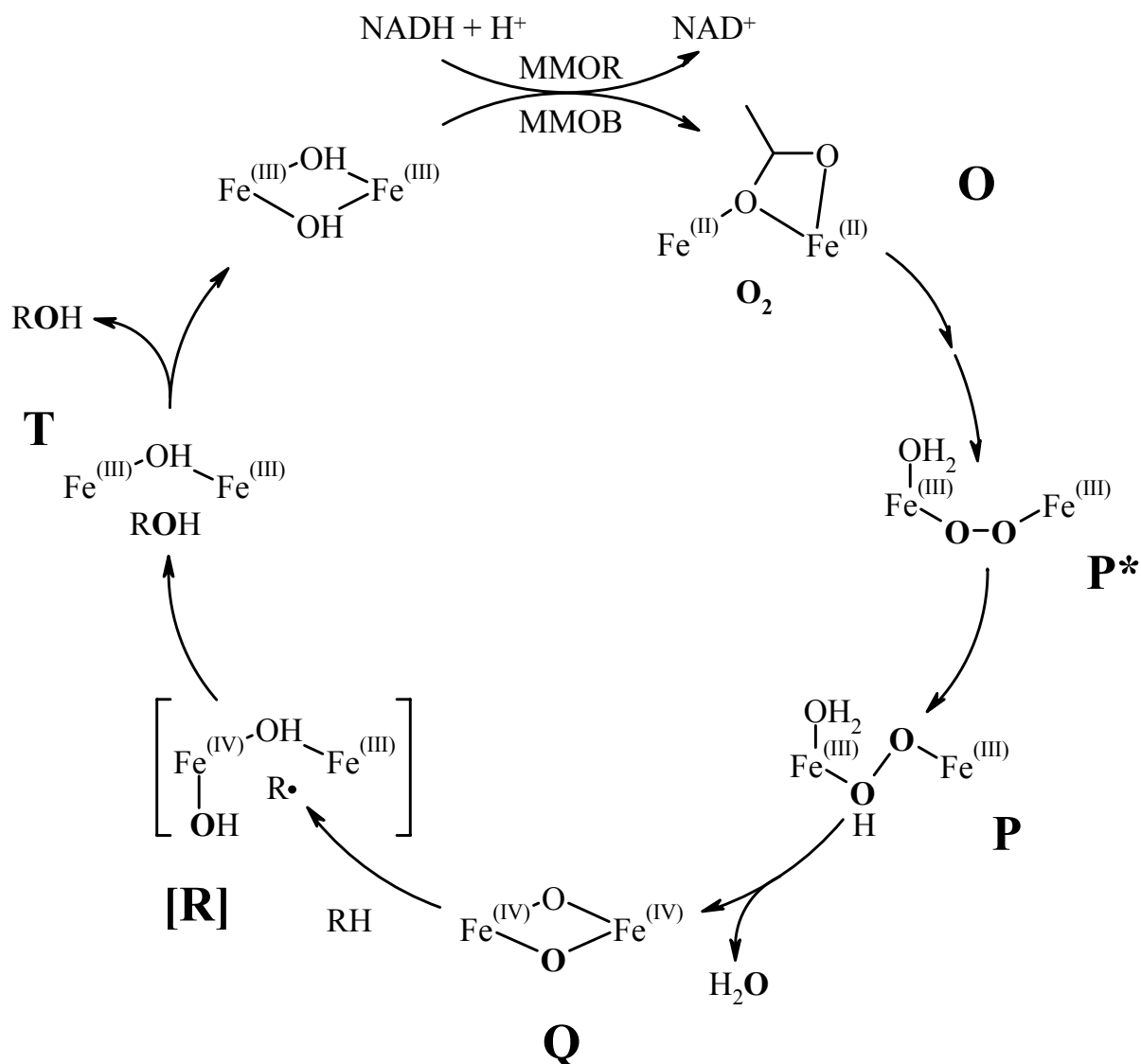


**Figure 1.5. The catalytic cycle of soluble MMO.** Oxygen atoms derived from molecular oxygen are shown in bold. Compounds O, P\*, P, Q, R, and T are described in the text. MMOR, reductase component of MMO; MMOB, component B of MMO. Adapted from (Wallar and Lipscomb, 1996; Brazeau, et al., 2001).

rearrangements clearly differ. The results suggest formation of an initial substrate radical intermediate (of at least 20 ps lifetime) that undergoes oxygen rebound, intramolecular rearrangement followed by oxygen rebound, or oxidation to a cationic intermediate that reacts with hydroxide (Brazeau, et al., 2001). Thus, analogous to P450, multiple mechanisms and oxidants may be involved in the hydroxylation of different substrates by MMO.



**Alkane monooxygenase** (AMO) of *P. putida* GPo1 is another member of the family of binuclear nonheme iron enzymes. It naturally catalyzes the  $\omega$ -hydroxylation of medium chain length alkanes (C<sub>5</sub>-C<sub>12</sub>) to alkanols, the first step in the degradation of alkanes through a set of enzymes encoded on two *alk* gene clusters on the catabolic OCT plasmid (Baptist, et al., 1963; Chakrabarty, et al., 1973; Kok, et al., 1989; van Beilen, et al., 1994b). AMO consists of an integral membrane protein, the hydroxylase component AlkB, and two soluble proteins, rubredoxin AlkG and rubredoxin reductase AlkT (Peterson, et al., 1966; Ruettinger, et al., 1974; Ruettinger, et al., 1977). Its substrate spectrum includes a wide range of linear, branched, and cyclic alkanes as well as alkyl benzenes (van Beilen, et al., 1994a). Furthermore, epoxidation of terminal alkenes, sulfoxidations, demethylations, and aldehyde formation have been reported (Katopodis, et al., 1984; May and Katopodis, 1986; Katopodis, et al., 1988; Fu, et al., 1991). Wildtype *P. putida* GPo1 and recombinant *Pseudomonas* and *E. coli* encoding the alkane monooxygenase genes (*alkBGT*) optionally combined with the genes for the alcohol dehydrogenase (*alkJ*) and the aldehyde dehydrogenase (*alkH*) have been used to produce aliphatic epoxides as well as primary alcohols and acids from alkenes and alkanes in an aqueous-organic two-liquid phase system (Schwartz and McCoy, 1977; de Smet, et al., 1983; Favre-Bulle, et al., 1991; Bosetti, et al., 1992; Favre-Bulle and Witholt, 1992; Favre-Bulle, et al., 1993; Wubbolts, et al., 1996a; Rothen, et al., 1998; Schmid, et al., 1998a). Studies on the topology of AlkB indicated a structure containing six transmembrane segments (van Beilen, et al., 1992). In this model, the amino terminus, two hydrophilic loops, and a large carboxy terminal domain are oriented towards the cytoplasm, and three very short loops are exposed to the periplasm. As MMOH, AlkB has been proposed to contain an active site diiron cluster, which is oxo- or hydroxo-bridged (Shanklin, et al., 1997; Hsu, et al., 1999). However, in contrast to water-soluble proteins of the diiron-carboxylate type (such as soluble MMO), in which the diiron centers are coordinated via histidines and the carboxyl groups of aspartate or glutamate, AlkB ligates the diiron core via histidines only. Thus, AlkB was suggested to represent a new type of nonheme diiron enzyme (Lange and Que, 1998). Sequence analyses indicated that a variety of nonheme integral membrane enzymes, including AlkB, contain a highly conserved 8-histidine motif (Shanklin, et al., 1994; Shanklin, et al., 1997). This motif was shown to be essential for catalytic activity in membrane bound rat stearoyl-CoA desaturase (Shanklin, et al., 1994). Studies with AlkB suggested that the 8-histidine motifs provide ligands for the O<sub>2</sub>-activating diiron clusters in integral membrane enzymes of this family (Shanklin, et al., 1997). As for the examination of the mechanism of MMO-catalyzed C-H bond oxygenation, norcarane was tested as substrate to distinguish

between radical and cation intermediates in AMO catalysis. Analogous to MMO, the results indicate the intermediacy of a carbon-centered substrate radical, in that case with a lifetime of approximately 1 ns (Austin, et al., 2000).

Recent genetic experiments have suggested that enzymes with high homology to AlkB, especially in the histidine-rich region, are widely distributed in nature (Smits, et al., 1999; Smits, et al., 2002; van Beilen, et al., 2002; Whyte, et al., 2002). Furthermore, sequence analyses revealed that the class of histidine cluster containing integral membrane proteins distributes among almost all organisms and includes many oxygen requiring enzymes such as epoxidases, acetylases, ketolases, decarboxylases, methyl oxidases, desaturases, hydroxylases, and enzymes capable of both hydroxylation and desaturation (Broun, et al., 1998; Shanklin and Whittle, 1999; Broadwater, et al., 2002). The dual ability for hydroxylation and desaturation also was found for soluble castor stearyl-ACP  $\Delta^9$  desaturase and MMO (Jin and Lipscomb, 2001; Behrouzian, et al., 2002), underscoring the similarity of the mechanisms among nonheme diiron enzymes of the soluble type, with diiron clusters rich in carboxylate ligands such as MMO, and the membrane-bound type, with histidine-coordinated diiron centers such as AMO.

**Xylene monooxygenase (XMO)** is another example for an integral membrane nonheme diiron enzyme containing a histidine cluster (Shanklin, et al., 1994). XMO initiates the degradation of toluene and xylenes in *P. putida* mt-2 by hydroxylation of a methyl side chain of the aromatic ring. Xylene degradation proceeds via an upper and two lower pathways, the *meta*- and the *ortho* cleavage pathways (Fig. 1.1). The upper pathway also includes XylB, a homodimeric member of the zinc-containing long chain alcohol dehydrogenase family (Shaw and Harayama, 1990; Shaw, et al., 1992; Shaw, et al., 1993), and XylC, a homodimeric benzaldehyde dehydrogenase (Shaw and Harayama, 1990; Shaw, et al., 1992; Shaw, et al., 1993), and yields benzoic acids. These carboxylic acid derivatives are then transformed to substrates of the Krebs cycle through the two lower pathways (Fig. 1.1). Using *E. coli* recombinants, XMO was shown to oxidize toluene and xylenes but also *m*- and *p*-ethyl-, methoxy-, nitro-, and chlorosubstituted toluenes, as well as *m*-bromosubstituted toluene to corresponding benzyl alcohol derivatives (Kunz and Chapman, 1981; Wubbolts, et al., 1994b). Furthermore, styrene is transformed into (*S*)-styrene oxide with an enantiomeric excess of 95% (Wubbolts, et al., 1994a; Wubbolts, et al., 1994b). *E. coli* recombinants containing XMO have been observed to catalyze the second step in the upper pathway, the oxidation of benzyl alcohols to corresponding aldehydes (Harayama, et al., 1986; Harayama,

et al., 1989). Even the conversion of benzaldehyde to benzoate, the third step in the upper pathway, could be observed, but was attributed to *E. coli* enzymes (Harayama, et al., 1989). Further studies performed in vitro with partially purified XMO showed no activity towards benzyl alcohol (Shaw and Harayama, 1995). The reasons for this discrepancy remained unclear.

XMO consists of two polypeptide subunits, encoded by *xylM* and *xylA* (Harayama, et al., 1989; Suzuki, et al., 1991). XylA, the NADH:acceptor reductase component, was characterized as electron transport protein transferring reducing equivalents from NADH to XylM (Shaw and Harayama, 1992). XylM, the hydroxylase component, is located in the membrane, and its activity with a pH optimum of 7 depends on phospholipids (Wubbolts, 1994; Shaw and Harayama, 1995). XylM has a 25% amino acid sequence homology with AlkB (Suzuki, et al., 1991) and contains six membrane-spanning helices in analogy to AlkB, (Wubbolts, 1994). Especially the location of the histidine residues of XylM matches those of AlkB, and the common histidines are distributed in 4 clusters of HXX(X)(H)H. Such similarities also suggest similar mechanisms.

The one-step oxygenation of styrene catalyzed by recombinant XMO in growing cells of *E. coli* was applied to produce (*S*)-styrene oxide on a 1.5-L scale with 25% (vol/vol) hexadecane as a second organic phase (Panke, et al., 1999b). Thereby, maximal productivities of up to 2 g per liter aqueous phase and hour and product concentrations of around 180 mM in the organic phase were reached. Furthermore, the wild-type strain *P. putida* mt-2 was used to oxidize methyl groups on aromatic heterocycles to the corresponding carboxylic acids (Kiener, 1992; 1995). With cells growing on *p*-xylene, a 5-methyl-2-pyrazinecarboxylic acid titer up to 24 g L<sup>-1</sup> was reached for the biotransformation of 2,5-dimethylpyranzine on a 15-m<sup>3</sup>-production scale. This system exploits the inability of the wild-type strain to further degrade heteroaromatic carboxylic acids. In *P. putida* mt-2, all three enzyme activities of the upper xylene degradation pathway are responsible for the three-step oxidation. Recently, wildtype *P. putida* mt-2 was shown to oxidize 2-methylquinoxaline to 2-quinoxalinecarboxylic acid in a similar manner, thus expanding the substrate spectrum of XMO to bicyclic heteroaromatic compounds containing a methyl group (Wong, et al., 2002). Thereby, a product concentration of around 10 g L<sup>-1</sup> and a yield of 86% were reached on an 8-L scale.

## **1.4. APPLICATION OF OXYGENASES**

The development of oxygenase-based bioprocesses suitable for industry faces hurdles that are not experienced by biocatalytic processes involving easy-to-use enzymes such as hydrolases, isomerases, or lyases. Oxygenases are often unstable, consist of multiple components, of which some might be membrane-bound, and require costly cofactors such as NAD(P)H (Duetz, et al., 2001). These issues constrict the use of isolated enzymes in practical applications (Faber, 2000). Despite promising progress in the application of isolated oxygenases including sophisticated cofactor regeneration systems (Schwaneberg, et al., 2000; Hollmann, et al., 2001; Urlacher and Schmid, 2002; Hollmann, et al., 2003), efforts towards the industrial application of oxygenases mainly have focused on whole-cell biocatalysis during the past two decades. This section of the introduction addresses general aspects in the practical application of oxygenases with a focus on *in vivo* biooxidation, which is a main topic of this thesis.

Critical issues include the structural complexity of substrates and the desired specificity of reactions, which require elaborate procedures for biocatalyst selection and/or engineering both involving efficient screening or selection strategies. Furthermore, intrinsic oxygenase properties such as often low catalytic rates, uncoupling, and multiple oxidation have to be considered. Physiological aspects in whole-cell biooxidations include product degradation, effects of (heterologous) expression and activity of oxygenases, cofactor recycling, and toxicity of substrates and products. The listed intrinsic oxygenase properties and physiological aspects can be tackled using biocatalyst engineering at the molecular level and biochemical process engineering. Moreover, bioprocess engineering faces challenges such as high oxygen requirements of the whole-cell biocatalyst, the danger of explosion hazard, and downstream processing. Below, these critical issues and strategies to overcome them are discussed.

### **1.4.1. BIOCATALYST SELECTION**

New processes can be based on the availability of an interesting new enzyme or the incidental identification of interesting products followed by the isolation of the responsible enzymes. Alternatively, it will be necessary to screen for organisms or enzymes catalyzing a desired reaction, or new enzyme activities may be developed by protein design or directed evolution. Due to the diverse physiological roles of oxygenases, it is a highly demanding task to find an

oxygenase that is suitable for a specific biocatalytic process among the available and yet to be discovered enzymes. Since screening for oxygenase products often requires highly sensitive assays due to structural product properties, low product levels, or excretion of unrelated hydroxylated compounds by microorganisms, high-throughput methods based on NMR or MS are of great interest (van Beilen, et al., 2003). New developments, such as high cell density microtiterplate cultures enabling high oxygen transfer rates (Duetz, et al., 2000; Doig, et al., 2002b), also facilitate the screening process. Various screening strategies are applied for oxygenases. These include traditional enrichment cultures, screening of literature and databases, high-throughput screening of a large collection of microbes, and screening of oxygenase clone libraries (van Beilen, et al., 2003).

## **1.4.2. INTRINSIC OXYGENASE PROPERTIES**

Enzymes have evolved to fulfill very specific and selective metabolic functions. Thus, in vivo enzyme activities and the regulation thereof fundamentally depend on the metabolic state of the cells and the position of in vivo reaction equilibria with respect to metabolic flux. Requirements of industrial applications of enzymes often differ from intrinsic enzyme properties evolved for optimal survival of a species in a specific environment. Biocatalyst engineering and biochemical process engineering provide a growing tool set to accomplish such application-related requirements.

### **1.4.2.1 SPECIFIC ACTIVITY**

A key aspect in the application of oxygenases is the specific catalytic rate, which is typically relatively low compared with hydrolytic enzymes, for instance. The specific activity of whole-cells can be increased by overexpression of oxygenases to high activity levels. This was attempted, e.g., by heterologous expression of xylene monooxygenase of *P. putida* mt-2 and styrene monooxygenase of *Pseudomonas* sp. strain VLB120 in *E. coli* resulting in specific activities for styrene epoxidation of 91 and 70-180 U (g of CDW)<sup>-1</sup>, respectively (Panke, et al., 1998b; Panke, et al., 1999b; Panke, et al., 2000). However, although such activities are relatively high, they did not reach or exceed the maximally measured activities of 185 U (g of CDW)<sup>-1</sup> and 200 U (g of CDW)<sup>-1</sup> for toluene degradation by wildtype *P. putida* mt-2 (Duetz, et al., 1998) and styrene oxidation by wildtype *P. putida* S12 containing a styrene monooxygenase similar to the VLB120-enzyme (Nöthe and Hartmans, 1994),

respectively. Thus, heterologous overexpression does not necessarily lead to higher activities, for which possible reasons are discussed in the subsequent sections. High-level expression in the natural host is another promising approach. An example is the overexpression of toluene dioxygenase and toluene *cis*-dihydrodiol dehydrogenase, the first two enzymes in the toluene degradation pathway of *P. putida* F1, in a mutant of the natural host unable to degrade 3-methylcatechol produced from toluene. Insertion of multiple gene copies of the two enzymes into the chromosome allowed a 5.5-fold increase of the specific activity as compared to the mutant containing single gene copies (Hüsken, et al., 2001a) and a maximal specific activity of 243 U (g of CDW)<sup>-1</sup> under optimized conditions (Hüsken, et al., 2002a).

A further possibility to enhance catalytic rates is protein engineering either by rational design or by directed evolution using a rapidly growing toolbox of molecular techniques (Arnold, 2001; Farinas, et al., 2001a; Bolon, et al., 2002; Patnaik, et al., 2002). Protein engineering can be used to address, beside the catalytic rate, also other enzyme properties such as specificity and stability (Cherry, 2000; Powell, et al., 2001; Cirino and Arnold, 2002; Zhao, et al., 2002). A remarkable example for an oxygenase tackled by protein engineering is the single component enzyme cytochrome P450 BM-3, which naturally hydroxylates long-chain fatty acids at subterminal positions. The substrate range of this enzyme was engineered allowing the hydroxylation of naturally poor or non-substrates such as smaller chain fatty acids (Ost, et al., 2000; Li, et al., 2001b), indole (Li, et al., 2000), alkanes (Farinas, et al., 2001b), alicyclic, aromatic, and heteroaromatic compounds (Appel, et al., 2001), and polycyclic aromatic hydrocarbons (Carmichael and Wong, 2001; Li, et al., 2001a). Multiple rounds of directed evolution have produced P450 BM-3 mutants capable of hydroxylating a variety of alkanes (C3 to C8) at initial turnover rates exceeding those of the wild-type enzyme towards the natural, fatty acid substrates and those of any known alkane hydroxylase (Glieder, et al., 2002). This mutant enzyme also showed higher activities towards fatty acids as compared to the wildtype enzyme. There are also examples of nonheme monooxygenases that have recently been engineered by directed evolution (Canada, et al., 2002; Meyer, et al., 2002a; Meyer, et al., 2002b). The flavoenzyme 2-hydroxybiphenyl 3-monooxygenase (HbpA) of *P. azelaica* HBP1 catalyzes the regioselective *ortho*-hydroxylation of a wide range of 2-substituted phenols to the corresponding catechols. Random mutagenesis resulted in enzyme variants with improved or novel activities towards 2-*tert*-butylphenol, guaiacol, and 2-*sec*-butylphenol (Meyer, et al., 2002a), as well as indole and derivatives thereof (Meyer, et al., 2002b). Continuous product removal by solid phase adsorption on a hydrophobic resin allowed the multi-gram scale production of 3-*tert*-butylcatechol using an improved variant of

HbpA in recombinant *E. coli* (Meyer, et al., 2003). The nonheme diiron enzyme toluene *ortho*-monooxygenase (TOM) of *Burkholderia cepacia* G4 converts toluene to 3-methylcatechol in a two-step reaction; it also oxidizes naphthalene and trichloroethylene, making TOM a potential biocatalyst for bioremediation (Luu, et al., 1995). TOM's ability to hydroxylate naphthalene and to degrade chlorinated compounds was improved using error-prone DNA shuffling (Canada, et al., 2002). Novel and improved molecular and computational techniques can be regarded as valuable tools for the optimization of enzyme activities and specificities of oxygenase-based biocatalysts.

#### 1.4.2.2 UNCOUPLING

In oxygenase catalysis, the reduction of molecular oxygen by two or four electrons can be uncoupled from substrate oxidation resulting in the formation of hydrogen peroxide or water. For whole-cell biocatalysis, this uncoupling has to be minimized because it leads to a loss of reduction equivalents from the host cell, an increased oxygen demand, and the production of toxic hydrogen peroxide (Lee, 1999). Uncoupling can occur in the absence of substrate and often is induced by compounds with a bad fit in the active site (Lee, 1999). This compound can be a poor substrate or a non-substrate such as the product of the oxygenase reaction (Suske, et al., 1997). Uncoupling can also occur when a crucial residue is mutated and thus can be a side effect of directed evolution (Miles, et al., 2000; Meyer, et al., 2002b). On the other hand, enzyme engineering can be used to reduce uncoupling as shown for HbpA (Meyer, et al., 2002a) and cytochrome P450cam (Jones, et al., 2001). Process engineering solutions such as in situ product removal can also reduce product-induced uncoupling as in the case of catechol production by recombinant *E. coli* containing HbpA (Held, et al., 1999b). The investigation of the exact molecular mechanisms of uncoupling may allow the development of biocatalyst and process engineering solutions for the minimization of uncoupling.

#### 1.4.2.3 MULTIPLE OXIDATION

Several oxygenases catalyze multiple oxidations of hydrocarbon substrates, which is a problem if a specific alcohol is the desired product. Such multiple oxidation activity may be due to a low (regio)specificity resulting in oxidation at multiple sites or in overoxidation of an alcohol product to the corresponding aldehyde and acid.

Both, oxidation at diverse carbon atoms and overoxidation were found for P450 BM-3, oxidizing fatty acids to subterminal hydroxy- and oxoproducts with a product diversity

depending on the dissolved oxygen concentration (Boddupalli, et al., 1992; Schneider, et al., 1999). Many other P450 enzymes have been reported to catalyze multiple oxidation of the same substrate. Examples are the oxidations of linalool and camphor to 8-oxolinalool and 5-ketocamphor, respectively (Ullah, et al., 1990), of ethanol via acetaldehyde to acetic acid (Bell-Parikh and Guengerich, 1999), and of fatty acids to diacids (Shet, et al., 1996). Furthermore, several P450 enzymes catalyze multistep reactions involved in steroid oxidation, e.g., P450s 27, 24, 19, 17 $\alpha$ , 14 $\alpha$ , 11 $\beta$  and P450scc (Hume, et al., 1984; Kellis and Vickery, 1987; Fischer, et al., 1989; Cali and Russell, 1991; Holmberg-Betsholtz, et al., 1993; Akiyoshi-Shibata, et al., 1994; Imai, et al., 1998; Yamazaki, et al., 1998).

Histidine cluster containing nonheme diiron enzymes have also been reported to catalyze multiple oxidations. For example, C-4 sterol methyl oxidase of *Saccharomyces cerevisiae* catalyzes the three-step oxidation of a methyl group to the carboxylic acid (Bard, et al., 1996). As mentioned above, alkane monooxygenase (AMO) oxidizes terminal alkanols to alkanals (May and Katopodis, 1986), and early reports suggested that xylene monooxygenase (XMO) catalyzes alcohol and aldehyde oxidations (Harayama, et al., 1986; Harayama, et al., 1989). In the case of XMO, such activities later were attributed to dehydrogenases present in the *E. coli* host (Harayama, et al., 1989; Shaw and Harayama, 1995).

The highest natural oxygenation activities were observed with enzymes, in which oxygenase and electron transfer components are fused naturally as in P450 BM-3 (Munro, et al., 2002) and nitric oxide synthase (Ortiz de Montellano, et al., 1998), enzymes showing significant overoxidation. The P450-catalyzed multistep oxidations of ethanol and of some steroids are considered to involve little or no dissociation of the reaction intermediates from the enzymes (Imai, et al., 1998; Yamazaki, et al., 1998; Bell-Parikh and Guengerich, 1999). Van Beilen et al. (2003) argued that the separation of the different cofactors in separate proteins, which slows down electron transfer, may be a result of evolutionary pressure towards mechanisms that allow the product to leave the enzyme before it is further oxidized. This suggests a trade-off between catalytic rate and reaction specificity (e.g., overoxidation). Thus, increasing the catalytic rate by protein engineering might lead to significant overoxidation, which mostly is undesired.



### 1.4.3. PHYSIOLOGICAL ASPECTS – BIOCATALYST STABILITY

#### 1.4.3.1. PRODUCT DEGRADATION

Oxygenases are generally part of catabolic or anabolic pathways involving downstream enzyme activities, which may lead to product degradation. The use of wildtype strains is useful when dead end products are produced, as in the oxidation of aromatic heterocycle methyl groups to the corresponding carboxylic acids by wildtype *P. putida* mt-2, which harbors the xylene degradation pathway (Kiener, 1992). However, when degradation of the desired product takes place, it will be necessary to block through-conversion of the desired intermediate by mutagenesis of the wildtype strain, or by introducing the genes of the desired enzymes into a host that is not able to degrade the product. In some cases, genetic engineering of the selected wildtype strain to avoid product consumption may be difficult due to, for instance, the presence of multiple enzyme activities attacking the product or unknown genetical properties. Then, heterologous expression, in vitro use, or further screening are possible alternatives. Further reasons that may favor heterologous expression are demanding cultivation, poor growth on minimal media, and suspected pathogenicity of the strain of interest.

#### 1.4.3.2. RECOMBINANT BIOCATALYSIS

Heterologous expression of oxygenases can be difficult and, as mentioned above, overexpression in a recombinant host does not necessarily result in higher activities than in the wildtype. The molecular environment in recombinant hosts may differ from the wildtype strain, which might complicate the stable and functional expression of oxygenases in recombinants. Critical factors include protein folding, protein stability, genetic stability, the ratio of multiple components, cofactor incorporation, the interactions of membrane-associated components with the host membrane, the requirement for additional proteins, and the formation of reactive oxygen species.

In the case of AMO, the enzyme components were less stable and the specific activity of the limiting oxygenase component AlkB was five or six times lower in recombinant *E. coli* than in *P. putida* GPo1 (Staijen, et al., 2000). Furthermore, the addition of sufficient iron is crucial (Staijen and Without, 1998). High-level expression of membrane bound components such as AlkB of AMO may destabilize the membrane and thus affect cell growth. AMO expression in *P. putida* and *E. coli* altered the membrane lipid composition and reduced the growth rate and

the stability of the AMO genes (Nieboer, et al., 1993; Chen, et al., 1995; Chen, et al., 1996). However, overexpression of AMO in *E. coli* compensated the lower specific enzyme activity and recombinants as active as the wildtype were constructed.

Genetic instability can be addressed by the insertion of the oxygenase genes into the chromosome of the host (Panke, et al., 1999a; Hüsken, et al., 2001a). Correct and sufficient cofactor incorporation into recombinant oxygenases might necessitate, beside the supply of metals such as iron, the addition of other cofactor precursors such as  $\delta$ -aminolevulinic acid in the case of heme proteins (Richardson, et al., 1995). Reasonable expression of eucaryotic P450 oxygenases in the cytosol instead of low levels in the membrane was reached by removing hydrophobic residues from the N-terminus (Miles, et al., 2000). A reactivating component was required as an additional protein in the case of catechol-2,3-dioxygenase (Hugo, et al., 1998). High specific styrene monooxygenase activities of  $180 \text{ U (g of CDW)}^{-1}$  in recombinant *E. coli* were reached by additionally expressing two genes encoding regulators, which control expression of the styrene monooxygenase genes at the transcriptional level (Panke, et al., 1998b). This procedure also alleviated a block that prevented translation when a heterologous promoter was used. High oxygenase activities are expected to enforce the formation of active oxygen species such as hydrogen peroxide, which affect host and oxygenase stability (Lee, 1999). This may limit the benefit of oxygenase overexpression.

However, despite the mentioned critical points, which need to be investigated in more detail, there are numerous reports on successful expression of oxygenases in recombinant hosts, especially in *E. coli* (Wahbi, et al., 1996; Parikh, et al., 1997; Shet, et al., 1997; Iwata, et al., 1998; Miles, et al., 2000; Doig, et al., 2001; Doig, et al., 2002a).

#### 1.4.3.3. COFACTOR RECYCLING IN WHOLE CELLS

Maximal turnover rates of NAD(P)H in whole cells were estimated based on exponential growth on glucose at a rate ( $\mu$ ) of  $2 \text{ h}^{-1}$  and a yield of 0.5 g of cells per g of glucose (Duetz, et al., 2001). This calculation resulted in a maximal NAD(P)H regeneration rate of  $720 \text{ U (g of CDW)}^{-1}$ , which has been considered to be sufficient to cover the demand of active heterologous oxygenases. Thereby, it was assumed that such a NAD(P)H regeneration capacity can be used for biotransformation instead of growth. However, processes exploiting in vivo oxygenation are often based on growing cells, in order to maintain high biocatalyst activities (Favre-Bulle, et al., 1991; Favre-Bulle and Witholt, 1992; Kiener, 1992; Favre-Bulle, et al., 1993; Wubbolts, et al., 1996a; Panke, et al., 1999b; Phumathon and Stephens,

1999; Panke, et al., 2000; Hüsken, et al., 2001b; Hüsken, et al., 2002a; Hüsken, et al., 2002b; Panke, et al., 2002). Furthermore, results obtained in several studies on whole-cell oxygenations at high specific rates indicate that resting cells or cells reaching the stationary phase after batch or fed-batch growth steadily lose their oxygenase activities despite of the supply of an energy source (Bosetti, et al., 1992; Favre-Bulle and Witholt, 1992; Wubbolts, et al., 1994a; Wubbolts, et al., 1996a; Prichanont, et al., 1998; Phumathon and Stephens, 1999; Hüsken, et al., 2001a; Hüsken, et al., 2002a; Maruyama, et al., 2003). This can be due to decreasing intracellular oxygenase levels and/or NAD(P)H shortage as a consequence of a reduced NAD(P)H regeneration rate, when the cells adapt their metabolic activity to the actual growth stage. Thus, the use of growing cells with high metabolic activities may guarantee the maintenance of high oxygenase levels and/or high NAD(P)H regeneration rates. However, during cell growth, various reactions, especially oxidative phosphorylation, also consume reduction equivalents (Russell and Cook, 1995). The presence of an active NAD(P)H-consuming oxygenase will thus have an impact on cell metabolism, decrease growth yields on energy sources, cause stress, and reduce growth rate, viability, and metabolic activity (Bosetti, et al., 1992; Phumathon and Stephens, 1999). Moreover, due to the complexity and flexibility of cell metabolism (Russell and Cook, 1995), a certain extent of oxygenase activity in growing cells might also cause an increase of the glucose uptake rate in order to accomplish the increased NAD(P)H demand. In such a case, overall NAD(P)H turnover rates might become higher than  $720 \text{ U (g of CDW)}^{-1}$ .

Up to the present, the interrelationship between cell growth, oxygenase overexpression, and intracellular NAD(P)H regeneration is poorly understood. Further investigations are required to elucidate if and to what extent cofactor recycling is limiting in whole-cell biooxidations. Based on this research, bioprocess engineering in order to optimally exploit cell metabolism and the introduction of additional cofactor regeneration activity may help maximizing in vivo oxygenation rates.

#### **1.4.3.4. TOXICITY OF SUBSTRATES AND PRODUCTS**

The majority of potentially interesting substrates and products of oxidative biotransformations is poorly water-soluble and/or toxic to living cells (Lilly, 1982; Nikolova and Ward, 1993; Salter and Kell, 1995; Lilly and Woodley, 1996; Leon, et al., 1998). This represents a major challenge for biochemical reaction engineering as whole cells are adapted to aqueous environments and process efficiency may be impaired in the presence of toxic chemicals. Typically, these drawbacks are circumvented by regulated substrate addition (Hack, et al.,

2000; Carragher, et al., 2001) and in situ product removal (Freeman, et al., 1993; Lye and Woodley, 1999), which is discussed below in section 1.4.4.

Small apolar substrates can readily diffuse into the cell membrane, which may be beneficial in the sense that no substrate uptake system is required and that substrate uptake does not limit biotransformation, which both may be the case for larger and polar substrates. However, as mentioned above, small apolar compounds often are toxic to living cells owing to different effects, of which membrane disintegration is believed to be the most prominent (Laane, et al., 1987; Sikkema, et al., 1995). Solvent toxicity correlates with its  $\log P_{\text{oct}}$ , the logarithm of the partition coefficient of a solvent in an octanol-water mixture (Laane, et al., 1987; Sikkema, et al., 1995). Solvents with a  $\log P_{\text{oct}}$  below 4.0 such as toluene ( $\log P_{\text{oct}} = 2.69$ ), styrene ( $\log P_{\text{oct}} = 2.95$ ), and xylenes ( $\log P_{\text{oct}} = 3.12 - 3.2$ ) are extremely toxic for most microorganisms because they disrupt the cell membrane structure. However, several bacterial strains can resist the presence of a solvent with a  $\log P_{\text{oct}} < 4$ . Such strains are termed solvent-tolerant. Ramos et al. recently published an excellent review on mechanisms of solvent tolerance in gram-negative bacteria (Ramos, et al., 2002). According to the current knowledge, the major mechanisms of solvent tolerance are adaptive alterations of the membrane fatty acids and phospholipid headgroup composition, energy-dependent efflux pumps exporting toxic compounds to the external medium, and formation of vesicles loaded with toxic compounds. Such mechanisms have mainly been characterized for *Pseudomonas* and *E. coli* strains and may be exploited in biocatalysis involving toxic organic substrates and products (de Bont, 1998; Ramos, et al., 2002).

The transfer of genes involved in solvent tolerance into a strain of interest may result in a more stable and more efficient biocatalyst. For example, the transfer of the genes for a solvent efflux system of solvent-resistant *P. putida* S12 into solvent-sensitive *P. putida* strains resulted in partial acquisition of solvent resistance by these strains (Kieboom, et al., 1998). Since often multiple mechanisms contribute to the solvent tolerance of a specific strain (Ramos, et al., 2002), transferring the genes for the biocatalytically active enzymes into a solvent-tolerant host may be even more promising. Following this strategy, the genes of *P. putida* F1 involved in the conversion of toluene to 3-methylcatechol were introduced into *P. putida* S12 (Wery, et al., 2000). Biotransformations were performed in a two-liquid phase system with octanol ( $\log P_{\text{oct}} = 2.92$ ) as second organic phase. However, overexpression of the genes of interest in a mutant of the relatively solvent-tolerant natural host (see section 1.4.2.1) proved to be more efficient in terms of biocatalyst activity as well as final product concentration achieved (Hüsken, et al., 2001b). The highly solvent-tolerant strain *P. putida*

DOT-T1E may be another promising host. This well-characterized strain contains several systems contributing to solvent-tolerance such as three efflux pumps (Ramos, et al., 1998; Mosqueda and Ramos, 2000; Rojas, et al., 2001) and a *cis/trans* isomerase acting on phospholipids and thus counteracting the increased membrane fluidity in the presence of organic solvents (Junker and Ramos, 1999). Further studies on the exploitation of such mechanisms of solvent tolerance in production strains are required to assess the feasibility of this promising approach for biocatalysis in the presence of low log  $P_{\text{oct}}$  solvents.

#### **1.4.4. BIOPROCESS ENGINEERING ASPECTS**

##### **1.4.4.1. IN SITU PRODUCT REMOVAL**

By removing the product from the aqueous biocatalyst environment, in situ product recovery methods can increase the productivity and/or yield of a biocatalytic reaction by different modes. These modes include overcoming inhibitory or toxic effects, reducing uncoupling, shifting unfavorable reaction equilibria, reducing the total number of downstream-processing steps, and minimizing product losses due to degradation, overoxidation, or uncontrolled release. Which in situ product removal technique is suitable for a specific system depends on the physical and chemical properties of the product (Freeman, et al., 1993). Such properties include volatility, molecular weight or size, solubility, charge, hydrophobicity, and specific functional groups of the molecule. In situ product removal techniques comprise evaporation via vacuum fermentation, gas stripping, or pervaporation, as well as size selective permeation, reversible complex formation, adsorption to or generation of a solid phase, and extraction into a second liquid phase. The latter two possibilities are the best-studied methods, have been considered the most appropriate techniques for in situ product recovery (Lye and Woodley, 1999), and will now be discussed in more detail.

##### **1.4.4.2. SOLID PHASE EXTRACTION**

Product removal by immobilization via adsorption onto polymeric matrices such as ion-exchange or hydrophobic resins has been demonstrated for a large variety of compounds including antibiotics, plant metabolites, fine chemicals, and even proteins (Voser, 1982; Hecht, et al., 1987; Freeman, et al., 1993; Lye and Woodley, 1999; Held, 2000).

An illustrative example including oxygenase catalysis is the production of 3-methylcatechol from toluene using toluene dioxygenase and *cis*-dihydrodiol dehydrogenase present in the

catechol-2,3-dioxygenase deficient mutant *P. putida* 2313 (Robinson, et al., 1992). Cycling a glucose fed-batch culture over a column containing activated charcoal allowed a 3–4-fold increase of the amount of 3-methylcatechol produced as compared to a process setup without in situ product removal. Thereby, toluene was continuously added in the vapor phase via an additional air stream, and a productivity of  $0.094 \text{ g L}^{-1} \text{ h}^{-1}$  was reached on a 5 L scale.

A similar approach was used for the conversion of fluorobenzene via fluorobenzene-*cis*-glycol to fluorocatechol by resting *P. putida* ML2 (Lilly and Woodley, 1996; Lynch, et al., 1997). The presence of fluorine as a substituent prevented further oxidation by catechol 1,2-dioxygenase present in the cells. The toxic effects of the substrate were minimized by continuously feeding fluorobenzene in order to maintain its concentration at a low nontoxic level. The polar and highly toxic product was removed by circulating the reaction mixture over a packed bed of the activated carbon Norit pK13. This procedure allowed a remarkable productivity of  $1.1 \text{ g L}^{-1} \text{ h}^{-1}$  on a 2 L scale.

An example illustrating the scalability of this in situ product removal method is the production of highly toxic substituted catechols from equally toxic phenols by recombinant *E. coli* containing HbpA (Held, et al., 1998; Held, et al., 1999b). The substrates were fed at a rate slightly below the maximal biooxidation rate. Efficient product removal and stabilization was achieved by pumping the reaction mixture, containing the biocatalyst, through an external loop with a fluidized bed of the hydrophobic resin Amberlite™ XAD-4. Successful scale up to 300 L allowed the production of 1 kg of 3-phenylcatechol from 2-phenylphenol with a reaction yield of 83% and an average productivity of  $0.4 \text{ g L}^{-1} \text{ h}^{-1}$  (Held, et al., 1999a; Held, 2000).

#### 1.4.4.3. TWO-LIQUID PHASE CONCEPT

Two-liquid phase systems can consist of an aqueous and an organic or two aqueous phases. In aqueous two-phase systems, the formation of two separate phases is achieved by adding two different high molecular weight compounds, such as dextran or polyethylene glycol, that are hygroscopic but immiscible in each other (Andersson and Hahn-Hägerdal, 1990; Kaul and Mattiason, 1991). In the present work, the two-liquid phase system is referred to as a system consisting of an aqueous medium and an organic, water-immiscible solvent, since only this system has been used for whole-cell biooxidations.

Organic-aqueous two-liquid phase systems present a valuable biotechnological tool for biotransformations of apolar compounds (Schwartz and McCoy, 1977; de Smet, et al., 1981b; Witholt, et al., 1990; Witholt, et al., 1992; Liu, et al., 1996; Wubbolts, et al., 1996a; Schmid,

et al., 1998a). The concept allows high overall concentrations of toxic apolar chemicals within the two-liquid phase system, by regulating substrate and product concentrations in the aqueous biocatalyst microenvironment, and simple product recovery (Furuhashi, et al., 1986; Woodley and Lilly, 1990; Leon, et al., 1998). Furthermore, the partitioning behavior of substrate and product can be exploited to avoid product inhibition, to guide equilibrium reactions into a desired direction, and to enhance the enantiomeric excess (Kawakami and Nakahara, 1994; Salter and Kell, 1995; Faber, 2000; Gerrits, et al., 2001b; Willeman, et al., 2002a). The choice of an appropriate organic phase is crucial and depends on a variety of parameters including toxic or inhibitory effects of the solvent on the cells (see section 1.4.3.4), solvent capacity for and partition coefficients of substrate and product, degradability by the biocatalyst, density difference to water, boiling point, flammability, toxicity to the operator, and price (Salter and Kell, 1995; Schmid, et al., 1998a).

Several studies on biotransformations based on oxygenase catalysis reported the use of the two-liquid phase concept. Selected examples are described below and summarized in Table 1.3. For reliable comparison of the different bioconversions, productivities with respect to the aqueous phase volume are given. Furthermore, the varying degree of development has to be considered.

In early studies, this concept was used to accumulate epoxyalkanes from alkenes via whole-cell catalysis based on wildtype *P. putida* GPO1 able to grow on alkanes and also 1-alkenes (Schwartz and McCoy, 1977; de Smet, et al., 1981a; de Smet, et al., 1981b; de Smet, et al., 1983). Thereby, pure alkene (de Smet, et al., 1981b; de Smet, et al., 1983) or alkene dissolved in cyclohexane (Schwartz and McCoy, 1977) were added as a second phase. In the former case, repeated exchange of the aqueous phase with a fresh culture (Cell Renewal Procedure) allowed to enhance the final product concentration (de Smet, et al., 1983). In this study, the highest overall productivity ( $0.08 \text{ g L}_{\text{tot}}^{-1} \text{ h}^{-1}$ , corresponding to  $0.16 \text{ g L}_{\text{aq}}^{-1} \text{ h}^{-1}$  with respect to the aqueous phase) was reached with an organic phase volume fraction of 50% (vol/vol) resulting in a product concentration in the organic phase of  $45 \text{ g L}_{\text{tot}}^{-1}$ . This concentration could be increased up to  $150 \text{ g L}_{\text{org}}^{-1}$  by reducing the organic phase volume fraction to 10% (vol/vol). An enantiomeric excess of 70% has been determined for the (*R*)-1,2-epoxyoctane product (de Smet, et al., 1981a), whereas 84% have been reported for (*R*)-7,8-epoxy-1-octene (May, et al., 1976).

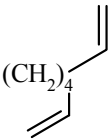
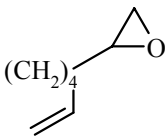
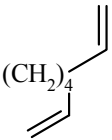
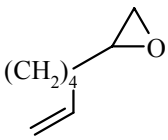
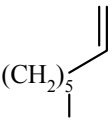
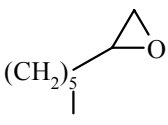
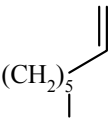
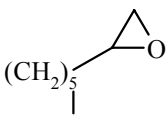
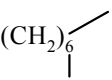
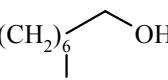
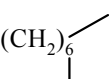
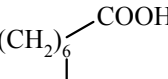
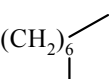
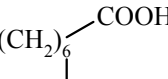
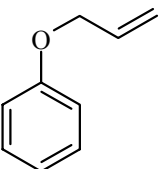
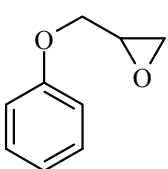
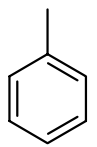
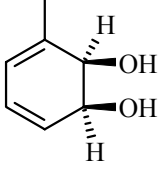
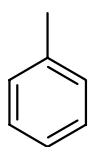
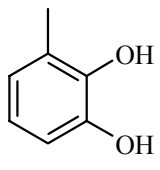
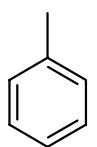
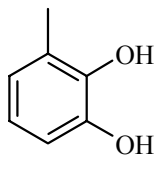
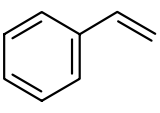
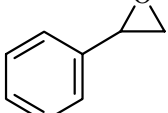
In a commercial epoxidation process, the Japan Energy Corporation (formerly Nippon Mining) uses wildtype *Rhodococcus rhodochrous* B-276, formerly known as *Nocardia corralina* B-276 (Furuhashi, et al., 1981), for the conversion of various alkenes (Furuhashi,

1986; 1992). The alkene monooxygenase of this strain has a very large substrate spectrum and is, in contrast to alkane monooxygenases such as the *P. putida* enzyme, specific for double bonds and also catalyzes subterminal epoxidations. C<sub>6</sub>-C<sub>12</sub> alk-1-enes and various aromatic olefins were diluted in a non-toxic carrier solvent (e.g. hexadecane or other alkanes) and converted by glucose-grown resting cells (Furuhashi, et al., 1986), whereas C<sub>13</sub>-C<sub>18</sub> alk-1-enes were directly added to a culture growing on these alkenes (Furuhashi, 1984). Enantiomeric excesses between 60 and 99% were reported for the products. With respect to the total volume, a product titer of 30 g L<sub>tot</sub><sup>-1</sup> and a productivity of 0.25 g L<sub>tot</sub><sup>-1</sup> h<sup>-1</sup> were achieved for (*R*)-1,2-epoxyoctane production on a 4 m<sup>3</sup> scale. For (*R*)-1,2-epoxytetradecane production in a 5 L fermenter, the respective numbers were 80 g L<sub>tot</sub><sup>-1</sup> and 0.56 g L<sub>tot</sub><sup>-1</sup> h<sup>-1</sup>. Glucose-grown *R. rhodochrous* B-276 have also been used in the epoxidation of smaller olefins (C<sub>3</sub> to C<sub>5</sub>), which were added via gas phase. Epoxide stripping via intense aeration resulted in productivities of up to 17 mmol L<sup>-1</sup> h<sup>-1</sup> (for propylene oxide) and was followed by extensive solvent absorption and distillation (Furuhashi, 1992). Thus, the use of the two-liquid phase concept as well as gas stripping renders Japan Energy able to commercially produce a large variety of epoxides.

More recent examples are the production of alkanols (Bosetti, et al., 1992) and octanoate (Favre-Bulle, et al., 1991; Favre-Bulle and Witholt, 1992; Wubbolts, et al., 1996a) from corresponding alkanes present as a second organic phase using growing recombinant *P. putida* and *E. coli*, respectively. The attained octanol productivity amounted to 0.088 g L<sub>aq</sub><sup>-1</sup> h<sup>-1</sup> during the first 10 h and to 0.053 g L<sub>aq</sub><sup>-1</sup> h<sup>-1</sup> over the total production period with low cell concentrations of around 1 (g of CDW) L<sub>aq</sub><sup>-1</sup> (Bosetti, et al., 1992). With cell concentrations of around 38 (g of CDW) L<sub>aq</sub><sup>-1</sup>, an octanoate productivity of 1.33 g L<sub>aq</sub><sup>-1</sup> h<sup>-1</sup> was reached for 5 h (Wubbolts, et al., 1996a). The production of octanoate, which accumulates in the aqueous phase, was also established in a continuous mode at a rate of 0.5 and 0.6 g L<sub>aq</sub><sup>-1</sup> h<sup>-1</sup> in the presence (Favre-Bulle, et al., 1993) and in the absence (Rothen, et al., 1998) of yeast extract, respectively. The production of octanol from octane was further studied with respect to downstream processing via phase separation and distillation (Mathys, et al., 1998a; Mathys, et al., 1998b), and with respect to industrial process design including a comprehensive economic evaluation (Mathys, et al., 1999).



Table 1.3. Examples for in vivo oxygenase catalysis in two-liquid phase systems.\*

Substrate	Product	Productivity [g L <sub>aq</sub> <sup>-1</sup> h <sup>-1</sup> ] <sup>a</sup>	Final [Product] <sup>b</sup>	Catalyst, scale <sup>c</sup> , and References
		0.13	39 g L <sub>org</sub> <sup>-1</sup>	Growing <i>P. putida</i> GPO1; scale: 100 ml (Schwartz and McCoy, 1977)
		0.23	45 g L <sub>org</sub> <sup>-1</sup> , <sup>d</sup>	Continuous cultivation of <i>P.</i> <i>putida</i> GPO1 in a membrane reactor; scale: 2 L (Doig, et al., 1999a)
		0.16	45 g L <sub>org</sub> <sup>-1</sup> , <sup>e</sup>	Growing <i>P. putida</i> GPO1; scale: 10-100 ml (de Smet, et al., 1983)
		0.25 [L <sub>tot</sub> <sup>-1</sup> ], <sup>f</sup>	30 g L <sub>org</sub> <sup>-1</sup> , <sup>f</sup>	Resting <i>R. rhodochrous</i> B- 276; scale: 4000 L (Furuhashi, 1992)
		0.053	5 g L <sub>org</sub> <sup>-1</sup>	Growing recombinant <i>P.</i> <i>putida</i> ; scale: 0.6 L (Bosetti, et al., 1992)
		1.33	6.6 g L <sub>aq</sub> <sup>-1</sup>	Fed-batch culture of recom- binant <i>E. coli</i> ; scale: 0.65 L (Wubbolts, et al., 1996a)
		0.6	1.9 g L <sub>aq</sub> <sup>-1</sup>	Continuous culture of re- combinant <i>E. coli</i> ; scale: 3 L (Rothen, et al., 1998)
		0.12	0.18 g L <sub>org</sub> <sup>-1</sup>	Resting <i>Mycobacterium</i> M156; scale: few ml (Prichanont, et al., 1998)
		9.5	57 g L <sub>aq</sub> <sup>-1</sup>	Resting <i>P. putida</i> UV4; scale: 1.7 L (Lilly and Woodley, 1996)
		0.11	6 g L <sub>org</sub> <sup>-1</sup> 0.27 g L <sub>aq</sub> <sup>-1</sup>	Growing mutant of <i>P. putida</i> F1; scale: 0.8 L (Hüsken, et al., 2001b)
		0.12	2.1 g L <sub>org</sub> <sup>-1</sup> 0.42 g L <sub>aq</sub> <sup>-1</sup>	Same strain growing in a membrane bioreactor; scale: 1.8 L (Hüsken, et al., 2002b)
		2	32.3 g L <sub>org</sub> <sup>-1</sup>	Growing recombinant <i>E.</i> <i>coli</i> ; scale: 30 L (Panke, et al., 2002)

## Legend of Table 1.3:

\*See text for further details concerning the individual examples listed. Subscripts: aq, aqueous phase; org, organic phase.

<sup>a</sup> overall productivity with respect to total production period and aqueous phase volume.

<sup>b</sup> final product concentration in the respective phase.

<sup>c</sup> working volume including both phases.

<sup>d</sup> epoxide accumulated in the organic phase reservoir (1 L, aqueous phase volume: 1 L).

<sup>e</sup> after 3 exchanges of the aqueous phase with a fresh culture (Cell Renewal Procedure).

<sup>f</sup> phase ratio was not reported; productivity and final product concentration are given with respect to the total volume.

In another study, phenyl glycidyl ether was produced from allyl phenyl ether by the use of resting cells of *Mycobacterium* M156 (Prichanont, et al., 1998). Hexadecane was chosen as organic carrier solvent, and specific epoxidation rates in the range of 5 to 6 U (g of CDW)<sup>-1</sup> were reached for 1.5 to 2 h, whereupon activity was lost. This translates to an aqueous phase based productivity of about 0.12 g L<sub>aq</sub><sup>-1</sup> h<sup>-1</sup> for the applied small-scale system with an aqueous phase volume fraction of 50% (vol/vol).

Toluene dioxygenase was used to produce toluene *cis*-glycol from toluene at productivities of 9.5 and 0.21 g L<sub>aq</sub><sup>-1</sup> h<sup>-1</sup> for *P. putida* UV4 and recombinant *E. coli*, respectively (Collins, et al., 1995; Lilly and Woodley, 1996; Tsai, et al., 1996; Phumathon and Stephens, 1999). The second organic phase consisted of tetradecane, and the rather polar product accumulated in the aqueous phase. Thus, in this case, the two-liquid phase setup was chosen only to continuously provide toxic substrate but not for in situ product extraction. 9.5 g L<sub>aq</sub><sup>-1</sup> h<sup>-1</sup> is the highest productivity reported for oxygenase based whole-cell biocatalysis in a two-liquid phase system and was achieved with 10-11 (g of CDW) L<sub>aq</sub><sup>-1</sup> resting *cis*-dihydrodiol dehydrogenase deficient *P. putida* UV4 during a production period of 6 h resulting in a product concentration of 57 g L<sub>aq</sub><sup>-1</sup> (Lilly and Woodley, 1996). This translates into a specific activity of 120 U (g of CDW)<sup>-1</sup>. With *E. coli*, a strategy including a toluene feed via vapor phase and no organic phase yielded the best results (productivity: 0.32 g L<sub>aq</sub><sup>-1</sup> h<sup>-1</sup>) (Phumathon and Stephens, 1999).

The same enzyme in combination with *cis*-dihydrodiol dehydrogenase was used to produce 3-methylcatechol in the presence of a second octanol phase. Therefore, the genes encoding these enzymes were overexpressed in a mutant of the natural host *P. putida* F1 (Hüsken, et al., 2001b) or introduced into solvent-tolerant *P. putida* S12 (Wery, et al., 2000) as described in the sections 1.4.2.1 and 1.4.3.4, respectively. The exposure of the cells to the two-liquid phase

system resulted in a long lag/adaptation time of up to 24 h without product formation. This may be due to the rather polar and thus slightly toxic solvent, which had to be chosen to sufficiently extract the relatively polar and toxic product, 3-methylcatechol. Productivities ranged from  $0.067 \text{ g L}_{\text{aq}}^{-1} \text{ h}^{-1}$  with recombinant *P. putida* S12 to  $0.11 \text{ g L}_{\text{aq}}^{-1} \text{ h}^{-1}$  with the mutant of *P. putida* F1. Using the latter strain in an aqueous one-phase system resulted in a similar productivity ( $0.1 \text{ g L}^{-1} \text{ h}^{-1}$ ) but in a lower overall product concentration (1.24 as compared to  $3.10 \text{ g L}_{\text{tot}}^{-1}$  in the two-liquid phase system).

A remarkable example for the use of the two-liquid phase concept for oxyfunctionalization is the enantioselective production of (*S*)-styrene epoxide from styrene. Therefore, two different enzymes were used in recombinant *E. coli*: XMO of *P. putida* mt-2 allowing an enantiomeric excess of 95% (Wubbolts, et al., 1994a; Wubbolts, et al., 1996a; Panke, et al., 1999b) and styrene monooxygenase of *Pseudomonas* sp. VLB120 with an even better enantiomeric excess (> 99%) for styrene epoxidation (Panke, et al., 1998b; Panke, et al., 2000). In contrast to the *Rhococcus* enzyme (see above), which catalyzes (*R*)-specific epoxidation of styrene, these enzymes are (*S*)-specific. Styrene monooxygenase, an optimized expression system, glucose-based fed-batch cultivation, the choice of bis(2-ethylhexyl)phthalate as organic carrier solvent present at a volume fraction of 50% (vol/vol), scale up to pilot-scale (30 L working volume), and downstream processing including phase separation and vacuum distillation enabled the production of 307 g (*S*)-styrene oxide (purity: >97%) (Panke, et al., 2002). The mean aqueous phase based productivity in the 16 h of biotransformation amounted to  $2 \text{ g L}_{\text{aq}}^{-1} \text{ h}^{-1}$ . Furthermore, stable whole-cell biocatalysts have been developed for the continuous production of (*S*)-styrene oxide (Panke, et al., 1999a). Xylene and styrene monooxygenase genes have been stably integrated into the chromosome of *P. putida* KT2440. The resulting biocatalysts showed specific activities rivalling those of multicopy plasmid based *E. coli* recombinants. However, the productivity of a preliminary continuous culture of *P. putida* containing the XMO genes on the chromosome was considerably lower ( $0.048 \text{ g L}_{\text{aq}}^{-1} \text{ h}^{-1}$ ) as compared to fed-batch cultures of recombinant *E. coli*.

A potential drawback of two-liquid phase biotransformations is the formation of stable emulsions, which may complicate phase separation. A possibility to avoid emulsification is to separate the two phases by a membrane (Vaidya, et al., 1992; Vaidya, et al., 1993; Vaidya, et al., 1994; Doig, et al., 1998; Doig, et al., 1999b; León, et al., 2001). The biocatalyst can also be entrapped in the membrane (especially in the case of isolated enzymes) and/or, in the case of more polar products, membranes can be used for product removal via cross-flow filtration, which allows biocatalyst retention during continuous operation (Lopez and Matson, 1997;

Giorno and Drioli, 2000; Goetz, et al., 2001; Iwan, et al., 2001; Wöltinger, et al., 2001). However, mass transfer limitation and biofilm formation may impair efficiency and scale up of biotransformations based on a membrane setup (Willaert, et al., 1999; de Carvalho and da Fonseca, 2002; Cánovas, et al., 2003).

Separation of aqueous and organic phase by a membrane was applied for the epoxidation of 1,7-octadiene to 1,2-epoxy-7,8-octene by *P. putida* GPO1 growing continuously in a membrane bioreactor (Doig, et al., 1999a). The organic phase consisted of a mixture of the biotransformation substrate 1,7-octadiene and the growth substrate heptane, which both partitioned over the membrane into the aqueous growth medium. In order to avoid mass transfer limitation, the two constituents of the organic phase were additionally fed directly into the aqueous medium. A dense silicone rubber membrane was used to contact the two phases and no phase breakthrough of either liquid, a major challenge associated with this technology, was observed. A productivity of  $0.23 \text{ g L}_{\text{aq}}^{-1} \text{ h}^{-1}$  was achieved, after optimization of the aqueous phase dilution rate.

The use of a membrane was also evaluated in the process described above for the production of 3-methylcatechol from toluene (Hüsken, et al., 2002b). Toluene was added via the air stream, and product extraction over the membrane was mass transfer limited. With a 1:2 ratio of the separated octanol and aqueous phases, the overall productivity was increased by 40% as compared to the two-liquid phase process with direct phase contact. The aqueous phase based productivities, however, were in a similar range (Table 1.3). The lack of the lag phase in the membrane-based process was attributed to reduced phase toxicity, when direct contact of the cells with the octanol phase is prevented.

Thus, the use of a membrane to separate the organic from the aqueous phase can, beside the avoidance of emulsion formation, further reduce toxic effects of the product and the carrier solvent. Moreover, this strategy allows decoupling the dilution rates of the two phases in continuous and semi-continuous processes. However, regarding an industrial application, the often limiting mass transfer over the membrane has to be improved, thus alleviating the need for large membrane areas.

In conclusion, as emphasized by the described processes involving toxic apolar reactants, in situ product removal methods facilitate the in vivo application of oxygenases, extend the applicability of biocatalytic oxyfunctionalization, and thus considerably enhance the commercial potential of such processes. Further research and development in this promising field is supposed to enable the straightforward implementation of a variety of oxygenase-based biooxidation processes in the chemical industry.

#### 1.4.4.4. OXYGEN TRANSFER AND EXPLOSION HAZARD

Many potential substrates and/or enzyme inducers for oxygenase catalysis are volatile and flammable. Since whole-cell biocatalysts performing oxygenation reactions require oxygen for the biotransformation as well as for endogenous respiration, high oxygen input rates are essential. The consequential danger of explosion hazard can be essentially overcome by the addition of inert carrier solvents such as hexadecane and bis(2-ethylhexyl)phthalate. In such systems, substrates and/or inducers can be added up to a volume fraction of 30% (vol/vol) of the organic phase without the danger of an explosion hazard (Schmid, et al., 1998a; Panke, et al., 2002). Furthermore, substrate concentrations can be maintained at a level below 30% (vol/vol) by a tailored feeding regime. In order to address safety issues in and to improve the performance of aerobic bacterial bioprocesses involving flammable organic solvents, Schmid et al. together with Bioengineering AG (Wald, Switzerland) have developed a high-pressure explosion proof bioreactor (Schmid, et al., 1999).

However, oxygen input into production scale bioreactors at high rates remains a big challenge. Based on air as oxygen source, an upper limit for oxygenase activity in living cells of 500 U per liter aqueous medium, corresponding to a productivity of 3 g L<sup>-1</sup> h<sup>-1</sup> for a 100 g mol<sup>-1</sup> product, was estimated for standard industrial scale reactors (van Beilen, et al., 2003). This estimation included endogenous respiration of 10 g cells per liter and assumed an oxygen transfer coefficient ( $k_{La}$ ) of 200 h<sup>-1</sup>. Improving the specific activity of whole-cell biocatalysts and thus lowering the cell concentration was considered to reduce the relative amount of oxygen required for respiration, which increases the upper limit for volumetric oxygenase activity. On the other hand, higher oxygen input rates may be achieved by technical solutions and via aeration by oxygen enriched air, if economically feasible.

### **1.4.5. PERSPECTIVES OF BIOCATALYTIC OXYFUNCTIONALIZATION**

Enzymes are optimized by nature for the survival of a species in a specific ecological environment and not to meet the requirements of industrial biocatalytic processes. Nevertheless, biochemical process engineering and modern DNA technology provide a variety of tools to develop and optimize a biocatalyst and a process setup (Burton, et al., 2002; Panke and Wubbolts, 2002; Patnaik, et al., 2002; Schmid, et al., 2002). The combined use of different concepts may allow the application of complex oxygenase systems for challenging reactions with high commercial potential such as the biosynthesis of chiral compounds, the specific oxyfunctionalization of complex molecules, and also the synthesis of medium-price chemicals (Mathys, et al., 1999). Recent developments and the large pool of oxygenases in nature (Ellis, et al., 2001; Hou, et al., 2003) augur well for the development of many and varied industrial biooxidation processes in the near future.

## 1.5. SCOPE OF THIS THESIS

This work was focused on the design and characterization of a whole-cell biocatalyst and a process for the regiospecific multistep oxidation of xylenes to benzaldehydes as an example for a complex biooxidation reaction with commercial potential. This was an approach to further assess the general feasibility of biocatalytic oxyfunctionalization for industrial applications.

Chapter 2 describes a further characterization of the upper xylene degradation pathway of *P. putida* mt-2 and shows that xylene monooxygenase (XMO) expressed in recombinant *E. coli* catalyzes the multistep oxygenation of toluene and pseudocumene to corresponding benzyl alcohols, benzaldehydes, and benzoic acids. In Chapter 3, the kinetics of this multistep reaction are analyzed and the potential of recombinant *E. coli* containing XMO for the production of the individual oxidation products is highlighted. Chapter 4 describes the development and optimization of an efficient two-liquid phase fed-batch process, which exploits the complex kinetics of the multistep oxidation of pseudocumene for the production of one specific oxidation product, 3,4-dimethylbenzaldehyde. Scale up of this process to a technical scale (30 L) including suitable downstream processing is topic of Chapter 5. Finally, a process model was developed in order to address several issues such as the mechanism of substrate uptake, cell metabolism, and bioconversion kinetics, which may influence the performance of this multistep biooxidation process (Chapter 6).





## CHAPTER 2

# **XYLENE MONOOXYGENASE CATALYZES THE MULTISTEP OXYGENATION OF TOLUENE AND PSEUDOCUMENE TO CORRESPONDING ALCOHOLS, ALDEHYDES AND ACIDS IN *ESCHERICHIA COLI* JM101.**

**Bruno Bühler, Andreas Schmid, Bernhard Hauer, and Bernard  
Witholt**

Journal of Biological Chemistry, 2000, 275(14):10085-10092.

## SUMMARY

Xylene monooxygenase of *Pseudomonas putida* mt-2 catalyzes the methylgroup hydroxylation of toluene and xylenes. In order to investigate the potential of xylene monooxygenase to catalyze multistep oxidations of one methyl group, we tested recombinant *E. coli* expressing the monooxygenase genes *xylM* and *xylA* under the control of the *alk* regulatory system of *P. putida* GPo1. Expression of xylene monooxygenase genes could efficiently be controlled by *n*-octane and dicyclopropylketone. Xylene monooxygenase was found to catalyze the oxygenation of toluene, pseudocumene, the corresponding alcohols, and the corresponding aldehydes. For all three transformations, <sup>18</sup>O incorporation provided strong evidence for a monooxygenation type of reaction, with *gem*-diols as the most likely reaction intermediates during the oxygenation of benzyl alcohols to benzaldehydes. In order to investigate the role of benzyl alcohol dehydrogenase (XylB) in the formation of benzaldehydes, *xylB* was cloned behind and expressed in concert with *xylMA*. In comparison to *E. coli* expressing only *xylMA*, the presence of *xylB* lowered product formation rates and resulted in back formation of benzyl alcohol from benzaldehyde. In *Pseudomonas putida* mt-2, XylB may prevent the formation of high concentrations of the particularly reactive benzaldehydes. In the case of high fluxes through the degradation pathways and low aldehyde concentrations, XylB may contribute to benzaldehyde formation via the energetically favorable dehydrogenation of benzyl alcohols. The results presented here characterize XylMA as an enzyme able to catalyze the multistep oxygenation of toluenes.

## INTRODUCTION

Xylene monooxygenase (XMO), encoded by the plasmid pWW0 of *Pseudomonas putida* mt-2, is a key enzyme system in the degradation of toluene and xylenes. XMO is a member of the alkyl-group hydroxylase family and hydroxylates the methyl side chain of the aromatic ring. This is the first step towards the production of a carboxylic acid (upper degradation pathway for xylenes) (Fig. 2.1), which is then transformed to substrates of the Krebs cycle through the *meta* cleavage pathway. The upper pathway enzymes are encoded by the upper operon (Fig. 2.1), whereas the *meta* cleavage pathway is encoded by the *meta* operon (Abril, et al., 1989; Harayama, et al., 1989; Harayama, et al., 1992; Ramos, et al., 1997; Williams, et al., 1997). XMO consists of two polypeptide subunits, encoded by *xyIM* and *xyIA* (Harayama, et al., 1989; Suzuki, et al., 1991). XylA, the NADH:acceptor reductase component, was characterized as electron transport protein transferring reducing equivalents from NADH to XylM (Shaw and Harayama, 1992). XylM, the hydroxylase component, is located in the membrane, and its activity depends on phospholipids and ferrous ion with a pH optimum of 7 (Wubbolts, 1994; Shaw and Harayama, 1995). The XylM amino acid sequence has a 25% homology with AlkB, the hydroxylase component of alkane hydroxylase of *Pseudomonas putida* (*oleovorans*) GPo1 (Suzuki, et al., 1991). Alkane hydroxylase is the first enzyme in the degradation of medium chain length alkanes through a set of enzymes encoded on two *alk* gene clusters on the catabolic OCT plasmid (Baptist, et al., 1963; Chakrabarty, et al., 1973; Kok, et al., 1989; van Beilen, et al., 1994b). Sequence analyses indicated that at least 11 nonheme integral membrane enzymes, including AlkB and XylM, contain a highly conserved 8-histidine motif (Shanklin, et al., 1994; Shanklin, et al., 1997). This motif was shown to be essential for catalytic activity in rat stearyl-CoA desaturase (Shanklin, et al., 1994). Based on studies of AlkB, the integral membrane enzymes of this family were proposed to contain diiron clusters as O<sub>2</sub>-activating sites, for which the 8-histidine motifs provide ligands (Shanklin, et al., 1997).

The second enzyme in the upper pathway is benzyl alcohol dehydrogenase (BADH), a homodimeric member of the zinc-containing long chain alcohol dehydrogenase family (Shaw and Harayama, 1990; Shaw, et al., 1992; Shaw, et al., 1993). This enzyme is encoded by the *xyIB* gene. The third enzyme in the upper pathway, benzaldehyde dehydrogenase (BZDH), is also a homodimer and is encoded by the *xyIC* gene (Shaw and Harayama, 1990; Shaw, et al., 1992).

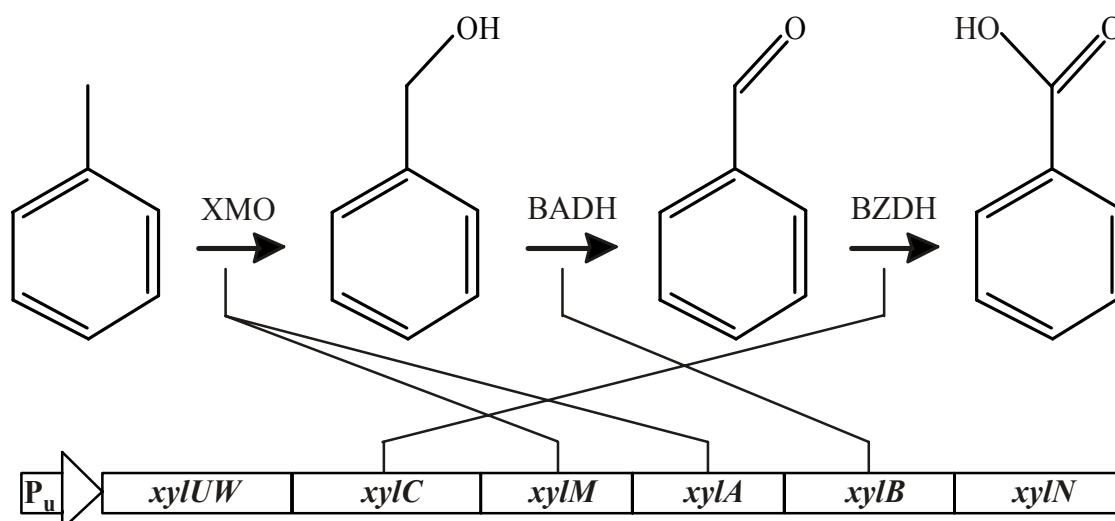


**Figure 2.1. Upper TOL pathway.** The consecutive oxidation of toluene to benzyl alcohol, benzaldehyde, and benzoic acid by enzymes of the upper TOL pathway and the organization of the *xyl* genes of the upper TOL operon are shown.  $P_u$ , upper TOL operon promoter; *xylUW*, genes with unknown function; *xylC*, gene encoding BZDH; *xylM*, gene encoding the terminal hydroxylase component of XMO; *xylA*, gene encoding the NADH:acceptor reductase component of XMO; *xylB*, gene encoding BADH; *xylN*, gene for a protein involved in substrate uptake (Kasai, et al., 2001).

Using *Escherichia coli* recombinants, XMO was shown to oxidize not only toluene and xylenes but also *m*- and *p*-ethyl-, methoxy-, nitro-, and chlorosubstituted toluenes, as well as *m*-bromosubstituted toluene to corresponding benzyl alcohol derivatives (Kunz and Chapman, 1981; Wubbolts, et al., 1994b). Styrene is transformed into (*S*)-styrene oxide with an enantiomeric excess of 95% (Wubbolts, et al., 1994b; Panke, et al., 1999b). In addition, XMO was observed to catalyze the second step in the upper pathway, the oxidation of benzyl alcohols to corresponding aldehydes in vivo (Harayama, et al., 1986; Harayama, et al., 1989). Even the conversion of benzaldehyde to benzoate, the third step in the upper pathway, could be observed, but was attributed to *E. coli* enzymes (Harayama, et al., 1989). Further studies performed in vitro with partially purified XylMA showed no activity towards benzyl alcohol (Shaw and Harayama, 1995). The reasons for this discrepancy remain unclear.

To investigate the ability of *E. coli* recombinants expressing *xylMA* to catalyze the multistep oxidation of one methyl group of toluene and xylenes in more detail, we used a recently developed expression system, expressing XMO genes via the *alk* regulatory system of *P. putida* (*oleovorans*) GPo1 (Panke, et al., 1999b). Expression of the first of the two previously

mentioned *alk* gene clusters is under control of *alkBp*, the *alk* promoter, and is initiated in the presence of the functional regulatory protein AlkS, which is encoded on the second *alk* gene cluster, and alkanes or other inducers such as dicyclopropylketone (DCPK) (Grund, et al., 1975; Wubbolts, 1994; Yuste, et al., 1998). In the present study, we show that XMO expressed via the *alk* regulatory system catalyzes the transformation of toluene and pseudocumene to the corresponding alcohols, aldehydes, and acids by consecutive monooxygenation reactions. Furthermore, we investigated the kinetics of these reactions in the absence and presence of BADH and show that the presence of BADH results in back formation of benzyl alcohol from benzaldehyde, thus lowering net aldehyde formation rates. The thermodynamics and the physiological role of the BADH catalyzed reaction and the involvement of a *gem*-diol intermediate in the XMO catalyzed alcohol oxygenation are discussed.

## MATERIALS AND METHODS

**Bacterial strains and plasmids.** Strains and plasmids used are listed in Table 2.1. To test the enzymatic activities of XylMA containing recombinants of *E. coli* JM101, an *E. coli* K-12 derivative, we used pBR322 derived expression vectors equipped with the *alk* regulatory system.

**Media, growth conditions, and materials.** Bacteria were either grown on Luria-Bertani (LB) broth (Difco, Detroit, MI) or on M9 minimal medium (Sambrook, et al., 1989) containing a 3-fold concentration of phosphate salts (M9\*) and 0.5% (wt/vol) glucose as single carbon source. When necessary, cultures were supplemented with kanamycin (final concentration, 50 mg L<sup>-1</sup>), ampicillin (100 mg L<sup>-1</sup>), chloramphenicol (30 mg L<sup>-1</sup>), thiamine (0.001% wt/vol), 1 mM indole, or 0.5 mM isopropyl-β-D-1-thiogalactopyranoside. Solid media contained 1.5% (wt/vol) agar. Liquid cultures were routinely incubated on horizontal shakers at 200 rpm and 30 or 37°C.

Restriction and DNA modification enzymes were obtained from Boehringer Mannheim (Rotkreuz, Switzerland), NEB (Schwalbach, Germany), Gibco (Basel, Switzerland), AGS (Heidelberg, Germany), or Promega (Zurich, Switzerland). The QIAprep Spin Miniprep Kit of Qiagen (Basel, Switzerland) was used to obtain small-scale plasmid DNA preparations

**Table 2.1. Bacterial strains and plasmids.**

Strain or plasmid	Characteristics	Source or reference
<b>Strains</b>		
<i>E. coli</i> DH5 $\alpha$	<i>supE44</i> $\Delta$ <i>lacU169</i> ( $\Phi$ 80 <i>lacZ</i> $\Delta$ M15) <i>hsdR17</i>	(Hanahan, 1983)
<i>E. coli</i> JM101	<i>recA1 endA1 gyrA96 thi-1 relA1</i> <i>supE thi-1</i> $\Delta$ ( <i>lac-proAB</i> ) F' <i>[traD26 proAB<sup>+</sup> lacI<sup>f</sup> lacZ</i> $\Delta$ M15]	(Sambrook, et al., 1989)
<b>Plasmids</b>		
pSPZ3	<i>alkS alkBp xylMA ori</i> pMB1; Km <sup>r</sup>	(Panke, et al., 1999b)
pRMAB	pSPZ3; <i>xylB</i> ; Km <sup>r</sup>	This study
pRS	pSPZ3; $\Delta$ <i>xylMA</i>	This study
pCKO4	<i>lacZ<math>\alpha</math> Pu xylWCMABN</i> ; pSC101 <i>oriV</i> ; Cm <sup>r</sup>	(Panke, et al., 1998a)
pGEM7Zf(+)	ColEI f1 <i>ori lacZ<math>\alpha</math></i> ; Ap <sup>r</sup>	Promega
pGEMAB	pGEM7Zf(+); <i>xylA<sup>*</sup>B</i> ; Ap <sup>r</sup>	This study

*A<sup>\*</sup>*, the plasmid contains only a part of the *xylA* gene.

following the supplier's protocol. Chemicals were obtained from Fluka (Buchs, Switzerland) (toluene, >99.5%; benzyl alcohol, >99%; benzaldehyde, >99%; benzoic acid, >99.5%; pseudocumene, ~99%; 3,4-dimethylbenzoic acid, ~97%), Aldrich (Buchs, Switzerland) (3,4-dimethylbenzyl alcohol, 99%), and Lancaster (Muehlheim, Germany) (3,4-dimethylbenzaldehyde, 97%).

**DNA manipulation and constructs.** Standard techniques were used for restriction analysis, cloning, and agarose gel electrophoresis (Sambrook, et al., 1989). Construction of pSPZ3 (Fig. 2.2), a pBR322 derivative, is described elsewhere (Panke, et al., 1999b). To insert the alcohol dehydrogenase gene *xylB* into the plasmid pSPZ3 directly downstream of the *xylA* gene, the 2.3-kilobase *XhoI/FspI* fragment of pCKO4 (Panke, et al., 1998a) containing *xylB* was first introduced into the *XhoI*- and *SmaI*-digested vector pGEM-7Zf(+) (Promega, Zurich, Switzerland) to yield pGEMAB. From this construct, the 2.3-kilobase fragment was cut out with *XhoI* and *BamHI* and ligated into the *XhoI*- and *BamHI*-digested plasmid pSPZ3. The resulting plasmid was called pRMAB (Fig. 2.2). As a negative control, pRS containing no *xyl* genes was constructed: pRMAB was digested with *BamHI* and *SmaI* and treated with Klenow enzyme. After isolation of the bigger fragment the vector was religated.

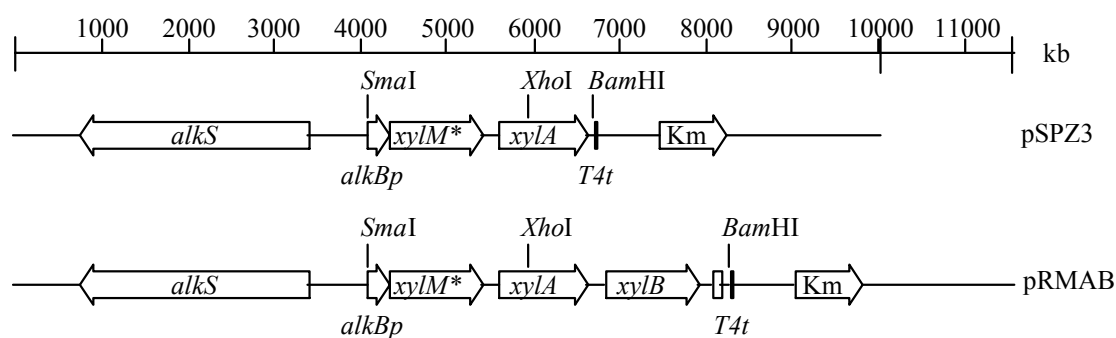


**Figure 2.2. Expression plasmids pSPZ3 and pRMAB; *xylMA* and *xylMAB* under the control of the *alk* regulatory system.** *alkBp*, promoter of the *alk* operon; *alkS*, gene for the positive regulator AlkS. *xylM\** and *xylA*, genes coding for the xylene monooxygenase (\* indicates that in *xylM* a *NdeI* site is removed); *xylB*, gene encoding BADH; Km, kanamycin resistance gene; *T4t*, phage T4 transcriptional terminator.

**Determination of enzyme activities in whole-cell assays.** Whole-cell biotransformations were carried out with *E. coli* JM101 recombinants that were incubated in 40 or 100 ml of medium in the presence of kanamycin. At an optical density at 450 nm ( $OD_{450}$ ) of  $\sim 0.3$ , cells were induced by the addition of 0.05% (vol/vol) DCPK or 0.1% (vol/vol) *n*-octane ( $10^{-5}$ -1% (vol/vol) for induction tests) and the incubation was continued for 3-3.5 h, at which time  $OD_{450}$  had typically increased to 0.8-0.9. The cells were harvested and resuspended to a cell dry weight (CDW) of  $2.5 \text{ g L}^{-1}$  in 50 mM potassium phosphate buffer, pH 7.4, containing 1% (wt/vol) glucose. Aliquots of 1 or 2 ml were distributed in stoppered Pyrex tubes and incubated horizontally on a rotary shaker at 250 rpm and  $30^\circ\text{C}$ . After 5 min, substrate was added to a final concentration of 1.5 mM from a 20-fold stock solution in ethanol. Due to the low solubility of 3,4-dimethylbenzoic acid in  $\text{H}_2\text{O}$ , substrates were added to a final concentration of 0.5 mM and CDW was reduced to  $1 \text{ g L}^{-1}$  when the formation of 3,4-dimethylbenzoic acid was expected. The reaction was carried out for 5 min in the shaker and then stopped by placing the samples in ice and immediately adding 40 or 80  $\mu\text{l}$  of a perchloric acid stock solution (10% vol/vol) to bring the suspension to pH 2.

One unit (U) is defined as the activity that produces 1  $\mu\text{mol}$  of total products in 1 min. Specific activity was expressed as activity per g CDW [ $\text{U (g of CDW)}^{-1}$ ]. Experiments were repeated at least three times independently.

**Product formation as a function of time.** Cells were grown, induced, collected, resuspended, and incubated with substrate as described for the whole-cell activity assays. To follow product formation over time, cell aliquots were incubated with the same substrate for different time periods (5, 10, 20, 30, 40, and 80 min). The reactions were stopped as described for the whole-cell activity assays and analyzed.

**Analysis of metabolites.** For high-performance liquid chromatography (HPLC) analysis, cells were removed by centrifugation ( $7800 \times g$ , 8 min), and the supernatants were analyzed. For the separation of benzyl alcohol, benzaldehyde, and benzoic acid, we used a Nucleosil C18 column (pore size, 100 Å; particle size, 5 µm; inner diameter, 25 cm  $\times$  4 mm) (Macherey-Nagel, Oensingen, Switzerland) with a mobile phase of 69.9% H<sub>2</sub>O, 30% acetonitrile, 0.1% H<sub>3</sub>PO<sub>4</sub> at a flow rate of 0.7 ml min<sup>-1</sup>. For the separation of 3,4-dimethylbenzyl alcohol, 3,4-dimethylbenzaldehyde, and 3,4-dimethylbenzoic acid, we used the same column at the same flow rate with a mobile phase of 64.9% H<sub>2</sub>O, 35% acetonitrile, 0.1% H<sub>3</sub>PO<sub>4</sub>. Detection was done using UV light at 210 nm.

For gas chromatography (GC) and gas chromatography-mass spectrometry (GC-MS) analysis, an equal volume of ice-cold ether containing 0.1 mM dodecane as an internal standard was added to samples. After addition of saturating amounts of sodium chloride, the water phase was extracted by vigorous shaking for 5 min at 30°C, and the phases were separated by centrifugation. The organic phase was dried over anhydrous sodium sulfate and analyzed. Gas chromatography was used to separate toluene/pseudocumene, the respective alcohols, aldehydes, and acids.

GC analysis was done on a gas chromatograph (Fisons Instruments, England) equipped with a fused silica capillary column OPTIMA-5 (25 m; inner diameter, 0.32 mm; film thickness, 0.25 µm) of Macherey-Nagel (Oensingen, Switzerland) with splitless injection and hydrogen as the carrier gas. The following temperature profile was applied: from 40 to 70°C at 15°C/min, from 70 to 105°C at 5°C/min, and from 105 to 240°C at 20°C/min. Compounds were detected with a flame ionization detector.

GC-MS analysis was performed on a Fisons MD 800 mass spectrometer and a gas chromatograph (Fisons Instruments, England) equipped with a CP-Sil 5CB column (Chrompack, the Netherlands) using split injection (20:1) and helium as the carrier gas. The temperature program was the same as described for GC analysis. Substances were identified by comparison of retention times with those of commercially available standards in both HPLC analysis and GC analysis and by GC-MS analysis.



**<sup>18</sup>O incorporation.** *E. coli* JM101 (pSPZ3) was grown, induced, harvested, and resuspended as described for the determination of enzyme activities in whole-cell assays. 1 ml of cell suspension was transferred to a Pyrex tube with a total volume of 8.3 ml, which was then sealed by using a butyl rubber stopper and a screw-on hole cap. Throughout the following steps, the cell suspension was mixed with a magnetic stirrer. The air in the head space of the Pyrex tube was removed to a reduced pressure of 20 mbar and replaced with nitrogen three times. The headspace was once again evacuated and brought to 80% of ambient pressure with nitrogen; following that, the Pyrex tube was filled with pure oxygen enriched with <sup>18</sup>O<sub>2</sub> (85 atom % <sup>18</sup>O). Following the final gas exchange, the cell suspension was incubated horizontally on a rotary shaker at 250 rpm and 30°C for 15 min to equilibrate the reaction medium. After equilibration, substrate was added by injection through the rubber stopper and the suspension was again incubated at 250 rpm and 30°C for different time periods depending on the substrate (toluene, 3 min; benzyl alcohol, 5 min; benzaldehyde, 90 min; pseudocumene, 5 min; 3,4-dimethylbenzyl alcohol, 20 min; 3,4-dimethylbenzaldehyde, 20 min). Incubation time was chosen as to allow a maximal formation of the desired products. Identical experiments were done with air in the headspace. The reactions were stopped by placing the samples on ice and immediately adding 40 µl of a perchloric acid stock solution (10% vol/vol) immediately followed by GC-MS analysis as described above.

## RESULTS

### Growth and induction kinetics of *E. coli* JM101 (pSPZ3).

XMO activities were investigated in *E. coli* JM101 *xylMA* recombinants. The *alk* regulatory system, which can be induced by *n*-octane or DCPK, was chosen to control the expression of the XMO genes, *xylMA*, on the plasmid pSPZ3 (Fig. 2.2).

XMO activity was followed after induction with 0.1% (vol/vol) *n*-octane (Fig. 2.3A) or 0.05% (vol/vol) DCPK (results not shown). XMO activity was quickly induced by both compounds, reaching a constant level of around 115 and 105 U (g of CDW)<sup>-1</sup> for *n*-octane and DCPK, respectively, after 3-3.5 h induction time. The growth rates of the induced cells were clearly reduced when compared to that of noninduced cells.

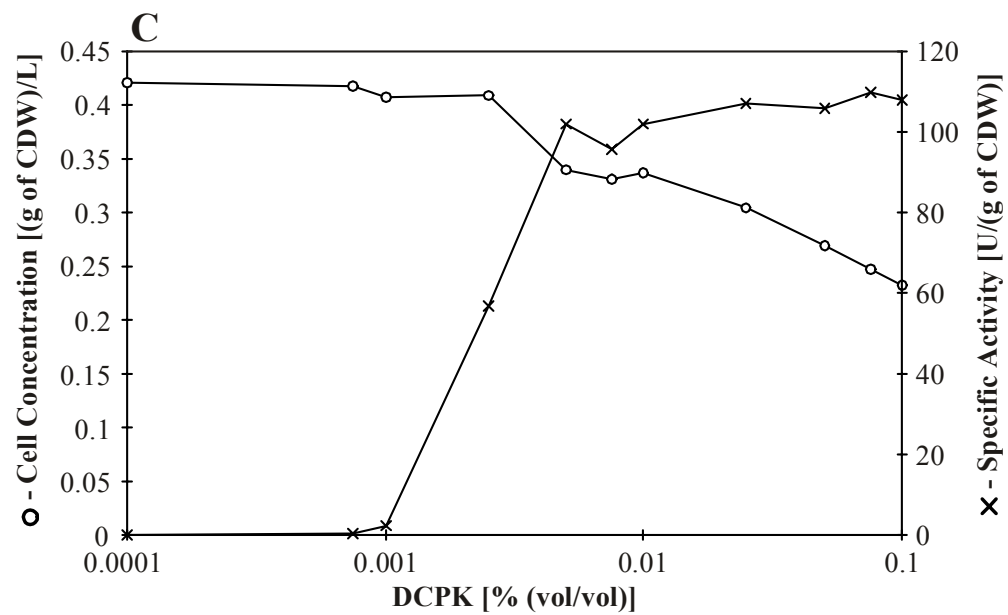
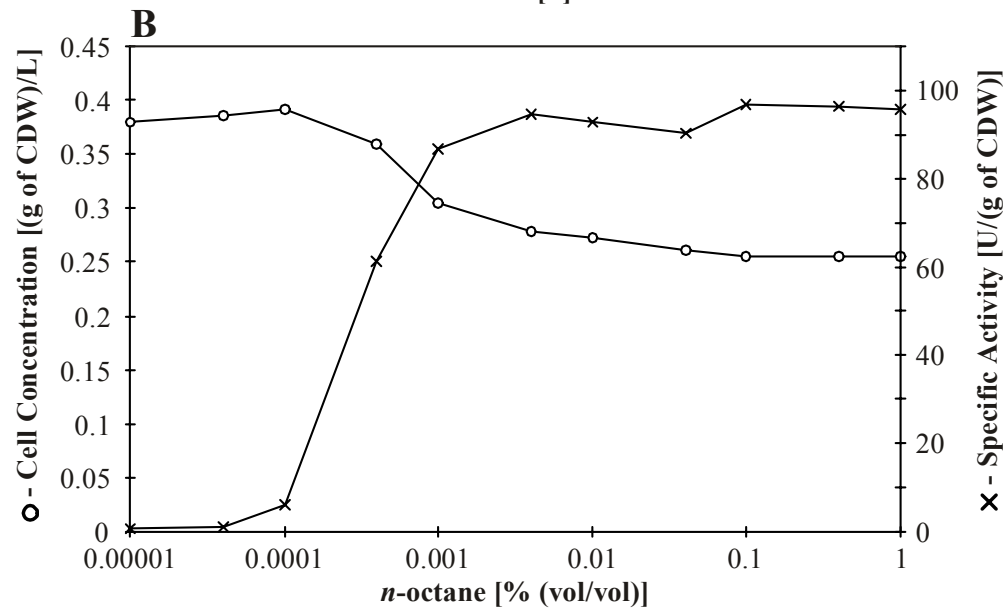
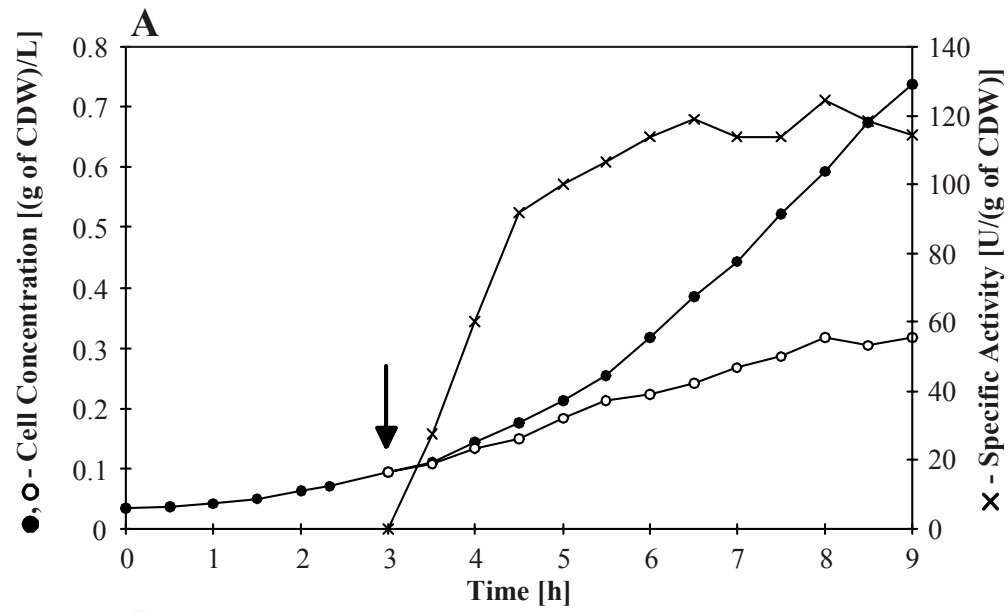


**Figure 2.3. Growth and induction kinetics of XMO in *E. coli* JM101 (pSPZ3).** Panel A shows the XMO activity and the cell concentration at different time intervals after induction by *n*-octane, whereas panels B and C show the same values 3.5 h after induction by different amounts of *n*-octane and DCPK, respectively. For each activity point a single culture was grown. The activity assays were performed as described under “Materials and Methods”. Pseudocumene (1.37 mM) was added to a suspension of resting cells of *E. coli* JM101 (pSPZ3) [2.04-2.44 (g of CDW) L<sup>-1</sup>] in 50 mM potassium phosphate buffer, pH 7.4, containing 1% (wt/vol) glucose. The specific activities are based on product formation during the initial 5 min of reaction. The arrow in panel A indicates when 0.1% (vol/vol) *n*-octane was added to induce XylMA synthesis. Closed circles, cell concentrations in uninduced cultures; open circles, cell concentrations in induced cultures; crosses, specific activities of induced cultures.

The dependence of XMO activity on inducer concentrations was determined by growing *E. coli* JM101 (pSPZ3) to 0.09 (g of CDW) L<sup>-1</sup> and inducing the cells with different amounts of *n*-octane and DCPK. After further growth for 3.5 h, cell concentrations and XMO activities were determined for each inducer concentration (Fig. 2.3, B and C). Very low monooxygenase activities [ $< 6 \text{ U (g of CDW)}^{-1}$ ] were measured when less than 0.0001% (vol/vol) octane or 0.001% (vol/vol) DCPK was added to the culture medium. Maximal induction was observed at DCPK concentrations above 0.005% (vol/vol), whereas for *n*-octane this value was observed at octane volume fractions above 0.001% (vol/vol).

The cell densities decreased in inducer concentration ranges where enzyme activities increased to a maximum. For higher concentrations of *n*-octane, they reached a constant value, whereas higher concentrations of DCPK provoked a further decrease of cell densities (Fig. 2.3, B and C). We therefore checked the direct influence of different inducer concentrations on the growth of *E. coli* JM101 without plasmid. High volume fractions of *n*-octane, up to 1% (vol/vol), had no influence on cell growth. In contrast, concentrations of DCPK above 0.01 % (vol/vol) led to a decreased growth rate. At a DCPK concentration of 0.5% (vol/vol), the cell concentration decreased from 0.09 to 0.073 (g of CDW) L<sup>-1</sup> during the 3.5 h of induction, indicating that high DCPK concentrations are toxic to *E. coli* host strains.

**Oxygenation of toluene and derivatives by xylene monooxygenase (XMO).**

*E. coli* JM101 *xylMA* recombinants were routinely induced by 0.1% (vol/vol) *n*-octane after growth to a cell density of 0.09 (g of CDW) L<sup>-1</sup>. After incubation for another 3-3.5 h and concomitant growth to 0.23-0.27 (g of CDW) L<sup>-1</sup>, product formation rates were determined.

XMO was shown to oxygenate toluene to benzyl alcohol, benzyl alcohol to benzaldehyde, and benzaldehyde to benzoic acid (Table 2.2). For the first two oxygenation reactions, activities as high as 95-100 U (g of CDW)<sup>-1</sup> were observed, whereas the oxygenation of benzaldehyde occurred at a lower rate of 10 U (g of CDW)<sup>-1</sup>. For pseudocumene, the results were similar: Pseudocumene was oxygenated to 3,4-dimethylbenzyl alcohol, 3,4-dimethylbenzyl alcohol to 3,4-dimethylbenzaldehyde, and 3,4-dimethylbenzaldehyde to 3,4-dimethylbenzoic acid. The hydroxylation of pseudocumene was also observed to take place at a rate of 100 U (g of CDW)<sup>-1</sup>, whereas 3,4-dimethylbenzaldehyde was formed more slowly at a rate of 50 U (g of CDW)<sup>-1</sup> and oxygenated to 3,4-dimethylbenzoic acid at a clearly higher rate [55 U (g of CDW)<sup>-1</sup>] than the oxygenation of benzaldehyde to benzoic acid. When the acids were added as substrates, no reaction products and no depletion of acids were detected.

As negative controls, the biotransformations were performed with uninduced *E. coli* JM101 carrying the plasmid pSPZ3 and with induced *E. coli* JM101 without plasmid. As an additional control to exclude any effect of the *alk* regulatory system on *E. coli*, we constructed plasmid pRS, still containing the *alkS* gene but lacking the *xyl* genes. No conversion products were detected in any of these control experiments when toluene, pseudocumene, or the corresponding alcohols were added as substrates (Table 2.2). However, when aldehydes were added as substrates in these experiments, they were reduced to alcohols at a constant rate (Table 2.3). The formation of 3,4-dimethylbenzoic acid could also be shown, but at a very low rate of 2-2.5 U (g of CDW)<sup>-1</sup> (Table 2.3). It can be concluded that at least 95% of acid formed by induced *E. coli* JM101 (pSPZ3) is due to the presence of XMO. No significant differences with respect to products formed and rates of formation between the routinely used inducer, 0.1% (vol/vol) *n*-octane, and the alternatively used 0.05% (vol/vol) DCPK were observed (results not shown).

**Table 2.2. Oxidation of toluene and derivatives by xylene monooxygenase.**

Substrate	Specific activity <sup>a</sup> [U (g of CDW) <sup>-1</sup> ]		
	<i>E. coli</i> JM101 (pSPZ3) induced <sup>b</sup>	<i>E. coli</i> JM101 (pSPZ3) uninduced	<i>E. coli</i> JM101 (pRS) induced <sup>b</sup>
Toluene	100	0	0
Benzyl alcohol	95	0	0
Benzaldehyde	10	SB <sup>c</sup>	SB <sup>c</sup>
Pseudocumene	100	0	0
3,4-Dimethyl- benzyl alcohol	50	0	0
3,4-Dimethyl- benzaldehyde	55	SB <sup>c</sup>	SB <sup>c</sup>

<sup>a</sup> The activity assay was performed as described under “Materials and Methods”. One unit is defined as the activity that produces 1  $\mu$ mol products in 1 min. Specific activity was calculated as an average activity based on the amount of products per g of CDW, formed in the first 5 min of reaction.

<sup>b</sup> Cells were induced by the addition of 0.1% (vol/vol) *n*-octane.

<sup>c</sup> SB, see below (Table 2.3).

**Table 2.3. Transformations of aldehydes in control experiments.**

Product formed	Specific activity <sup>a</sup> [U (g of CDW) <sup>-1</sup> ]			
	Benzaldehyde as substrate		3,4-Dimethylbenzaldehyde as substrate	
	<i>E. coli</i> JM101 (pSPZ3) uninduced	<i>E. coli</i> JM101 (pRS) induced <sup>b</sup>	<i>E. coli</i> JM101 (pSPZ3) uninduced	<i>E. coli</i> JM101 (pRS) induced <sup>b</sup>
Alcohol	19	15	9.4	8.3
Acid	0.5	0	2.2	2.4

<sup>a</sup> see footnote *a* in Table 2.2.

<sup>b</sup> see footnote *b* in Table 2.2.

### **<sup>18</sup>O incorporation experiments.**

These experiments were done to determine how in the above reactions alcohols, aldehydes, and acids are formed from toluene, pseudocumene, and possibly also other substituted toluenes. One possibility is the consecutive incorporation of single atoms from dioxygen into a methyl substituent of the aromatic ring via a monooxygenase reaction. A second possibility is that aldehydes and acids are formed from benzyl alcohol and 3,4-dimethylbenzyl alcohol via oxidation reactions catalyzed by dehydrogenases.

Toluene, pseudocumene, and the corresponding alcohols and aldehydes were incubated with whole cells of *E. coli* JM101 (pSPZ3) with normal air or an <sup>18</sup>O<sub>2</sub>-enriched atmosphere (85 atom % <sup>18</sup>O) as described under "Materials and Methods". Following incubation, reaction mixtures were extracted with diethyl ether and analyzed by gas chromatography-mass spectrometry. Products showing mass spectra characteristic of benzyl alcohol, benzaldehyde, benzoic acid, 3,4-dimethylbenzyl alcohol, 3,4-dimethylbenzaldehyde, and 3,4-dimethylbenzoic acid have been detected. Panels A and B of Figure 2.4 show the mass spectra of 3,4-dimethylbenzyl alcohol formed from pseudocumene after incubation with air (A) and with an <sup>18</sup>O<sub>2</sub>-enriched atmosphere (B). The fragmentation patterns of the two spectra clearly show that one atom of dioxygen was incorporated into 3,4-dimethylbenzyl alcohol during the course of the reaction. The ratio of the M<sup>+</sup> + 2 to M<sup>+</sup> molecular ion peaks (Fig 2.4B) is 85:15 for both the *m/z* 136 (3,4-dimethylbenzyl alcohol) and the *m/z* 121 (methyl-benzyl alcohol species) peaks.

We observed a rapid exchange of oxygen during incubation of benzaldehyde and 3,4-dimethylbenzaldehyde with H<sub>2</sub><sup>18</sup>O (60 atom % <sup>18</sup>O), the exchange being faster for benzaldehyde than for 3,4-dimethylbenzaldehyde. After 5 and 20 min of incubation, 40 and 50%, respectively, of the oxygen in benzaldehyde was <sup>18</sup>O. For 3,4-dimethylbenzaldehyde, these values amounted to 11 and 25%. This rapid oxygen exchange in aldehydes precluded a quantitative measurement of <sup>18</sup>O incorporation into the aldehydes during the oxidation of toluene, pseudocumene, and the corresponding alcohols by XMO.

Nevertheless, the mass spectra of 3,4-dimethylbenzaldehyde formed from 3,4-dimethylbenzyl alcohol (Fig. 2.4, C and D) showed a minor enrichment of <sup>18</sup>O in the aldehyde (2.1%) for the reaction under an <sup>18</sup>O<sub>2</sub>-enriched atmosphere (D). Assuming a monooxygenase reaction for the oxidation of the alcohols with the formation of a diol followed by spontaneous unspecific dehydration, 42.5% M<sup>+</sup> + 2 ion enrichment would be expected in the absence of oxygen exchange with solvent water. When pseudocumene was added as substrate, after two oxygenation steps only 5% enrichment of the M<sup>+</sup> + 2 ion was observed for 3,4-

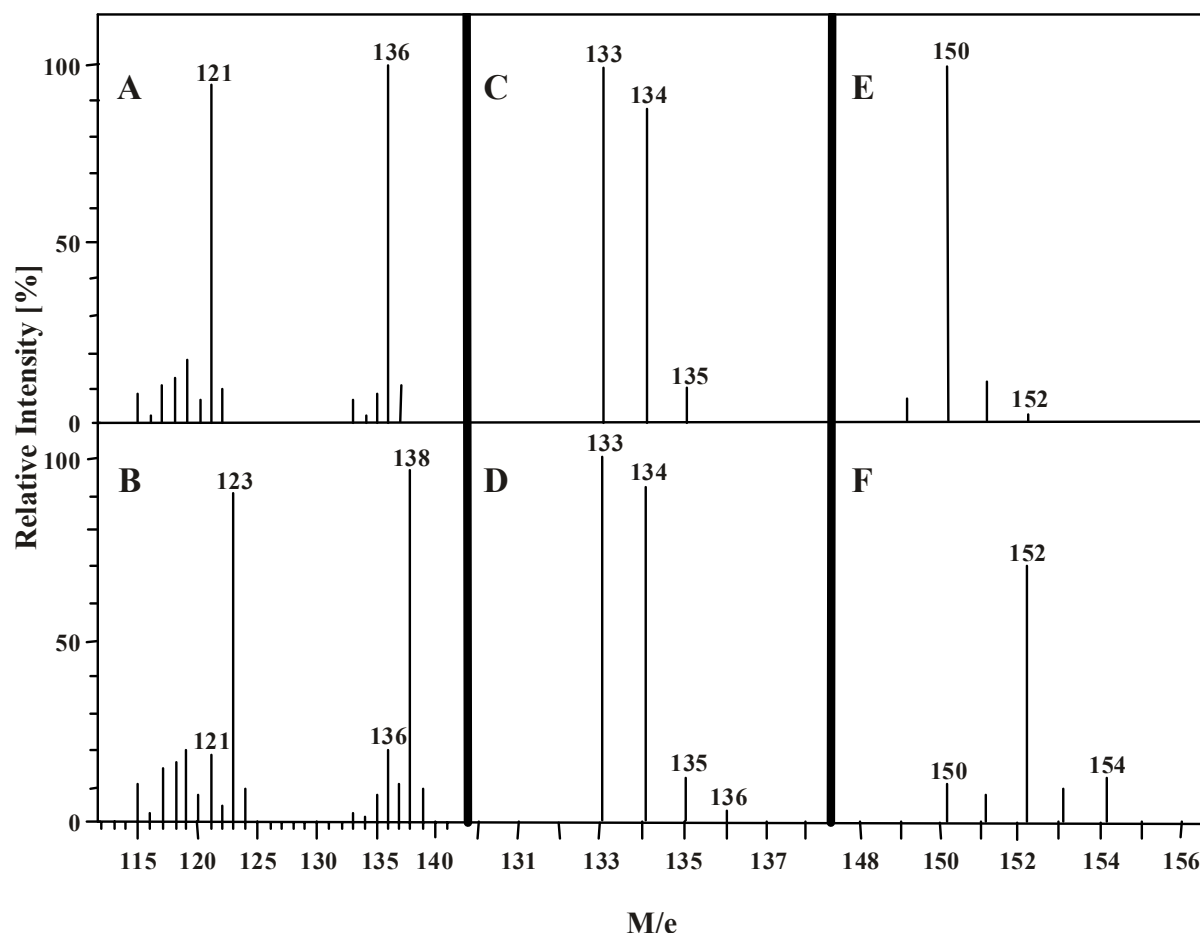


**Figure 2.4. Mass spectra of products formed by *E. coli* JM101 (pSPZ3) in air (A, C, and E) and in an  $^{18}\text{O}_2$ -enriched atmosphere (B, D and F).** Panels A and B show the mass spectrometry analysis of 3,4-dimethylbenzyl alcohol produced from pseudocumene, panels C and D the analysis of 3,4-dimethylbenzaldehyde produced from 3,4-dimethylbenzyl alcohol, and panels E and F the analysis of 3,4-dimethylbenzoic acid produced also from 3,4-dimethylbenzyl alcohol.

dimethylbenzaldehyde (expected: 72%) (results not shown). This low level of  $^{18}\text{O}$  enrichment in the aldehyde can again be explained by the rapid exchange of oxygen in aldehydes.

When 3,4-dimethylbenzaldehyde was added as substrate in an  $^{18}\text{O}_2$ -enriched atmosphere, the molecular ion value of the emerging acid increased by 2 atomic mass units over the value obtained in air (results not shown). In this case, the ratio between  $M^+ + 2$  and  $M^+$  was 85:15, indicating that the XMO catalyzed formation of the acid from the aldehyde requires the introduction of one oxygen atom from molecular oxygen. When two such monooxygenation steps are involved in the XMO catalyzed formation of 3,4-dimethylbenzoic acid from 3,4-dimethylbenzyl alcohol, the incorporation of two  $^{18}\text{O}$  atoms into the acid is expected in an

$^{18}\text{O}_2$ -enriched atmosphere. Ignoring the rapid exchange of oxygen in aldehydes, this would result in a ratio of 8.6:55.3:36.1 between the three molecular ion values 150, 152, and 154 of the formed acid. We indeed observed the incorporation of two  $^{18}\text{O}$  atoms into the acid in an  $^{18}\text{O}_2$ -enriched atmosphere (Fig. 2.4, E and F). The ratio of the three normalized molecular ion values 150, 152, and 154 was 10:80:10 (F).

For toluene and its derivatives as substrates and products analogous results were obtained. Again, formation of benzyl alcohol from toluene and of benzoic acid from benzaldehyde in an  $^{18}\text{O}_2$ -enriched atmosphere resulted in an increase of the molecular ion value by 2 atomic mass units. Because of the already mentioned fact that the oxygen exchange in benzaldehyde is faster than in 3,4-dimethylbenzaldehyde, the intensity of the observed  $\text{M}^+ + 2$  ion of benzaldehyde formed from toluene under  $^{18}\text{O}_2$ -enriched atmosphere was lower (3.4%) than for 3,4-dimethylbenzaldehyde formed from pseudocumene. For benzaldehyde formed from benzyl alcohol, the  $\text{M}^+ + 2$  ion was completely absent (results not shown).

### **Kinetics of oxygenation reactions in *E. coli* JM101 (pSPZ3).**

To follow product formation over time, cells were incubated with the same substrate for different time periods. When toluene or pseudocumene were added as substrates, the consecutive accumulation of the corresponding alcohols, aldehydes, and acids was observed (Figs. 2.5A and 2.6A). As also found in the activity assays, benzyl alcohol, 3,4-dimethylbenzyl alcohol, and benzaldehyde were formed at high rates, 3,4-dimethylbenzaldehyde and 3,4-dimethylbenzoic acid were formed at intermediate rates, and benzoic acid accumulated slowly. In the first 5 min, products were formed from either pseudocumene or toluene with a specific activity of  $100 \text{ U (g of CDW)}^{-1}$  (Table 2.2). Between 5 and 10 min, benzaldehyde was formed at a rate of  $80 \text{ U (g of CDW)}^{-1}$ , whereas 3,4-dimethylbenzaldehyde was formed more slowly [ $37 \text{ U (g of CDW)}^{-1}$ ]. Acid formation started when toluene or pseudocumene had completely disappeared, at rates of 3.2 and  $21 \text{ U (g of CDW)}^{-1}$  for benzoic acid and 3,4-dimethylbenzoic acid, respectively, between 10 and 30 min. A low level of benzyl alcohol always remained. Between 40 and 80 min, the level of benzyl alcohol started to increase again, whereas the benzaldehyde level decreased (Fig. 2.5A). Pseudocumene, 3,4-dimethylbenzyl alcohol, and 3,4-dimethylbenzaldehyde were completely used up to form 3,4-dimethylbenzoic acid (Fig. 2.6A).



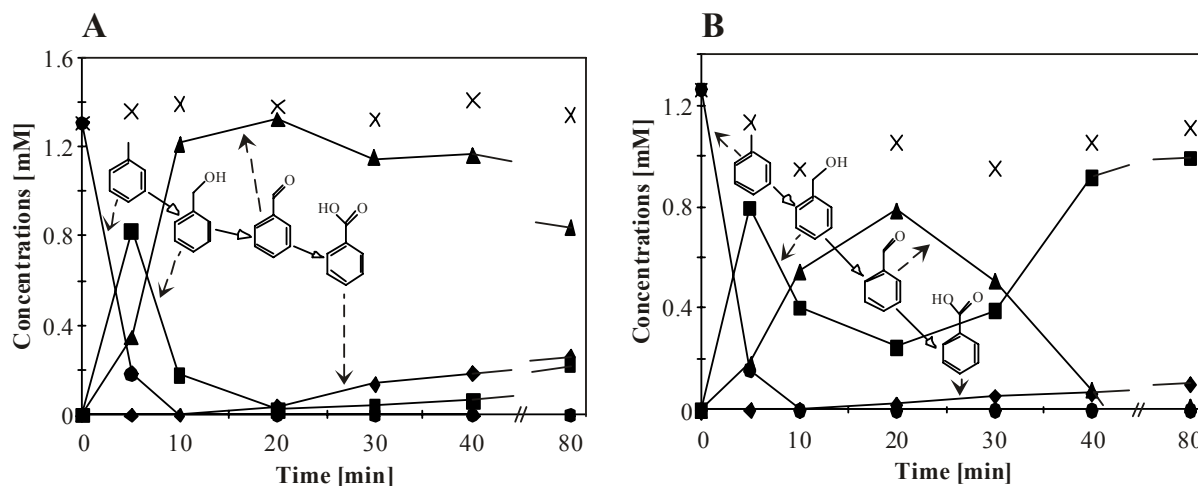


**Figure 2.5.** Oxidation of toluene by *E. coli* JM101 (pSPZ3) (A) and *E. coli* JM101 (pRMAB) (B). The assay was performed as described under “Materials and Methods”. Toluene (1.37 mM) was added to a suspension of resting *E. coli* JM101 (pSPZ3/pBRMAB) [2.07-2.14 (g of CDW) L<sup>-1</sup>] in 50 mM potassium phosphate buffer, pH 7.4, containing 1% (wt/vol) glucose. Circles, toluene; squares, benzyl alcohol; triangles, benzaldehyde; diamonds, benzoic acid; crosses, sum of the four concentrations.

When 3,4-dimethylbenzyl alcohol was added as the substrate, 3,4-dimethylbenzaldehyde was formed at a rate of 50 U (g of CDW)<sup>-1</sup> (Table 2.2), whereas 3,4-dimethylbenzoic acid was formed at a rate of 23 U (g of CDW)<sup>-1</sup> between 10 and 30 min (Fig. 2.6C). With benzyl alcohol as a substrate, the benzaldehyde formation rate amounted to 95 U (g of CDW)<sup>-1</sup> and benzoic acid formed at a constant rate of 2.9 U (g of CDW)<sup>-1</sup> (results not shown). In contrast to benzyl alcohol, 3,4-dimethylbenzyl alcohol was completely converted to the acid in this same time period.

3,4-Dimethylbenzoic acid was formed at a rate of 55 U (g of CDW)<sup>-1</sup> (Table 2.2) when 3,4-dimethylbenzaldehyde was added as substrate (Fig. 2.6E), and after 20 min already was the predominant species. Slow and constant formation of benzoic acid [3 U (g of CDW)<sup>-1</sup>] was observed when benzaldehyde was added as substrate (results not shown). Here, the initial rate in the first 5 min was 10 U (g of CDW)<sup>-1</sup> (Table 2.2).

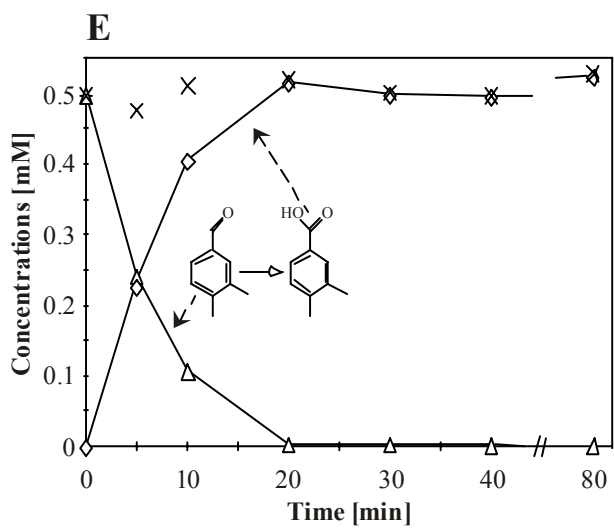
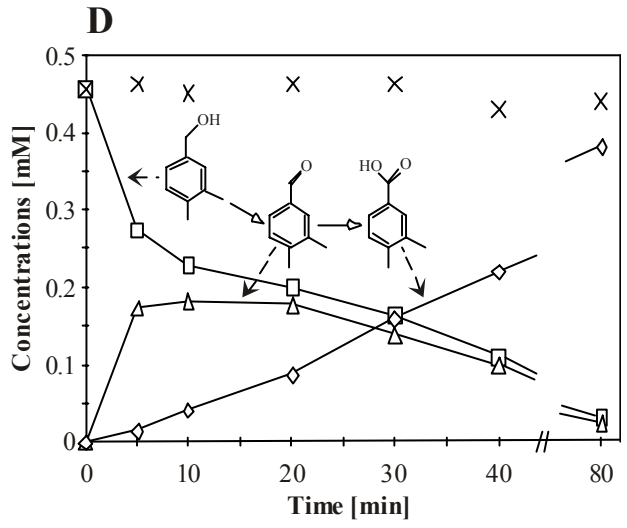
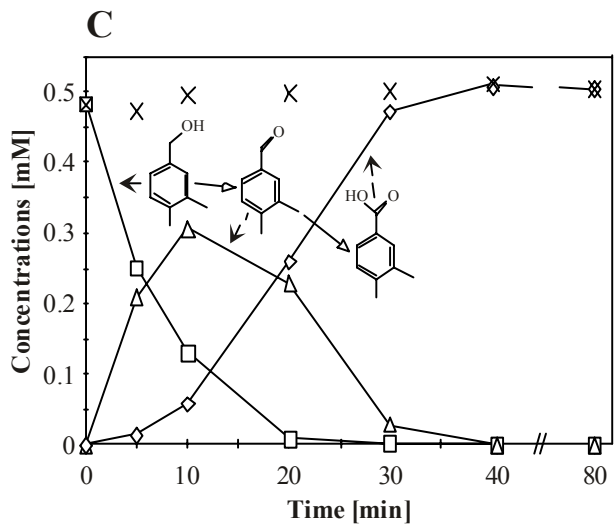
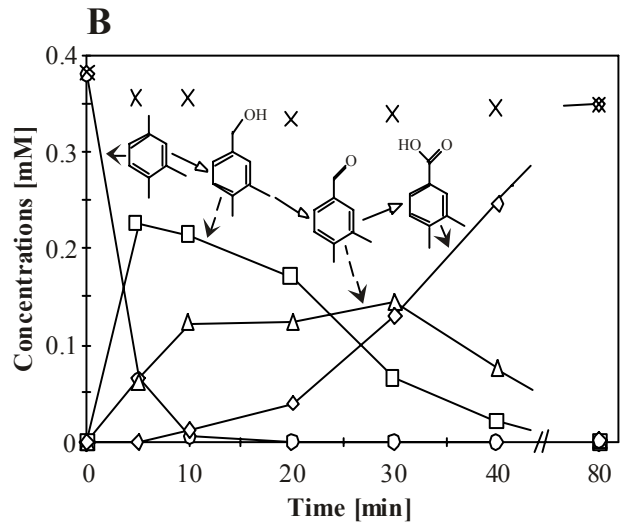
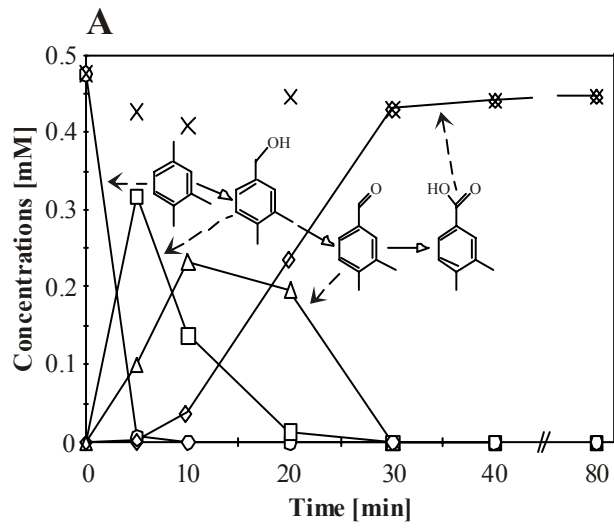


**Figure 2.6. Oxidation of pseudocumene, the corresponding alcohol and the corresponding aldehyde by *E. coli* JM101 (pSPZ3) (A, C, and E) and *E. coli* JM101 (pRMAB) (B and D).** The assay was performed as described in “Materials and Methods”. Substrates (0.46 mM) were added to a suspension of resting *E. coli* JM101 (pSPZ3/pBRMAB) [0.86-0.92 (g of CDW) L<sup>-1</sup>] in 50 mM potassium phosphate buffer, pH 7.4, containing 1% (wt/vol) glucose. A and B show the oxidation of pseudocumene, C and D show the oxidation of 3,4-dimethylbenzyl alcohol, and E shows the oxidation of 3,4-dimethylbenzaldehyde. Circles, pseudocumene; squares, 3,4-dimethylbenzyl alcohol; triangles, 3,4-dimethylbenzaldehyde; diamonds, 3,4-dimethylbenzoic acid; crosses, sum of the four concentrations.

### Conversions of toluene and pseudocumene by *E. coli* JM101 (pRMAB).

We tested whether the presence of BADH together with XMO increased or decreased the rate of aldehyde formation from toluene and pseudocumene. The latter is a distinct possibility because several other alcohol dehydrogenases catalyze reactions with an equilibrium on the side of the alcohol at physiological pH. Consequently, BADH might decrease the net rate of aldehyde formation. On the other hand, a two-step oxidation of toluene (pseudocumene) via benzyl alcohol (3,4-dimethylbenzyl alcohol) to benzaldehyde (3,4-dimethylbenzaldehyde) catalyzed by XMO in concert with BADH might result in increased formation rates of the aldehydes since reduced nicotinamide cofactors oxidized by XMO would be regenerated by BADH. To clarify these questions, we cloned the BADH gene *xylB* into pSPZ3 directly downstream of the *xylA* gene. The resulting plasmid was called pRMAB (Fig. 2.2).

Biotransformations by *E. coli* JM101 carrying plasmid pRMAB were in fact clearly different from those by *E. coli* JM101 (pSPZ3). Toluene was transformed to its corresponding products with an initial specific activity of 87 U (g of CDW)<sup>-1</sup>. The corresponding values for benzyl alcohol, pseudocumene, and 3,4-dimethylbenzyl alcohol were 66, 73 and 42 U (g of CDW)<sup>-1</sup>, respectively. The presence of BADH clearly reduced the level of oxidation products formed by XMO. Here also we followed product formation over 80 min. When toluene was added, we observed consecutive accumulation of benzyl alcohol, benzaldehyde, and benzoic acid (Fig. 2.5B). Between 5 and 10 min, benzaldehyde was formed at a rate of 34 U (g of CDW)<sup>-1</sup> and the acid accumulated at a rate of 1 U (g of CDW)<sup>-1</sup> between 10 and 40 min. After about 20 min, the level of benzyl alcohol started to increase again. After 80 min, almost no benzaldehyde remained and a very low amount of benzoic acid was formed. When benzyl alcohol was added as a substrate, analogous results were obtained (results not shown); the level of the aldehyde decreased after about 20 min, whereas the alcohol was formed. Clearly,

expression of BADH together with XMO caused a considerable reduction of benzaldehyde to benzyl alcohol, indicating that formation of benzaldehyde is not enhanced by additional BADH.

When pseudocumene was added as a substrate, we again observed consecutive accumulation of 3,4-dimethylbenzyl alcohol, 3,4-dimethylbenzaldehyde, and 3,4-dimethylbenzoic acid (Fig. 2.6B). Between 5 and 10 min, 3,4-dimethylbenzaldehyde was formed at a rate of 15 U (g of CDW)<sup>-1</sup>. The acid accumulated at about the same rate [13 U (g of CDW)<sup>-1</sup>] between 30 and 40 min. After the rapid formation of the alcohol, the aldehyde level remained quite high for 20 min. Nevertheless, at the end of the reaction, alcohol and aldehyde were completely transformed to the acid. 3,4-Dimethylbenzaldehyde and 3,4-dimethylbenzoic acid were formed when 3,4-dimethylbenzyl alcohol was added as substrate (Fig. 2.6D). Between 20 and 30 min, the acid was formed with a specific activity of 8 U (g of CDW)<sup>-1</sup>, and the aldehyde concentration never exceeded the alcohol concentration. The continued presence of 3,4-dimethylbenzyl alcohol indicates that besides the oxygenations there is a simultaneous reduction of aldehyde to alcohol for which BADH seems to be responsible.

## DISCUSSION

### **The *alk* regulatory system as an expression system for XMO.**

*E. coli* recombinants expressing the *xylMA* genes have been used to oxidize styrene to (*S*)-styrene oxide on a 2-L reactor scale (Wubbolts, et al., 1994a; Wubbolts, et al., 1996b). However, activity has been limited, and this is probably due to insufficient expression of the *xyl* genes in *E. coli*. The *alk* regulatory system of *P. putida* (*oleovorans*) GPO1 is not subject to catabolite repression in *E. coli*, and expression of the *alk* genes in glucose grown *E. coli* W3110 via the *alk* regulatory system permits accumulation of the membrane located alkane hydroxylase AlkB up to 10-15% of total cell protein (Nieboer, et al., 1993; Staijen, et al., 1999). The *alk* regulatory system has therefore been used to increase the volumetric activities of *E. coli* recombinants producing (*S*)-styrene oxide, based on a 5-fold increase of the expression of *xylMA* via the *alk* regulatory system, resulting in styrene oxidation activities of up to 91 U (g of CDW)<sup>-1</sup> (Panke, et al., 1999b).

In the present study, we used related constructs and reached specific activities between 100 and 120 U (g of CDW)<sup>-1</sup> for toluene and pseudocumene as substrates. Compared to earlier

studies with *E. coli* expressing *xylMA*, this corresponds to a 10 to 20-fold activity increase (Harayama, et al., 1986; Wubbolts, et al., 1994b). Cells were rapidly induced by both *n*-octane and DCPK, but *n*-octane was a better inducer than DCPK, because with *n*-octane maximal induction is reached at lower concentrations than with DCPK (Fig. 2.3). Induced cells grew more slowly, indicating a stress effect either of the gene products or of the inducers themselves. Growth was reduced most when XMO expression was maximal. This stress effect has been described before (Wubbolts, et al., 1994b; Nieboer, 1996). Additionally, DCPK concentrations in excess inhibit cell growth. For *n*-octane in water this is not the case, most probably because of its very low solubility.

**XMO catalyzes the oxygenation not only of toluene and xylenes but also of the corresponding alcohols and aldehydes.**

The results obtained in the present study show that XMO has aromatic alcohol and aldehyde oxidation activities to form the corresponding acids via monooxygenation reactions. Uninduced *E. coli* JM101 (pSPZ3) and induced *E. coli* JM101 (pRS) as controls did not carry out these biotransformations.

The oxidation of benzyl alcohols by XMO has been reported by Harayama *et al.* (Harayama, et al., 1986; Harayama, et al., 1989), but in a later study including *in vitro* experiments, the authors concluded that XMO is not responsible for such activity (Shaw and Harayama, 1995). Instead, chromosomally encoded dehydrogenases of the *E. coli* host, which transform benzyl alcohol to benzoate, were supposed to be responsible for the transformation of benzyl alcohol to benzoate (Harayama, et al., 1989). However, the incorporation of  $^{18}\text{O}$  into the products, observed in this study and discussed below, provides strong evidence for a monooxygenation type of reaction catalyzed by XMO.

In control experiments, in which aldehydes were incubated with uninduced *E. coli* JM101 (pSPZ3) and induced *E. coli* JM101 (pRS), we observed the reduction of aldehydes to alcohols. These transformations, rather than the oxidation of alcohols, can be explained by the action of *E. coli* alcohol dehydrogenases that catalyze an equilibrium lying, for thermodynamic reasons, on the side of the alcohols. The net formation of benzyl alcohol in the end of the biotransformation of toluene by *E. coli* JM101 (pSPZ3) (Fig. 2.5A) can also be attributed to *E. coli* dehydrogenases, and this activity becomes significant because XMO loses activity with time.

Two significant differences were observed between the consecutive oxygenation of toluene and pseudocumene. 3,4-Dimethylbenzyl alcohol is oxygenated more slowly than benzyl

alcohol and 3,4-dimethylbenzoic acid is formed at a clearly higher rate than benzoic acid. This indicates that there are differences in the effect of varying substitutions on the specific activities of XMO towards oxidized substrates (alcohols and aldehydes) compared to that towards unoxidized substrates like toluene and pseudocumene, which are hydroxylated at a very similar rate.

Another interesting finding is that the acids were not formed until toluene or pseudocumene had disappeared more or less completely. This points to a higher affinity of XMO for toluene and pseudocumene than for the corresponding aldehydes.

### **The presence of BADH results in the back formation of benzyl alcohol from benzaldehyde.**

In cells containing BADH, the aldehydes accumulate at a clearly lower rate. BADH seems to drastically increase the effect of the *E. coli* dehydrogenases; the equilibrium of this dehydrogenase reaction seems to lie on the side of the alcohol. In fact, the Gibbs energy change of the dehydrogenation of benzyl alcohol, calculated according to the group contribution method of Mavrovouniotis (Mavrovouniotis, 1990; 1991), is 5 kcal/mol or, calculated according to the Gibbs energies of formation given by Dean (Dean and Lange, 1985), 4 kcal/mol. (The Gibbs energy change of the oxygenation of benzyl alcohol amounts to -100 kcal/mol.) On the basis of these values, an equilibrium constant between benzyl alcohol and benzaldehyde of around  $10^{-3}$  can be assumed. The estimated ratio between the equilibrium concentrations of benzaldehyde and benzyl alcohol including an NAD/NADH ratio of 10.6 in *E. coli* under aerobic conditions and glucose excess (Leonardo, et al., 1996) amounts to 1:100. In addition, BADH was reported to have lower  $K_m$  and higher  $V_{max}$  values for the reverse reaction (from aldehydes to alcohols) compared with the forward reaction, whereas the optimal pH, at which the measurements were performed, was 9.4 for the forward and 5.7 for the reverse reaction (Shaw and Harayama, 1990; Shaw, et al., 1992; Shaw, et al., 1993). For benzyl alcohol and benzaldehyde, Shaw et al. (Shaw, et al., 1993) found  $K_m$  values of 155 and 65  $\mu\text{M}$  and  $V_{max}$  values of 320 and 4800  $\mu\text{mol min}^{-1} \text{mg}^{-1}$  for the forward and the reverse reaction, respectively, in 100 mM glycine.

After only 20 min, there was net formation of benzyl alcohol by *E. coli* JM101 (pRMAB). This was not observed for *E. coli* JM101 (pSPZ3) as the biocatalyst (Fig. 2.5B).

Here, the following question arises: what could be the physiological roles of BADH and BZDH in the natural host *P. putida* (pWW0), when XMO alone is able to catalyze all reactions from the unoxidized substrates to the carboxylic acids? Concerning BZDH, the

answer seems to be evident: In the absence of BZDH and in the presence of unoxidized substrate (e.g. toluene and pseudocumene), the corresponding aldehydes would not be oxidized because of their low affinity to XMO. In addition, for benzaldehyde, the oxygenation rate is quite low, which could also be the case for other aromatic aldehydes. Thus, BZDH may be necessary for the efficient formation of acids in its native host. When the fluxes from the alcohols to the acids and through the *meta* cleavage pathway are high, which again requires highly active BZDH, the concentrations of intermediates like benzaldehyde would be very low, and BADH could also catalyze a part or even most of the aldehyde formation. The dehydrogenation of alcohols and aldehydes is favorable for the host because reducing equivalents are produced rather than consumed, as is the case for the first oxygenation step. In addition, accumulation of these toxic intermediates in the cytosol is prevented. In the case of high concentrations of these intermediates, BADH could, by aldehyde reduction, preserve low concentrations of the particularly reactive aldehydes.

**The most probable mechanism for alcohol oxidation includes the formation of a *gem*-diol as an intermediate.**

The quantitative  $^{18}\text{O}$  incorporation into aromatic alcohols and acids characterized the formation of these compounds as monooxygenation reactions. Alcohol oxidation to carbonyl products is usually mediated by pyridine nucleotide-dependent dehydrogenases like BADH. However, XMO catalyzes the NADH-dioxygen-dependent oxidation of benzyl alcohol and 3,4-dimethylbenzyl alcohol to the corresponding aldehydes (Table 2.2). Similar reactions are also catalyzed by the alkane hydroxylase of *P. putida* (*oleovorans*) GPO1, which was reported to catalyze the oxygenative formation of medium chain length alkanals from terminal alkanols (May and Katopodis, 1986), and by ammonia-grown cells of *Nitrosomonas europaea*, which also oxidizes toluene through benzyl alcohol to benzaldehyde (Keener and Arp, 1994). Rabbit liver P-450 (forms 2B4 and 2E1) (Vaz and Coon, 1994) and purified naphthalene dioxygenase from *Pseudomonas* sp. strain NCIB 9816-4 (Lee and Gibson, 1996) were reported to oxidize benzyl alcohol and 1-phenylethyl alcohol. Because of the rapid exchange of oxygen in aldehydes, both studies concentrated on the 1-phenylethyl alcohol oxidation to evaluate possible mechanisms. Vaz and Coon suggested that the mentioned forms of P-450 oxidize the alcohol to a carbon radical followed by coupling of oxygen to form a *gem*-diol intermediate which undergoes nonstereospecific dehydration to yield acetophenone (Vaz and Coon, 1994). Another possible mechanism, not utilized by either of the two P-450 forms, involves desaturation to form an enol intermediate followed by tautomerization to acetophenone.

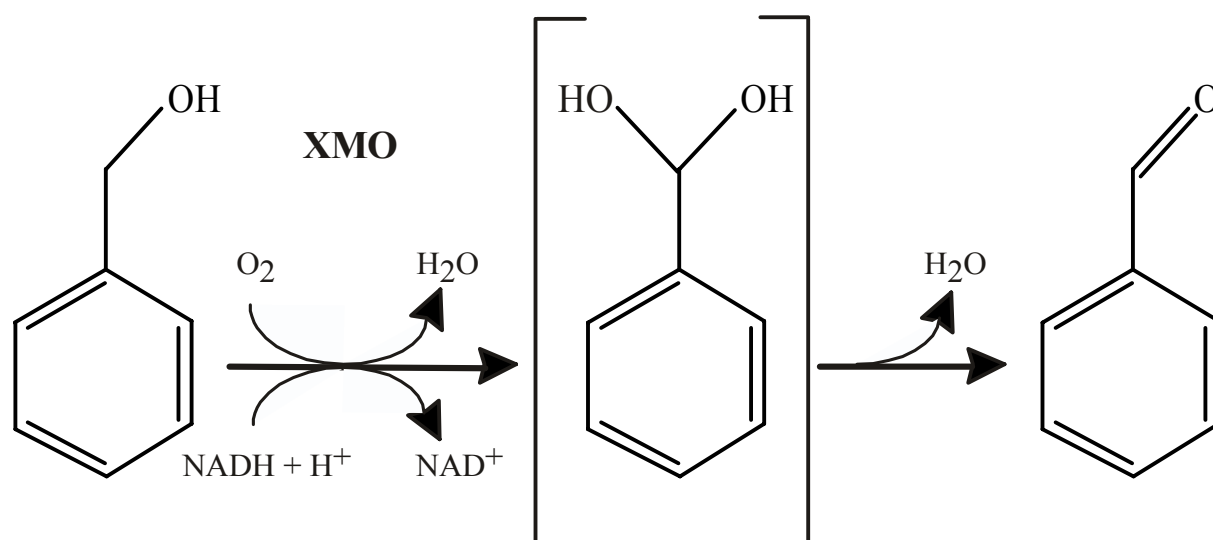


**Figure 2.7. Monoxygenation of benzyl alcohol by XMO; proposed formation of a *gem*-diol.** XMO indicates xylene monoxygenase of *P. putida* mt-2 expressed in *E. coli* JM101 (pSPZ3).

In the case of naphthalene dioxygenase and 1-phenylethyl alcohol, despite the fact that no <sup>18</sup>O from molecular dioxygen was found to be incorporated into acetophenone, Lee and Gibson (Lee and Gibson, 1996) suggested that both mechanisms could contribute to product formation. They argued that stereospecific dehydration of putative *gem*-diol intermediates, which has been proposed for other oxidations (Spain, et al., 1989; Robertson, et al., 1992), could occur with the aid of a basic amino acid residue in the active site of the enzyme. Lee and Gibson as well as Vaz and Coon suggested that the formation of a *gem*-diol intermediate could account for the oxidation of benzyl alcohol to benzaldehyde by naphthalene dioxygenase and the two forms of P-450, respectively. In the case of XMO, the signals for the M<sup>+</sup> + 2 ion in the mass spectrum of 3,4-dimethylbenzaldehyde (2.1%) (Fig. 2.4D) and for the M<sup>+</sup> + 4 ion in the mass spectrum of 3,4-dimethylbenzoic acid (10%) (Fig. 2.4F), formed from the corresponding alcohol, indicate the monoxygenation of the alcohol and as a result the formation of a *gem*-diol intermediate followed by nonstereospecific dehydration yielding the aldehyde (Fig. 2.7). After 20 min of incubation of 3,4-dimethylbenzaldehyde in water containing 60% H<sub>2</sub><sup>18</sup>O under conditions similar to those of the enzymatic reaction, but with 3,4-dimethylbenzyl alcohol, potassium phosphate, glucose, and the cells omitted, only 25% of the oxygen was exchanged. Therefore, it can not be completely excluded that stereospecific dehydration also contributes to aldehyde formation. The results presented in this study



strongly suggest that the most probable mechanism for alcohol oxidation by XMO includes the formation of a *gem*-diol as an intermediate.

The ability of XMO to catalyze three consecutive oxygenation steps at high rates makes it a very interesting nonheme iron enzyme. The *in vitro* characterization of this enzyme is an approach that, based on the high activity of XMO, will hopefully allow a detailed analysis of this interesting reaction.

## **ACKNOWLEDGMENTS**

We thank Sven Panke for providing plasmids and for helpful discussions and Hans Peter E. Kohler for the gift of  $^{18}\text{O}_2$ .



## CHAPTER 3

# **CHARACTERIZATION AND APPLICATION OF XYLENE MONOOXYGENASE FOR MULTISTEP BIOCATALYSIS**

**Bruno Bühler, Bernard Witholt, Bernhard Hauer, and Andreas  
Schmid**

Applied and Environmental Microbiology, 2002, 68(2):560-568

## SUMMARY

Xylene monooxygenase of *Pseudomonas putida* mt-2 catalyzes multistep oxidations of one methyl group of toluene and xylenes. Recombinant *E. coli* expressing the monooxygenase genes *xylM* and *xylA* catalyze the oxygenation of toluene, pseudocumene, the corresponding alcohols, and the corresponding aldehydes, all by a monooxygenation type of reaction (see Chapter 2). Using *E. coli* expressing *xylMA* we investigated the kinetics of this one-enzyme three-step biotransformation. We found that unoxidized substrates like toluene and pseudocumene inhibit the second and the third oxygenation steps and that the corresponding alcohols inhibit the third oxygenation step. These inhibitions might promote the energetically more favorable alcohol and aldehyde dehydrogenations in the wildtype. Growth of *E. coli* was strongly affected by low concentrations of pseudocumene and its products. Toxicity and solubility problems were overcome by the use of a two-liquid phase system with bis(2-ethylhexyl)phthalate as carrier solvent, allowing high overall substrate and product concentrations. In a fed-batch based two-liquid phase process with pseudocumene as substrate, we observed the consecutive accumulation of aldehyde, acid, and alcohol. Our results indicate that, depending on the reaction conditions, the product formation could be directed to one specific product.

## INTRODUCTION

During the last decades, the microbial degradation pathways of aromatic and aliphatic hydrocarbons have received a lot of scientific interest because of the high potential of the involved enzyme systems for environmental (Shannon and Unterman, 1993) and preparative applications (Witholt, et al., 1990; Schmid, et al., 2001). These pathways are usually initiated by an oxygenase-catalyzed chemo-, regio-, and stereoselective hydroxylation of the hydrocarbons, a reaction for which often no organic chemical counterpart is known (Harayama, et al., 1992; Faber, 2000).

The xylene degradation pathway of *Pseudomonas putida* mt-2 and its initiating oxygenase, the xylene monooxygenase (XMO), are among the best-studied examples for aromatic hydrocarbon degradation (Williams and Murray, 1974; Worsey and Williams, 1975; Burlage, et al., 1989; Ramos, et al., 1997). The enzymes for xylene degradation are encoded on a catabolic plasmid, the TOL plasmid pWW0. XMO is the first enzyme in the upper degradation pathway for toluene and xylenes, in which a carboxylic acid is formed (Abril, et al., 1989; Harayama, et al., 1989; Williams, et al., 1997). The upper pathway also involves benzyl alcohol dehydrogenase and benzaldehyde dehydrogenase, which catalyze the oxidation of benzyl alcohols via benzaldehydes to benzoic acids (Shaw and Harayama, 1990; Shaw, et al., 1992; Shaw, et al., 1993). The carboxylic acid is then transformed to substrates of the Krebs cycle through the *meta* cleavage pathway (Franklin, et al., 1981; Harayama, et al., 1984; van der Meer, et al., 1992; Ramos, et al., 1997).

XMO consists of two polypeptide subunits, encoded by *xyIM* and *xyIA* (Harayama, et al., 1989; Suzuki, et al., 1991). XylA, the NADH:acceptor reductase component is an electron transport protein transferring reducing equivalents from NADH to XylM (Shaw and Harayama, 1992). XylM, the hydroxylase component, is located in the membrane, and its activity depends on phospholipids and ferrous ion with a pH optimum of 7 (Wubbolts, 1994; Shaw and Harayama, 1995).

The substrate spectrum of XMO was investigated, with focus on preparative applications: XMO expressed in *E. coli* oxidizes toluene and xylenes but also *m*- and *p*-ethyl-, methoxy-, nitro-, and chlorosubstituted toluenes, as well as *m*-bromosubstituted toluene to corresponding benzyl alcohol derivatives (Kunz and Chapman, 1981; Wubbolts, et al., 1994b). Furthermore, styrene is transformed into (*S*)-styrene oxide with an enantiomeric excess (ee) of 95% (Wubbolts, et al., 1994a; Wubbolts, et al., 1994b). The one-step oxygenation of styrene

catalyzed by recombinant XMO in growing cells of *E. coli* was applied to produce (*S*)-styrene oxide on a 2-liter scale with hexadecane as second organic phase (Panke, et al., 1999b).

The wild-type strain *P. putida* mt-2 was used to oxidize methyl groups on aromatic heterocycles to the corresponding carboxylic acids (Kiener, 1992). In large-scale fermentations, a 5-methyl-2-pyrazinecarboxylic acid titer up to 20 g L<sup>-1</sup> was reached. This system exploits the inability of the wild-type strain to further degrade heteroaromatic carboxylic acids. In *P. putida* mt-2, all three enzyme activities of the upper xylene degradation pathway are responsible for the three-step oxidation. Early reports suggested that XMO also catalyzes alcohol and aldehyde oxidations (Harayama, et al., 1986; Harayama, et al., 1989). Later, such activities were attributed to dehydrogenases present in the *E. coli* host (Harayama, et al., 1989; Shaw and Harayama, 1995). Recently, we verified by *in vivo* experiments that XMO indeed catalyzes the oxidation of benzyl alcohols and benzaldehydes, both via a monooxygenation type of reaction (Chapter 2). *E. coli* cells expressing XMO genes under the control of the *alk* regulatory system (Grund, et al., 1975; Wubbolts, 1994; Yuste, et al., 1998; Staijen, et al., 1999) were used for these experiments.

Potential preparative *in vivo* applications of XMO are hampered by low water solubilities and high toxicities of possible substrates and products, limiting the performance of aqueous systems. Nonconventional reaction media such as an aqueous-organic two-liquid phase system are promising alternatives (Schwartz and McCoy, 1977; de Smet, et al., 1981b). A second immiscible phase can act as a reservoir for substrate and products, regulating the concentration of such compounds in the biocatalyst microenvironment, minimizing toxicity, and simplifying product recovery (Witholt, et al., 1992; Wubbolts, et al., 1996a; Leon, et al., 1998).

In the present study, we characterized the multistep oxidation of substrates like pseudocumene and toluene by whole cells of *E. coli* containing XMO with the aims of clarifying the natural role of such a multistep catalysis and identifying possible applications. The biotechnological conversion of pseudocumene is of special interest because a controlled regio- and chemospecific multistep oxidation of only one methyl group is difficult to achieve by purely chemical methods. We determined the kinetics of the one-enzyme multistep reaction and analyzed the whole-cell biocatalyst in a two-liquid phase biotransformation on a 2-liter scale. Our results indicate that, depending on the reaction conditions, product formation may be directed to one specific product, either benzylic alcohols, aldehydes, or acids.

## MATERIALS AND METHODS

**Bacterial strain and plasmid.** *E. coli* JM101 (*supE thi Δ(lac-proAB)* F'[*traD36 proAB<sup>+</sup> lacI<sup>f</sup> lacZΔM15*]) (Messing, 1979), an *E. coli* K-12 derivative, was used as recombinant host strain. As expression vector, we used the pBR322-derived plasmid pSPZ3 containing the XMO genes *xylM* and *xylA* under the control of the *alk* regulatory system (Panke, et al., 1999b). The QIAprep Spin Miniprep Kit (Qiagen, Basel, Switzerland) was used to prepare plasmid DNA following the supplier's protocol.

**Media and growth conditions.** Bacteria were either grown in Luria-Bertani (LB) broth (Difco, Detroit, MI) or in M9\* minimal medium, which was identical to M9 mineral medium (Sambrook, et al., 1989) except that it contained a threefold-higher concentration of phosphate salts to increase the buffer capacity and did not contain calcium chloride. Glucose was added to the M9\* mineral medium at a concentration of 0.5% (wt/vol) as single carbon source or to complex media at a concentration of 1% (wt/vol) for catabolite repression of tryptophanase synthesis in *E. coli*. Tryptophanase is involved in the formation of indole on complex media; indole can subsequently be converted to indigo by XMO (Mermod, et al., 1986; Mc Fall and Newman, 1996). When necessary, cultures were supplemented with kanamycin (final concentration, 50 mg L<sup>-1</sup>), thiamine (10 mg L<sup>-1</sup>), and 1 ml L<sup>-1</sup> of trace element solution US\*, which contained 1 M hydrochloric acid and (per liter) 4.87 g of FeSO<sub>4</sub>·7H<sub>2</sub>O, 4.12 g of CaCl<sub>2</sub>·2H<sub>2</sub>O, 1.50 g of MnCl<sub>2</sub>·4H<sub>2</sub>O, 1.05 g of ZnSO<sub>4</sub>, 0.30 g of H<sub>3</sub>BO<sub>3</sub>, 0.25 g of Na<sub>2</sub>MoO<sub>4</sub>·2H<sub>2</sub>O, 0.15 g of CuCl<sub>2</sub>·2H<sub>2</sub>O and 0.84 g of disodium EDTA·2H<sub>2</sub>O. Solid media contained 1.5% (wt/vol) agar. Liquid cultures were routinely incubated in baffled Erlenmeyer flasks shaken at 200 rpm and 30°C.

**Chemicals.** Chemicals were obtained from Fluka (Buchs, Switzerland) (toluene, >99.5%; benzyl alcohol, >99%; benzaldehyde, >99%; benzoic acid, >99.5%; pseudocumene, ~99%; 3,4-dimethylbenzoic acid, ~97%; bis(2-ethylhexyl)phthalate (BEHP), 97%), Aldrich (Buchs, Switzerland) (3,4-dimethylbenzyl alcohol, 99%), Lancaster (Muehlheim, Germany) (3,4-dimethylbenzaldehyde, 97%) and Acros Organics (Geel, Belgium) (*n*-octane, >98.5%).

**Analysis of metabolites.** For the separation of *n*-octane, toluene/pseudocumene, the respective alcohols, aldehydes, and acids we used gas chromatography (GC) as described in Chapter 2. Alternatively, benzyl alcohol, benzaldehyde, and benzoic acid were separated via high-performance liquid chromatography (HPLC), using a Nucleosil C18 HD column (100-Å pore size, 5-μm particle size, 25 cm by 4 mm inner diameter) (Macherey-Nagel, Oensingen,

Switzerland) with a mobile phase of 64.9% H<sub>2</sub>O-35% acetonitrile-0.1% H<sub>3</sub>PO<sub>4</sub> at a flow rate of 0.7 ml/min. For the separation of 3,4-dimethylbenzyl alcohol, 3,4-dimethylbenzaldehyde and 3,4-dimethylbenzoic acid we used the same column at the same flow rate with a mobile phase of 59.9% H<sub>2</sub>O-40% acetonitrile-0.1% H<sub>3</sub>PO<sub>4</sub>. The UV detector was set at a wavelength range of 210 to 265 nm.

**Whole-cell assays.** Whole-cell assays to study the kinetics and inhibitions of the three monooxygenation steps catalyzed by XMO included cell growth, induction, resting cell biotransformations at a 1-ml scale, and sample preparation for GC and HPLC analysis and were performed as described in Chapter 2 with the following modifications: *xylMA* expression was induced by *n*-octane (0.1%, vol/vol) exclusively, and cell concentrations in the resting-cell biotransformations varied between 0.1 and 1.1 g of cell dry weight (CDW) per liter.

In experiments to follow product formation over time, samples of cells were incubated with the same substrates for different time periods (0 to 80 min). The assays were carried out twice independently. Initial specific activities were calculated as average activities based on the sum of all products formed in 5 min of reaction. One unit (U) is defined as the activity that forms 1 μmol of total products in 1 min. Specific activity was expressed as activity per gram of CDW [U (g of CDW)<sup>-1</sup>].

$V_{\max}$  and  $K_s$  for pseudocumene, toluene, and their derivatives were determined in reactions carried out for 5 min except for the aldehydes as substrate (10 min of reaction) with various substrate concentrations (0.04 to 30 mM). Specific activities were calculated based on the amount of products formed.  $V_{\max}$  and  $K_s$  values were calculated using the program Leonora, designed to analyze enzyme kinetic data and described by Cornish-Bowden (Cornish-Bowden, 1995). Experiments were repeated at least three times independently.

**Determination of toxicities of pseudocumene and its metabolites for *E. coli* JM101.** The toxicities of pseudocumene, 3,4-dimethylbenzyl alcohol, 3,4-dimethylbenzaldehyde, and 3,4-dimethylbenzoic acid were determined with *E. coli* JM101 incubated in complete M9\* medium. After reaching the exponential growth phase, the culture was subdivided into sterile baffled Erlenmeyer flasks with screw-on caps containing a Teflon seal to avoid evaporation, and the different compounds were added to concentrations between 0 and 40 mM. Subsequently, incubation was continued and growth was determined by monitoring the optical density at 450 nm. An optical density of one corresponded to 0.29 g of CDW per liter. The effect of BEHP, containing 1% (vol/vol) *n*-octane and different amounts of pseudocumene on growth of *E. coli* JM101 was determined by a similar procedure. After subdividing an exponentially growing culture, an equal volume of organic phase was added



and incubation was continued. One culture was further incubated without a second phase as a control.

**Two-liquid phase culture.** Freshly transformed *E. coli* JM101 cells harboring plasmid pSPZ3 were inoculated into a 3 ml LB medium preculture, grown overnight at 30°C, and diluted 100-fold in 100 ml of M9\* mineral medium. The resulting culture was incubated for approximately 10 h (during which time the cells entered the stationary phase) and used as an inoculum for the biotransformation reaction mixture. The biotransformation reaction was carried out in a stirred tank reactor with two Rushton turbine impellers, four baffles, and a total volume of 3 L (Preusting, et al., 1993; Wubbolts, et al., 1996a). Seals and O-rings were made out of solvent-resistant Viton. The reactor contained 0.9 L of a mineral medium composed of 8.82 g KH<sub>2</sub>PO<sub>4</sub>, 10.85 g K<sub>2</sub>HPO<sub>4</sub>, 8.82 g Na<sub>2</sub>HPO<sub>4</sub>, 1.0 g NH<sub>2</sub>Cl, 0.5 g NaCl, 0.49 g MgSO<sub>4</sub>·7H<sub>2</sub>O, 5 g glucose, 10 mg thiamine, 50 mg kanamycin, and 1 ml trace element solution US\* per liter. The composition of US\* is described in Chapter 2. The pH was maintained at 7.1 using 25% NH<sub>4</sub>OH and 34% phosphoric acid. After inoculation with 100 ml of the preculture, the reactor was aerated at a rate of 0.5 L min<sup>-1</sup> and was stirred at 1500 rpm for 10 to 12 hours (overnight), which resulted in a culture in the stationary phase containing approximately 3 (g of CDW) L<sup>-1</sup>. This culture of 1 L in volume was supplemented with 4 ml of US\* trace element solution and 4 ml of a 1% (wt/vol) thiamine solution. Subsequently, the culture was fed at a rate of 10 g h<sup>-1</sup> with an aqueous solution containing (per liter) 450 g of glucose, 50 g of yeast extract (Difco, Detroit, Mich.), and 9 g of MgSO<sub>4</sub>·7H<sub>2</sub>O, adjusted to pH 3 with hydrochloric acid. One hour after feed initiation, 1 L of the organic phase was added, resulting in a phase ratio of 0.5. The organic phase consisted of BEHP as the carrier solvent, which contained 1% (vol/vol) *n*-octane as an inducer of the *alk* regulatory system and 2% (vol/vol) pseudocumene as the substrate. Concomitantly, the stirrer speed was increased to 2000 rpm. Organic phase addition served as the time point of induction. Foam formation was limited by the addition of antifoam 289 (Sigma, Buchs, Switzerland).

**Process analytics.** The dissolved oxygen tension (DOT) was determined with an autoclavable amperometric probe (Mettler Toledo, Greifensee, Switzerland). Cell concentrations in the aqueous phase and octane, pseudocumene, 3,4-dimethylbenzyl alcohol, 3,4-dimethylbenzaldehyde, and 3,4-dimethylbenzoic acid concentrations in the organic phase as well as in the aqueous phase of the reactor were monitored over time. To do this, 2-ml samples were withdrawn from the reactor at regular intervals and added to 2-ml Eppendorf tubes. The reaction was stopped by placing the samples on ice and immediately acidifying them to pH 2 by the addition of 40 µl of perchloric acid stock solution (10%, vol/vol). The

samples were centrifuged to separate the phases, and the position of the interphase was marked. The organic phase was removed, diluted 50-fold with diethyl ether supplemented with dodecane as an internal standard, dried over sodium sulfate, and analyzed by GC to determine substrate, product, and octane concentrations. Then, 0.5 ml of the aqueous supernatant of each centrifuged sample was removed with a syringe into and extracted with an equal volume of diethyl ether as described in Chapter 2. Subsequently, the ether phase was analyzed by GC to determine the concentrations in the aqueous phase. The remaining aqueous supernatant was completely removed and discarded. The cell pellet was resuspended in an amount of M9\* medium corresponding to the original amount of aqueous supernatant, and the optical density at 450 nm was determined.

The apparent volumetric productivities and specific product formation rates were calculated as averages for intervals between two data points. The term “apparent” refers to the fact that activities may have been limited by substrate availability. Furthermore, since aldehyde and acid accumulation from pseudocumene demands multistep catalysis, apparent specific aldehyde and acid formation rates require doubled and threefold specific biocatalyst activities, respectively.

## RESULTS

### **Product formation patterns in the presence of two substrates.**

Recently, we showed that whole cells of *E. coli* JM101 containing XMO catalyze the multistep oxidation of toluene and pseudocumene via corresponding alcohols and aldehydes to benzoic acids (Chapter 2). When benzaldehydes were added as substrates, the cells transformed benzaldehyde and 3,4-dimethylbenzaldehyde to the corresponding acids at initial rates of 10 and 55 U (g of CDW)<sup>-1</sup>, respectively. In contrast, when toluene and pseudocumene were added as substrates, we observed that benzoic acids did not form until concentrations of toluene or pseudocumene reached low levels (Chapter 2).

In order to investigate this phenomenon in more detail, cells were incubated with the same amounts of toluene and benzaldehyde for different time periods (Fig. 3.1A). Benzoic acid was not formed until the toluene concentration reached a value as low as 0.05 mM, although benzaldehyde was present from the start of the reaction. Analogous biotransformations were carried out with pseudocumene and 3,4-dimethylbenzaldehyde as substrates (Fig. 3.1B). The

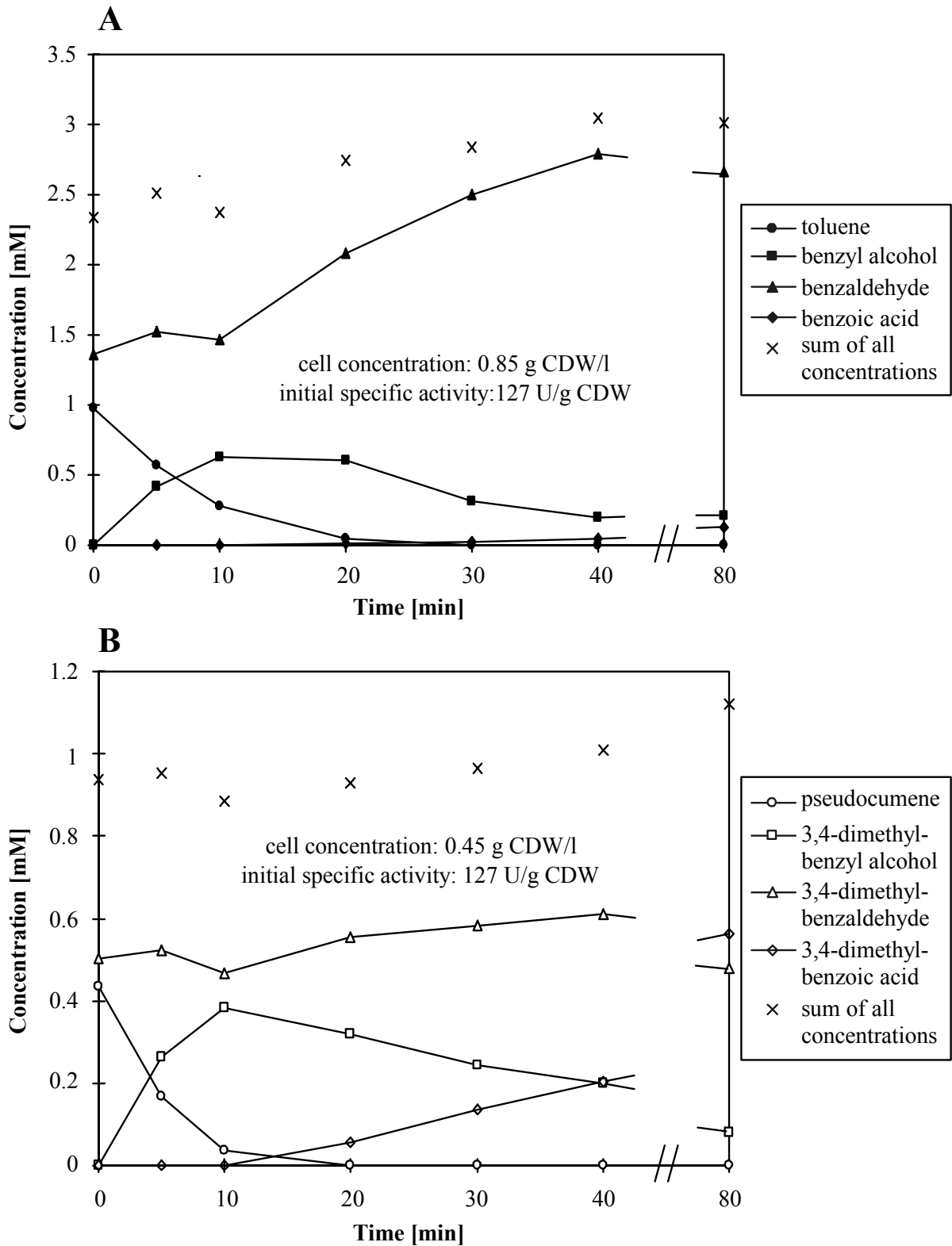


**Figure 3.1. Product formation after simultaneous addition of toluene and benzaldehyde (A) and of pseudocumene and 3,4-dimethylbenzaldehyde (B) to resting *E. coli* JM101 (pSPZ3) in 50 mM potassium phosphate buffer, pH 7.4, containing 1% (wt/vol) glucose. The assay was performed as described in Materials and Methods.**

corresponding acid started to be formed at a pseudocumene concentration below 0.036 mM. These results demonstrate that acid formation is completely prevented in the presence of toluene or pseudocumene.

We also tested the influence of pseudocumene and toluene on alcohol oxidation. Cells were incubated with equal amounts of pseudocumene and 3,4-dimethylbenzyl alcohol (Fig. 3.2A). After the reaction started, the alcohol accumulated at a high rate of  $109 \text{ U (g of CDW)}^{-1}$ , whereas the aldehyde accumulated at a rate as low as  $9 \text{ U (g of CDW)}^{-1}$ . Then, at reduced pseudocumene concentrations, the mean aldehyde formation rate increased to  $25 \text{ U (g of CDW)}^{-1}$ . After 10 min, a pseudocumene pulse established pseudocumene concentrations similar to those observed in the beginning of the reaction. The product formation pattern between 10 and 20 min of reaction looked very similar to the product formation pattern in the first 10 min. The aldehyde formation rate was reduced to  $8.5 \text{ U (g of CDW)}^{-1}$ , whereas the alcohol accumulated at a high rate of  $115 \text{ U (g of CDW)}^{-1}$ . At reduced pseudocumene concentrations, the aldehyde formation rate recovered to  $25 \text{ U (g of CDW)}^{-1}$ . The acid slowly accumulated when pseudocumene had completely disappeared from the reaction mixtures. Figure 3.2B shows the comparison between the aldehyde formation rates in the experiment shown in Figure 3.2A with the pseudocumene pulse after 10 min and the aldehyde formation rates in an identical experiment without pseudocumene pulse. In both experiments, initial aldehyde formation rates were identical and low, but increased as pseudocumene concentrations decreased. Without pseudocumene pulse, the aldehyde formation rate reached  $30 \text{ U (g of CDW)}^{-1}$  and remained roughly constant, whereas the pseudocumene addition after 10 min clearly reduced the aldehyde formation rate. Toluene also reduced the aldehyde formation rate, but only at concentrations above 0.5 mM and to a lesser extent than pseudocumene (results not shown). The presence of pseudocumene or toluene obviously not only prevents aldehyde oxidation but also reduces the alcohol oxidation rate. For the impairment of alcohol oxidation, higher pseudocumene or toluene concentrations are required than for the prevention of aldehyde oxidation.

In order to investigate the product formation pattern in the presence of 3,4-dimethylbenzyl alcohol and 3,4-dimethylbenzaldehyde, similar amounts of the two substrates were incubated with induced *E. coli* JM101 (pSPZ3) (Fig. 3.3). Initially, only alcohol was oxidized. Aldehyde oxidation started after the concentrations of alcohol and aldehyde had decreased and increased, respectively. For benzyl alcohol and benzaldehyde as substrates a similar product formation pattern with an initial aldehyde formation rate of  $123 \text{ U (g of CDW)}^{-1}$  was obtained.

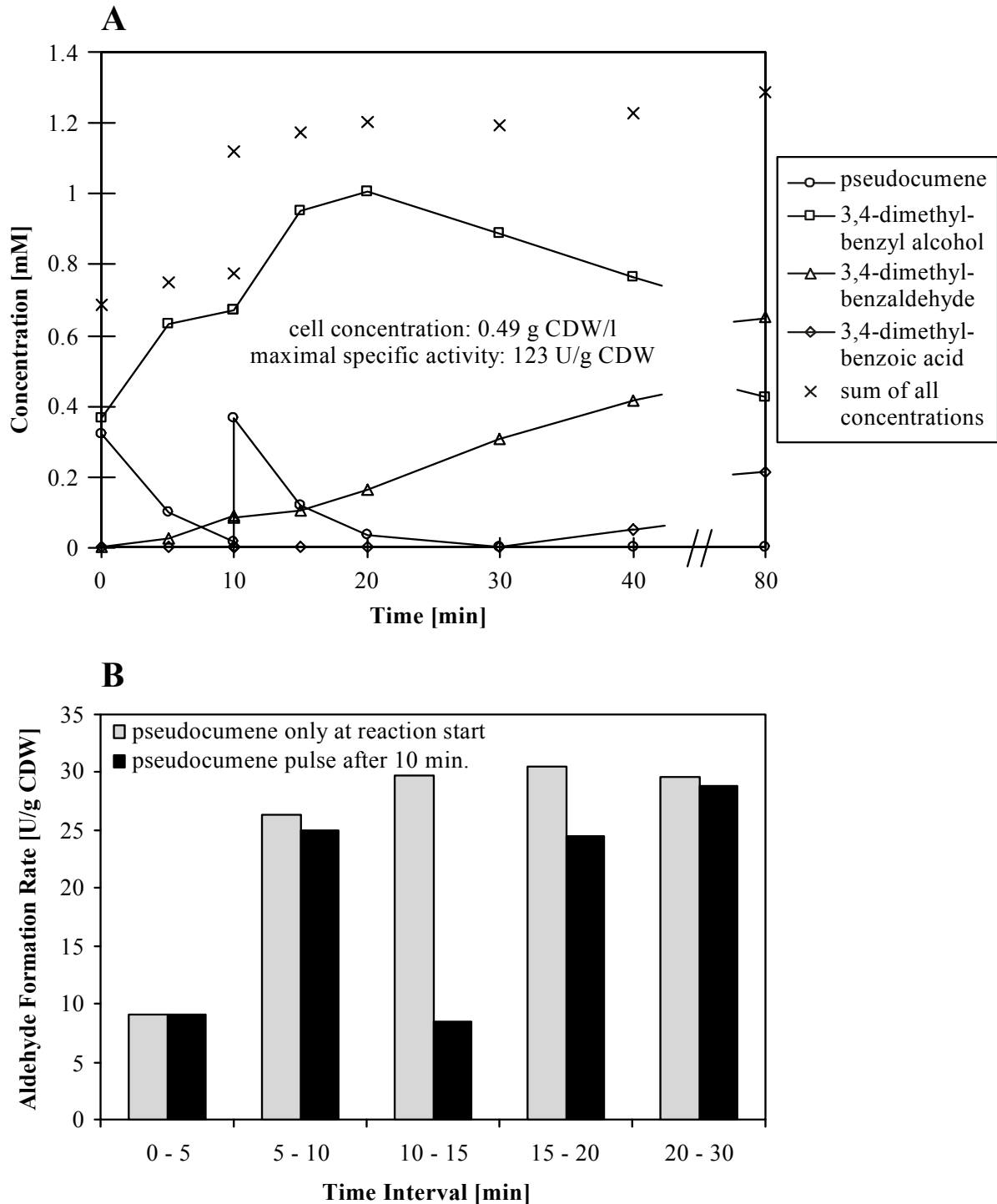


**Figure 3.2.** Product formation after simultaneous addition of pseudocumene and 3,4-dimethylbenzyl alcohol to resting *E. coli* JM101 (pSPZ3) in 50 mM potassium phosphate buffer, pH 7.4, containing 1% (wt/vol) glucose. Assays were performed as described in Materials and Methods. (A) Product formation pattern. After 10 min, pseudocumene was pulsed to the reaction mixtures. (B) Comparison of aldehyde formation rates in reactions with and without pseudocumene pulse. The aldehyde formation rates are calculated as average activities per gram of CDW in different time intervals.

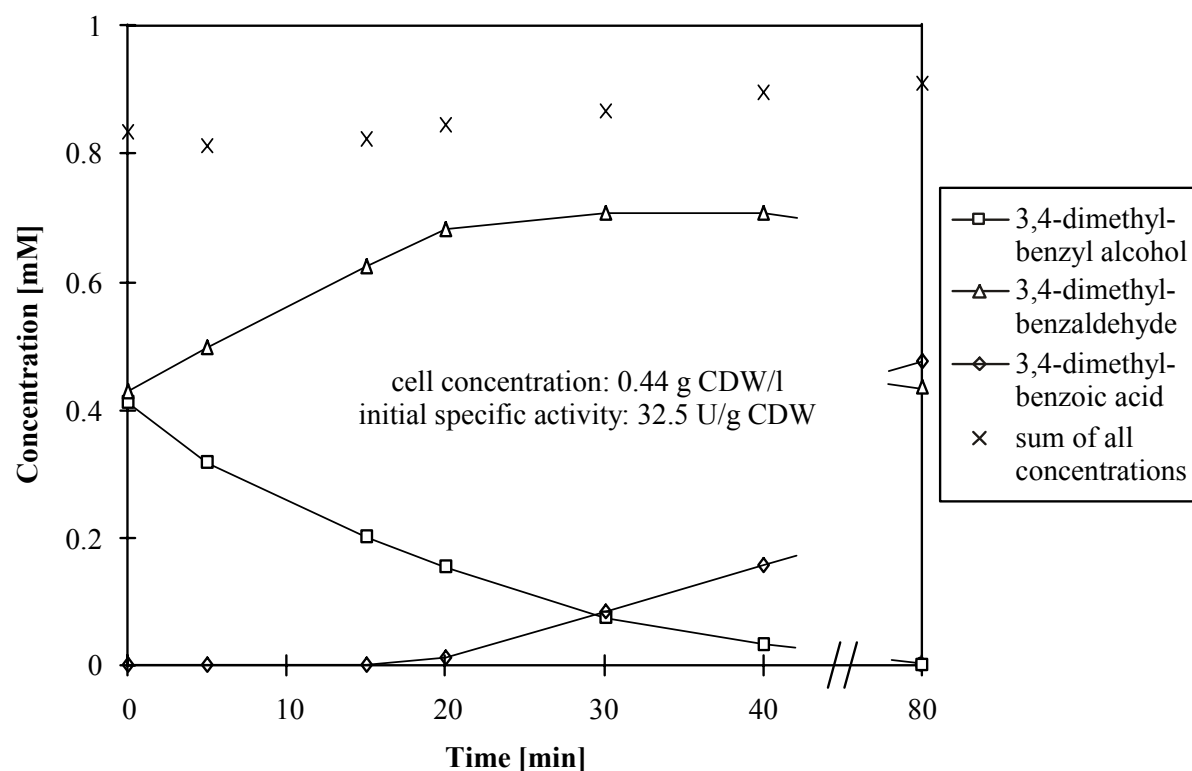


**Figure 3.3. Product formation after simultaneous addition of 3,4-dimethylbenzyl alcohol and 3,4-dimethylbenzaldehyde to resting *E. coli* JM101 (pSPZ3) in 50 mM potassium phosphate buffer, pH 7.4, containing 1% (wt/vol) glucose. Assays were performed as described in Materials and Methods.**

Obviously, not only pseudocumene and toluene but also the corresponding alcohols prevent acid formation. The inhibition of acid formation by the alcohols seems to be weaker than the inhibition by pseudocumene and toluene, since alcohol concentrations must be higher than toluene and pseudocumene concentrations to prevent acid formation.

#### **$V_{\max}$ and $K_s$ values of *E. coli* JM101 (pSPZ3) for different substrates.**

In Chapter 2, we speculated that the biocatalyst might take up toluene and pseudocumene more efficiently than corresponding aldehydes, which would explain the lack of acid formation in the presence of unoxidized substrates such as toluene and pseudocumene. In order to evaluate this presumption and to learn more about the catalytic features of XMO present in *E. coli*, we investigated the kinetics of the consecutive in vivo oxygenation of xylenes to benzoic acids. Apparent maximal reaction velocities ( $V_{\max}$ ) and substrate uptake

**Table 3.1. Apparent<sup>a</sup>  $V_{\max}$  and  $K_s$  values of *E. coli* JM101 (pSPZ3) for different substrates.**

Substrate	Apparent <sup>a</sup> $V_{\max}$ [U (g of CDW) <sup>-1</sup> ]	Apparent <sup>a</sup> $K_s$ [ $\mu$ M]	$V_{\max}/K_s$ [U $\mu$ M <sup>-1</sup> (g of CDW) <sup>-1</sup> ]
Pseudocumene	351 $\pm$ 8	202 $\pm$ 8	1.7
3,4-Dimethylbenzyl alcohol	93 $\pm$ 3	24 $\pm$ 4	3.9
3,4-Dimethylbenzaldehyde <sup>b</sup>	$\geq$ 560	$\geq$ 8000	ND <sup>c</sup>
Toluene	134 $\pm$ 9	87 $\pm$ 17	1.5
Benzyl alcohol	225 $\pm$ 9	85 $\pm$ 4	2.6
Benzaldehyde <sup>b</sup>	$\geq$ 18	$\geq$ 20000	ND <sup>c</sup>

<sup>a</sup> The term “apparent” refers to the fact that these kinetic values were determined for whole cells. Values are means  $\pm$  standard errors.

<sup>b</sup> The kinetic values for benzaldehydes could not be determined accurately because relevant substrate concentrations were in a range at which measurements were hampered by toxicity and limited solubility of the substrates.

<sup>c</sup> ND, not determined.

constants ( $K_s$ , corresponding to the substrate concentrations at which whole cells show half-maximal transformation rates) were determined by whole-cell assays (Table 3.1). The term “apparent” is used because the kinetic values were determined with whole cells.

The cells showed Michaelis-Menten like kinetics for the formation of benzyl alcohols from pseudocumene or toluene and the formation of benzaldehydes from benzyl alcohols. For the natural substrate pseudocumene, we found a higher uptake constant than for the corresponding alcohol, whereas the maximal reaction velocity of pseudocumene oxidation was higher than of 3,4-dimethylbenzyl alcohol oxidation. The kinetic values for benzaldehydes were difficult to determine because the relevant substrate concentrations were in a range at which measurements were hampered by toxicity and limited solubility of the substrates. Furthermore, for 3,4-dimethylbenzaldehyde as substrate, we observed a sigmoid rather than a hyperbolic (Michaelis-Menten like) dependency of the reaction rate on the substrate concentration. This dependency was linear for benzaldehyde as substrate in a concentration range of 1 to 30 mM. Surprisingly, at concentrations above the solubility of 3,4-dimethylbenzaldehyde in aqueous solution ( $>4$  mM), increasing aldehyde amounts still caused increasing reaction rates, suggesting aldehyde uptake from organic-phase droplets.

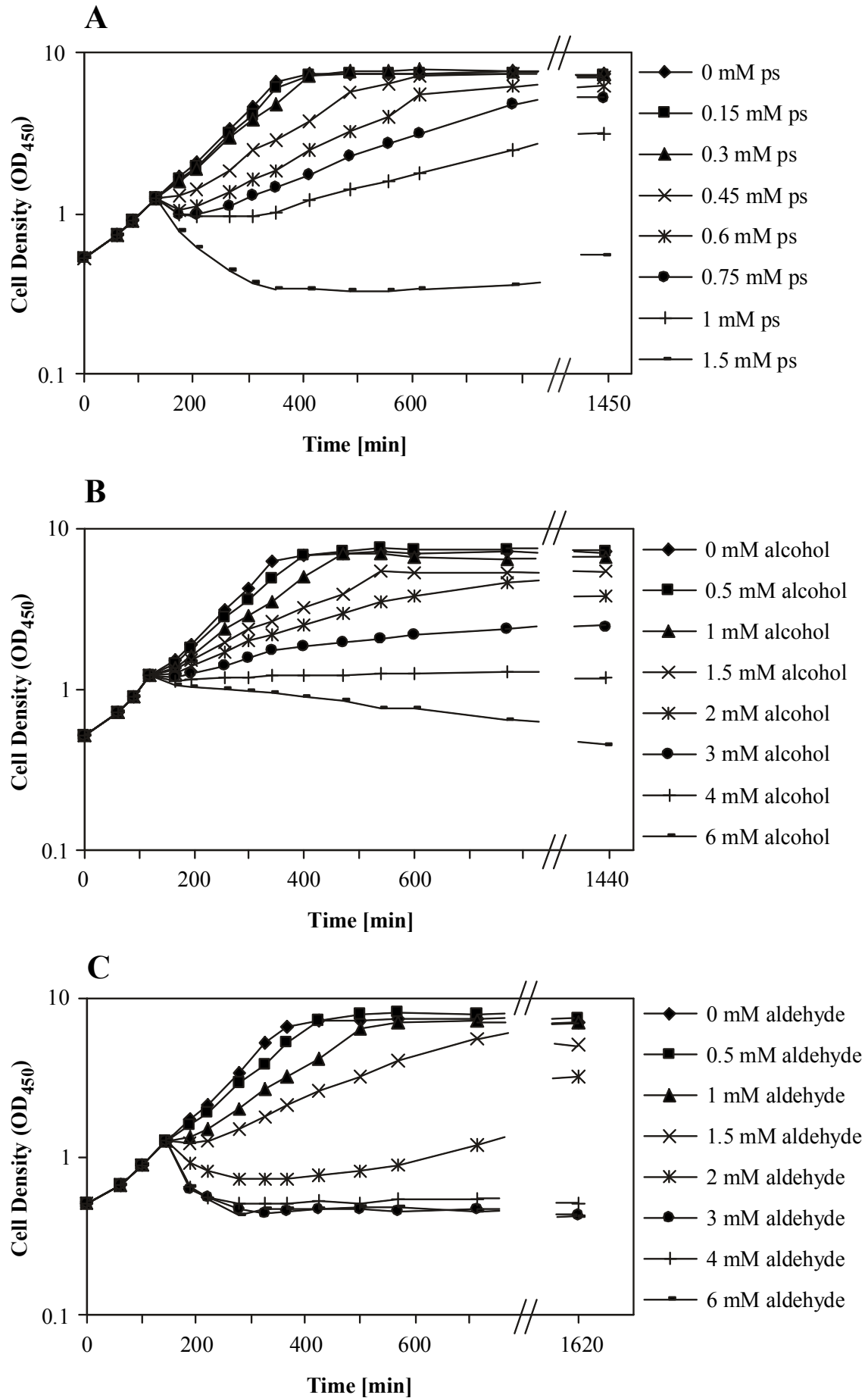
Nevertheless, we were able to estimate lower limits for the  $K_s$  values of the aldehydes (Table 3.1). The minimal  $V_{\max}$  values presented in Table 3.1 correspond to the maximal reaction velocities measured experimentally. The uptake of benzaldehydes by the biocatalyst is in fact significantly less efficient than the uptake of toluene and pseudocumene.

### **Toxicities of pseudocumene and its derivatives for *E. coli* in an aqueous medium.**

Xylenes as well as their oxidized derivatives are expected to be toxic to microorganisms such as *E. coli*. Metabolically active cells are essential to maintain biocatalytic activity of *E. coli* (pSPZ3) because NADH, a cofactor of the XMO-catalyzed oxidations, must be regenerated by the *E. coli* host. Therefore, the toxicities of substrates and products are important parameters for a possible preparative application of XMO in recombinant *E. coli*.

We tested the toxicities of pseudocumene and its products to cultures of *E. coli* JM101 by monitoring growth at different substrate and product concentrations (Fig. 3.4). The formation of a second liquid phase caused initial decreases in optical density because of cell lysis and changes in cell morphology (as observed under the microscope). Pseudocumene reduced growth already at low concentrations, and complete inhibition of growth was observed at concentrations above 1 mM (Fig. 3.4A). Only slightly weaker toxicities were observed for 3,4-dimethylbenzyl alcohol (Fig. 3.4B) and 3,4-dimethylbenzaldehyde (Fig. 3.4C) with complete growth inhibition above concentrations of 3 and 2 mM, respectively. The start of growth 4 h after the addition of 3,4-dimethylbenzaldehyde to a concentration of 2 mM (Fig. 3.4C) may be explained by aldehyde reduction to the less toxic alcohol through the action of unspecific dehydrogenases of the *E. coli* host, as reported in Chapter 2. 3,4-Dimethylbenzoic acid was considerably less toxic; concentrations above 24 mM were necessary to completely inhibit growth (Fig. 3.4D). Panel E of Figure 3.4 illustrates the influence of varying inhibitor concentrations on the growth rate. Thus, the concentrations of pseudocumene and the corresponding alcohol and aldehyde in the microenvironment of the cells have to be kept low for practical application of *E. coli* JM101 (pSPZ3) as a biocatalyst. A two-liquid phase system with a second phase consisting of an organic solvent offers a possible solution to accomplish this requirement.





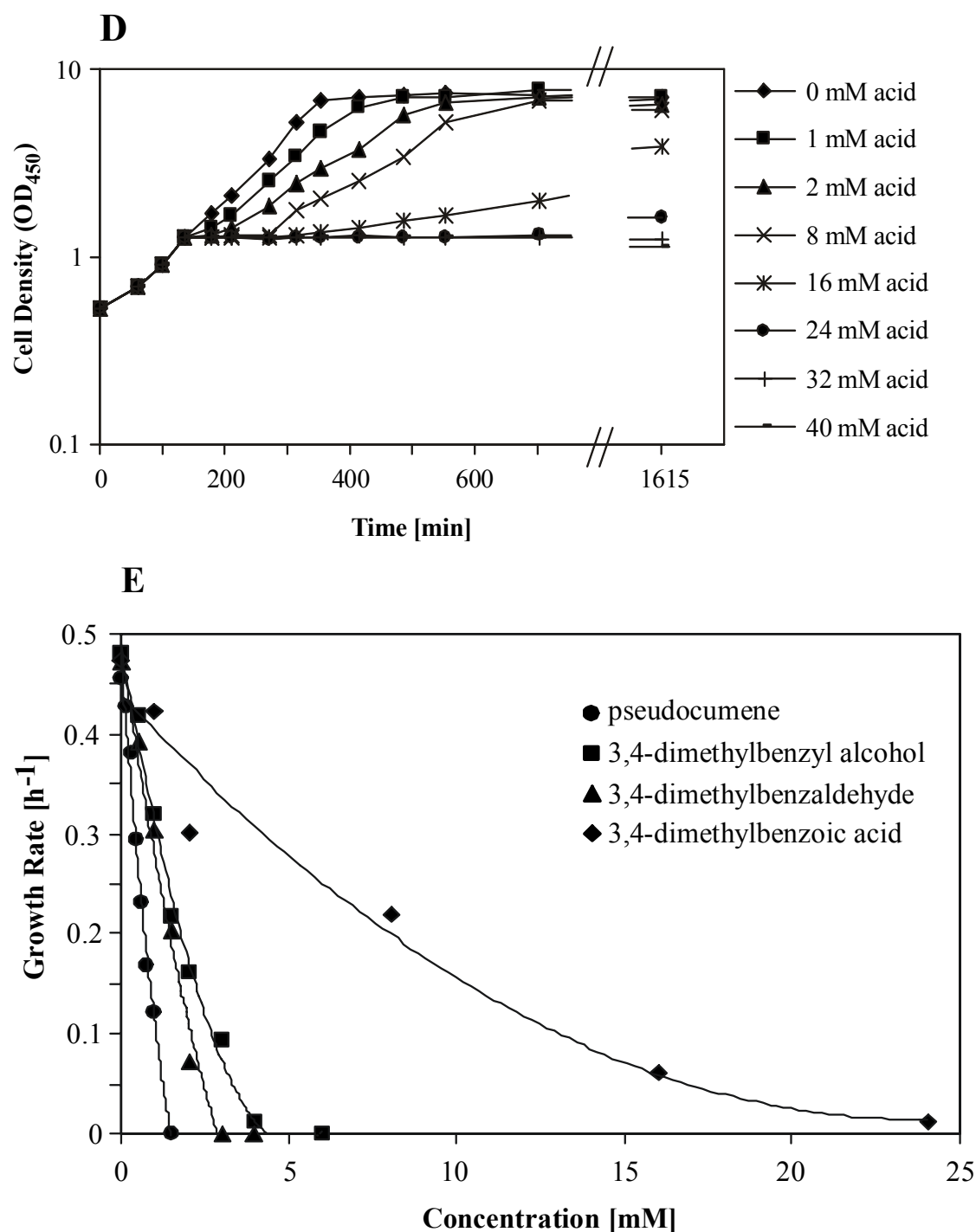


**Figure 3.4.** Growth of *E. coli* JM101 after addition of different amounts of pseudocumene (ps) (A), 3,4-dimethylbenzyl alcohol (alcohol) (B), 3,4-dimethylbenzaldehyde (aldehyde) (C) and 3,4-dimethylbenzoic acid (acid) (D). Panel E shows the dependence of the growth rate on varying inhibitor concentrations. After entering exponential growth, a 400-ml culture was split into 40-ml subcultures, to which different amounts of the substance of interest were added. Experimental details are described in Materials and Methods.

**Fed-batch-based biotransformation in a two-liquid phase system.**

We used BEHP for the investigation of the multistep biotransformation of pseudocumene by *xylMA*-expressing recombinant *E. coli* in a two-liquid phase system. In order to ensure the suitability of BEHP for our system, we examined the effect of BEHP and different concentrations of pseudocumene in BEHP on growth of *E. coli* JM101 (Fig. 3.5). To simulate the conditions in the biotransformation system, the organic phase, present at a phase ratio of 0.5, contained 1% (vol/vol) *n*-octane, the inducer of *xylMA* expression in *E. coli* JM101 (pSPZ3). BEHP containing up to 10% (vol/vol) pseudocumene had no effect on cell growth. Higher pseudocumene concentrations increasingly reduced the growth rate and with more than 25% (vol/vol) of pseudocumene in the organic phase no growth was observed. The use of BEHP allows the addition of large amounts of pseudocumene to the biotransformation reaction mixture and thereby meets the main demand for a second liquid organic phase.

To analyze the product formation pattern in the BEHP/M9\* two-liquid phase system, we performed biotransformations in fed-batch mode. This approach was based on our previous experiments designed to produce (*S*)-styrene oxide from styrene (Wubbolts, et al., 1996a; Panke, et al., 1999b; Panke, et al., 2000). The biotransformation was started one hour after feed initiation by the addition of the organic phase containing 2% (vol/vol) pseudocumene and 1% (vol/vol) *n*-octane as inducer for *xylMA* expression. Results are shown in Figure 3.6 and were confirmed by repeating the experiment. Substrate and product concentrations (Fig. 3.6A) were calculated as the sum of the concentrations in the organic and the aqueous phase for each compound and correspond to the doubled overall concentrations in the total volume.

Aldehyde and alcohol formation began about 1 h after addition of the second phase, confirming the short induction period observed in shaking flask experiments (Chapter 2). The subsequent biotransformation can be divided into three stages. In the first stage, pseudocumene was directly channeled through two oxygenation steps, and 3,4-dimethylbenzaldehyde accumulated as sole product to a concentration of 65 mM. The second stage was characterized by a complete cessation of aldehyde accumulation and exclusive formation of 3,4-dimethylbenzoic acid at pseudocumene concentrations below 90 mM. In the third stage, 3,4-dimethylbenzyl alcohol accumulated at a very low rate to a concentration of 13.5 mM, the aldehyde concentration remained constant, and the acid concentration increased slightly. The final concentrations of pseudocumene and 3,4-dimethylbenzaldehyde amounted to 16 and 63 mM, respectively. The aqueous pseudocumene, alcohol, and aldehyde concentrations remained very low during the whole experiment, whereas the acid accumulated to concentrations of 48.5 and 6.5 mM in the aqueous and organic phase, respectively. Such

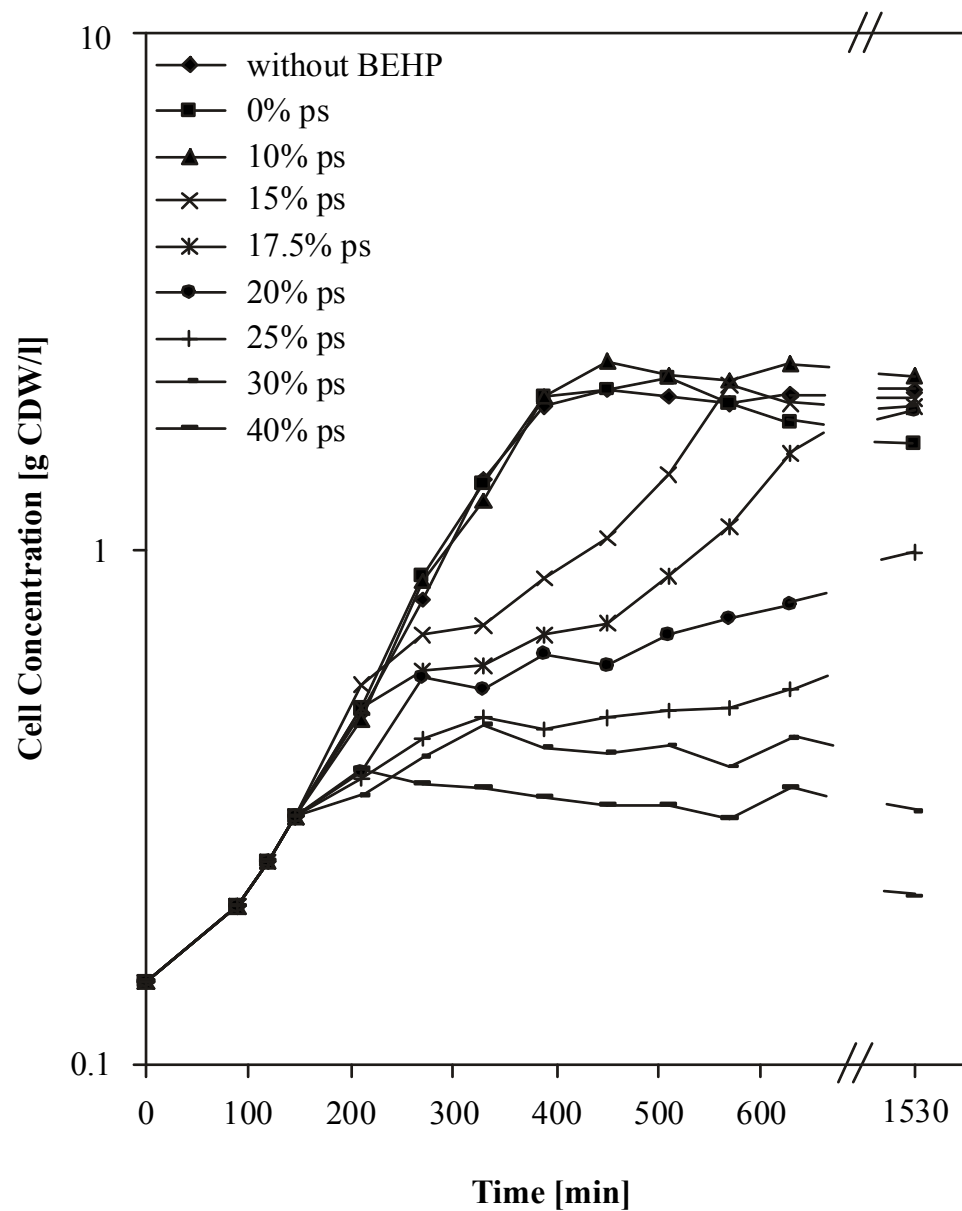


**Figure 3.5. Growth of *E. coli* JM101 in the absence and in the presence of BEHP containing different volume fractions of pseudocumene.** After reaching exponential growth a 200-ml culture was split into 20-ml subcultures, to which no or 20 ml BEHP containing different volume fractions of pseudocumene (ps) was added. Experimental details are described in Materials and Methods.

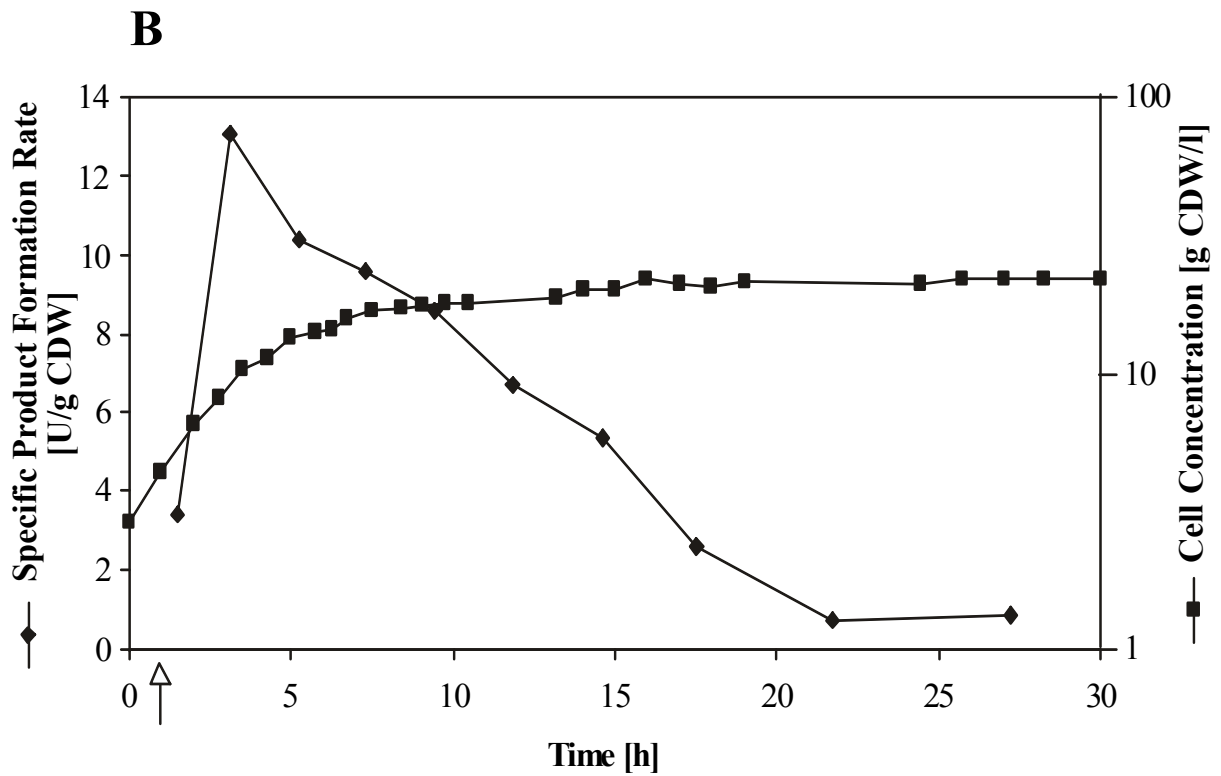
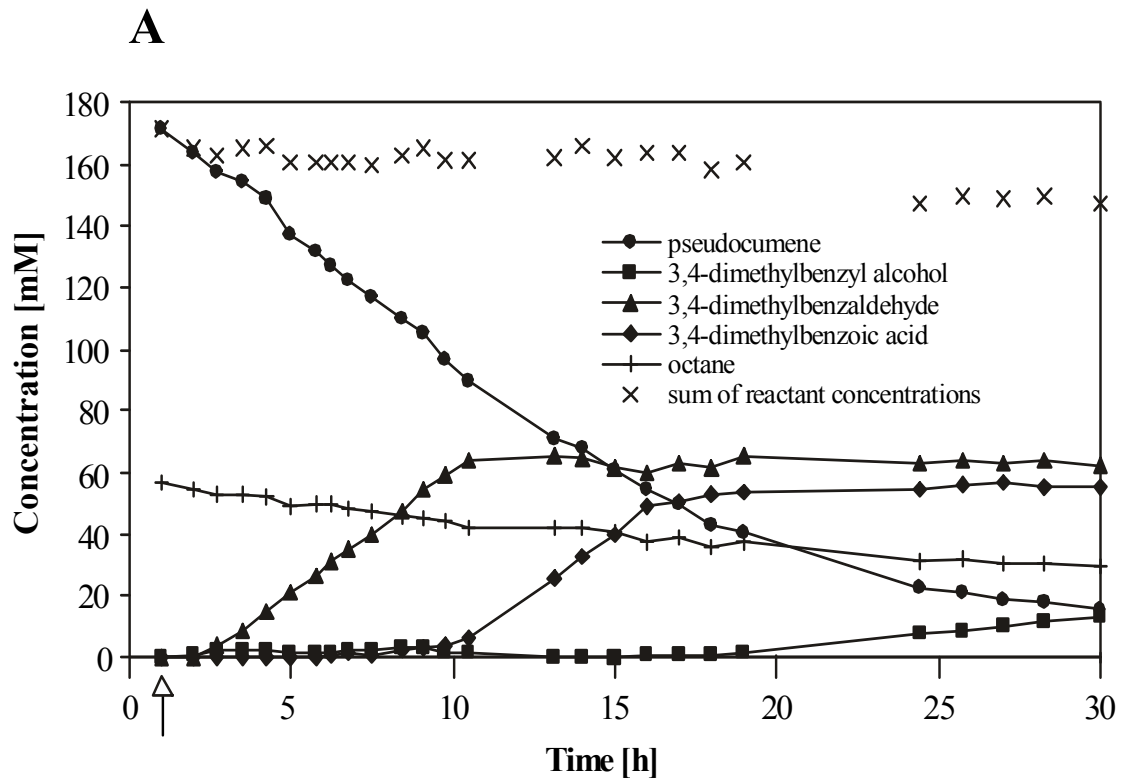


**Figure 3.6. Fed-batch based two-liquid phase biotransformation with *E. coli* JM101 (pSPZ3) at a phase ratio of 0.5.** The second organic phase consisted in BEHP as the organic carrier solvent, 2% (vol/vol) pseudocumene and 1% (vol/vol) *n*-octane (as the inducer). Addition of the organic phase occurred 1 h after feed initiation (arrow). Experimental details of the fed-batch are described in Materials and Methods. (A) Reactant and octane concentrations during the fed-batch experiment. All concentrations represent the sum of the respective concentrations in the organic and aqueous phases. (B) Formation of *E. coli* JM101 (pSPZ3) biomass and development of the specific product formation rate, which was calculated by determining the rate of total product formation per gram of CDW as the average for an interval between two data points.

aqueous acid concentrations are expected to be toxic for *E. coli* JM101 (Fig. 3.4). The octane concentration decreased continuously during the biotransformation, which is due to its volatility and gives an indirect measure of substrate stripping by aeration, which caused a slight decrease of the total reactant concentration.

As expected, growth continued after organic phase addition without any interruption (Fig. 3.6B). After 4 h of exponential growth, the culture was limited by oxygen over 5 h. Linear growth to a cell dry weight of 17 g L<sup>-1</sup> after 7.5 h of fed-batch cultivation was followed by slow growth to a maximal cell density of 22 g L<sup>-1</sup>. The specific activity concerning the formation of all three products, referred to as specific product formation rate, was maximal 2 h after induction in growing cells at 13 U (g of CDW)<sup>-1</sup>, then decreased continuously, and was low during the third stage of the biotransformation (Fig. 3.6B). The maximal volumetric activity concerning the formation of one specific product, in this case 3,4-dimethylbenzaldehyde, amounted to 133 U L<sub>aq</sub><sup>-1</sup>, corresponding to a maximal volumetric productivity of 1.1 g L<sub>aq</sub><sup>-1</sup> h<sup>-1</sup>. This productivity was reached 3.5 h after induction and remained constant for 7 h.

The biocatalyst *E. coli* JM101 (pSPZ3), cultivated in a fed-batch mode, supported the accumulation of 3,4-dimethylbenzaldehyde, 3,4-dimethylbenzoic acid, and 3,4-dimethylbenzyl alcohol in three consecutive stages of the biotransformation.

## DISCUSSION

### Kinetic properties of *E. coli* JM101 (pSPZ3).

The high specific product formation rates observed in this study for resting cells of *E. coli* JM101 (pSPZ3) containing XMO together with results obtained earlier with this system indicate that pSPZ3 is highly suited for *xylMA* expression under the control of the *alk* promoter (Chapter 2; Panke, et al., 1999b). The efficient inhibition of the XMO-catalyzed aldehyde oxygenation by toluene and pseudocumene might be explained by the high uptake constants for aldehydes (Table 3.1) and competitive inhibition. Besides substrate affinity, kinetics of biocatalysts based on whole cells are determined by various factors such as membrane permeability and cofactor availability. Pseudocumene and toluene also reduce aldehyde formation rates, which cannot be explained by competitive inhibition, since the biocatalyst has lower apparent specificity constants ( $V_{\max}/K_s$ ) for pseudocumene and toluene than for corresponding alcohols (Table 3.1). Moreover, higher concentrations of 3,4-dimethylbenzyl alcohol than of pseudocumene are needed to inhibit aldehyde oxidation, which is not expected regarding the  $V_{\max}/K_s$  values. Therefore, also the lack of acid formation in the presence of pseudocumene cannot only be ascribed to competitive inhibition. A comparison with earlier experiments using the same whole cells and unoxidized substrates (e.g., toluene and pseudocumene, Chapter 2) shows that pseudocumene and toluene oxidation rates are not reduced in the presence of alcohols or aldehydes, another argument against substrate competition. Transient accumulation and degradation of substrate, product, and inhibitor impeded kinetic analyses of the mutual inhibitions.

Nevertheless, the results presented in this study indicate that the inhibitions by pseudocumene and toluene are not purely competitive, whereas the inhibition of aldehyde oxygenation by the corresponding alcohols may be. The presence of unoxidized substrates might induce an enzyme conformation in which their own oxidation is favored over alcohol and aldehyde oxidation. P450 monooxygenases, for instance, were proposed to undergo conformational changes caused by salt (Yun, et al., 1996), inhibitor (Raag, et al., 1993), or substrate (Poulos, et al., 1995; Ueng, et al., 1997) or during the reaction (Bell-Parikh and Guengerich, 1999), e.g., by transition from the ferric to the ferrous state (Raag and Poulos, 1989). A hypothesis assuming a single active site and not necessarily requiring a conformational change comprises that unoxidized substrates bind to a putative substrate access channel, to which the membrane might also contribute, and thereby inhibit the access of more polar substrates to the active site.

Considering that the natural host *P. putida* mt-2 synthesizes three enzymes for the three oxidation steps of the upper pathway, the ability of XMO to catalyze all reactions from the unoxidized substrates to the carboxylic acids is surprising. An analogous example is the bile acid synthesis pathway, in which sterol side chain oxidations from alcohol to carboxylic acid can proceed by sterol 27-hydroxylase, also responsible for alcohol formation, but also by the action of alcohol and aldehyde dehydrogenases (Cali and Russell, 1991; Holmberg-Betsholtz, et al., 1993). This dual ability was suggested to be an example of evolution producing functional similarity from disparate structures and mechanisms.

In our case, a recombinant strain of *P. putida* KT2440 expressing only the XMO genes from its chromosome (Panke, et al., 1999a) grew on benzoic acid by the action of enzymes of the *ortho* cleavage pathway encoded on the chromosome but not on toluene provided via gas phase (results not shown). The lack of growth on toluene could be caused by an inhibition of alcohol and aldehyde oxygenation by toluene. Nevertheless, early in evolution XMO might have been the only enzyme in the upper pathway catalyzing the three-step oxidation at low rates with a high demand for reducing equivalents. Later, dehydrogenases catalyzing energetically more favorable reactions, in which reducing equivalents are produced and not consumed, might have evolved. Such dehydrogenations might have become favored through the inhibition of alcohol and aldehyde oxygenation by xylenes.

The high specificity constants of XMO-containing *E. coli* for benzyl alcohols are surprising, but in the wild-type a high catalytic efficiency in alcohol oxygenation might be necessary, because the equilibrium catalyzed by XylB, the benzyl alcohol dehydrogenase, lies on the side of the alcohols (Chapter 2). With purified XylB, Shaw et al. found  $K_m$  values of 155 and 65  $\mu\text{M}$  and  $V_{\text{max}}$  values of 320 and 4800  $\mu\text{mol min}^{-1} \text{mg}^{-1}$  for benzyl alcohol (forward reaction) and benzaldehyde (reverse reaction), respectively (Shaw, et al., 1993). As suggested in Chapter 2, XylB may prevent the formation of high intracellular concentrations of the particularly reactive benzaldehydes. In the case of high fluxes through the degradation pathways and low aldehyde concentrations, XylB contributes to aldehyde formation. Thus, at high concentrations of unoxidized substrates, the inhibition of alcohol oxygenation could promote alcohol dehydrogenation. Furthermore, the inhibition of the second and the third oxygenation step of the XMO-catalyzed reaction cascade by unoxidized substrates may explain why the alcohol and aldehyde oxidation activities of XMO have not been more widely reported.



**One-enzyme multistep catalysis – mechanism and examples.**

At least 11 nonheme integral membrane enzymes, including XylM, contain a highly conserved 8-histidine motif (Shanklin, et al., 1994; Shanklin, et al., 1997), which is essential for catalytic activity. Based on studies on the alkane hydroxylase of *P. putida* GPO1, such integral membrane enzymes were proposed to contain diiron clusters as O<sub>2</sub>-activating sites, for which the 8-histidine motifs provide ligands (Shanklin, et al., 1997). Furthermore, alkane hydroxylase of *P. putida* catalyzes the oxygenative formation of medium chain length alkanals from terminal alkanols (May and Katopodis, 1986), also part of a multistep oxygenation. The histidine cluster containing C-4 sterol methyl oxidase of *Saccharomyces cerevisiae* catalyzes, like XMO, the three-step oxidation of a methyl group to the carboxylic acid (Bard, et al., 1996). Purified naphthalene dioxygenase from *Pseudomonas* sp. strain NCIB 9816–4 and ammonia-grown cells of *Nitrosomonas europaea* catalyze, among other reactions, the oxidation of toluene via benzyl alcohol to benzaldehyde but not to benzoic acid (Keener and Arp, 1994; Lee and Gibson, 1996). Methane monooxygenase of *Methylosinus trichosporium*, another nonheme monooxygenase with diiron clusters as O<sub>2</sub>-activating sites, is functionally similar to cytochrome P450 enzymes (Rataj, et al., 1991; Bell and Guengerich, 1997). P450 monooxygenases also catalyze the oxidation of toluenes (White and McCarthy, 1986; Ling and Hanzlik, 1989), benzyl alcohols (Vaz and Coon, 1994), and benzaldehydes, which also cause enzyme deactivation by heme adduct formation (Raner, et al., 1997; Kuo, et al., 1999). Furthermore, P450 monooxygenases catalyze the multistep oxidations of linalool and camphor to 8-oxolinalool and 5-ketocamphor, respectively (Ullah, et al., 1990), of ethanol via acetaldehyde to acetic acid (Bell-Parikh and Guengerich, 1999), and of fatty acids to diacids (Shet, et al., 1996) and to subterminal hydroxy- and oxoproducts with a product diversity depending on the dissolved oxygen concentration (Schneider, et al., 1999). Like C-4 sterol methyl oxidase, several P450 enzymes also catalyze multistep reactions involved in steroid oxidation, e.g., P450s 27, 24, 19, 17 $\alpha$ , 14 $\alpha$ , 11 $\beta$  and P450<sub>scc</sub> (Hume, et al., 1984; Kellis and Vickery, 1987; Fischer, et al., 1989; Cali and Russell, 1991; Holmberg-Betsholtz, et al., 1993; Akiyoshi-Shibata, et al., 1994; Imai, et al., 1998; Yamazaki, et al., 1998). These reactions usually consist of two or three consecutive two-electron oxidation steps. The large number of multistep oxidations, which could be further extended, shows that multistep reactions are widespread among oxygenases.

As in the XMO-catalyzed oxidation of benzyl alcohols (Chapter 2), the formation of *gem*-diol intermediates, which spontaneously dehydrate to the more stable carbonyl compounds, was also proposed in the alcohol oxidation step of most of the cited steroid oxidations as well as in

the P450-catalyzed oxidations of ethanol (Bell-Parikh and Guengerich, 1999), 8-hydroxylinalool (Ullah, et al., 1990), hydroxy fatty acids (Shet, et al., 1996; Schneider, 1998), and benzyl alcohols (Vaz and Coon, 1994). Another example for an enzyme capable of multistep catalysis is dehydroquinase, which performs several different consecutive chemical reactions in one active site and thus prevents the formation of unwanted by-products by specific interactions with the substrate (Carpenter, et al., 1998). The P450-catalyzed multistep oxidation of ethanol and of some steroids is considered to involve little exchange of the reaction intermediates with the medium. However, in the XMO-catalyzed multistep oxygenation, substantial exchange of intermediates with the medium must be assumed, since transient accumulation and degradation of alcohol and aldehyde intermediates occur (Chapter 2) (Figs. 3.1, 3.2, and 3.3).

#### **Product formation patterns in the BEHP/M9\* two-liquid phase fed-batch system.**

Cyclic hydrocarbons can be toxic to bacteria, inhibiting a potential whole-cell-based biocatalytic process; Sikkema *et al.* reviewed mechanisms of membrane toxicity of hydrocarbons (Sikkema, et al., 1995). In our study, we also found pseudocumene as well as 3,4-dimethylbenzyl alcohol, and 3,4-dimethylbenzaldehyde to be toxic at low concentrations. We therefore chose the two-liquid phase concept to overcome toxicity and solubility problems (Freeman, et al., 1993; Wubbolts, et al., 1996a; Leon, et al., 1998). As expected for very hydrophobic solvents (Laane, et al., 1987), BEHP ( $\log P_{\text{oct}}$  9.6) did not affect bacterial growth when used as second organic phase and proved to be highly suited to prevent substrate toxicity.

In fed-batch-based two-liquid phase biotransformations of pseudocumene, the products 3,4-dimethylbenzyl alcohol, 3,4-dimethylbenzaldehyde, and 3,4-dimethylbenzoic acid accumulated in three diverse stages. The exclusive accumulation of the aldehyde during the first stage suggests that pseudocumene concentrations in the system were high enough to inhibit aldehyde oxidation but not to inhibit alcohol oxidation. The switch from aldehyde to acid accumulation in the second stage may be explained by pseudocumene concentrations falling below an inhibitory limit at around 90 mM in the organic phase. At this point of the biotransformation, the aqueous pseudocumene concentration was below the detection limit of 20  $\mu\text{M}$ . An inhibitory limit in the aqueous phase below 20  $\mu\text{M}$  is in accordance with the results shown in Figure 3.1, which suggest that the inhibitory limit is below 36  $\mu\text{M}$ . The slow alcohol accumulation accompanied by a slight increase of the acid concentration during the third stage of the biotransformation might be ascribed to low XMO activities, which might be

exceeded by the transformation of aldehyde to alcohol by the non-specific alcohol dehydrogenase activity of *E. coli* (Chapter 2). The accumulation of mainly one product in each of the three stages of the biotransformation indicates that the use of the two-liquid phase concept may allow the accumulation of a single product in a kinetically controlled one-enzyme multistep process.

### **Factors influencing biocatalyst activity.**

The parallel decreases in substrate concentration and specific product formation rate in two-liquid phase biotransformations point to substrate limitation. The maximal product formation rate of  $13 \text{ U (g of CDW)}^{-1}$  was much lower than  $127 \text{ U (g of CDW)}^{-1}$ , the maximal specific activity measured for resting cells. The results of resting-cell experiments are not expected to coincide perfectly with the results of fed-batch experiments. However, the huge difference between the specific product formation rates nevertheless strongly suggests substrate limitation during the fed-batch experiment. Moreover, the exclusive formation of 3,4-dimethylbenzaldehyde in the beginning of the biotransformation also indicates substrate limitation. The exclusive accumulation of the aldehyde is only possible when the alcohol oxidation rate equals or exceeds the pseudocumene oxidation rate. According to the kinetic values for the first two oxidation steps (Table 3.1), exclusive aldehyde accumulation from pseudocumene requires clearly limiting pseudocumene concentrations, at which the lower uptake constant of the biocatalyst for 3,4-dimethylbenzyl alcohol than for pseudocumene dominates the higher maximal reaction velocity of pseudocumene oxidation.

High aqueous substrate and product concentrations also can impair biocatalyst activity in two-liquid phase systems (Kawakami and Nakahara, 1994). The avoidance of toxic aqueous substrate and product concentrations is crucial for the maintenance of high biocatalyst activities (Leon, et al., 1998). Aqueous concentrations of pseudocumene, 3,4-dimethylbenzyl alcohol, and 3,4-dimethylbenzaldehyde did not reach toxic levels and had no obvious effect on biocatalyst activity in the fed-batch experiments, but we observed toxic aqueous acid concentrations, which may have affected cell metabolism. Furthermore, the metabolic activity of the cells, which is necessary for NADH regeneration, is reduced in the late stationary phase anyway.

In general, at the beginning of the biotransformation, the specific product formation rate was dependent on the amount of pseudocumene present in the two-liquid phase system. With progression of the biotransformation, most probably biocatalyst activities were increasingly

influenced by toxic acid concentrations and other factors, such as the metabolic state of the cells in the late stationary phase.

### **Possible strategies towards the accumulation of a single product**

The exclusive accumulation of 3,4-dimethylbenzyl alcohol might be achieved by high pseudocumene concentrations in the BEHP/M9\* two-liquid phase system. At high substrate concentrations, we expect higher biocatalyst activities and, besides aldehyde formation, alcohol accumulation when the high  $V_{\max}$  of the pseudocumene oxidation dominates the low  $K_s$  for the alcohol (Table 3.1). Furthermore, high pseudocumene concentrations are expected to inhibit aldehyde formation, which could be further minimized by coexpression of benzyl alcohol dehydrogenase (Chapter 2). Exclusive 3,4-dimethylbenzaldehyde formation can be reached via substrate concentrations at which the alcohol oxidation rate equals or exceeds the pseudocumene oxidation rate. Coexpression of dehydrogenases is expected to impair aldehyde accumulation. Finally, exclusive 3,4-dimethylbenzoic acid formation may be reached by maintaining the organic pseudocumene concentration below 90 mM or by coexpression of benzaldehyde dehydrogenase and possibly also benzyl alcohol dehydrogenase.

The two dehydrogenases may also have contributed to the production of carboxylic acids from aromatic heterocycles in an industrial process developed by Lonza AG using the wild-type strain *Pseudomonas putida* mt-2 (Kiener, 1992). Acid production is limited in the BEHP/M9\* two-liquid phase system because the deprotonated form of the acid is poorly extracted by BEHP and therefore exerts toxic effects on the cells.

By controlling the pseudocumene concentration in a two-liquid phase system and selective coexpression of dehydrogenases, the process presented may be driven to the exclusive accumulation of the alcohol, aldehyde, or acid derivative of pseudocumene. This principle might also apply to other substrates of XMO. The experimental application of these strategies and the further characterization of the presented kinetically controlled multistep biotransformation system are topics of ongoing research.

### **ACKNOWLEDGMENTS**

This work was supported by the BASF Corporation (Ludwigshafen, Germany).

We thank Jim Spain for critical reading of the manuscript.

## CHAPTER 4

# **USE OF THE TWO-LIQUID PHASE CONCEPT TO EXPLOIT KINETICALLY CONTROLLED MULTISTEP BIOCATALYSIS**

**Bruno Bühler, Irene Bollhalder, Bernhard Hauer, Bernard  
Witholt, and Andreas Schmid**

Biotechnology and Bioengineering, 2003, 81(6):683-694.

## SUMMARY

The two-liquid phase concept was used to develop a whole-cell biocatalytic system for the efficient multistep oxidation of pseudocumene to 3,4-dimethylbenzaldehyde. Recombinant *Escherichia coli* cells were employed to express the *Pseudomonas putida* genes encoding xylene monooxygenase, which catalyzes the multistep oxygenation of one methyl group of toluene and xylenes to corresponding alcohols, aldehydes, and acids. A fed-batch based two-liquid phase bioconversion was established with bis(2-ethylhexyl)phthalate as organic carrier solvent and a phase ratio of 0.5; the product formation pattern, the impact of the nutrient feeding strategy, and the partitioning behavior of the reactants were studied. On the basis of the favorable conditions provided by the two-liquid phase system, engineering of the initial pseudocumene concentration allowed exploiting the complex kinetics of the multistep reaction for the exclusive production of 3,4-dimethylbenzaldehyde. Further oxidation of the product to 3,4-dimethylbenzoic acid could be inhibited by suitable concentrations of pseudocumene or 3,4-dimethylbenzyl alcohol. The optimized biotransformation setup includes a completely defined medium with high iron content and a nutrient feeding strategy avoiding severe glucose limitation as well as high inhibitory glucose levels. Using such a system on a 2-L scale, we were able to produce, within 14.5 h, 30 g of 3,4-dimethylbenzaldehyde as predominant reactant in the organic phase and reached a maximal productivity of 1.6 g per liter liquid volume per hour. The present study implicates that the two-liquid phase concept is an efficient tool to exploit the kinetics of multistep biotransformations in general.

## INTRODUCTION

Ongoing research activities are continuously revealing enzyme catalyzed chemical reactions of industrial interest (Faber, 2000; Schmid, et al., 2001; Burton, et al., 2002). Regio- and stereoselective biooxidations, an important field in biocatalysis, are often cofactor dependent (e.g., NADH, NADPH) and catalyzed by multicomponent enzyme systems, of which some are membrane associated. Thus, whole-cell in vivo cultures are usually favored over the use of isolated enzymes. Many potentially interesting substrates and products of such biotransformations are poorly water-soluble and/or toxic to living cells (Lilly, 1982; Nikolova and Ward, 1993; Salter and Kell, 1995; Leon, et al., 1998). Typically, these drawbacks are circumvented by regulated substrate addition and in situ product recovery (Freeman, et al., 1993; Lye and Woodley, 1999).

Two-liquid phase systems, consisting of an aqueous medium and an organic, water-immiscible solvent, present a valuable biotechnological tool for biotransformations of apolar compounds (Schwartz and McCoy, 1977; de Smet, et al., 1981b; Witholt, et al., 1992; Liu, et al., 1996; Wubbolts, et al., 1996a; Panke, et al., 2000). The concept allows high overall concentrations of toxic apolar chemicals within the two-liquid phase system, by regulating substrate and product concentrations in the aqueous biocatalyst microenvironment, and simple product recovery (Furuhashi, et al., 1986; Woodley and Lilly, 1990; Wubbolts, et al., 1994a; Leon, et al., 1998). Furthermore, the partitioning behavior of substrate and product can be exploited to avoid product inhibition, to guide equilibrium reactions into a desired direction, and even to enhance the enantiomeric excess (Kawakami and Nakahara, 1994; Salter and Kell, 1995; Faber, 2000; Gerrits, et al., 2001b; Willeman, et al., 2002a).

It is reasonable that the two-liquid phase concept might also be useful to control multistep biocatalysis. In Chapters 2 and 3, we characterized an interesting multistep reaction, which is catalyzed by xylene monooxygenase (XMO) of *Pseudomonas putida* mt-2. The membrane-associated XMO is the first enzyme in the upper xylene degradation pathway, in which toluene and xylenes are oxidized to corresponding carboxylic acids (Worsey and Williams, 1975; Abril, et al., 1989; Harayama, et al., 1992), consists of two polypeptide subunits (Harayama, et al., 1989; Suzuki, et al., 1991), the nonheme iron monooxygenase component XylM (Wubbolts, 1994; Shaw and Harayama, 1995) and the NADH:acceptor reductase component XylA (Shaw and Harayama, 1992), and it has a broad substrate range (Kunz and Chapman, 1981; Wubbolts, et al., 1994b). The *alk* regulatory system of *P. putida* GP01

(formerly known as *P. oleovorans* GPo1 = TF4-1L = ATCC 29347) (Grund, et al., 1975; Staijen, et al., 1999; van Beilen, et al., 2001) was successfully used for *xylMA* expression in recombinant *E. coli* (Panke, et al., 1999b). In Chapter 2, we demonstrated that such a whole-cell biocatalyst catalyzes the multistep oxidation of toluene and pseudocumene via benzyl alcohols and benzaldehydes to corresponding carboxylic acids, all steps via a monooxygenation type of reaction. Kinetic analyses of this multistep reaction showed that the substrates toluene and pseudocumene, as well as the corresponding alcohols, inhibit aldehyde oxygenation and that elevated substrate concentrations also weakly inhibit alcohol oxygenation (Chapter 3). The kinetics together with results of preliminary two-liquid phase biotransformations indicated that, depending on the reaction conditions, the product formation may be directed to one specific product.

The biocatalytic production of aromatic aldehydes from cheap substrates like xylenes is of particular interest, since enzymatic transformations are generally highly specific. Benzaldehydes represent important ingredients of natural flavors and fragrances and serve as synthons for a variety of polymers, pharmaceuticals, and fine chemicals (Bruehne and Wright, 1985; Falbe and Regitz, 1995). XMO based single-enzyme multistep catalysis is considered to suit the production of benzaldehydes best, since benzyl alcohol dehydrogenase, the second enzyme of the upper xylene degradation pathway (Shaw and Harayama, 1990; Shaw, et al., 1992; Shaw, et al., 1993), catalyzes an equilibrium lying, for thermodynamic reasons, on the side of benzyl alcohols (Chapter 2).

In this chapter, we report the utilization of the two-liquid phase concept to direct the kinetically controlled multistep bioconversion of pseudocumene to the accumulation of 3,4-dimethylbenzaldehyde (DMB-aldehyde). In fed-batch based two-liquid phase biotransformations with bis(2-ethylhexyl)phthalate (BEHP) as organic carrier solvent, we studied the product formation pattern, the impact of the nutrient feeding strategy, and the partitioning behavior of the reactants. As a proof of concept, an optimized biotransformation with DMB-aldehyde as predominant product is presented.



## MATERIALS AND METHODS

**Bacterial strain, plasmid, and chemicals.** *E. coli* JM101 (*supE thi Δ(lac-proAB) F'*[*traD36 proAB*<sup>+</sup> *lacI*<sup>f</sup> *lacZΔM15*]) (Messing, 1979), an *E. coli* K-12 derivative, was used as recombinant host strain. As expression vector, we used the pBR322-derived plasmid pSPZ3 containing the XMO genes *xy/MA* under the control of the *alk* regulatory system (Panke, et al., 1999b). The QIAprep Spin Miniprep Kit of Qiagen (Basel, Switzerland) was used to prepare plasmid DNA following the supplier's protocol. Chemicals were obtained from Fluka (Buchs, Switzerland) [pseudocumene, ~99%; 3,4-dimethylbenzoic acid (DMB-acid), ~97%; bis(2-ethylhexyl)phthalate (BEHP), 97%], Aldrich (Buchs, Switzerland) [3,4-dimethylbenzyl alcohol (DMB-alcohol), 99%], Lancaster (Muehlheim, Germany) [3,4-dimethylbenzaldehyde (DMB-aldehyde), 97%], and Acros Organics (Geel, Belgium) [*n*-octane, >98.5%].

**Media and growth conditions.** Bacteria were either grown in Luria-Bertani (LB) broth (Difco, Detroit, Mich.) or minimal media, MS or RB. Solid media contained 1.5% (wt/vol) agar and shaking flask cultures were routinely incubated on horizontal shakers at 200 rpm and 30°C. Complex media contained 50 mg L<sup>-1</sup> kanamycin and 10 g L<sup>-1</sup> glucose to avoid indigo formation (Panke, et al., 1999b). The MS medium is derived from M9 mineral medium (Sambrook, et al., 1989) and contained per liter 8.82 g KH<sub>2</sub>PO<sub>4</sub>, 10.85 g K<sub>2</sub>HPO<sub>4</sub>, 8.82 g Na<sub>2</sub>HPO<sub>4</sub>, 1.0 g NH<sub>2</sub>Cl, 0.5 g NaCl, 0.49 g MgSO<sub>4</sub>·7H<sub>2</sub>O, 5 g glucose, 10 mg thiamine, 50 mg kanamycin, and 1 ml trace element solution US\*, of which the composition is described in Chapter 2. NaOH (10 M) was used to adjust the pH to 7.1. Medium engineering resulted in the use of RB medium, which is derived from a medium developed for high cell density cultivations of *E. coli* and known to minimize the tendency of *E. coli* to form acetic acid (Riesenberg, et al., 1991). RB medium was composed of 13.3 g KH<sub>2</sub>PO<sub>4</sub>, 4.0 g (NH<sub>4</sub>)<sub>2</sub>HPO<sub>4</sub>, and 1.7 g citric acid per liter, sterilized, adjusted to pH 6.8 using 25% NH<sub>4</sub>OH and to pH 7.1 using NaOH (10 M), and supplemented with 1.2 g MgSO<sub>4</sub>·7H<sub>2</sub>O, 5 g glucose or glycerol, 10 mg thiamine, 50 mg kanamycin, and 1 ml US\* per liter. Other refinements were the increase of the FeSO<sub>4</sub>·7H<sub>2</sub>O content in US\* from 4.87 to 8.87 g L<sup>-1</sup> resulting in trace element solution US<sup>Fe</sup>, the addition of 5 (instead of 1) ml US<sup>Fe</sup> to 1 liter batch medium, and batch and fed-batch cultivation without kanamycin. An initial glucose (or glycerol) concentration of 7 g L<sup>-1</sup> allowed batch growth to 4-4.5 (g of CDW) L<sup>-1</sup>, which guaranteed optimal bioconversion performance.

**Analysis of metabolites.** The quantitative analysis of *n*-octane, pseudocumene, DMB-alcohol, DMB-aldehyde, and DMB-acid was performed via gas chromatography (GC) and high-performance liquid chromatography (HPLC) as described in Chapters 2 and 3, respectively.

**Determination of partition coefficients in the BEHP/MS two-liquid phase system.** Varying amounts of pseudocumene, DMB-alcohol, DMB-aldehyde, and DMB-acid were added to equal volumes (1 ml) of BEHP and complete MS medium containing either glucose or glycerol. The system was allowed to equilibrate under vigorous shaking and left overnight without shaking. The phases were separated by centrifugation. The organic and aqueous phases were diluted in and extracted with diethyl ether, respectively. The concentrations in the two phases were determined by GC and HPLC, and the partition coefficients were calculated. Measurements were performed at least three times independently.

**Two-liquid phase cultures.** A stirred tank reactor with a total volume of 3 L (Preusting, et al., 1993; Wubbolts, et al., 1996a) was used for the biotransformations. Precultivation and batch cultivation of freshly transformed *E. coli* JM101 (pSPZ3) were performed as described in Chapter 3. The pH was maintained at 7.1 using 25% NH<sub>4</sub>OH and 34% phosphoric acid. Batch cultures were stirred at 1500 rpm for 9 to 12 hours (overnight), during which time the initial carbon source and metabolic by-products (e.g., acetic acid) were consumed completely, whereupon the cultures were supplemented with (per liter) additional 4 ml of trace element solution and 4 ml of a 1% (wt/vol) thiamine solution. Subsequently, fed-batch cultivation was initiated by continuously adding 4-20 g h<sup>-1</sup> of an aqueous feeding solution, which was filter-sterilized. The feeding solution contained per liter 450 g glucose, 9 g MgSO<sub>4</sub>·7H<sub>2</sub>O, and optionally 50 g yeast extract (Difco, Detroit, MI), when MS medium was used, and 730 g glucose (or 1160 g glycerol) and 19.6 g MgSO<sub>4</sub>·7H<sub>2</sub>O, when RB medium was used. One hour after feed initiation, the biotransformation was started by the addition of 1 L organic phase consisting of bis(2-ethylhexyl)phthalate (BEHP) as carrier solvent, 1% (vol/vol) *n*-octane as inducer of the *alk* regulatory system, and variable amounts of pseudocumene as substrate (time point of induction). Concomitantly, the stirrer speed was increased to 2000 rpm. Foam formation was limited by the addition of antifoam 289 (Sigma, Buchs, Switzerland).

**Bioconversion analytics.** The dissolved oxygen tension (DOT) was determined with an autoclavable amperometric probe (Mettler Toledo, Greifensee, Switzerland). Cell densities as well as octane, pseudocumene, DMB-alcohol, DMB-aldehyde, and DMB-acid concentrations in the organic and the aqueous phase were determined as described in Chapter 3 and monitored over time. The apparent volumetric productivities and specific product formation

rates were calculated as averages for intervals between two data points. The term “apparent” refers to the fact that activities may have been limited by substrate availability. Furthermore, since DMB-aldehyde and DMB-acid accumulation from pseudocumene demand multiple oxidation steps catalyzed by a single monooxygenase, apparent accumulation rates cannot be related directly to specific DMB-aldehyde and DMB-acid formation rates. Aqueous phase concentrations of glucose, glycerol, and acetic acid were determined by the use of enzymatic kits provided by Roche Diagnostics (Rotkreuz, Switzerland) and Sigma (Buchs, Switzerland). Diastix reagent strips (Bayer, Zurich, Switzerland) were used for preliminary estimation of glucose concentrations. Alternatively, acetic acid concentrations were determined by GC, using a HP 5890 Series II gas chromatograph (Hewlett Packard, Palo Alto, USA) equipped with a fused silica capillary column PERMABOND CW20M (25 m; inner diameter, 0.25 mm; film thickness, 0.25  $\mu$ m) from Macherey-Nagel (Oensingen, Switzerland) with helium as the carrier gas. Fifty  $\mu$ l aqueous culture supernatant were mixed with 350  $\mu$ l distilled water, 50  $\mu$ l phosphoric acid (85%), and 50  $\mu$ l of 100 mM sodium butyrate as an internal standard. After injection the following temperature profile was applied: 85°C for 0.5 min, from 85 to 110°C at 12°C/min, from 110 to 200°C at 70°C/min, and 200°C for 2.5 min. Compounds were detected with a flame ionization detector.

## RESULTS

In Chapter 2, we demonstrated that recombinant *E. coli* containing XMO catalyze the multistep oxygenation of pseudocumene and toluene to corresponding benzylic alcohols, aldehydes, and acids. Furthermore, we reported that two-liquid phase biotransformations based on growing fed-batch cultures with BEHP as organic carrier solvent containing pseudocumene showed consecutive accumulation of DMB-aldehyde, DMB-alcohol, and DMB-acid (Chapter 3). Table 4.1 contains key parameters of such a biotransformation, which is referred to as biotransformation I in the present chapter. Based on kinetic analyses, the switch from exclusive accumulation of DMB-aldehyde in a first stage to exclusive accumulation of DMB-acid in a second stage was explained by inhibition of DMB-aldehyde oxidation by pseudocumene at organic phase concentrations above 90 mM but not below. In order to evaluate, whether the two-liquid phase concept can be used to efficiently produce

**Table 4.1. Two-liquid phase biotransformations with varying initial pseudocumene concentrations and feed rates.\***

Parameter	Unit	Biotransformations			
		I <sup>a</sup>	II	III	IV
Initial [pseudocumene] <sub>org</sub>	mM	165	840	320	163+2*41
Feed rate	g·h <sup>-1</sup>	10	10	20->10	20->15->12
DMB-aldehyde production period (from induction on)	h	9.5	14	17	25.5
[Pseudocumene] <sup>b</sup>	mM	90	540	10.5	29
[DMB-alcohol] <sup>b</sup>	mM	1.2	204	75	66
[DMB-acid] <sup>b</sup>	mM	6.4	2.6	7.2	5.8
<b>[DMB-aldehyde]<sup>b</sup></b>	<b>mM</b>	<b>64</b>	<b>118</b>	<b>216</b>	<b>140</b>
<b>DMB-aldehyde produced</b>	<b>g</b>	<b>7.4</b>	<b>15.8</b>	<b>29</b>	<b>18.8</b>
Molar yield	%	39	14	67	58
Maximal specific activity <sup>c</sup>	U (g of CDW) <sup>-1</sup>	13.5	42	28	13.5
Maximal specific activity <sub>ald</sub>	U (g of CDW) <sup>-1</sup>	13	15	14	13
Maximal volumetric activity <sub>ald</sub>	U L <sub>aq</sub> <sup>-1</sup>	133	200	340	167
Average volumetric activity <sub>ald</sub>	U L <sub>aq</sub> <sup>-1</sup>	112	150	212	91
Cell concentration 10 h after feed initiation	(g of CDW) L <sub>aq</sub> <sup>-1</sup>	18	16.5	25	23

\* Subscripts: org, organic phase; aq, aqueous phase; ald, referring to DMB-aldehyde formation.

<sup>a</sup> Adapted from Chapter 3.

<sup>b</sup> Sum of respective organic and aqueous phase concentrations after DMB-aldehyde production period.

<sup>c</sup> Based on sum of all products.

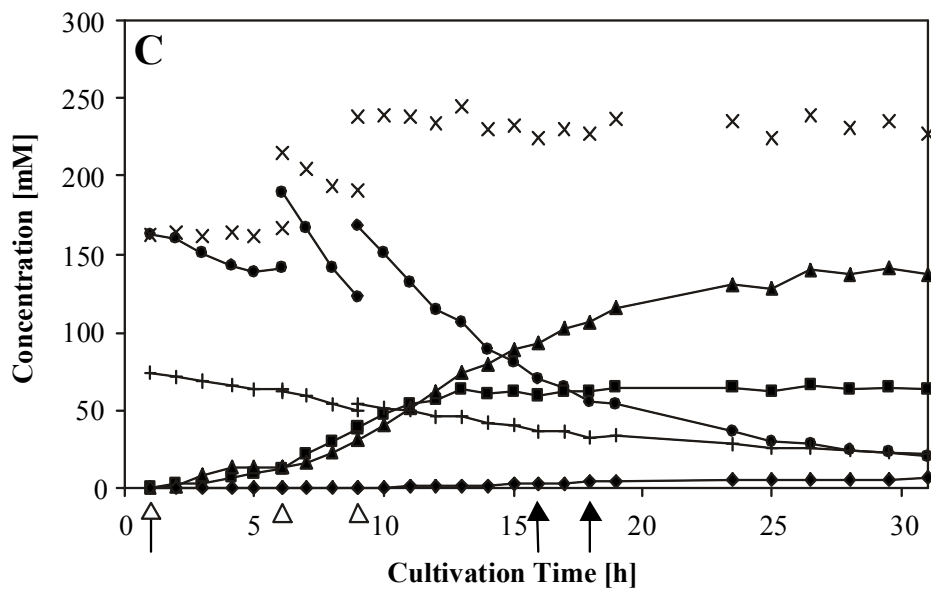
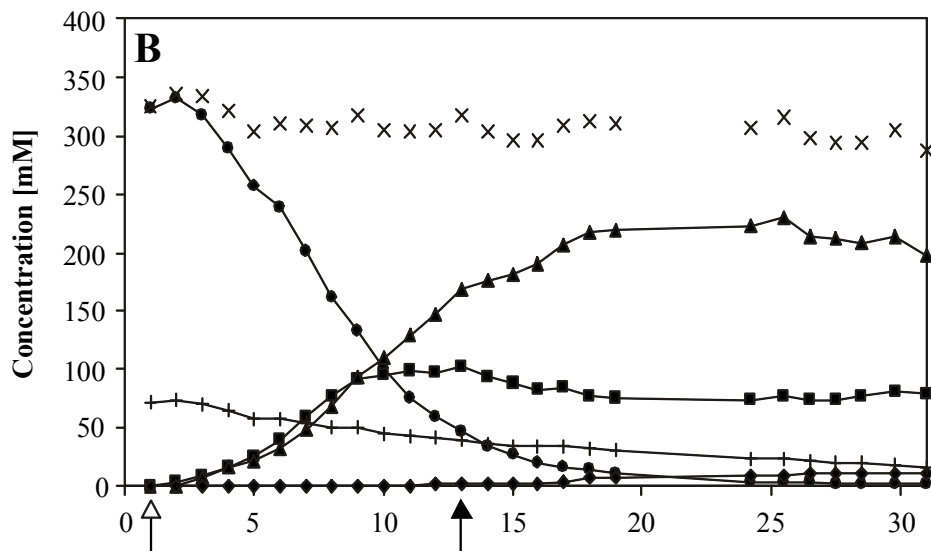
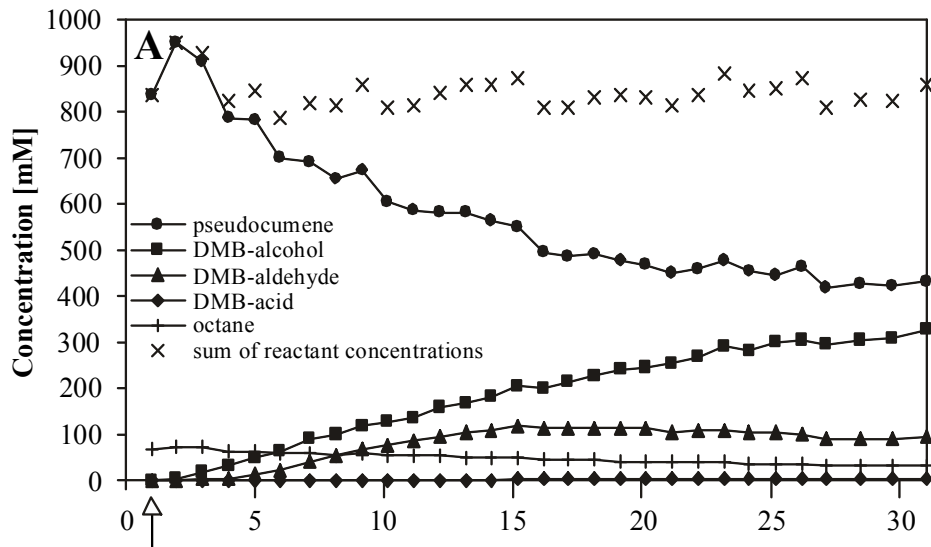
DMB-aldehyde via a kinetically controlled multistep oxidation of pseudocumene, we investigated the characteristics of such biotransformations. In a second part, we present the resulting optimizations and their final implementation.

## BIOCONVERSION CHARACTERISTICS

In order to analyze the product formation pattern, the impact of the nutrient feeding strategy, and the partitioning behavior of the reactants, we performed biotransformations with varying initial pseudocumene concentrations, feed rates, and feed compositions and we determined partition coefficients in the absence of cells. In initial biotransformation experiments, *E. coli* JM101 (pSPZ3) were grown in MS mineral medium (see Materials and Methods). The results of three representative experiments (biotransformations II, III, and IV) are shown in Figure 4.1 and summarized in Table 4.1. Reactant concentrations represent the sum of respective organic and aqueous phase concentrations. Specific product formation rates are based on the sum of all products formed over time and correspond to the pseudocumene oxidation rates. Below, the impact of the substrate concentration, variations of feed rate and feed composition, and reactant partitioning are treated in three separate sections.

### **Substrate concentration.**

To study product formation at high substrate concentrations, we performed an experiment with an initial pseudocumene concentration of 840 mM in the organic phase (biotransformation II, Fig. 4.1, A and D). Feed and aeration rates were set at 10 g h<sup>-1</sup> and 0.5 L min<sup>-1</sup>, respectively. The culture was not oxygen limited throughout the whole experiment. Growth was not affected by the organic phase and the cell concentration increased to 20 (g of CDW) L<sup>-1</sup>. After a short induction period, DMB-alcohol and DMB-aldehyde accumulated simultaneously, DMB-alcohol at a higher rate than DMB-aldehyde (Fig. 4.1A). Fourteen hours after organic phase addition, the aqueous alcohol concentration had increased to 5.6 mM, which is toxic for *E. coli* JM101 (Chapter 3). Thereafter, DMB-alcohol accumulated as the only product. Overall, only minor DMB-acid accumulation was observed. The maximal specific product formation rate [42 U (g of CDW)<sup>-1</sup>] was significantly higher than in biotransformation I (Table 4.1). This points to a rate limitation of the first oxidation step by the substrate concentration. During the biotransformation, the specific product formation rate decreased continuously (Fig. 4.1D), which can be ascribed to the decreasing pseudocumene concentration and to toxic effects of increasing aqueous DMB-alcohol concentrations. The maximal specific DMB-aldehyde formation rate [15 U (g of CDW)<sup>-1</sup>] was only slightly higher than in biotransformation I (Table 4.1), suggesting the existence of a critical pseudocumene concentration, above which the DMB-alcohol oxidation rate no longer increases and DMB-alcohol also accumulates.



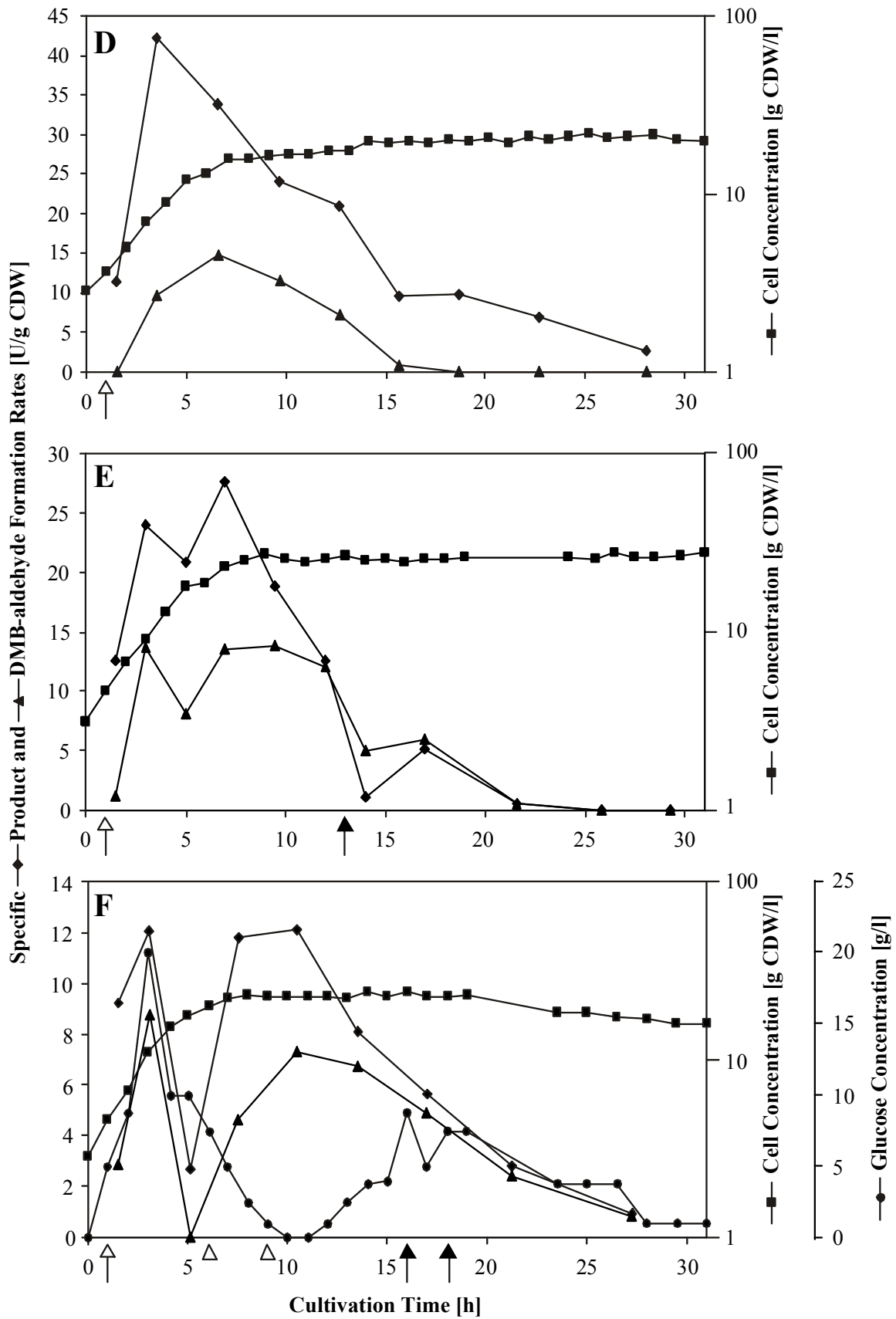


**Figure 4.1. Fed-batch based two-liquid phase biotransformations using the MS medium, *E. coli* JM101 (pSPZ3) as biocatalyst, and BEHP as organic carrier solvent containing variable volume fractions of pseudocumene and 1% (vol/vol) *n*-octane (phase ratio: 0.5).** Addition of the organic phase occurred 1 h after feed initiation (open arrow). Experimental details are described in Materials and Methods. (A and D) Biotransformation II: initial organic pseudocumene concentration, 840 mM; feed rate, 10 g h<sup>-1</sup>. (B and E) Biotransformation III: initial organic pseudocumene concentration, 320 mM; initial feed rate, 20 g h<sup>-1</sup>, after 13 h reduced to 10 g h<sup>-1</sup> (closed arrow). (C and F) Biotransformation IV: initial organic pseudocumene concentration, 163 mM; two pseudocumene pulses (5 ml, arrowheads); initial feed rate, 20 g h<sup>-1</sup>, after 16 and 18 h reduced to 15 and 12 g h<sup>-1</sup>, respectively (closed arrows). (A-C) Course of reactant and octane concentrations. All concentrations represent the sum of the respective concentrations in the organic and the aqueous phase. (D-F) Course of biomass formation and specific DMB-aldehyde and product (sum of all products) formation rates calculated as averages for intervals between two data points. (F) Additionally, the course of glucose concentration is shown.

In order to define such a critical pseudocumene concentration, biotransformations with lower initial pseudocumene concentrations were carried out. Panels B and E of Figure 4.1 show an experiment with an initial organic substrate concentration of 320 mM (biotransformation III). Simultaneous DMB-aldehyde and DMB-alcohol accumulation was followed by exclusive DMB-aldehyde formation and DMB-alcohol consumption (Fig. 4.1B). This indicates that the DMB-alcohol formation rate exceeds the DMB-aldehyde formation rate above but not below pseudocumene concentrations of about 150 mM. The lack of significant DMB-acid accumulation at pseudocumene concentrations below 90 mM can be explained by the high aqueous DMB-alcohol concentration (2.5–1.7 mM) in the time period under consideration. In Chapter 3, we showed that benzyl alcohols also inhibit benzaldehyde oxygenation. The exclusive DMB-aldehyde formation at substrate concentrations between 150 and 90 mM and the inhibition of DMB-aldehyde oxygenation by DMB-alcohol at pseudocumene concentrations below 90 mM may be exploited for the production of DMB-aldehyde

#### **Feed rate and feed composition.**

Since the availability of glucose is crucial for cofactor regeneration and growth to high cell (biocatalyst) concentrations, a higher initial feed rate (20 instead of 10 g h<sup>-1</sup>) was tested in biotransformation III (Fig. 4.1, B and E). The reactor was aerated at a rate of 1 L min<sup>-1</sup>, and the culture was oxygen limited between 4 and 6 h of fed-batch cultivation. As a consequence of the higher feed rate, cells grew faster to a higher cell density, with a maximum at 27 (g of CDW) L<sup>-1</sup>. The specific product and DMB-aldehyde formation rates were transiently reduced



4 h after induction followed by an increase to maxima of 28 and 14 U (g of CDW)<sup>-1</sup>, respectively (Fig. 4.1E). The specific DMB-aldehyde formation rate remained high for 11 h and its maximum was similar as in biotransformation II, indicating that specific activities are independent of the cell concentration. After 13 h, harsh glucose limitation, caused by a feed rate reduction from 20 to 10 g h<sup>-1</sup>, reduced biocatalyst activity. However, the higher glucose feed rate over 13 h enabled higher cell concentrations and thereby improved volumetric DMB-aldehyde formation rates (Table 4.1).

Severe glucose limitation was prevented in biotransformation IV (Fig. 1, C and F). The initial organic pseudocumene concentration amounted to 163 mM, and 5 ml pseudocumene were pulsed twice. Feed and aeration rate were set at 20 g h<sup>-1</sup> and 1 L min<sup>-1</sup>, respectively. Growth was similar as in biotransformation III, and a short-term oxygen limitation was observed after 3.5 h. After the expected accumulation of DMB-aldehyde and little DMB-alcohol in the beginning of the biotransformation, specific activities decreased to very low levels and only DMB-alcohol was formed. Two observations point to an inhibition of biocatalyst activity by high glucose concentrations: the high glucose concentration (20 g L<sup>-1</sup>) 1 h before activity loss and the retrieval of specific activities, when cell growth caused a decrease of the glucose concentration. As described above, a transient activity reduction was also observed in biotransformation III even though to a lower extent, which may be due to the lower maximal glucose concentration as a consequence of the higher cell concentration before feed initiation [3.1 instead of 2.8 (g of CDW) L<sup>-1</sup>]. A harmful effect of oxygen limitation on biocatalyst activity can be ruled out, since, in biotransformation I (Table 4.1), oxygen limitation for as long as 5 h had no detectable influence on biocatalyst activity (Chapter 3).

The two pseudocumene additions during biotransformation IV increased the pseudocumene concentration to 190 and 170 mM, respectively (Fig. 4.1C). Thus, DMB-alcohol and DMB-aldehyde accumulated simultaneously after recovery of biocatalyst activity. The switch to exclusive DMB-aldehyde accumulation and the lack of DMB-acid formation confirmed the product formation pattern depicted above. High volumetric DMB-aldehyde productivities could be maintained for 6 h between 9 and 15 h of fed-batch cultivation with high cell and low glucose concentrations. After 11 h, the glucose concentration increased due to the decreasing metabolic activity of stationary phase cells. In order to avoid inhibitory glucose concentrations, the feed rate was reduced twice, to 15 and 12 g h<sup>-1</sup>. On the one hand, preventing severe glucose limitation and thus providing enough substrate for NADH regeneration prolonged the aldehyde production period. On the other hand, high glucose concentrations seem to provoke low biocatalyst activities.

Furthermore, we tested the influence of yeast extract on the performance of the bioconversion. A feed without yeast extract might be advantageous, since yeast extract stabilizes emulsions and thereby complicates phase separation. The undefined nature of yeast extract may generally be a drawback in product work up. In comparable experiments (initial substrate concentration: 120 mM; feed rate: 10 g h<sup>-1</sup>), yeast extract had no influence on the product formation pattern. Exclusive DMB-aldehyde formation was followed by DMB-acid accumulation. However, omitting yeast extract slightly reduced the specific activity and the growth rate in the exponential growth phase (Table 4.2). Since XMO is an iron-containing enzyme, the additional iron in yeast extract might have allowed faster growth and bioconversion (Staijen and Witholt, 1998). Moreover, yeast extract in the feeding solution allowed growth to higher cell concentrations (Table 4.2), which can be attributed to additional growth substrates provided with yeast extract. The higher cell densities and specific activities obtained with yeast extract resulted in higher volumetric aldehyde formation rates. A higher iron content in the medium and optimization of the feeding strategy might compensate for the absence of yeast extract in the feeding solution.

#### **Partitioning behavior of the reactants.**

As reported in Chapter 3, pseudocumene, DMB-alcohol, and DMB-aldehyde are highly and DMB-acid is moderately toxic for *E. coli* JM101 (Table 4.3). The two-liquid phase concept was chosen to overcome toxicity and solubility problems. As required, the chosen carrier solvent BEHP does not affect growth of *E. coli* JM101 (Panke, et al., 2000), and pseudocumene can be added up to a volume fraction of 10% of the organic phase without any influence on the growth behavior of *E. coli* JM101 (Chapter 3). In order to evaluate toxicities, kinetics, and effectiveness of product extraction, we determined the partition coefficients for all reactants in the BEHP based two-liquid phase system (Table 4.3). We found a very high partition coefficient for pseudocumene, enabling high overall substrate levels in the system. The more polar DMB-alcohol and DMB-aldehyde also partition mainly into the organic phase, whereas most of the DMB-acid is found in the aqueous phase at neutral pH. In the case of pseudocumene depletion, the considerably lower partition coefficient for DMB-alcohol than for DMB-aldehyde offers the possibility to inhibit DMB-aldehyde oxidation by relatively low overall DMB-alcohol concentrations. Furthermore, the high partition coefficient for DMB-aldehyde allows high overall product levels and facilitates down-stream processing. Partition coefficients were not influenced by the presence of glucose and glycerol in the reaction medium.

**Table 4.2. Influence of yeast extract.\***

Parameter	Unit	With yeast extract <sup>a</sup>	Without yeast extract <sup>a</sup>
Growth rate <sup>b</sup>	h <sup>-1</sup>	0.36	0.31
Maximal specific activity <sup>c</sup>	U (g of CDW) <sup>-1</sup>	13	10
Maximal cell concentration	(g of CDW) L <sub>aq</sub> <sup>-1</sup>	22	12.5
Maximal volumetric activity <sub>ald</sub>	U L <sub>aq</sub> <sup>-1</sup>	95	55

\* Subscripts: aq, aqueous phase; ald, referring to DMB-aldehyde formation.

<sup>a</sup> In the feeding solution.

<sup>b</sup> In the exponential growth phase of the fed-batch.

<sup>c</sup> Based on sum of all products.

**Table 4.3. Partition coefficients in a two-liquid phase system with BEHP as carrier solvent.\***

Substance	Partition coefficient $K_p$ <sup>a</sup>	Critical concentration [mM] <sup>b</sup>
Pseudocumene	24,300 ± 1500	0.5 - 1
DMB-alcohol	50 ± 3	2 - 4
DMB-aldehyde	906 ± 20	1 - 3
DMB-acid	0.118 ± 0.005	16 - 24

\* The aqueous phase consisted of complete MS medium containing 5 g L<sup>-1</sup> glucose. Phase ratio: 0.5.

<sup>a</sup> The partition coefficient  $K_p$  is specified as the concentration in the organic phase divided by the concentration in the aqueous phase.

<sup>b</sup> Concentration range in an aqueous one-phase system, in which toxic effects were observed; adapted from Chapter 3.

In order to evaluate the partitioning behavior during the biotransformations, we compared measured aqueous reactant concentrations with aqueous concentrations calculated via partition coefficients from organic concentrations. Data for the comparison shown in Figure 4.2 were taken from biotransformation IV. Similar correlations were observed in all biotransformation experiments performed. Since pseudocumene concentrations in the aqueous

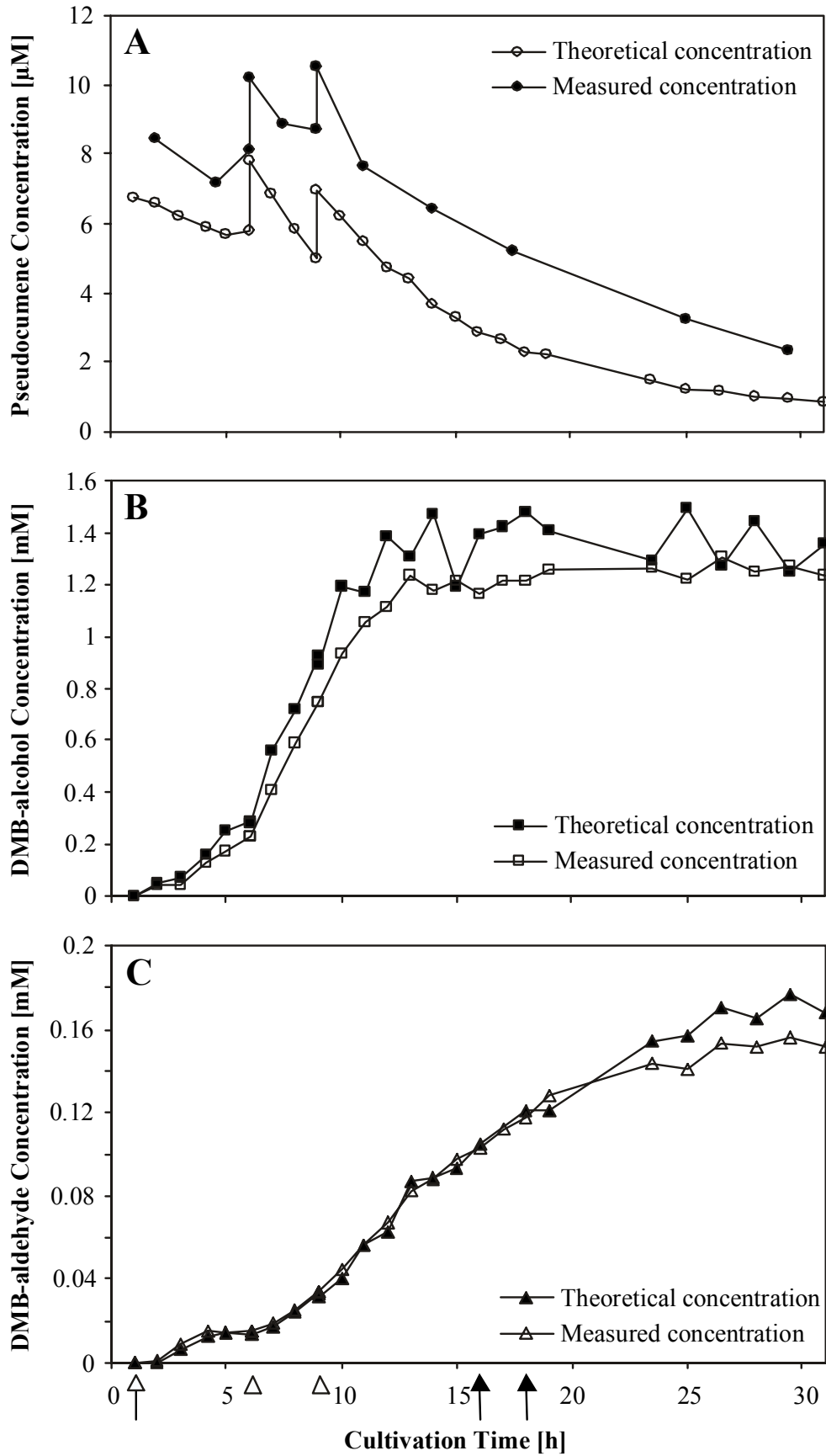


**Figure 4.2. Comparison of concentrations measured in the aqueous phase and theoretical concentrations calculated from concentrations in the organic phase and partition coefficients.** Data for the comparison were taken from biotransformation IV (Table 4.1). (A) Pseudocumene concentrations (averages of temporally consecutive determinations); (B) DMB-alcohol concentrations; (C) DMB-aldehyde concentrations. For further specifications see legend of Figure 4.1.

phase were close to the detection limit, data variance was 30-50%. In addition, very minor organic phase contaminations in aqueous phase samples cause major distortions of results. Considering all possible sources of error and the high variance, the pseudocumene concentrations measured in the aqueous phase correlated well with concentrations derived from organic phase concentrations and partition coefficients (Fig. 4.2A). Better correlations were found for DMB-alcohol and DMB-aldehyde (Fig. 2, B and C). For pseudocumene and DMB-alcohol, measured aqueous concentrations tended to exceed concentrations calculated via the partition coefficients. DMB-aldehyde concentrations measured in the aqueous phase exceeded the theoretical values only at the very end of the biotransformation, when cell lysis, due to the surfactant-like nature of cell debris, is expected to cause higher solubilities. For DMB-acid such a comparison was not made, since stopping the reaction in the samples by acidification and concomitant protonation of DMB-acid significantly changed its partitioning behavior. Obviously, the presence of cells and varying nutrient concentrations did not substantially influence the partitioning behavior of pseudocumene, DMB-alcohol, and DMB-aldehyde.

As shown in Chapter 3, a pseudocumene volume fraction of 25% in the organic phase severely inhibits growth. According to the partition coefficient, such an organic pseudocumene concentration corresponds to an aqueous concentration of 75  $\mu\text{M}$ . However, pseudocumene up to a concentration of 300  $\mu\text{M}$  only marginally affected growth of *E. coli* JM101 in an aqueous one-phase system (Chapter 3). When exposed to the two-liquid phase system, the cells sense more pseudocumene than present in the aqueous phase. The divergence of measured aqueous pseudocumene concentrations from concentrations calculated via the partition coefficient (Fig. 4.2A) is too small and unsure to completely explain such sensitivity to pseudocumene. An alternative explanation is that direct interaction between cells and solvent droplets might have additional toxic effects, thus increasing the apparent sensitivity to aqueous phase pseudocumene. Accordingly, and for toluene as substrate, tetradecane as carrier solvent, and *P. putida* as biocatalyst, Collins et al. (Collins, et

al., 1995) found that the toluene concentration in the organic phase is critical and that, at subtoxic toluene levels in the aqueous phase, the biocatalyst can be inactivated via the interface.

Altogether, the partitioning behavior of the reactants in the BEHP-based two-liquid phase system seems to be suitable for DMB-aldehyde production from pseudocumene.

### OPTIMIZATION OF THE BIOCONVERSION

Medium engineering resulted in the use of RB medium with increased iron content (see Materials and Methods). On the basis of the minimal iron requirement of recombinant *E. coli* containing a nonheme iron monooxygenase, which was reported to be  $3 \mu\text{mol (g of CDW)}^{-1}$  (Staijen and Witholt, 1998), the total amount of iron in the biotransformation medium corresponds to the threefold amount minimally required for  $30 \text{ (g of CDW) L}^{-1}$  monooxygenase containing *E. coli* and is supposed to accomplish also the iron requirement in the stationary phase. Under non-oxygen limited conditions, acetic acid formation normally is prevented by glucose limitation. However, biotransformation experiments with our system and RB medium showed that glucose limitation reduces, but does not completely prevent acetic acid formation, which may be explained by additional metabolic stress caused by the synthesis and presence of active XMO. Biocatalyst activity was not influenced by acetic acid concentrations up to  $20 \text{ g L}^{-1}$  (results not shown), even though cell growth was reported to be inhibited by far lower acetic acid concentrations (Luli and Strohl, 1990). Further improvements were achieved by engineering the initial glucose concentration and omitting kanamycin (see Materials and Methods). Unexpectedly, cultivation without kanamycin in the biotransformation medium allowed good plasmid stability and had no impact on bioconversion performance. Omitting kanamycin simplifies wastewater treatment in the down-stream processing. The described changes allowed omitting yeast extract in the feeding solution and reduced medium costs in general.

#### **Implementation: repeated fed-batch.**

As a proof of concept, we performed two consecutive biotransformations (biotransformations V and VI), including all the changes described above. In order to simplify the up-stream processing and to shorten the overall bioconversion time, we chose a repeated fed-batch mode of cultivation in the absence of kanamycin. After batch and 15.5 h of fed-batch cultivation, biotransformation V was stopped and the reaction broth was removed from the bioreactor

except for 10 ml of the emulsion, which served as an inoculum for a second batch culture in fresh medium. The following 15.3 h of fed-batch cultivation included biotransformation VI. The initial aeration rate was  $1 \text{ L min}^{-1}$  in both biotransformations. By regulating aeration rate and stirrer speed, the DOT was kept above 10% saturation. For both biotransformations, we chose initial substrate concentrations of about 4.3% (vol/vol) in the organic phase. Key bioconversion parameters are summarized in Table 4.4.

The product formation patterns of the two consecutive biotransformations were very similar (Fig. 4.3, A and D). Simultaneous accumulation of DMB-alcohol and DMB-aldehyde was followed by exclusive DMB-aldehyde formation and DMB-alcohol consumption. At the end of biotransformation V, DMB-aldehyde accounted for 92% of all reactants in the organic phase. Prolongation of biotransformation VI may also have resulted in a further reduction of DMB-alcohol and pseudocumene concentrations. In the two biotransformations, again, only minor DMB-acid accumulation was observed. The maximal specific product and DMB-aldehyde formation rates were equal in both experiments and similar to the rates measured in biotransformation III (Table 4.1, Fig. 4.1E). The volumetric DMB-aldehyde productivities reached maxima at the beginning of the stationary phase, when cell concentrations and specific DMB-aldehyde formation rates were highest (Fig. 4.3). Considering that two oxygenation steps are involved in the formation of DMB-aldehyde from pseudocumene, the average volumetric DMB-aldehyde formation rates of about  $250 \text{ U L}_{\text{aq}}^{-1}$  correspond to average volumetric oxygenation rates of  $500 \text{ U L}_{\text{aq}}^{-1}$ .

By choosing an initial feed rate of  $12.2 \text{ g h}^{-1}$ , accumulation of glucose to inhibitory levels was avoided. After initial glucose accumulation, increasing cell densities caused a decrease of glucose concentrations (Fig. 4.3, C and F). Glucose limitation caused a switch from exponential to linear growth. In order to support high cell concentrations, the feed rate was increased stepwise. In both fed-batch cultivations, glucose limitation resulted in a reduced formation of acetic acid. During biotransformation VI, the acetic acid concentration even decreased when the culture entered glucose limitation. In the stationary phase, glucose accumulated and acetic acid formation increased.

The very similar performance of the two consecutive biotransformations (Table 4.4) indicates that *xy/IMA* expression was stable without selection pressure for 50 h and 11 generations, which was confirmed by selective plating (data not shown). In the end of the biotransformations, similar product concentrations and yields were achieved. However, we

**Table 4.4. Optimized two-liquid phase biotransformations.\***

Parameter	Unit	Glucose as C-source		Glycerol as C-source
		Biotransformation V	Biotransformation VI	Biotransformation VII
Growth rate <sup>a</sup>	h <sup>-1</sup>	0.37	0.33	0.25
Maximal CDW reached	g liter <sup>-1</sup>	30	27.5	25
Biotransformation time (from induction on)	h	14.5	14.25	16.7
Initial [pseudocumene] <sub>org</sub>	mM	315	300	400
[Pseudocumene] <sup>b</sup>	mM	9	23	90
[DMB-alcohol] <sup>b</sup>	mM	10	37	75
[DMB-acid] <sup>b</sup>	mM	9	4.6	15
<b>[DMB-aldehyde]<sup>b</sup></b>	<b>mM</b>	<b>220</b>	<b>206</b>	<b>200</b>
<b>DMB-aldehyde produced</b>	<b>g</b>	<b>29.5</b>	<b>27.6</b>	<b>26.8</b>
Molar yield	%	70	69	50
Maximal specific activity <sup>c</sup>	U (g of CDW) <sup>-1</sup>	27	27	45
Maximal specific activity <sub>ald</sub>	U (g of CDW) <sup>-1</sup>	16	16	22
Maximal volumetric activity <sub>ald</sub>	U liter <sub>aq</sub> <sup>-1</sup>	390	320	340
Average volumetric activity <sub>ald</sub>	U liter <sub>aq</sub> <sup>-1</sup>	253	241	200
Average productivity <sub>ald</sub>	g liter <sub>tot</sub> <sup>-1</sup> h <sup>-1</sup>	1	1	0.8

\* Subscripts: org, organic phase; aq, aqueous phase; ald, referring to DMB-aldehyde formation.

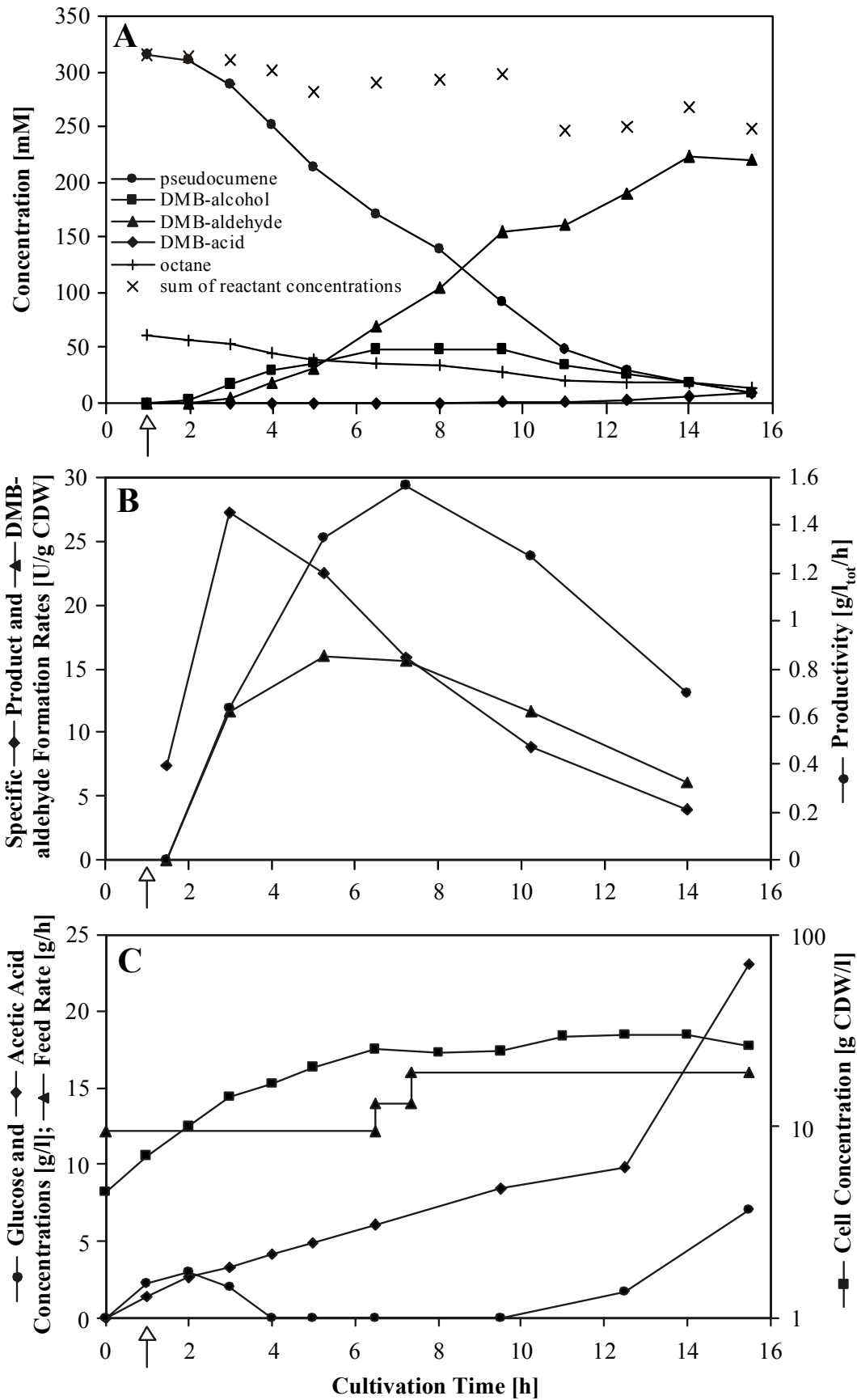
<sup>a</sup> In the exponential growth phase of the fed-batch.

<sup>b</sup> Sum of respective organic and aqueous phase concentrations at the end of the biotransformation.

<sup>c</sup> Based on sum of all products.

observed a difference in oxygen demand, which was higher in biotransformation V. In biotransformation VI, increasing the stirrer speed sufficed to meet the increasing oxygen demand, whereas in biotransformation V, additionally, an increase of the aeration rate was necessary. The diverse aeration during the two bioconversions resulted in differential pseudocumene and octane evaporation.





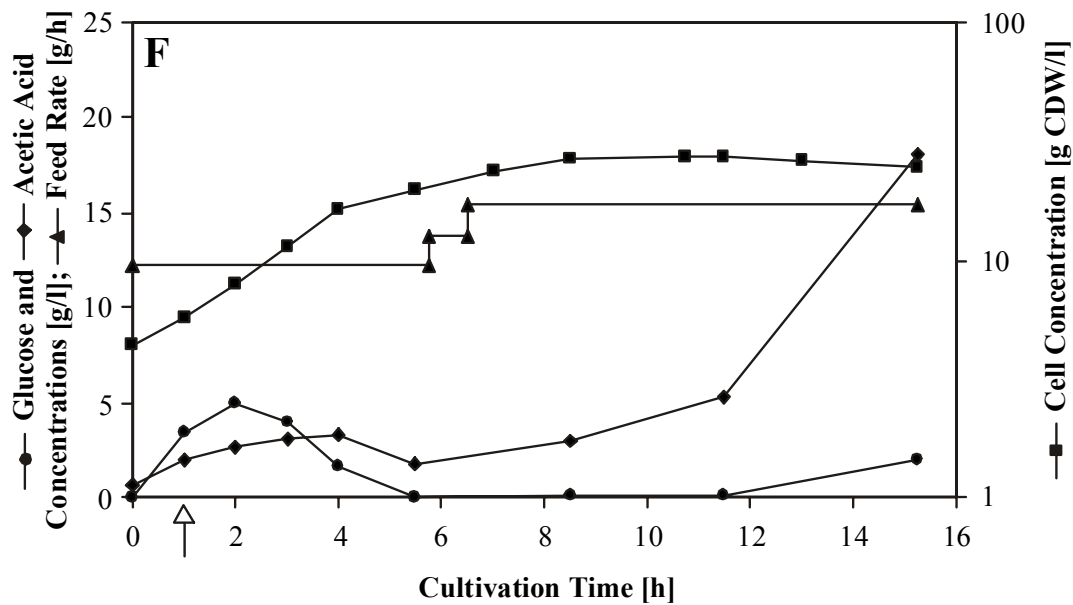
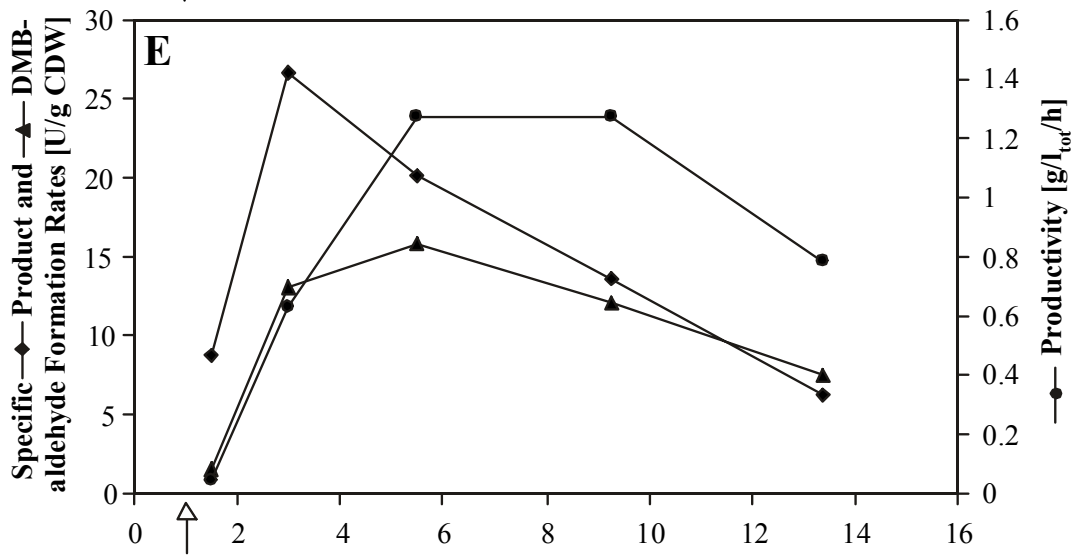
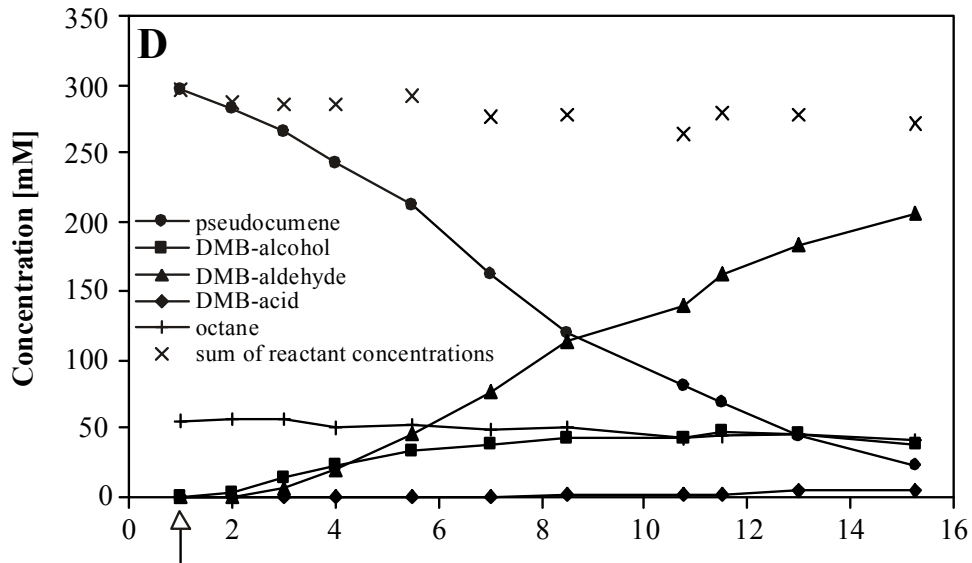


**Figure 4.3. Repeated fed-batch based biotransformations using the optimized RB medium without kanamycin.** The proceeding was as described for Fig. 4.1. (A, B, and C) Biotransformation V. (D, E, and F) Biotransformation VI. (A and D) Course of reactant and octane concentrations. All concentrations represent the sum of the respective concentrations in the organic and the aqueous phase. (B and E) Course of DMB-aldehyde productivity and specific DMB-aldehyde and product (sum of all products) formation rates, calculated as averages for intervals between two data points. (C and F) Course of glucose and acetic acid concentrations, biomass formation, and feed rate.

Finally, we evaluated the efficiency of the bioconversion with glycerol instead of glucose as growth substrate. *E. coli* is known to produce less acetic acid when grown on glycerol. As expected, growth on glycerol was slower than on glucose, and acetic acid accumulated only in the stationary phase. Similar maximal cell densities were reached. However, specific product and DMB-aldehyde formation rates were higher. Furthermore, the substrate concentration, at which the cultures switched from simultaneous accumulation of DMB-alcohol and DMB-aldehyde to exclusive DMB-aldehyde formation, increased from 150 mM to about 250 mM, and the substrate concentration, below which significant DMB-acid formation was observed, increased from 90 to 190 mM. Such different characteristics suggest that higher DMB-aldehyde concentrations may be reached by the use of higher initial substrate concentrations and glycerol as growth substrate. In Table 4.4, such an experiment (biotransformation VII) is compared with biotransformations V and VI. However, the high specific DMB-aldehyde formation rate drastically decreased when the cells entered the stationary phase, and the lower growth rate reduced the initial DMB-aldehyde productivity. Therefore, initially formed DMB-alcohol was not transformed to DMB-aldehyde and significant amounts of pseudocumene remained in the bioconversion mixture. The DMB-aldehyde yield was relatively low, whereas similar product concentrations were reached as with glucose grown cells (Table 4.4). The advantage of the growth substrate glycerol as compared to glucose consists of higher specific activities; the disadvantages are higher residual concentrations of DMB-alcohol and pseudocumene, a shorter period with high biocatalyst activity, slower growth, a more difficult phase separation, and the higher price. This characterizes glucose as the superior source of carbon and energy.

Overall, a two-liquid phase bioconversion with glucose as growth substrate and BEHP as organic carrier solvent containing 4.3% (vol/vol) of pseudocumene allowed the production of DMB-aldehyde as predominant reactant in the organic phase at a molar yield of 70% and a final organic phase concentration of 220 mM.

## DISCUSSION

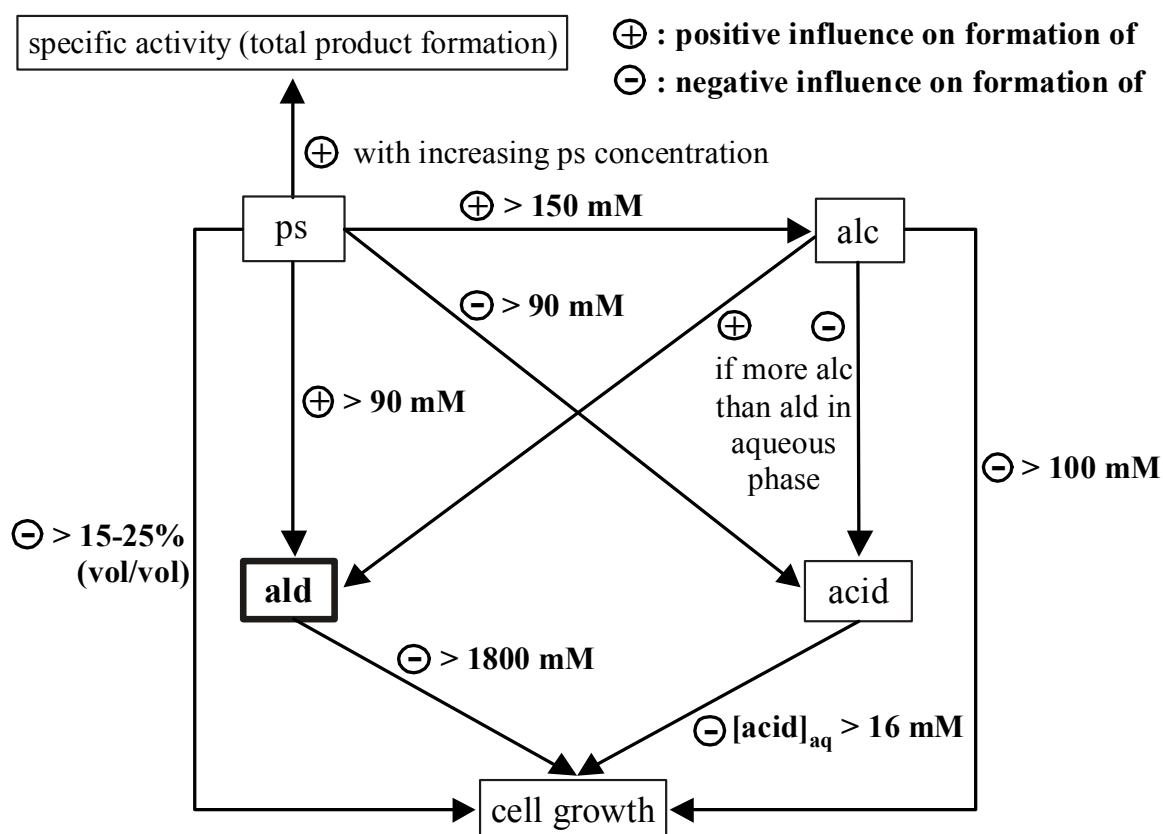
### Product formation patterns in two-liquid phase fed-batch cultures.

Figure 4.4 summarizes the influences of varying reactant concentrations on pseudocumene conversion and cell growth in the BEHP-based two-liquid phase system. Results presented here and in Chapter 3 show that the biocatalyst activity is limited by substrate availability. DMB-acid formation is inhibited above an organic pseudocumene concentration of 90 mM, and DMB-aldehyde accumulates as the only product. Furthermore, DMB-aldehyde and DMB-alcohol accumulated simultaneously above a second critical organic pseudocumene concentration around 150 mM. This can be explained comparing the kinetic parameters of pseudocumene oxidation [ $V_{\max}$ : 351 U (g of CDW)<sup>-1</sup>;  $K_s$ : 202  $\mu$ M;  $V_{\max}/K_s$ : 1.7 U  $\mu$ M<sup>-1</sup> (g of CDW)<sup>-1</sup>] and DMB-alcohol oxidation [ $V_{\max}$ : 93 U (g of CDW)<sup>-1</sup>;  $K_s$ : 24  $\mu$ M;  $V_{\max}/K_s$ : 3.9 U  $\mu$ M<sup>-1</sup> (g of CDW)<sup>-1</sup>] (Chapter 3). At low pseudocumene concentrations, the lower substrate uptake constant  $K_s$  of the biocatalyst for the DMB-alcohol dominates the higher maximal reaction velocity  $V_{\max}$  of pseudocumene oxidation and all pseudocumene is directly converted to DMB-aldehyde. At high pseudocumene concentrations, the higher reaction velocity of pseudocumene oxidation causes DMB-alcohol accumulation.

Moreover, the presence of DMB-alcohol with a far lower partition coefficient than pseudocumene allowed efficient inhibition of DMB-acid formation below organic pseudocumene concentrations of 90 mM. Transiently accumulated DMB-alcohol could be transformed to the desired DMB-aldehyde without substantial accumulation of undesired DMB-acid (Fig. 4.3A). When toxic aqueous DMB-alcohol concentrations (Fig. 4.1, A and D) or inhibitory glucose levels (Fig. 4.1, C and F) reduced biocatalyst activity, only DMB-alcohol accumulated at a low rate. There, as in the case of toxic aqueous DMB-acid concentrations (Chapter 3), the transformation of DMB-aldehyde to DMB-alcohol by non-specific alcohol dehydrogenase activities of *E. coli* may have exceeded the low XMO activity.

### Impact of aqueous pseudocumene concentrations on product formation.

According to the partition coefficient of pseudocumene, the critical organic phase concentrations (150 and 90 mM) correspond to aqueous phase concentrations of 6.2 and 3.7  $\mu$ M. With glycerol instead of glucose in the aqueous medium, the partitioning behavior did not change (data not shown). Nevertheless, the critical substrate concentrations in the organic phase shifted to higher levels (~250 and 190 mM) and correspond to 10.3 and 7.8  $\mu$ M in the



**Figure 4.4. Scheme showing influences of varying reactant concentrations** (in the organic phase if not specified else) **on product formation and cell growth in two-liquid phase biotransformations.** aq, aqueous phase; ps, pseudocumene; alc, DMB-alcohol; ald, DMB-aldehyde; acid, DMB-acid.

aqueous phase. This suggests that the changes in the product formation pattern might not only depend on the aqueous substrate concentration, but also on the nature of the emulsion, which might change in the presence of the highly viscous glycerol. Furthermore, when pseudocumene uptake is assumed to depend only on aqueous phase concentrations, the switch from simultaneous accumulation of DMB-alcohol and DMB-aldehyde to exclusive DMB-aldehyde formation is expected at an aqueous pseudocumene concentration in the range of the  $K_s$  value for pseudocumene. However, the critical aqueous pseudocumene concentrations calculated via the partition coefficient are up to two orders of magnitude below the  $K_s$  value, again indicating that product formation cannot depend only on aqueous substrate concentrations.

Figure 4.5 shows a comparison of measured and calculated reaction velocities for the first oxidation step from pseudocumene to corresponding alcohol. The measured reaction velocities are based on product formation during the biotransformation experiments. Maximally possible reaction velocities were calculated using the Lineweaver-Burk equation and aqueous pseudocumene concentrations determined according to the partition coefficient. In biotransformations I and IV with initial pseudocumene concentrations around 160 mM (Fig. 4.5A), the measured reaction rates after full induction correspond well with - and even slightly exceed - the theoretical maxima except during the transient activity reduction at high glucose concentrations. Towards the end of the biotransformations, the measured rates fell below the calculated rates. This occurred earlier in biotransformation I, which is due to emerging toxic DMB-acid concentrations. In the repeated fed-batch experiment, the measured rates exceeded the theoretical maxima by 50 to 100% (Fig. 4.5B). Similarly, with glycerol as growth substrate, the initial reaction velocity also exceeded the theoretical value, but rapidly decreased to low levels early in the biotransformation (Fig. 4.5C). Thus, the experimentally measured rates are in the same order of magnitude as - but clearly tend to exceed - the theoretical maxima derived from aqueous pseudocumene concentrations.

The relatively high pseudocumene oxidation rates, the observation that the product formation pattern does not directly depend on aqueous substrate concentrations, and the lower aqueous toxicity limit in the two-liquid phase system as compared to the aqueous one-phase system point to direct interaction between cells and solvent droplets. Such a direct contact and even substrate uptake directly from the organic phase were assumed, e.g., for long chain alkanes (Goswami and Singh, 1991; Schmid, et al., 1998c), menthyl acetate (Westgate, et al., 1995), and trichlorophenol (Ascón-Cabrera and Lebeault, 1995). In general, we conclude that the pseudocumene oxidation rate and the product formation pattern depend on the amount of pseudocumene present in the organic phase and that organic pseudocumene concentrations below 150 mM (250 mM with glycerol instead of glucose as growth substrate) also limit the DMB-aldehyde formation rate.

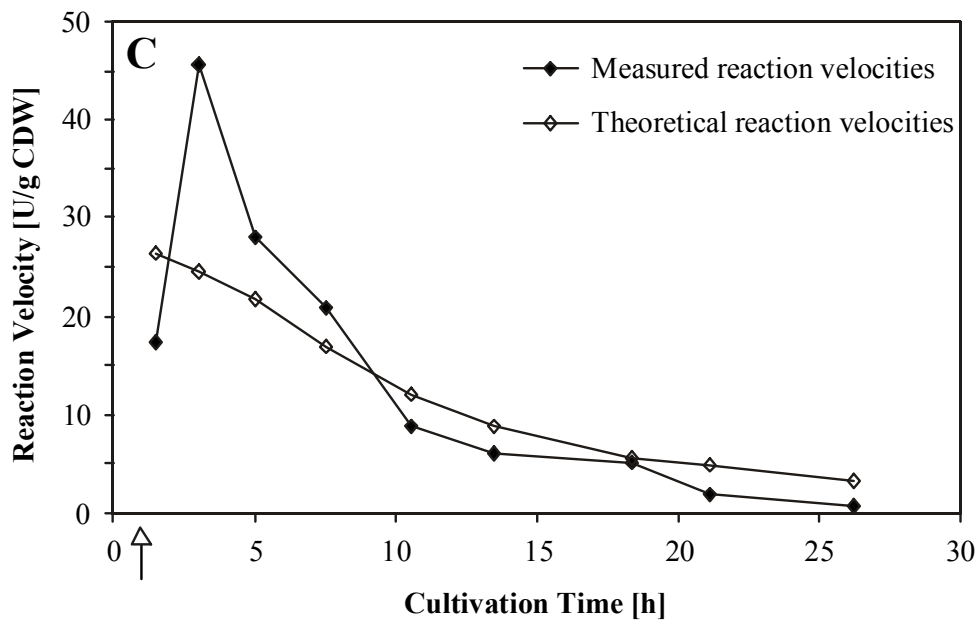
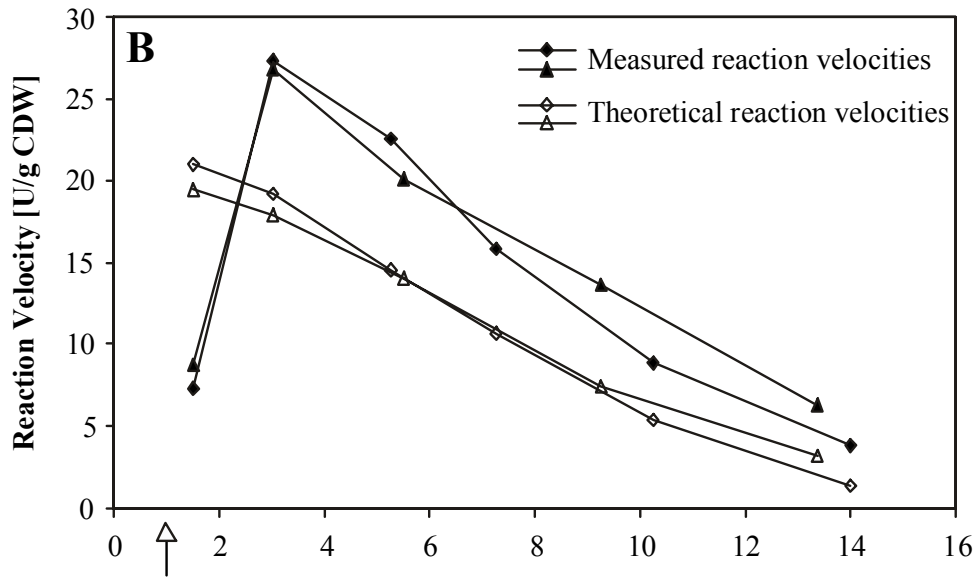
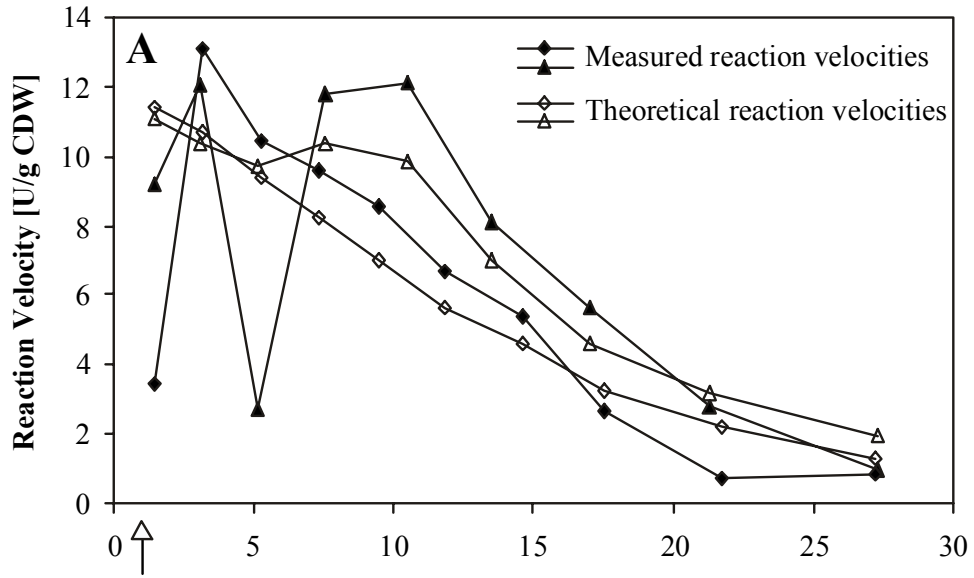


**Figure 4.5. Comparison of measured reaction velocities of pseudocumene oxidation and theoretical values corresponding to maximally possible reaction velocities** calculated via Lineweaver-Burk equation and aqueous pseudocumene concentrations derived from the partition coefficient. (A) Results for biotransformation I (Chapter 3) (diamonds) and IV (triangles). (B) Results for biotransformation V (diamonds) and VI (triangles). (C) Results for biotransformation VII with glycerol as growth substrate.

### **Factors limiting biocatalyst performance.**

Beside substrate limitation and inhibitory effects of toxic aqueous DMB-alcohol and DMB-acid concentrations, decreasing metabolic activity of the cells may also limit biocatalyst activity. Reduced metabolic activity may impair heterologous gene expression and NADH regeneration. Glucose limitation causes such a reduction of viability (Hewitt, et al., 1999; Hewitt, et al., 2000). In our case, prevention of severe glucose limitation prolonged the aldehyde production period significantly (Fig. 4.1). However, the slow decrease of the DMB-aldehyde formation rate in the late stationary phase indicates that decreasing metabolic activity also reduces biocatalyst performance when glucose is not limiting. Acetic acid, which vigorously accumulated in the stationary phase, may also have affected cell metabolism and thus biocatalyst activity. Moreover, high aqueous glucose concentrations seemed to inhibit biocatalyst activity although growth was not affected (Fig. 4.1F). An adequate feeding strategy appears to be crucial to reach optimal productivity in the fed-batch bioconversion.

### **The optimized bioconversion system.**

In the optimized system (Fig. 4.3), we could avoid inhibitory DMB-alcohol and DMB-acid levels, high glucose concentrations, and severe glucose limitation. Because of the low biocatalyst activity in the late stationary phase, the optimal biotransformation time is limited to 14-17 h. Thus, lower feed rates and concomitant slower growth might be an approach to prolong the production period.

Above a pseudocumene concentration of 150 mM (250 mM with glycerol), it is not the pseudocumene oxidation but the DMB-alcohol oxidation that limits the production of DMB-aldehyde from pseudocumene. The specific DMB-aldehyde oxidation rate never exceeded 16 U (g of CDW)<sup>-1</sup> [22 U (g of CDW)<sup>-1</sup> with glycerol], also at high DMB-alcohol concentrations. The measured DMB-alcohol oxidation rates never reached the maximally possible DMB-alcohol oxidation rates calculated via aqueous DMB-alcohol concentrations and the corresponding Lineweaver-Burk equation. Consequently, the second oxidation step is limited



by other factors than the amount of DMB-alcohol present in the two-liquid phase system. A limitation by the mass transfer from organic to aqueous phase is improbable because DMB-alcohol is produced in the aqueous phase. Also in aqueous one-phase systems, maximally possible DMB-alcohol oxidation rates were not reached when substrate as well as biocatalyst concentrations were high (Chapters 2 and 3).

In a biotransformation of 14.5 h duration, we achieved a final product concentration of 220 mM in the organic phase and a volumetric activity of up to  $390 \text{ U L}_{\text{aq}}^{-1}$ , corresponding to an oxygenation activity of  $780 \text{ U L}_{\text{aq}}^{-1}$  (Table 4.4). There are two possibilities to improve the volumetric productivity of the presented bioconversion. First, higher biocatalyst concentrations would lead to higher volumetric productivities since specific activities were found to be independent of the cell concentration. The second possibility is the increase of the specific DMB-aldehyde formation rate, which is limited by the rate of DMB-alcohol oxygenation. Therefore, it will be of special interest to investigate the factors influencing the oxygenation of DMB-alcohol.

### **Perspectives of the two-liquid phase concept.**

The two-liquid phase approach is very powerful in preventing substrate and product toxicity for the system presented in this study. The use of BEHP as second organic liquid phase enabled us to provide pseudocumene at an organic phase concentration optimal for the exclusive production of DMB-aldehyde (Fig. 4.3). The low toxicity of BEHP for humans (Hasmall, et al., 2000) and its poor flammability (boiling point,  $386^{\circ}\text{C}$ ; flash point,  $199^{\circ}\text{C}$ ) are other advantages. The tendency of BEHP to form stable emulsions was reduced significantly by omitting yeast extract from the feeding solution. BEHP is a relatively inexpensive pure solvent and can be recycled in a potential production setup. Due to its beneficial properties, the BEHP-based two-liquid phase system may serve now as a basis for the development of a scalable process exploiting the multistep bioconversion of pseudocumene for the production of DMB-aldehyde.

Clearly, the results presented in this study show that the two-liquid phase concept is a highly feasible method to direct kinetically controlled multistep reactions, such as the oxygenation of xylenes, to desired intermediates, such as aromatic aldehydes. This qualifies the two-liquid phase concept as an efficient tool to exploit the kinetics of multistep biotransformations in general.



## CHAPTER 5

# **CHEMICAL BIOTECHNOLOGY FOR THE SPECIFIC OXYFUNCTIONALIZATION OF HYDROCARBONS ON A TECHNICAL SCALE**

**Bruno Bühler, Irene Bollhalder, Bernhard Hauer, Bernard  
Witholt, and Andreas Schmid**

Biotechnology and Bioengineering, 2003, 82(7):833-842.

## SUMMARY

Oxygenases catalyze, among other interesting reactions, highly selective hydrocarbon oxyfunctionalizations, which are important in industrial organic synthesis but difficult to achieve by chemical means. Many enzymatic oxygenations have been described, but few of these have been scaled up to industrial scales, due to the complexity of oxygenase based biocatalysts and demanding process implementation. We have combined recombinant whole-cell catalysis in a two-liquid phase system with fed-batch cultivation in an optimized medium and developed an industrially feasible process for the kinetically controlled and complex multistep oxidation of pseudocumene to 3,4-dimethylbenzaldehyde using the xylene monooxygenase of *Pseudomonas putida* mt-2 in *E. coli*. Successful scale up to 30 L working volume using downscaled industrial equipment allowed a productivity of 31 g L<sup>-1</sup> d<sup>-1</sup> and a product concentration of 37 g L<sup>-1</sup>. These performance characteristics meet present industry requirements. Product purification resulted in the recovery of 469 g high value 3,4-dimethylbenzaldehyde at a purity of 97% and an overall yield of 65%. This process illustrates the general feasibility of industrial biocatalytic oxyfunctionalization.

## INTRODUCTION

Selective oxyfunctionalization of petrochemicals is a major topic in industrial organic synthesis (Wittcoff and Reuben, 1996), as recognized by the 2001 chemistry Nobel Prize, awarded to Sharpless for his work on chirally catalyzed oxidation reactions (Katsuki and Sharpless, 1980). Nature has much to offer in this area, given the many oxidation reactions catalyzed by oxygenases that occur in microbial metabolic pathways (Leadbetter and Foster, 1959; Witholt, et al., 1990; Harayama, et al., 1992; Faber, 2000). These enzymes use molecular oxygen to introduce oxygen in specific substrates providing an effective and sustainable approach to oxyfunctionalization, since highly reactive oxidants are avoided.

Oxygenases are usually cofactor dependent, often multicomponent, and/or membrane-associated enzyme systems, which constricts the use of isolated enzymes in practical applications (Faber, 2000; Li, et al., 2002). Instead, efforts during the past two decades have focused on whole-cell biocatalysis. Various solutions to issues such as biocatalyst stability, narrow substrate range, low volumetric productivities, and process setup have been developed based on improved screening strategies (Wahler and Reymond, 2001b; a), the use of recombinant strains (Lin, et al., 1999; Panke, et al., 2000; Panke, et al., 2002), biocatalyst engineering (Arnold, 2001; Zhao, et al., 2002), regulated substrate addition (Hack, et al., 2000), and *in situ* product recovery (Lye and Woodley, 1999). However, despite these promising approaches, very few industrial biooxidation processes have been developed thus far for the production of high value compounds (Schmid, et al., 2001).

In this paper, we describe initial steps in the development of such a process, in this case for the production of aromatic aldehydes, which serve as ingredients of natural flavors and fragrances and as synthons for a variety of polymers, pharmaceuticals, and fine chemicals. Chemical C-H bond activation via carbonylation or oxygen addition usually requires the use of expensive and hazardous reactants and catalysts and often yields product mixtures complicating product isolation (Carelli, et al., 1999; Thomas, et al., 1999). Thus, we consider it worth exploring the biocatalytic production of aromatic aldehydes from cheap substrates such as xylenes via selective C-H bond functionalization. The enzyme system which we use for this oxidation is the xylene monooxygenase (XMO) of *Pseudomonas putida* mt-2 (Worsey and Williams, 1975; Harayama, et al., 1989), which consists of a NADH:acceptor reductase component (XylA) (Shaw and Harayama, 1992) and a membrane bound hydroxylase component (XylM) (Shaw and Harayama, 1995). This nonheme iron enzyme has a broad

substrate range (Wubbolts, et al., 1994b) and initiates xylene degradation by the specific hydroxylation of one methyl group (Abril, et al., 1989). We have demonstrated that recombinant *E. coli* expressing the *xylMA* genes under control of the *alk* regulatory system (Panke, et al., 1999b) and thus containing the integral membrane enzyme XMO catalyze the monooxygenation not only of toluene and pseudocumene but also of the corresponding benzyl alcohols and benzaldehydes (Chapter 2). Thus, one single recombinant enzyme system (XylMA) can specifically produce desired benzaldehydes from xylenes.

We report here on specific and efficient biocatalytic hydrocarbon oxidation achieved by XMO based recombinant whole-cell catalysis in a two-liquid phase system combined with fed-batch cultivation in an optimized medium. We used downscaled industrial equipment to assess the scalability and were able to produce the toxic and unstable 3,4-dimethylbenzaldehyde (DMB-aldehyde) from equally toxic but inexpensive pseudocumene via a sophisticated multistep catalysis process using the complex XMO system. To our knowledge, this is the first report on a scalable integrated process for selective biooxidation of a non-functionalized hydrocarbon allowing good productivity, yield, and product concentration.

## MATERIALS AND METHODS

**Strain and precultivation.** *E. coli* JM101 (*supE thi Δ(lac-proAB) F'[traD36 proAB<sup>+</sup> lacI<sup>q</sup> lacZΔM15]*) (Messing, 1979), an *E. coli* K-12 derivative, was used as recombinant host strain. As expression vector, we used the pBR322 derived plasmid pSPZ3 containing the XMO genes *xylM* and *xylA* under the control of the *alk* regulatory system (Panke, et al., 1999b). All growth steps were carried out at 30°C. *E. coli* JM101 (pSPZ3) transformants were selected on Luria-Bertani broth (LB) plates (Sambrook, et al., 1989) containing 50 mg L<sup>-1</sup> kanamycin and 10 g L<sup>-1</sup> glucose to avoid indigo formation (Panke, et al., 1999b). To increase the reproducibility, freshly transformed cells served as inoculum for 3-ml LB cultures supplemented with glucose and kanamycin as before. These cultures were diluted 100-fold with 100 ml of RB minimal medium (Chapter 4) complemented with per liter, 2 ml of 1 M magnesium sulfate, 5 g glucose, 1 ml of 1% (wt/vol) thiamine, 50 mg kanamycin, and 1 ml trace element solution US<sup>Fe</sup> (Chapter 4). Such precultures were transferred into a 3-L stirred tank reactor, in which biotransformations on a 2-L scale or precultivations for large-scale experiments were performed. The details of the reactor system and its instrumentation have

been described (Wubbolts, et al., 1996a). For precultivations the reactor contained 1.9 L of mineral medium of identical composition as for the culture before. The pH in the reactor was kept at 7.1 or 7.4 by the addition of 25% (wt/vol) ammonium water or 30% phosphoric acid. One and a half liters of such cultures were used as inocula for biotransformations on a 30-L scale.

**Biotransformation setup.** Thirty liter biotransformations were performed in a 42-L stirred tank reactor with regulated temperature, pH, stirrer speed, aeration, and internal pressure (New MBR, Zurich, Switzerland). Data collection occurred every 30 s with the Caroline II software (PCS, Wetzikon, Switzerland) on an OS/9 operating system. Mixing was achieved with 2 six-bladed Rushton turbine impellers. Two-liter experiments were carried out in a 3-L reactor (see above). Maintenance of pH was achieved as described above. Typical biotransformation procedures as developed and optimized earlier (Chapters 3 and 4) started with batch cultivation (Fig. 5.1). Depending on the scale, the batch culture volumes amounted to 1 or 15 L. Before sterilization, the reactors contained salts equivalent to 0.9 or 13.5 L of RB medium dissolved in 0.85 or 12.5 L water. After sterilization, the reactor contents were supplemented aseptically with, per liter culture volume, 2.5 ml of 1 M magnesium sulfate, 14 ml of a 50% (wt/vol) glucose solution, 1 ml of a 1% (wt/vol) thiamine solution, and 5 ml of trace element solution US<sup>Fe</sup>. Omitting kanamycin had no impact on process efficiency (Chapter 4). The pH was adjusted to 6.8 with 25% (wt/vol) ammonium water and to pH 7.1 or 7.4 with 10 M NaOH and the volume to 0.9 or 13.5 L with water. After inoculation, batch cultivation was performed at a stirring speed of 1,500 and 600 rpm and an aeration of 1 and 15 L min<sup>-1</sup> on small and large scale, respectively. After initial glucose and metabolic by-products (e.g., acetic acid) had completely been consumed, a feed of 73 % (wt/vol) glucose and 19.6 g L<sup>-1</sup> magnesium sulfate was initiated. Furthermore, the culture was supplemented with, per liter, 5 ml of trace element solution US<sup>Fe</sup> and 4 ml of 1% (wt/vol) thiamine, and *xylMA* expression was induced by the addition of 0.02% (vol/vol) dicyclopropyl ketone (DCPK, 95%, Aldrich, Buchs, Switzerland) or 0.1% (vol/vol) *n*-octane (>98.5%, Acros, Geel, Belgium). After 1-1.5 h of fed-batch growth, the biotransformation was started by the addition of a volume of organic phase equivalent to the culture volume. The organic phase consisted of bis(2-ethylhexyl)phthalate (BEHP, 97%, Fluka, Buchs, Switzerland) as the carrier solvent, variable amounts of pseudocumene (99%, Fluka), and 1% (vol/vol) *n*-octane. Adjusting stirrer speed and aeration and, if necessary, oxygen admixture prevented oxygen limitation. Sampling and determination of reactant concentrations in both phases and glucose, acetic acid, and cell concentrations in the aqueous phase were performed as described in Chapters 3

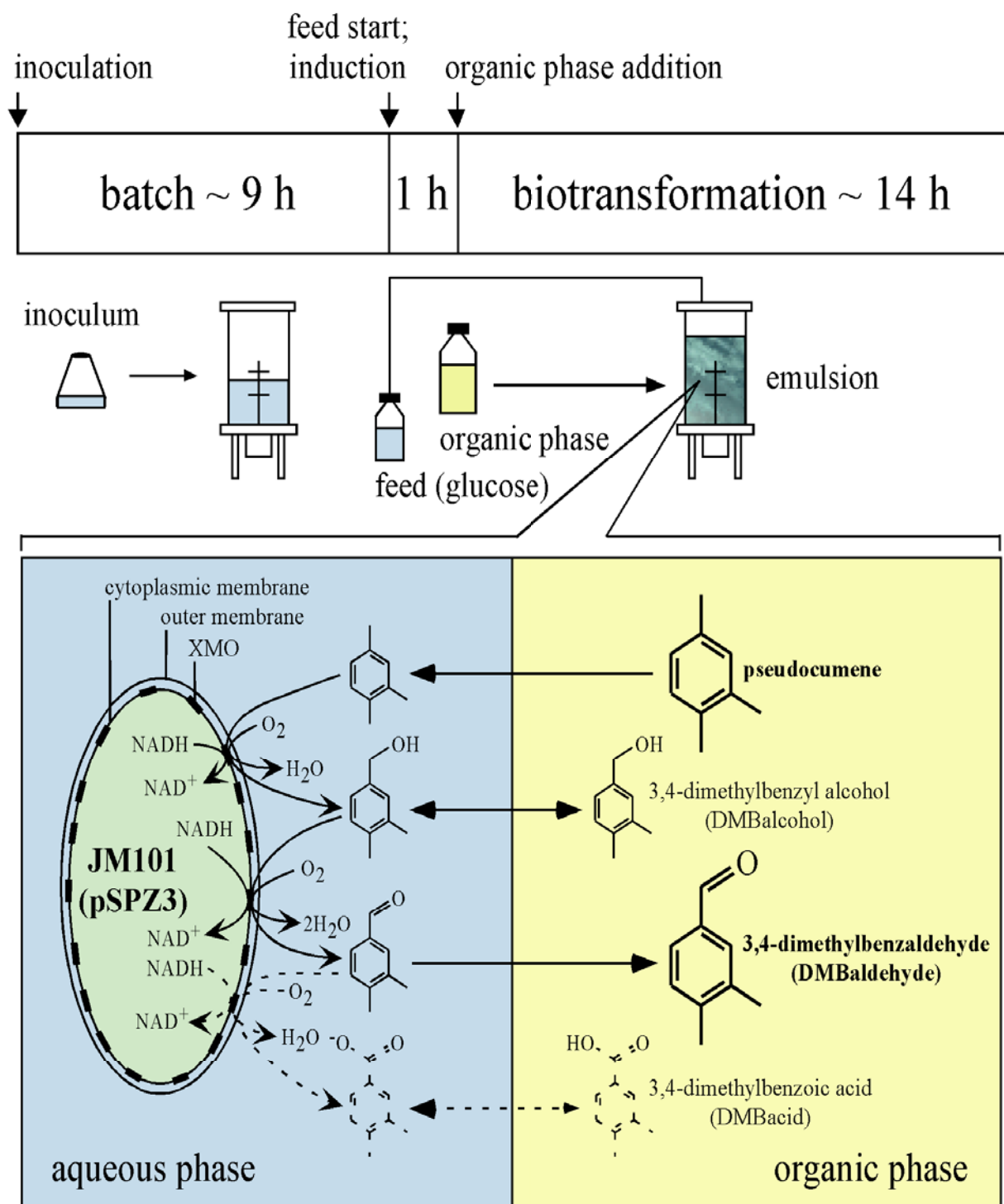


**Figure 5.1. Biotransformation process.** Batch growth is followed by fed-batch cultivation and the two-liquid phase biooxidation of pseudocumene. Pseudocumene, DMB-alcohol, and DMB-aldehyde, but not DMB-acid (at neutral pH) mainly partition into the organic phase (Chapter 4).



and 4. Foam formation was limited by the addition of antifoam 289 (Sigma, Buchs, Switzerland). Volumetric productivities and specific product formation rates were calculated for intervals between two sampling points. One Unit is defined as the activity that produces 1  $\mu\text{mol}$  of product per minute.

**Downstream processing.** After harvesting, the two phases were separated by centrifugation for 30 min at 8400 g in a Haereus-Christ Cryofuge 8000 centrifuge (Haereus, Zurich, Switzerland). The organic phase was supplemented with dry sodium sulfate and stored at 4°C. After filtration, DMB-aldehyde was purified by fractionated distillation at a pressure of 0.1 mbar. At this pressure and room temperature, *n*-octane (boiling point [bp], 126°C) and pseudocumene (bp, 169°C) condensed in the dry ice containing cryo trap. Organic phase portions of 4.5 L were heated to 110°C, when distillate of a temperature of 35°C condensed in the cooler. During distillation, the temperature at the still was raised to 190°C and the temperature of the distillate increased to 55°C. This fraction contained DMB-aldehyde (bp: 233°C) at a purity of 97% as determined by GC and HPLC, whereas traces of 3,4-dimethylbenzyl alcohol (DMB-alcohol; bp: 218-221°C; melting point [mp]: 62-65°C) sublimed in the cooler and 3,4-dimethylbenzoic acid (DMB-acid; mp: 165-167°C) as well as BEHP (bp: 384°C) remained in the still. It was essential that the DMB-alcohol content in the organic phase was as low as possible, since the separation of DMB-alcohol and DMB-aldehyde was difficult during such a purification procedure.

## RESULTS

### **Multistep laboratory-scale oxidation of pseudocumene to DMB-aldehyde.**

The laboratory-scale process is outlined in Figure 5.1. Recombinant *E. coli* JM101 expressing the XMO genes under control of an alkane responsive regulatory system (Panke, et al., 1999b) were used as biocatalyst. After precultivation of the cells, the bioreactor was inoculated. Following batch growth in 1 L of minimal medium, a feed of glucose and magnesium sulfate was initiated and XMO synthesis was induced with DCPK or *n*-octane (see Materials and Methods). The biotransformation started with the addition of 1 L of organic phase consisting of BEHP as the carrier solvent, which contained the substrate pseudocumene and 1% (vol/vol) *n*-octane to maintain continuous induction. This procedure resulted from characterization and optimization work described in the Chapters 3 and 4. In such a system, high overall concentrations of the toxic and poorly water-soluble reactants could be added to the two-

liquid phase system without inhibiting bacterial growth and DMB-aldehyde accumulated to high concentrations. Glucose was fed continuously as the carbon and energy source to maximize biocatalyst concentrations and volumetric productivities. The left column in Table 5.1 lists relevant parameters of such a biotransformation (experiment 1).

We found that the medium pH influences the bioconversion efficiency. Figure 5.2 shows a biotransformation (experiment 2) performed at the same conditions as experiment 1 except for the pH, which was 7.4 and enabled better productivity than biotransformation at pH 7.1. At constant aeration ( $1 \text{ L min}^{-1}$ ) and stirrer speed (2000 rpm), the dissolved oxygen tension (DOT) never decreased below 50% saturation. The initial simultaneous accumulation of DMB-alcohol and DMB-aldehyde was followed by the formation of DMB-aldehyde only, after the pseudocumene concentration had decreased below 150 mM. This and the lack of significant DMB-acid formation can be attributed to the complex kinetics of the multistep oxidation of pseudocumene and the favorable partitioning behavior of the reactants in the two-liquid phase system. We have previously shown that the presence of pseudocumene and DMB-alcohol inhibits DMB-aldehyde oxidation (Chapters 3 and 4). Furthermore, substrate limitation in the first oxidation step, as indicated by the parallel decrease of the pseudocumene concentration and the specific pseudocumene oxidation rate (Fig. 5.2), causes a switch from the simultaneous accumulation of DMB-alcohol and DMB-aldehyde to the formation of DMB-aldehyde only (Chapter 4). As full induction is reached only after about 3 h (Chapter 2), specific product and DMB-aldehyde formation rates increased at the beginning of the bioconversion (Fig 5.2B). After the induction period, the specific DMB-aldehyde formation rate remained high at around  $40 \text{ U (g of CDW)}^{-1}$  until cell growth ceased, whereupon it decreased steadily in the stationary phase (Fig 5.2). However, the increase of the medium pH from 7.1 to 7.4 significantly enhanced the specific activities but lowered growth rates and maximal cell concentrations (Table 5.1). Since such a pH difference has no effect on the growth of wildtype *E. coli* JM101, the impaired growth of biocatalytically active *E. coli* JM101 (pSPZ3) points to a metabolic burden of the high specific activities for the host strain as observed for alkane hydroxylation (Bosetti, et al., 1992). Overall, volumetric productivity and final product concentration were significantly improved by the pH increase to 7.4.

**Table 5.1. Process characteristics at varying pH and scale.\***

Parameter	Unit	Experiment			
		1 <sup>a</sup>	2	3	4
Working volume	L	2	2	30	30
pH		7.1	7.4	7.4	7.1→7.4
Growth rate <sup>b</sup>	h <sup>-1</sup>	0.35	0.24	0.25	0.34
Maximal CDW reached	g L <sub>aq</sub> <sup>-1</sup>	30	18	15.5	20
Biotransformation time <sup>c</sup>	h	14.5	13	14.5	14
Initial [pseudocumene] <sub>org</sub>	mM	315	500	400	355
Final [DMB-aldehyde] <sub>org</sub>	mM	220	330	254	274
DMB-aldehyde produced	g L <sub>org</sub> <sup>-1</sup>	29.5	44.3	34.1	36.8
Molar yield	%	70	66	64	77
Product share in all reactants <sup>d</sup>	%	92	80	76	97
Maximal specific activity <sup>e</sup>	U (g of CDW) <sup>-1</sup>	27	61	65	51
Maximal specific activity <sub>ald</sub>	U (g of CDW) <sup>-1</sup>	16	43	36	30
Maximal volumetric activity <sub>ald</sub>	U L <sub>aq</sub> <sup>-1</sup>	390	710	440	500
Maximal productivity <sub>ald</sub>	g L <sub>tot</sub> <sup>-1</sup> h <sup>-1</sup>	1.6	2.9	1.8	2
Average productivity <sub>ald</sub>	g L <sub>tot</sub> <sup>-1</sup> h <sup>-1</sup>	1	1.7	1.2	1.3

\*All experiments were carried out under the same conditions at varying pH and scale (organic carrier solvent, BEHP; phase ratio, 0.5; for details see Materials and Methods). CDW: cell dry weight. Subscripts: org, organic phase; aq, aqueous phase; tot, total volume; ald, referring to DMB-aldehyde formation.

<sup>a</sup> Adapted from Chapter 4.

<sup>b</sup> In the exponential growth phase.

<sup>c</sup> Second phase addition is defined as the start point.

<sup>d</sup> In the organic phase at the end of the biotransformation.

<sup>e</sup> Based on the sum of all products formed (corresponds to the specific pseudocumene oxidation rate).

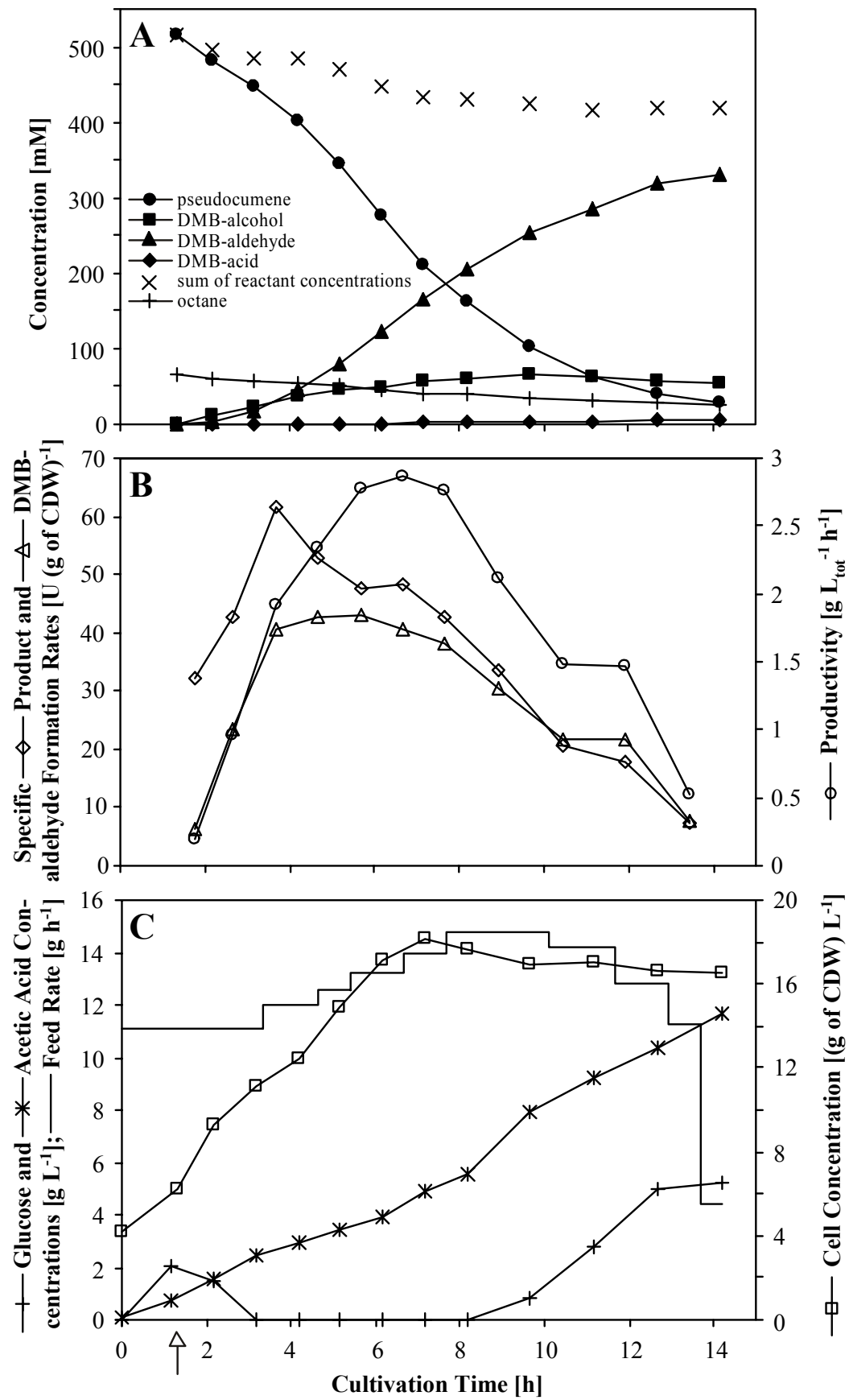
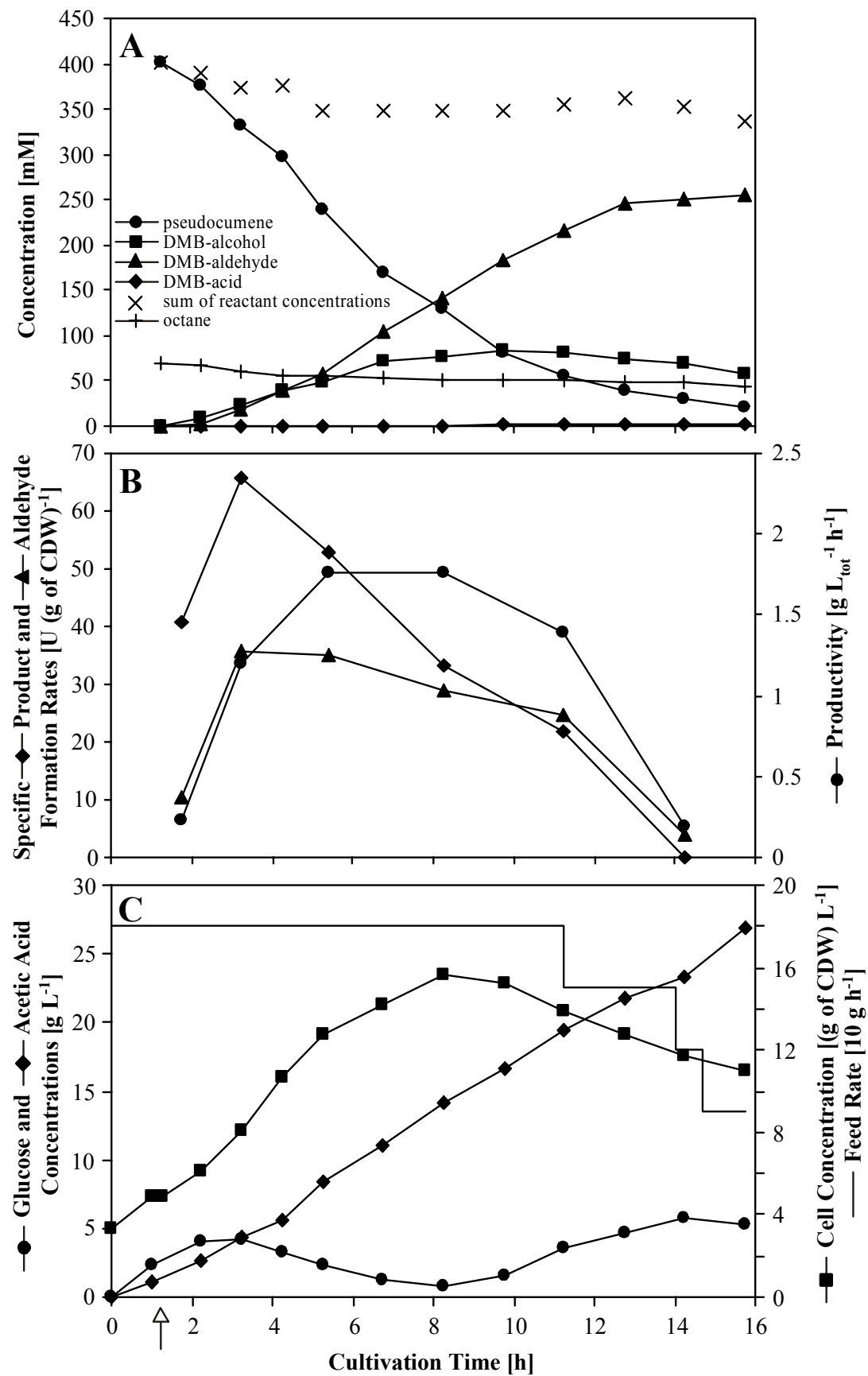


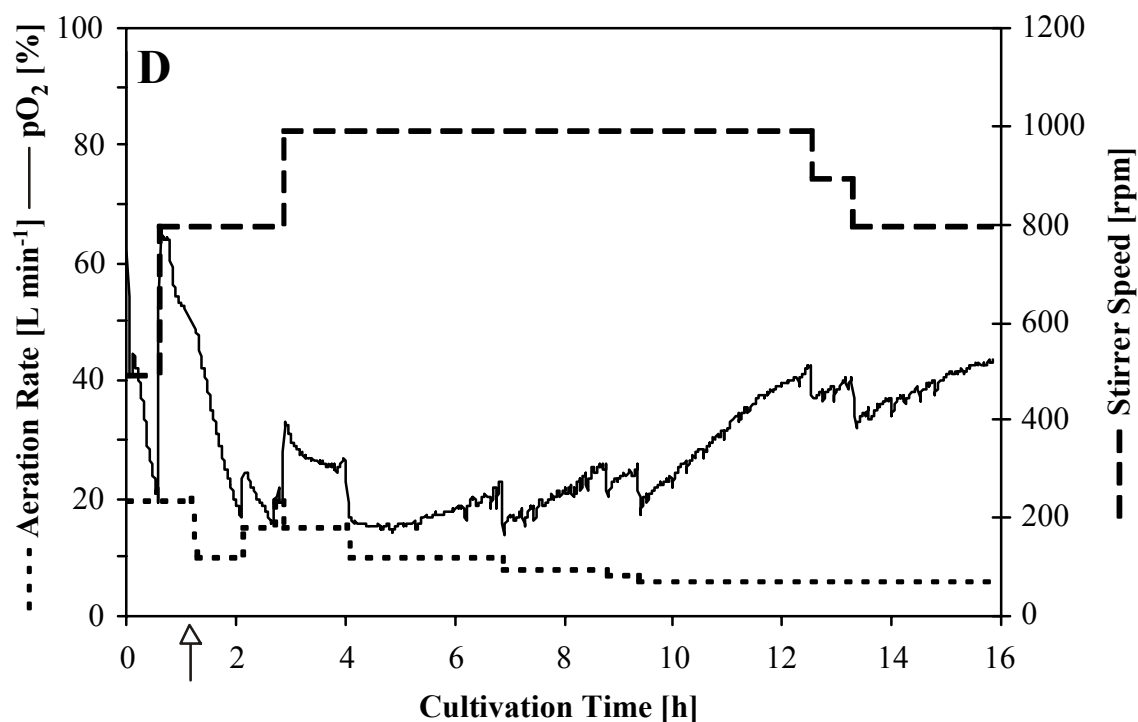
**Figure 5.2. Fed-batch based two-liquid phase biotransformation on a 2-liter scale (pH 7.4) with *E. coli* JM101 (pSPZ3) as biocatalyst and BEHP as organic carrier solvent (experiment 2).** After batch growth of a 1 L culture, cells were induced and a glucose feed was initiated (time 0), and, 1.33 h later, the biotransformation was started by the addition of 1 L organic phase (arrow). For details see Materials and Methods. (A) Reactant and octane concentrations represent the sum of the respective concentrations in the organic and the aqueous phase. (B) Specific DMB-aldehyde and product formation rates and DMB-aldehyde volumetric productivities are calculated for intervals between two sampling points. The specific product formation rate is based on the sum of all products formed in a time interval and is synonymous to the specific pseudocumene oxidation rate. (C) Course of glucose and acetic acid concentrations, biomass formation, and glucose feed rate.

### Scale up of the bioconversion to technical scale.

In order to evaluate the scalability of the two-liquid phase biooxidation system, we carried out the biotransformation in a 42-L bioreactor containing 15 L of minimal medium and 15 L of organic phase (experiment 3, Table 5.1, Fig. 5.3). The lower power input of maximally 5 W L<sup>-1</sup> in the 42-L reactor, as compared to 60 W L<sup>-1</sup> in previous experiments, and an aeration rate of 15 L min<sup>-1</sup> sufficed to maintain the DOT above 15%. Product formation and growth behavior were similar to that seen on laboratory-scale. However, lower cell concentrations and slightly lower specific DMB-aldehyde formation rates as compared to laboratory-scale reduced the average productivity from 1.7 to 1.2 g L<sup>-1</sup> h<sup>-1</sup>.

To ensure complete conversion and thus facilitate product isolation, the initial pseudocumene concentration was reduced (experiment 4, Table 5.1). Furthermore, to reach higher biocatalyst concentrations in combination with high biocatalyst activities, we introduced a pH shift from 7.1 via 7.2 to 7.4. As intended, DMB-aldehyde was the predominant product at the end of the biotransformation and high cell concentrations were combined with high biocatalyst activities (Fig. 5.4). After induction and pH shift, the specific DMB-aldehyde formation rate and thus productivity remained high until cell growth ceased. Also in experiment 3, the productivity decreased in the stationary phase (Fig. 5.3). This illustrates the necessity of metabolically active cells for optimal process performance as detailed in Chapter 4.

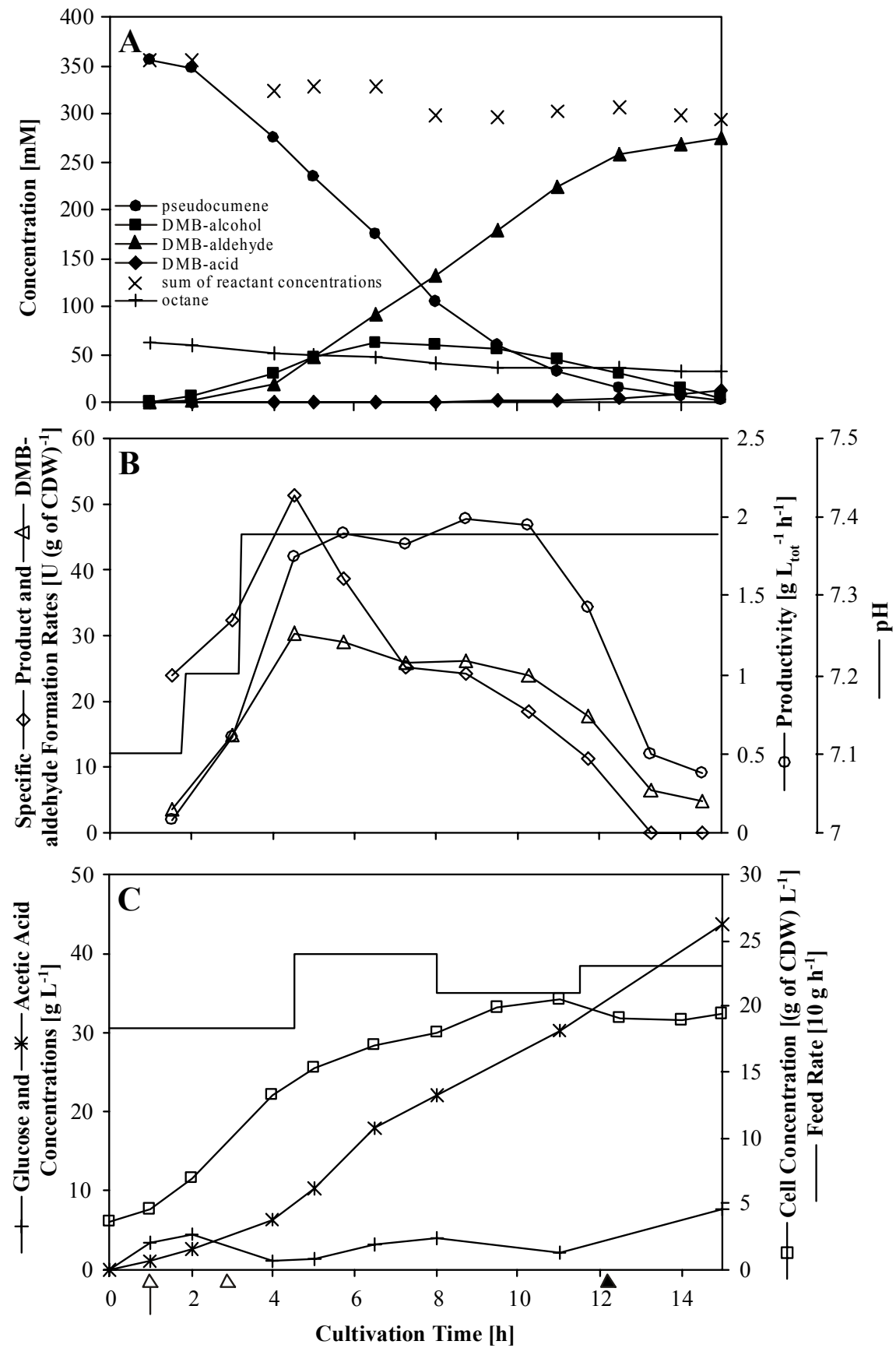




**Figure 5.3. Fed-batch based two-liquid phase biotransformation on a 30-liter scale (pH 7.4) with *E. coli* JM101 (pSPZ3) as biocatalyst and BEHP as organic carrier solvent (experiment 3).** Time 0 indicates induction and initiation of a glucose feed to a 15 L culture grown in batch mode. After 1.25 h, the biotransformation was started by the addition of 15 L organic phase (arrow). For details see Materials and Methods. (A, B, and C) As described for Fig. 5.2. (D) Course of stirrer speed, dissolved oxygen tension (DOT), and aeration rate.

At the beginning of the biotransformation in experiment 4 (Fig. 5.4) at pH 7.1, the oxygen requirement apparently exceeded the available oxygen. Increasing the power input to the maximum of  $5 \text{ W L}^{-1}$  at a stirrer speed of 1000 rpm and the aeration rate to a maximum of  $50 \text{ L min}^{-1}$  did not satisfy the oxygen requirement of the cells. Thus, the reactor was aerated with an air-oxygen mixture.

A molar yield of 100% was not reached because aeration of the reactor caused substrate evaporation. Overall, the up scaled two-liquid phase process allowed the production of 550 g DMB-aldehyde, a final product share in all reactants of 97% in the organic phase, and a maximal productivity of  $2 \text{ g L}_{\text{tot}}^{-1} \text{ h}^{-1}$ .





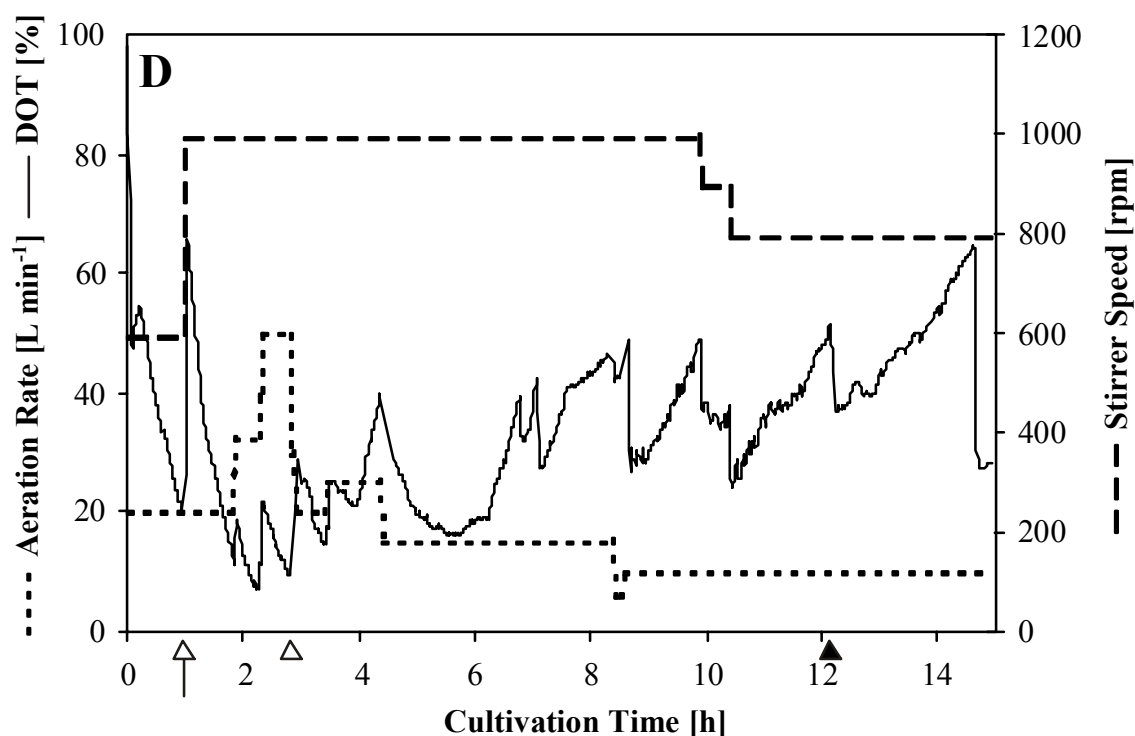


**Figure 5.4. Biocatalytic synthesis of DMB-aldehyde from pseudocumene by *E. coli* JM101 (pSPZ3) on a 30-liter scale (experiment 4).** Time 0 indicates induction and initiation of a glucose feed to a 15 L culture grown in batch mode. After 1 h, the biotransformation was started by the addition of 15 L organic phase (arrow). For details see Materials and Methods. (A, B, and C) As described for Fig. 5.2. In panel B, additionally, the course of the pH in the reactor is shown. (D) Course of stirrer speed, dissolved oxygen tension (DOT), and aeration rate. Due to the high oxygen demand, the reactor was aerated with an air-oxygen mixture, which was readjusted several times. Open and closed arrowheads indicate start and stop of oxygen admixture, respectively.

### Downstream processing.

In situ product extraction in the two-liquid phase system enabled a straightforward downstream processing consisting of phase separation, drying the organic phase over sodium sulfate, and vacuum distillation. Phase separation was achieved by centrifugation and resulted in the recovery of 13.5 L dry organic phase corresponding to 90% of the apolar phase originally added in experiment 4 (Fig. 5.5). During harvesting and phase separation, acetic acid production by the cells caused a pH decrease. Thus, DMB-acid increasingly partitioned into the organic phase, due to its protonation. However, this had no impact on further product purification. A single distillation of the organic phase at a pressure of 0.1 mbar yielded 469 g DMB-aldehyde at a purity of 97% (GC, HPLC). <sup>1</sup>H-NMR analysis confirmed the identity of the product (results not shown).

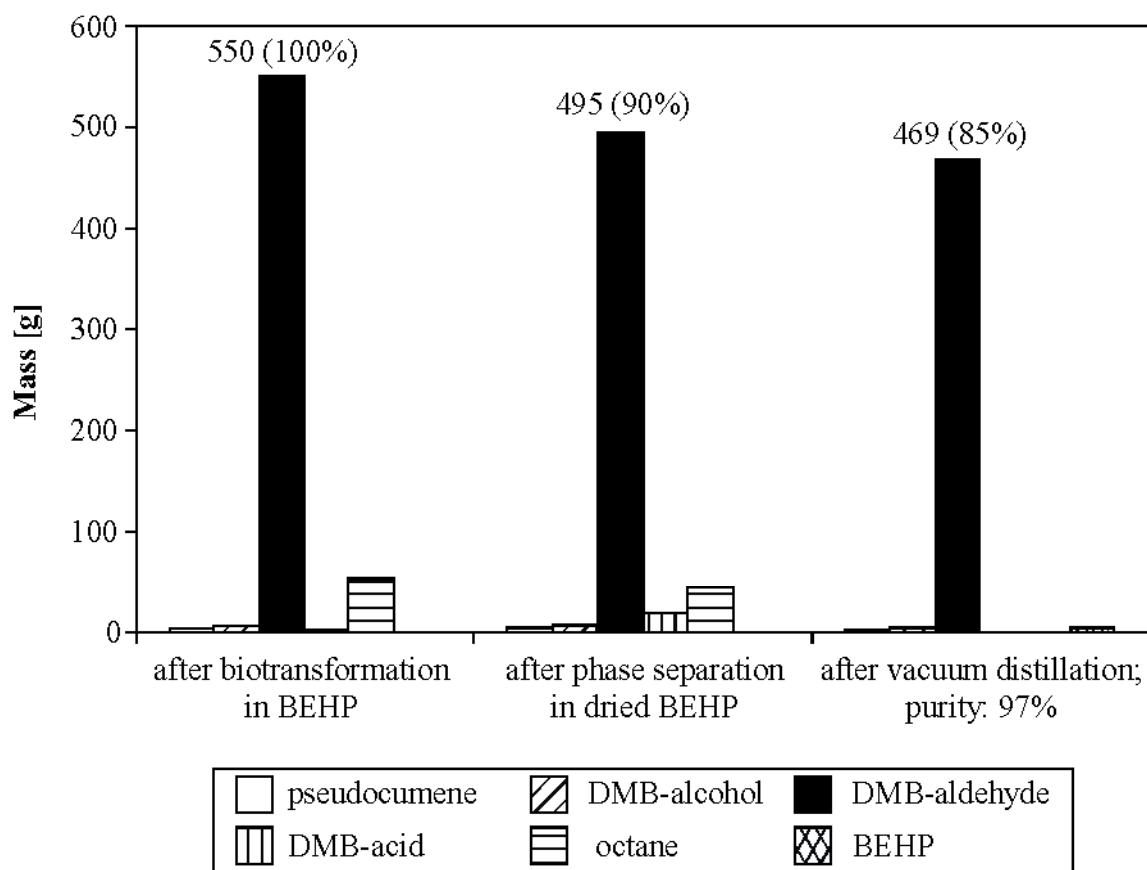


**Figure 5.5. Efficiency of the downstream processing.** Phase separation via centrifugation is followed by drying over sodium sulfate and filtration yielding 90% of the organic phase volume initially added in experiment 4 (Fig. 5.4). Fractionated distillation at a pressure of 0.1 mbar yielded 97% pure DMB-aldehyde. The overall purification yield amounted to 85%.

## DISCUSSION

### Recombinant whole-cell biocatalysis.

Complex cofactor dependent enzymes such as oxygenases are normally used *in vivo* to enable inexpensive cofactor regeneration (Faber, 2000; Li, et al., 2002). This approach has been useful when dead end products are produced, as in the oxidation of aromatic heterocycle methyl groups to the corresponding carboxylic acids by wildtype *P. putida* mt-2, which harbors the xylene degradation pathway (Kiener, 1992). Aromatic aldehydes such as DMB-aldehyde are, however, further metabolized in *Pseudomonas* strains, which reduces yields. Such product degradation was efficiently prevented by the use of recombinant *E. coli*, which could be grown to high cell densities on glucose as a cheap source of carbon and energy.

Expression of the XMO genes under *alk* regulatory control, which has been shown to support high levels of inducible monooxygenase activities in *E. coli* (Chapter 2; Nieboer, et al., 1993; Panke, et al., 1999b; Panke, et al., 2000), enabled high volumetric productivities on a technical scale.

### **Fed-batch cultivation in an optimized medium.**

In order to maintain high oxygenase activities over time, we employed growing cells with high metabolic activity, which were expected to provide enough energy for efficient cofactor regeneration and oxygenase synthesis (Doig, et al., 1999a; Faber, 2000). Cells were cultivated in fed-batch mode in a medium optimized for *E. coli* and *xylMA* expression (Chapter 4; Riesenberg, et al., 1991), and high and stable productivities were indeed reached during growth. In the stationary phase, when metabolic activity and viability of the cells decreased, biocatalyst activities declined independently from the reactant concentrations (Chapter 4), for an optimal biotransformation time of about 14 h for the chosen process setup. Also with respect to genetic stability, *E. coli* JM101 (pSPZ3) proved to be a suitable biocatalyst, since plasmid as well as biocatalyst activity remained stable for 11 generations without selection pressure during two successive biotransformations performed in a repetitive fed-batch mode of cultivation (Chapter 4). Similarly, Favre-Bulle et al. reported segregational and structural stability for as long as 29 generations in *E. coli* HB101 (pGEc47) without selection pressure, but highly varying genetic stabilities in different *E. coli* host strains (Favre-Bulle, et al., 1993). This genetic stability permits the elimination of antibiotics from these industrial bioprocesses, which is useful from an economical and ecological point of view. The feasibility of a repetitive fed-batch mode of cultivation also emphasizes the possibility to reuse the biocatalyst. Such a reuse, however, still necessitates cell growth.

### **Two-liquid phase concept.**

Hydrocarbons and their oxidized products are often poorly water-soluble and toxic or inhibitory for the biocatalyst. In situ product removal, including the use of membrane reactors, solid phase extraction, and two-phase systems, is commonly used to overcome these hurdles (Leon, et al., 1998; Lye and Woodley, 1999). In two-liquid phase processes, the properties of the chosen recyclable organic carrier solvent are of special importance (Bruce and Daugulis, 1991; Salter and Kell, 1995; Schmid, et al., 1998a). The use of BEHP with its low flammability and low toxicity to *E. coli* (Chapter 3; Panke, et al., 2000) and humans (Hasmall, et al., 2000) allowed the safe operation of a 42-L stirred tank reactor with a 50%

volume fraction of this solvent. Furthermore, substrate and product toxicity were efficiently prevented and high pseudocumene mass transfer rates from the organic phase to the cells were reached. As outlined in Chapter 4, DMB-alcohol oxidation is the limiting step in the overall biotransformation. By optimizing the medium pH, the specific activities including the DMB-alcohol oxidation rate were significantly enhanced. The BEHP based two-liquid phase system allowed exploiting the complex kinetics of the multistep oxidation of pseudocumene to produce high concentrations of DMB-aldehyde as the predominant product in the organic phase. Furthermore, this concept facilitated product isolation.

### **Industrial feasibility.**

Two-liquid phase processes have thus far mostly operated at laboratory scale. In order to assess the industrial feasibility of biocatalytic hydrocarbon oxyfunctionalization, we used a reactor with an estimated power input ( $5 \text{ W L}^{-1}$ ) close to values typically reached on industrial scales (Woodley, 1990; Manfredini and Manfredini, 1996). A pilot scale of 20-30 L often serves as a platform for scalability evaluation of industrial processes and for scale up to production ( $50\text{--}100 \text{ m}^3$ ). Requirements for industrial oxidation processes include productivities between 10 and  $60 \text{ g L}^{-1} \text{ d}^{-1}$ , high biocatalyst stability, high yields (60 – 80%), product concentrations of  $10\text{--}100 \text{ g L}^{-1}$ , and simple product recovery (Straathof, et al., 2002). Schmid et al. envisioned volumetric activities in the range of  $200\text{--}1000 \text{ U L}^{-1}$  for large-scale two-liquid phase processes considering future developments in biocatalyst and reactor engineering (Schmid, et al., 1998a). Taking an average volumetric activity of  $100 \text{ U L}^{-1}$  for alkane hydroxylation, Mathys et al. demonstrated the economic feasibility of such processes based on a detailed modeling analysis (Mathys, et al., 1999). We now achieved for the first time an average volumetric activity of  $330 \text{ U L}_{\text{aq}}^{-1}$  with a maximum at  $500 \text{ U L}_{\text{aq}}^{-1}$  for a technical-scale two-step oxygenation process. This corresponds to an overall oxygenation activity of  $1000 \text{ U L}_{\text{aq}}^{-1}$  or  $500 \text{ U L}_{\text{tot}}^{-1}$ . The resulting productivity of  $31 \text{ g L}_{\text{tot}}^{-1} \text{ d}^{-1}$ , a final DMB-aldehyde concentration of  $37 \text{ g L}^{-1}$  in the organic phase, and an isolated product yield of 65% (conversion yield: 77%) clearly illustrate the practical feasibility of large-scale two-liquid phase processes and point to the high potential of biocatalytic hydrocarbon oxidation in organic synthesis. Another recent example is the use of recombinant *E. coli* containing styrene monooxygenase of *Pseudomonas* sp. VLB120 for the enantioselective single step oxidation of the styrene vinyl function to produce (*S*)-styrene oxide with an enantiomeric excess of >99% at a purity of >97% (Panke, et al., 2002).

**Perspectives.**

Enzymes are optimized by nature for the survival of a species in a specific ecological environment and not to meet the requirements of industrial biocatalytic processes. Nevertheless, biochemical engineering and modern DNA technology provide a variety of tools to develop and optimize a biocatalyst and a process setup (Burton, et al., 2002; Panke and Wubbolts, 2002; Patnaik, et al., 2002; Schmid, et al., 2002). The present example shows that the combined use of different concepts allows the application of complex enzyme systems such as oxygenases for complex reactions such as kinetically controlled multistep reactions. The clear feasibility of biocatalytic oxyfunctionalization on a technical scale and the large pool of oxygenases in nature (Ellis, et al., 2001) augur well for the development of many and varied industrial scale hydrocarbon oxidations in the coming decade.

**ACKNOWLEDGMENTS**

The authors thank H.-J. Feiten and D. Meyer for their excellent technical assistance and F. Hollmann for NMR analyses.



## CHAPTER 6

# **MODELING AND SIMULATION OF A WHOLE-CELL MULTISTEP BIOOXIDATION PROCESS IN A TWO- LIQUID PHASE SYSTEM**

**Bruno Bühler, Adrie J. J. Straathof, Bernard Witholt, and  
Andreas Schmid**

## SUMMARY

A process model for whole-cell biocatalysis in a two-liquid phase system including cell growth and bioconversion kinetics was developed. The reaction considered is the kinetically controlled multistep oxidation of pseudocumene to 3,4-dimethylbenzaldehyde catalyzed by recombinant *Escherichia coli* expressing the *Pseudomonas putida* genes encoding xylene monooxygenase, which catalyzes the successive oxygenation of one methyl group of xylenes to corresponding alcohols, aldehydes, and acids. The biocatalytic process includes cells growing in fed-batch mode and a two-liquid phase system consisting of bis(2-ethylhexyl)phthalate as organic carrier solvent and an aqueous minimal medium at a phase ratio of 0.5. The process model comprises a description of the bioconversion kinetics, mass transfer kinetics, cell growth, and mass balances for both the aqueous and the organic phase. Key theoretical results correlated well with experimental biotransformations. Bioconversion kinetics and consistent process simulation indicated the occurrence of direct substrate uptake from organic phase droplets and provided evidence for a competition for NADH between xylene monooxygenase and the respiratory chain with its consequential impact on bioconversion and cell growth. The introduction of a pH-dependent feedback inhibition of the NADH consuming bioconversions allowed good simulations of biotransformation experiments performed at varying pH, scale, and initial substrate concentration. Moreover, modeling indicated a product inhibition in the second oxidation step, which could be confirmed experimentally. A sensitivity analysis for the aqueous-organic mass transfer coefficient showed that this transfer is not critical for the process performance and emphasized the efficient substrate-cell transfer in the investigated two-liquid phase process. The presented model provides a basis for complete theoretical description, characterization, and optimization of biooxidation processes based on growing cells.



## INTRODUCTION

Regio- and stereoselective biooxidations are an important field in biocatalysis (Faber, 2000; Schmid, et al., 2001; Burton, et al., 2002; Schmid, et al., 2002). Such reactions are often cofactor dependent (e.g., NADH, NADPH) and catalyzed by multicomponent enzyme systems, of which some are membrane associated. Thus, living whole-cells are usually favored over the use of isolated enzymes. Such potential preparative in vivo applications are often hampered by low water solubilities and high toxicities of possible substrates and products, limiting the performance of aqueous systems. Nonconventional reaction media such as an aqueous-organic two-liquid phase system are promising alternatives (Schwartz and McCoy, 1977; de Smet, et al., 1981b). A second immiscible phase can act as a reservoir for substrate and products, regulating the concentration of such compounds in the biocatalyst microenvironment, minimizing toxicity, and simplifying product recovery (Woodley and Lilly, 1990; Witholt, et al., 1992; Salter and Kell, 1995; Leon, et al., 1998).

Here, we focus on a two-liquid phase process for the production of aromatic aldehydes, which serve as ingredients of natural flavors and fragrances and as synthons for a variety of polymers, pharmaceuticals, and fine chemicals (Bruehne and Wright, 1985; Falbe and Regitz, 1995). Synthetic chemical strategies such as carbonylation or oxygen addition usually require the use of expensive and hazardous reactants and catalysts and often yield product mixtures complicating product isolation (Carelli, et al., 1999; Thomas, et al., 1999). Thus, we consider it worth exploring the biocatalytic production of aromatic aldehydes via selective multistep biooxidation of cheap substrates such as xylenes with benzyl alcohols as intermediates using the two-liquid phase concept as a tool to control multistep whole-cell biocatalysis.

The enzyme system we use for this oxidation is the xylene monooxygenase (XMO) of *Pseudomonas putida* mt-2 (Worsey and Williams, 1975; Harayama, et al., 1989), which consists of a NADH:acceptor reductase component (XylA) (Shaw and Harayama, 1992) and a membrane bound hydroxylase component (XylM) (Shaw and Harayama, 1995). This nonheme iron enzyme has a broad substrate range (Wubbolts, et al., 1994b) and initiates xylene degradation by the specific hydroxylation of one methyl group (Abril, et al., 1989). We have demonstrated that recombinant *E. coli* expressing the *xylMA* genes under control of the *alk* regulatory system (Panke, et al., 1999b) catalyze the monooxygenation not only of toluene and pseudocumene but also of the corresponding benzyl alcohols and benzaldehydes (Chapter 2). The kinetic analysis of this multistep reaction showed that the substrates toluene

and pseudocumene as well as the corresponding alcohols inhibit aldehyde oxygenation, and that elevated substrate concentrations also weakly inhibit alcohol oxygenation (Chapter 3). As an example for selective multistep biooxidation, we further investigated the bioconversion of pseudocumene to 3,4-dimethylbenzaldehyde (DMB-aldehyde) involving 3,4-dimethylbenzyl alcohol (DMB-alcohol) as intermediate and 3,4-dimethylbenzoic acid (DMB-acid) as potential by-product (Fig. 6.1A). The development and optimization of a two-liquid phase process with bis(2-ethylhexyl)phthalate (BEHP) as organic carrier solvent and recombinant *E. coli* as biocatalyst allowed to direct this complex kinetically controlled multistep bioconversion to the exclusive production of the desired DMB-aldehyde (Chapter 4). Fed-batch growth guaranteed efficient NADH regeneration. Successful scale up to a technical 30-L scale and straightforward product purification resulted in the recovery of 469 g DMB-aldehyde at a purity of 97% and an overall yield of 65% (Chapter 5).

Due to the lack of a comprehensive theory for such whole-cell biooxidations, process optimization has so far been carried out by an empirical approach. The influence of all known parameters was investigated experimentally, and these parameters were optimized one by one. This approach allowed obtaining suitable biotransformation conditions. A detailed process model based on knowledge gained by the empirical approach will facilitate process characterization and optimization especially when other substrates are used, leading to considerable savings in experimental effort and enabling a straightforward scale up. Furthermore, such a mathematical model is a promising approach towards a comprehensive theory for whole-cell biooxidations in general.

This chapter describes the development of a model for whole-cell biocatalysis in a two-liquid phase system including cell growth and bioconversion kinetics. The primary goal is to use the model to further characterize and optimize the multistep biooxidation of pseudocumene to DMB-aldehyde in the BEHP-based two-liquid phase system. The model allowed studying specific issues such as substrate transfer from the solvent to the cells, pH dependency, impact of the bioconversion on cell metabolism, the inhibitions of the different reaction steps by the reactants, and the impact of organic-aqueous mass transfer.

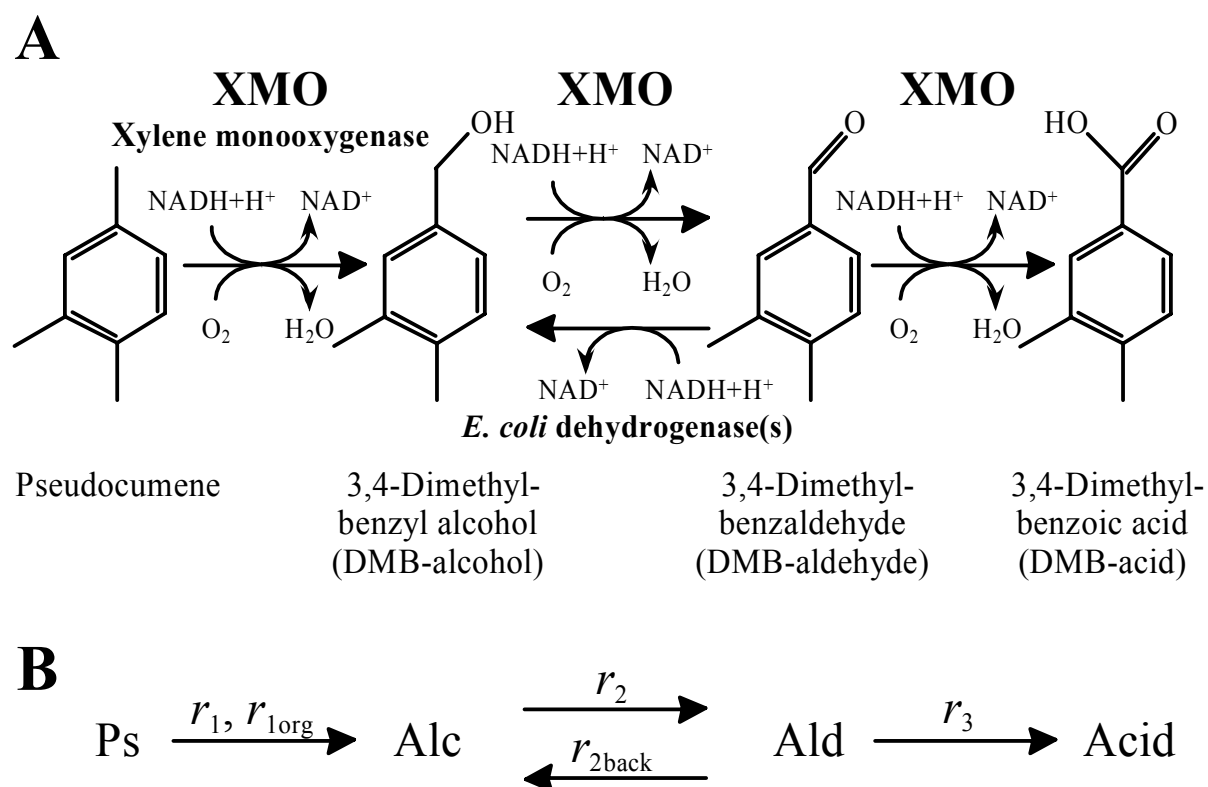


**Figure 6.1.** Bioconversion reactions catalyzed by *E. coli* JM101 (pSPZ3). Panel A shows the consecutive oxygenation of pseudocumene to DMB-alcohol, DMB-aldehyde, and DMB-acid catalyzed by xylene monooxygenase (XMO) and the back reaction from DMB-aldehyde to DMB-alcohol catalyzed by dehydrogenase(s) of the *E. coli* host. Panel B assigns the bioconversion rates  $r_1$ ,  $r_{1\text{org}}$ ,  $r_2$ ,  $r_{2\text{back}}$ , and  $r_3$  used in the modeling (see Modeling Aspects section) to the individual reaction steps. As in the subscripts of the modeling parameters, pseudocumene, DMB-alcohol, DMB-aldehyde, and DMB-acid are indicated as Ps, Alc, Ald, and Acid, respectively.

## MODELING ASPECTS

The process model described in this chapter is designed for whole-cell biocatalysis in a stirred tank reactor containing a biphasic liquid consisting of aqueous minimal medium and an organic phase at a volume ratio of about 1:1 (Chapters 3, 4, and 5). Cells and the growth substrate glucose are considered to reside in the aqueous phase only. For the cells, no stable adsorption to and no presence in the organic phase were observed under the microscope. The biotransformation compounds are considered to partition between both phases.

### Volume calculation

Calculation of the concentration profiles during bioconversion requires knowledge of the phase volumes. The precise organic-aqueous volume ratio fluctuates during the experiments because the organic phase is added only after about 1 h, both phases are sampled, there is a feed of glucose during the experiment, pH control requires addition of acid or base, and some evaporation occurs. For calculation of the phase volumes, the two latter sources of volume change are neglected, since the volume changes caused thereby are minor. Furthermore, it is assumed that the reactions, the phase mixing, the mass transfer between the two phases, and temperature differences do not cause significant volume changes.

The volumes of the aqueous and organic phases are  $V^{\text{aq}}$  and  $V^{\text{org}}$ , respectively. The subscript 0 is used to indicate the initial volume, which for the aqueous phase is the volume at the beginning of fed-batch cultivation ( $t_0$ ) and for the organic phase the volume at the time of its addition ( $t_{\text{org}}$ ) to the fed-batch culture. The aqueous glucose feed flow  $F$  may be changing during the bioconversion and hence is a function of time. Both phases are sampled during the experiment at regular intervals, and for simplicity this is expressed as a continuous sample flow  $F_{\text{sample}}$ , the same for both phases. The volumes are calculated using the following equations:

$$V^{\text{aq}} = V_0^{\text{aq}} + (F - F_{\text{sample}}) \cdot t \quad [\text{L}_{\text{aq}}] \quad (1)$$

$$V^{\text{org}} = 0 \quad \text{for } t < t_{\text{org}} \quad [\text{L}_{\text{org}}] \quad (2.1)$$

$$V^{\text{org}} = V_0^{\text{org}} - F_{\text{sample}} \cdot t \quad \text{for } t \geq t_{\text{org}} \quad [\text{L}_{\text{org}}] \quad (2.2)$$

### Biomass growth

The bioconversion rates are proportional to the biomass concentration ( $C_X$ ). Thus, a good prediction of  $C_X$  is needed, which is calculated using its macroscopic balance:

$$\begin{aligned} \text{accumulation} &= \text{production} - \text{flow out} \\ \frac{d(V^{\text{aq}} \cdot C_X)}{dt} &= V^{\text{aq}} \cdot r_X - F_{\text{sample}} \cdot C_X \quad [\text{g h}^{-1}] \quad (3) \end{aligned}$$

This equation can be integrated using the boundary condition  $C_{X,0}$  at  $t_0$ . It is assumed that the rate of biomass accumulation ( $r_X$ ) depends on the aqueous glucose concentration ( $C_{\text{Glc}}^{\text{aq}}$ ) and the dissolved oxygen concentration ( $C_{\text{O}_2}^{\text{aq}}$ ):

$$r_X = \frac{C_{\text{Glc}}^{\text{aq}}}{K_{s,\text{Glc}} + C_{\text{Glc}}^{\text{aq}}} \cdot \frac{C_{\text{O}_2}^{\text{aq}}}{K_{s,\text{O}_2} + C_{\text{O}_2}^{\text{aq}}} \cdot \mu_{\text{max}} \cdot C_X \quad [(\text{g of CDW}) \text{ L}_{\text{aq}}^{-1} \text{ h}^{-1}] \quad (4)$$

The Monod constants  $K_s$  are  $0.0018 \text{ g L}_{\text{aq}}^{-1}$  and  $2 \cdot 10^{-6} \text{ mmol L}_{\text{aq}}^{-1}$  for glucose and oxygen, respectively (Atkinson and Mavituna, 1991). Growth is also influenced by the biotransformation. The overproduction and presence of a heterologous monooxygenase as well as high bioconversion rates can have impeding or deleterious consequences for the host and its metabolism. This is due to additional protein synthesis, integration of enzyme components into the membrane, formation of reactive oxygen species, consumption of reduction equivalents (NADH), and the formation of toxic products, which need to be excreted (Nieboer, et al., 1993; Chen, et al., 1995; Chen, et al., 1996; Neubauer, et al., 2003; van Beilen, et al., 2003). Such effects lead to acetic acid formation and growth inhibition (Park and Schmid, unpublished results). Due to yet insufficient knowledge in this context, bioconversion related growth inhibition was not included in the model, and the maximum specific growth rate  $\mu_{\text{max}}$  was varied among and during the biotransformations depending on pH, time after induction, and scale. The growth parameters are summarized in Table 6.1 and discussed in the Modeling and Simulation Results section.

### Glucose concentration

The glucose concentration is calculated using the following macroscopic balance:

$$\text{accumulation} = \text{flow in} - \text{flow out} - \text{consumption} \quad [\text{g h}^{-1}] \quad (5)$$

$$\frac{d(V^{\text{aq}} \cdot C_{\text{Glc}}^{\text{aq}})}{dt} = F \cdot C_{\text{Glc}}^{\text{feed}} - F_{\text{sample}} \cdot C_{\text{Glc}}^{\text{aq}} - V^{\text{aq}} \cdot r_{\text{Glc}}$$

This equation can be integrated using the boundary condition  $C_{\text{Glc},0}^{\text{aq}} = 0$  at  $t_0$ . The feed flow contains the glucose concentration in the feeding solution  $C_{\text{Glc}}^{\text{feed}}$  ( $450$  or  $730 \text{ g L}_{\text{feed}}^{-1}$ ). In the feeding solution containing  $450 \text{ g L}_{\text{feed}}^{-1}$  glucose, additionally,  $50 \text{ g L}_{\text{feed}}^{-1}$  yeast extract is present. This is considered by increasing the maximal biomass yield on glucose and by reducing the maintenance requirements. The glucose consumption rate is described by:

$$r_{\text{Glc}} = \frac{r_X}{Y_{\text{X/Glc}}^{\text{max}}} + \frac{r_{\text{P,NADH}}}{Y_{\text{P/Glc}}^{\text{max}}} + m_{\text{Glc}} \cdot C_X \quad [\text{g L}_{\text{aq}}^{-1} \text{ h}^{-1}] \quad (6)$$

Thus, the glucose consumption depends on the maximum yields of biomass and biotransformation product on glucose  $Y_{\text{X/Glc}}^{\text{max}}$  and  $Y_{\text{P/Glc}}^{\text{max}}$ , respectively, on the maintenance coefficient for glucose  $m_{\text{Glc}}$ , on the biomass formation rate  $r_X$ , and on the total NADH coupled

**Table 6.1. Growth parameters for the simulation of the reaction systems.\***

Parameter	Unit	Conditions		
		pH 7.1	pH 7.1, ye <sup>a</sup>	pH 7.4
$K_{s,\text{Glu}}$	$\text{g L}_{\text{aq}}^{-1}$	0.0018	0.0018	0.0018
$K_{s,\text{O}_2}$	$\text{mmol L}_{\text{aq}}^{-1}$	$2 \cdot 10^{-6}$	$2 \cdot 10^{-6}$	$2 \cdot 10^{-6}$
Initial $\mu_{\text{max}}$	$\text{h}^{-1}$	0.38	0.38	0.34 (0.3) <sup>b</sup>
Initial $m_{\text{Glc}}$	$\text{g g}^{-1} \text{h}^{-1}$	0.01	0.005	0.04
$Y_{\text{X/Glc}}^{\text{max } c}$	$\text{g g}^{-1}$	0.5	0.59	0.42 (0.33) <sup>b</sup>
$Y_{\text{P/Glu}}^{\text{max}}$	$\text{mmol mCmol}^{-1}$	1.67	1.67	1.67
$Y_{\text{P/O}_2}^{\text{max}}$	$\text{mmol mmol}^{-1}$	1	1	1
$(k_L a)_{\text{O}_2}^d$	$\text{h}^{-1}$	1300 (1500)	1300 (1500)	1300 (1500)

\* The growth parameters apply for the simulations using both model 1 and 2 for the rate equations of the biotransformation.

<sup>a</sup> Cultivations with yeast extract in the feeding solution.

<sup>b</sup> Values apply for the modeling of biotransformations on a 2-L scale. The numbers in brackets apply for 30-L biotransformations.

<sup>c</sup>  $Y_{\text{X/O}_2}^{\text{max}}$  is dependent on  $Y_{\text{X/Glc}}^{\text{max}}$  as described in the Modeling Aspects section (equation 10).

<sup>d</sup>  $(k_L a)_{\text{O}_2}$  values for cultivations on a 2-L scale at a stirrer speed of 2000 rpm and 2500 rpm (brackets).  $(k_L a)_{\text{O}_2}$  values for cultivations on a 30-L scale are discussed in the Modeling and Simulation Results section.

bioconversion rate  $r_{\text{P,NADH}}$ .  $r_{\text{P,NADH}} (= r_1 + r_{\text{1org}} + r_2 + r_{\text{2back}} + r_3$ , see Biotransformation) represents the sum of the rates of NADH consuming reaction steps including the oxygenation steps catalyzed by XMO and the back reaction from DMB-aldehyde to DMB-alcohol catalyzed by *E. coli* dehydrogenases (Chapter 2). An estimate for  $Y_{\text{P/Glc}}^{\text{max}}$  is that per mol glucose 10 mol NADH can be produced by the microorganism; hence,  $Y_{\text{P/Glc}}^{\text{max}}$  is 1.667 mol product per C-mol glucose. It must be considered that uncoupling of the bioconversion related NADH oxidation from the biotransformation reactions may occur, thus leading to an underestimation of the bioconversion related glucose consumption in the model. Furthermore, due to overflow metabolism and metabolic stress caused by the presence of the heterologous monooxygenase and high bioconversion rates (as mentioned above), glucose will be transformed into acetic acid or other metabolites instead of CO<sub>2</sub>. Since the exact interrelationship of acetic acid formation is not known, this side reaction is not included in the model leading to inaccuracies in the prediction of the glucose concentration.

### Oxygen concentration

Biomass growth also depends on the dissolved oxygen concentration. However, the dissolved oxygen tension (DOT) was generally maintained above 10% throughout the experimental biotransformations except for some experiments including yeast extract as additional growth substrate. Nevertheless, the oxygen concentration is considered in the model and is calculated using its macroscopic balance:

$$\begin{aligned} \text{accumulation} &= \text{oxygen transfer rate} - \text{consumption} \\ \frac{d(V^{\text{aq}} \cdot C_{\text{O}_2}^{\text{aq}})}{dt} &= V^{\text{aq}} \cdot \varphi_{\text{O}_2} - V^{\text{aq}} \cdot r_{\text{O}_2} \quad [\text{mmol h}^{-1}] \quad (7) \end{aligned}$$

It is assumed that the influence of glucose feed and sampling are negligible. The oxygen concentration in equilibrium  $C_{\text{O}_2}^*$  is about 0.2 to 0.3 mmol L<sup>-1</sup> in aqueous fermentation medium aerated with air (Onken and Liefke, 1989; Royce and Thornhill, 1991) and here was assumed to be 0.25 mmol L<sub>aq</sub><sup>-1</sup>. Thus, equation 7 can be integrated using the boundary condition  $C_{\text{O}_2,0}^{\text{aq}} = C_{\text{O}_2}^* = 0.25 \text{ mmol L}_{\text{aq}}^{-1}$  at  $t_0$ . The oxygen transfer rate from gas phase to aqueous phase is described by:

$$\varphi_{\text{O}_2} = (k_L a)_{\text{O}_2} \cdot (C_{\text{O}_2}^* - C_{\text{O}_2}^{\text{aq}}) \quad [\text{mmol L}_{\text{aq}}^{-1} \text{ h}^{-1}] \quad (8)$$

In the presence of organic solvents, the volumetric mass transfer coefficient,  $(k_L a)_{\text{O}_2}$ , can be somewhat higher than usual. However, viscous organic solvents such as BEHP may impair mass transfer efficiency. For the lab-scale reactor used (2 L working volume) and aqueous medium a maximal  $(k_L a)_{\text{O}_2}$  of 1800 h<sup>-1</sup> was estimated (Schmid, 1997). Here, based on the modeling of experimental biotransformations, we assumed a  $(k_L a)_{\text{O}_2}$  of 1500 and 1300 h<sup>-1</sup> at a stirrer speed of 2500 (maximum) and 2000 rpm, respectively. For simplicity, only maximal stirrer speeds were considered and initial increases from lower stirrer speeds were neglected. The oxygen consumption rate ( $r_{\text{O}_2}$ ) depends on the maximum yields of biomass and biotransformation product on oxygen  $Y_{\text{X}/\text{O}_2}^{\text{max}}$  and  $Y_{\text{P}/\text{O}_2}^{\text{max}}$ , respectively, biomass growth, maintenance, and the rates of all O<sub>2</sub> consuming oxidation steps catalyzed by XMO,  $r_1$ ,  $r_{1\text{org}}$ ,  $r_2$ , and  $r_3$  (see Biotransformation):

$$r_{\text{O}_2} = \frac{r_{\text{X}}}{Y_{\text{X}/\text{O}_2}^{\text{max}}} + \frac{r_1 + r_{1\text{org}} + r_2 + r_3}{Y_{\text{P}/\text{O}_2}^{\text{max}}} + m_{\text{O}_2} \cdot C_{\text{X}} \quad [\text{mmol L}_{\text{aq}}^{-1} \text{ h}^{-1}] \quad (9)$$

The maximum yield of biotransformation steps on oxygen  $Y_{P/O_2}^{\max} = 1 \text{ mol mol}^{-1}$  is derived from the stoichiometry of monooxygenases. The maximum yield of biomass on oxygen  $Y_{X/O_2}^{\max}$ , is derived from the stoichiometry of formation of biomass assuming a composition of  $\text{CH}_{1.8}\text{O}_{0.5}\text{N}_{0.2}$  (Atkinson and Mavituna, 1991):



It can be derived that the coefficients for water and oxygen are  $b = 1.3 - 0.9 \cdot Y_{X/\text{Glc}}^{\max}$  and

$a = 1.15 - 1.2 \cdot Y_{X/\text{Glc}}^{\max}$ . Then,  $a = Y_{O_2/\text{Glc}} = \frac{Y_{X/\text{Glc}}^{\max}}{Y_{X/O_2}^{\max}}$ , so

$$Y_{X/O_2}^{\max} = \frac{1}{\frac{1.15}{Y_{X/\text{Glc}}^{\max}} - 1.2} \quad [\text{mCmol mmol}^{-1}] \quad (10)$$

The oxygen maintenance coefficient,  $m_{O_2}$ , can be derived from the stoichiometry of glucose respiration. This leads to:

$$m_{O_2} \quad [\text{mmol} \cdot \text{mCmol}^{-1} \cdot \text{h}^{-1}] = m_{\text{Glc}} \quad [\text{mCmol} \cdot \text{mCmol}^{-1} \cdot \text{h}^{-1}] \quad (11)$$

It must be considered that these stoichiometries are not exactly correct when yeast extract is present in the feeding solution. Furthermore, uncoupling of  $\text{O}_2$  consumption from monooxygenation in XMO catalysis and acetic acid formation (see above) may result in an error in predictions of the oxygen concentration.

### Biotransformation

The biotransformation compounds are pseudocumene, 3,4-dimethylbenzyl alcohol (DMB-alcohol), 3,4-dimethylbenzaldehyde (DMB-aldehyde), and 3,4-dimethylbenzoic acid (DMB-acid), indexed by the subscripts Ps, Alc, Ald, and Acid, respectively, in the bioconversion parameters (Fig. 6.1). The reaction rates between these compounds are sequentially  $r_1$ ,  $r_2$ , and  $r_3$ . The biotransformation compounds will be partly in the organic phase. For pseudocumene, we assume uptake also from the organic phase and release as DMB-alcohol into the aqueous phase. Thus,  $r_1$  is split into an apparent rate for pseudocumene uptake from the organic phase  $r_{1\text{org}}$  and an apparent rate for pseudocumene uptake from the aqueous phase  $r_1$  (Fig. 6.1B). Furthermore, a dehydrogenation type back reaction from aldehyde to alcohol is taking place in *E. coli* (Chapter 2). Thus,  $r_2$  is split into  $r_2$  (forward reaction) and  $r_{2\text{back}}$  (reverse reaction) (Fig. 6.1B). The species balances for the aqueous phase are:



*accumulation = transfer rate – flow out + production – consumption*

$$\frac{d(V^{\text{aq}} \cdot C_{\text{Ps}}^{\text{aq}})}{dt} = V^{\text{aq}} \cdot \varphi_{\text{Ps}} - F_{\text{sample}} \cdot C_{\text{Ps}}^{\text{aq}} - V^{\text{aq}} \cdot r_1 \quad [\text{mmol h}^{-1}] \quad (12.1)$$

$$\frac{d(V^{\text{aq}} \cdot C_{\text{Ald}}^{\text{aq}})}{dt} = V^{\text{aq}} \cdot \varphi_{\text{Ald}} - F_{\text{sample}} \cdot C_{\text{Ald}}^{\text{aq}} + V^{\text{aq}} \cdot (r_1 + r_{\text{org}} - r_2 + r_{2\text{back}}) \quad [\text{mmol h}^{-1}] \quad (12.2)$$

$$\frac{d(V^{\text{aq}} \cdot C_{\text{Acid}}^{\text{aq}})}{dt} = V^{\text{aq}} \cdot \varphi_{\text{Acid}} - F_{\text{sample}} \cdot C_{\text{Acid}}^{\text{aq}} + V^{\text{aq}} \cdot (r_2 - r_{2\text{back}} - r_3) \quad [\text{mmol h}^{-1}] \quad (12.3)$$

$$\frac{d(V^{\text{aq}} \cdot C_{\text{Ps}}^{\text{aq}})}{dt} = V^{\text{aq}} \cdot \varphi_{\text{Ps}} - F_{\text{sample}} \cdot C_{\text{Ps}}^{\text{aq}} + V^{\text{aq}} \cdot r_3 \quad [\text{mmol h}^{-1}] \quad (12.4)$$

These equations can be integrated using the boundary conditions  $C_0^{\text{aq}} = 0$  at  $t_{\text{org}}$ .

Since pseudocumene is volatile, pseudocumene evaporation from the organic phase is considered. The pseudocumene evaporation rate is described by:

$$r_{\text{evap}} = k_{\text{evap}} \cdot C_{\text{Ps}}^{\text{org}} \quad [\text{mmol L}_{\text{org}}^{-1} \text{h}^{-1}] \quad (13)$$

The evaporation rate constant for pseudocumene ( $k_{\text{evap}}$ ) calculated from the reactant balances in the biotransformation experiments amounts to  $0.025 \text{ h}^{-1}$ . Alternatively, assuming ideal conditions and that the air flow leaving the reactor is saturated with pseudocumene, the evaporation rate can be calculated based on the aeration rate, the vapor pressure of pure pseudocumene, and the mole fraction, at which pseudocumene is present in the organic phase. The vapor pressure of pure pseudocumene at  $25^\circ\text{C}$  is 2.1 mm Hg (<http://esc.syrres.com/interkow/physdemo.htm>) and was estimated to be 2.6 mm Hg at  $30^\circ\text{C}$  according to the equation of Clausius-Clapeyron. When a constant aeration rate of  $1.5 \text{ L}_{\text{air}} \text{ min}^{-1} \text{ L}_{\text{org}}^{-1}$  is assumed (the experimental aeration rate varied between 1 and  $2 \text{ L}_{\text{air}} \text{ min}^{-1} \text{ L}_{\text{org}}^{-1}$ ), this gives an estimated evaporation rate constant of  $0.0069 \text{ h}^{-1}$ . This value is in the same order of magnitude but about 3 times lower than the experimental  $k_{\text{evap}}$ , which can be attributed to the non-ideal conditions in the gaseous and liquid phases during the biotransformation.

The species balance for pseudocumene in the organic phase is:

*accumulation = –transfer rate – flow out – consumption – evaporation*

$$\frac{d(V^{\text{org}} \cdot C_{\text{Ps}}^{\text{org}})}{dt} = -V^{\text{aq}} \cdot \varphi_{\text{Ps}} - F_{\text{sample}} \cdot C_{\text{Ps}}^{\text{org}} - V^{\text{aq}} \cdot r_{1\text{org}} - V^{\text{org}} \cdot r_{\text{evap}} \quad [\text{mmol h}^{-1}] \quad (14.1)$$

This can be integrated using the boundary condition  $C_{p,s,0}^{\text{org}}$  at  $t_{\text{org}}$ . Analogous equations apply to DMB-alcohol, DMB-aldehyde, and DMB-acid in the organic phase, but their initial concentrations will be zero and there will be no consumption and no evaporation (low volatility).

The transfer rate of the reactants from the organic to the aqueous phase is:

$$\varphi_a = (k_L a)_{\text{org/aq}} \cdot \left( \frac{C_a^{\text{org}}}{K_{p,a}} - C_a^{\text{aq}} \right) \quad [\text{mmol L}_{\text{aq}}^{-1} \text{ h}^{-1}] \quad (15)$$

The subscript a refers to the biotransformation compound considered. The mass transfer coefficient  $(k_L a)_{\text{org/aq}}$  was assumed to be the same for all reactants and similar to the oxygen mass transfer coefficient (1300 – 1500  $\text{h}^{-1}$ ). On a technical scale, a significantly lower  $(k_L a)_{\text{org/aq}}$  of 500  $\text{h}^{-1}$  was assumed. Such values for  $(k_L a)_{\text{org/aq}}$  are in the same range as reported for other two-liquid phase processes performed in stirred tank reactors and with similar reactants, considering the varying power input in the different systems (Cruickshank, et al., 2000; Willeman, et al., 2002a; Willeman, et al., 2002d). Furthermore, a sensitivity analysis will be presented for  $(k_L a)_{\text{org/aq}}$ . The molar partition coefficients of the reactants between the organic and aqueous phase,  $K_{p,a}$  have been determined as described in Chapter 4.

For the rate equations of the biotransformation, two different models are used.

**Model 1.** The first model involves Michaelis-Menten equations for  $r_1$ ,  $r_{1\text{org}}$ ,  $r_2$ ,  $r_{2\text{back}}$ , and  $r_3$ , partly including inhibition terms for the individual reactants. Evidence for such inhibitions was presented earlier (Chapters 2, 3, and 4). Since these results indicated that the inhibitions are not purely competitive, rate equations including competitive (equation 16.1) and non competitive (equation 16.2) inhibitions were formulated and tested.

$$r_n = \frac{q_{\text{max},n} \cdot \frac{C_a^{\text{aq}}}{K_{m,a}} \cdot C_X}{1 + \frac{C_a^{\text{aq}}}{K_{m,a}} + \frac{C_b^{\text{aq}}}{K_{i,b,n}}} \quad [\text{mmol L}_{\text{aq}}^{-1} \text{ h}^{-1}] \quad (16.1)$$

$$r_n = \frac{q_{\text{max},n} \cdot \frac{C_a^{\text{aq}}}{K_{m,a}} \cdot C_X}{1 + \frac{C_a^{\text{aq}}}{K_{m,a}} + \frac{C_b^{\text{aq}}}{K_{i,b,n}} + \frac{C_a^{\text{aq}} \cdot C_b^{\text{aq}}}{K_{m,a} \cdot K_{i,b,n}}} \quad [\text{mmol L}_{\text{aq}}^{-1} \text{ h}^{-1}] \quad (16.2)$$

The subscripts a and b mark the parameters for the transformed and the inhibiting compound, respectively, and n the reaction step considered. In the absence of inhibiting compounds, these equations become normal Michaelis-Menten equations. The Michaelis-Menten constants  $K_m$  and the maximal reaction velocities  $q_{\max}$  for  $r_1$ ,  $r_2$ , and  $r_3$  are taken from Chapter 3, where  $q_{\max}$  was termed  $V_{\max}$ , assuming that the substrate uptake constants  $K_s$  given in Chapter 3 are actually  $K_m$  values. For  $r_{1\text{org}}$ , a Michaelis-Menten equation including the same  $q_{\max}$  as for  $r_1$  and a constant specific for substrate uptake directly from the organic phase,  $K_{m,\text{Ps,org}}$ , are assumed. Whereas  $r_1$ ,  $r_{1\text{org}}$ , and  $r_{2\text{back}}$  are supposed to be free of inhibitions by other reactants,  $r_2$  is assumed to be non competitively inhibited by pseudocumene (Chapter 3) and competitively or non competitively by the product DMB-aldehyde. The rate for the third reaction,  $r_3$ , is assumed to be non competitively inhibited by pseudocumene and DMB-alcohol (Chapter 3). The inhibition constants,  $K_{i,b,n}$ , as well as  $K_{m,\text{Ps,org}}$  were obtained by model fitting. For  $r_{2\text{back}}$ , a normal Michaelis-Menten equation was used, neglecting the forward reaction DMB-alcohol  $\rightarrow$  DMB-aldehyde in the dehydrogenation equilibrium. This is considered appropriate since an equilibrium constant of 0.01 was estimated earlier for the dehydrogenase reaction catalyzed by *E. coli* (pSPZ3) (Chapter 2). The parameters  $q_{\max,2\text{back}} = 14 \text{ U (g of CDW)}^{-1} = 0.84 \text{ mmol (g of CDW)}^{-1} \text{ h}^{-1}$  and  $K_{m,\text{Ald,back}} (=K_{s,\text{Ald,back}}) = 0.237 \text{ mM}$  were determined in this study as described in the Materials and Methods section.

**Model 2.** The second model considers that biotransformation and oxidative phosphorylation, in which NADH is consumed for energy (ATP) generation, compete for NADH. The rates of both may be decreased by high overall biotransformation rates causing NADH shortage (Park and Schmid, unpublished results). In the case of the biotransformation rates, this effect can be termed “feedback inhibition”. Thus, regarding the biotransformation, we tentatively introduced such an inhibition into the rate equations of the individual oxygenation reactions and called it metabolic inhibition. This metabolic inhibition is assumed to be a non competitive type of inhibition of the XMO catalyzed reactions by the total reaction rate  $r_{\text{P,NADH}} = r_1 + r_{1\text{org}} + r_2 + r_{2\text{back}} + r_3$ , corresponding to the total biotransformation related NADH consumption rate. Furthermore, a metabolic inhibition coefficient  $M_i$  (the same for all reaction steps) is introduced. Then, e.g., the equation for  $r_1$  becomes:

$$r_1 = \frac{q_{\max,1} \cdot \frac{C_{\text{Ps}}^{\text{aq}}}{K_{m,\text{Ps}}} \cdot C_X}{1 + \frac{C_{\text{Ps}}^{\text{aq}}}{K_{m,\text{Ps}}} + \frac{r_{\text{P,NADH}}}{M_i} + \frac{C_{\text{Ps}}^{\text{aq}} \cdot r_{\text{P,NADH}}}{K_{m,\text{Ps}} \cdot M_i}} \quad [\text{mmol L}_{\text{aq}}^{-1} \text{ h}^{-1}] \quad (17)$$

Analogous equations apply to  $r_{1\text{org}}$ ,  $r_2$ , and  $r_3$ . A potential metabolic inhibition of  $r_{2\text{back}}$ , which is catalyzed by dehydrogenase(s) of *E. coli* and not by XMO, would necessitate a different specific metabolic inhibition constant. For simplicity and because of the low absolute rate of this reaction, such a potential metabolic inhibition was neglected.

The rates except for  $r_{2\text{back}}$  will be dependent on the dissolved oxygen concentration. Since oxygen was not limiting in experimental biotransformations, this dependence is neglected. Furthermore, it must be considered that, in the beginning of the experimental bioconversions, full induction of the XMO activity only was reached after 1-2 h. This induction phenomenon was not included in the model. However, due to the low initial cell (biocatalyst) concentrations, this had only a minor impact on the bioconversion pattern. The bioconversion parameters for the simulation of the reaction systems according to model 2 for the rate equations are summarized in Table 6.2 and discussed in the Modeling and Simulation Results section.

### Simulation procedure

The left hand side of the aforementioned macroscopic balances was transformed into:

$$\frac{d(V \cdot C)}{dt} = V \cdot \frac{dC}{dt} + C \cdot \frac{dV}{dt} \quad (18)$$

Since the volume is known as a function of time according to equations 1, 2.1, or 2.2,  $dV/dt$  can be evaluated. Subsequently, differential equations can be obtained, in which  $dC/dt$  is explicit. As a representative example for all balance equations, the equation for the aqueous glucose concentration becomes:

$$\frac{dC_{\text{Glc}}^{\text{aq}}}{dt} = \frac{F \cdot C_{\text{Glc}}^{\text{feed}} - F_{\text{sample}} \cdot C_{\text{Glc}}^{\text{aq}} - V^{\text{aq}} \cdot r_{\text{Glc}} - C_{\text{Glc}}^{\text{aq}} \cdot \frac{dV^{\text{aq}}}{dt}}{V^{\text{aq}}} = -r_{\text{Glc}} + \frac{F \cdot (C_{\text{Glc}}^{\text{feed}} - C_{\text{Glc}}^{\text{aq}})}{V^{\text{aq}}} \quad (19)$$

**Table 6.2. Bioconversion parameters for the simulation of the reaction systems according to model 2 for the rate equations.\***

Parameter	Value	Unit
$q_{\max,1}$	21.06	mmol (g of CDW) <sup>-1</sup> h <sup>-1</sup>
$q_{\max,2}$	5.58	mmol (g of CDW) <sup>-1</sup> h <sup>-1</sup>
$q_{\max,2back}$	0.84	mmol (g of CDW) <sup>-1</sup> h <sup>-1</sup>
$q_{\max,3}$	72	mmol (g of CDW) <sup>-1</sup> h <sup>-1</sup>
$K_{m,Ps}$	0.202	mmol L <sub>aq</sub> <sup>-1</sup>
$K_{m,Alc}$	0.024	mmol L <sub>aq</sub> <sup>-1</sup>
$K_{m,Ald,back}$	0.24	mmol L <sub>aq</sub> <sup>-1</sup>
$K_{m,Ald}$	1	mmol L <sub>aq</sub> <sup>-1</sup>
$K_{m,Ps,org}$	850-1000	mmol L <sub>org</sub> <sup>-1</sup>
$K_{i,Ps,2}$	0.03	mmol L <sub>aq</sub> <sup>-1</sup>
$K_{i,Ald,2}$	0.004	mmol L <sub>aq</sub> <sup>-1</sup>
$K_{i,Ps,3}$	0.0002	mmol L <sub>aq</sub> <sup>-1</sup>
$K_{i,Alc,3}$	0.002	mmol L <sub>aq</sub> <sup>-1</sup>
$k_{\text{evap}}$	0.0069	h <sup>-1</sup>
$M_i$		
pH 7.1	1.08	mmol (g of CDW) <sup>-1</sup> h <sup>-1</sup>
pH 7.4	8.4	mmol (g of CDW) <sup>-1</sup> h <sup>-1</sup>
$K_{p,Ps}$	24300	L <sub>aq</sub> L <sub>org</sub> <sup>-1</sup>
$K_{p,Alc}$	50	L <sub>aq</sub> L <sub>org</sub> <sup>-1</sup>
$K_{p,Ald}$	906	L <sub>aq</sub> L <sub>org</sub> <sup>-1</sup>
$K_{p,Acid}$	0.118	L <sub>aq</sub> L <sub>org</sub> <sup>-1</sup>
$(k_L a)_{\text{org/aq}}$		
2-L scale	1300 (1500) <sup>a</sup>	h <sup>-1</sup>
30-L scale	500	h <sup>-1</sup>

\* All inhibition constants apply to non competitive inhibitions except for  $K_{i,Ald,2}$ , which applies to a competitive inhibition. The growth parameters used are listed in Table I. CDW: cell dry weight.

<sup>a</sup>  $(k_L a)_{\text{org/aq}}$  values at a stirrer speed of 2000 rpm and 2500 rpm (brackets).

## MATERIALS AND METHODS

**Bacterial strain, plasmid, and chemicals.** *E. coli* JM101 (*supE thi Δ(lac-proAB) F'[traD36 proAB<sup>+</sup> lacI<sup>f</sup> lacZΔM15]*) (Messing, 1979), an *E. coli* K-12 derivative, was used as recombinant host strain. As expression vector, we used the pBR322 derived plasmid pSPZ3 containing the XMO genes *xylMA* under the control of the *alk* regulatory system of *P. putida* GPo1 (Panke, et al., 1999b). The High Pure Plasmid Isolation Kit of Roche Diagnostics (Mannheim, Germany) was used to prepare plasmid DNA following the supplier's protocol. Chemicals were obtained from Fluka (Buchs, Switzerland) (pseudocumene, ~99%; DMB-acid, ~97%; BEHP, 97%), Aldrich (Buchs, Switzerland) (DMB-alcohol, 99%), Lancaster (Muehlheim, Germany) (DMB-aldehyde, 97%), and Acros Organics (Geel, Belgium) (*n*-octane, > 98.5%).

**Media and growth conditions.** Bacteria were either grown in Luria-Bertani (LB) broth (Difco, Detroit, Mich.) or minimal media, MS or RB (Chapter 4). In all cases, the growth temperature was 30°C. Complex media contained 50 mg L<sup>-1</sup> kanamycin and 10 g L<sup>-1</sup> glucose to avoid indigo formation (Panke, et al., 1999b). Minimal media contained per liter 5 or 7 g glucose, 10 mg thiamine, 50 mg kanamycin and 1 ml trace element solution US<sup>Fe</sup>, of which the composition is described in Chapters 3 and 4. Solid media contained 1.5% (wt/vol) agar. Shaking flask cultures were routinely incubated on horizontal shakers at 200 rpm. The setup and the procedure of the two-liquid phase biotransformations at different scales and pH as well as the process analytics have been described in Chapters 3, 4, and 5.

**Analysis of metabolites.** The quantitative analysis of *n*-octane, pseudocumene, 3,4-dimethylbenzyl alcohol, 3,4-dimethylbenzaldehyde and 3,4-dimethylbenzoic acid was performed via gas chromatography (GC) and high-performance liquid chromatography (HPLC) as described in Chapters 2 and 3.

**Whole-cell assays.** Whole-cell assays to study the kinetics and pH dependency of the three monooxygenation steps catalyzed by XMO included cell growth, induction, resting cell biotransformations at a 1 ml scale, and sample preparation for GC and HPLC analysis and were performed as described in Chapter 2 including induction by 0.1% (vol/vol) *n*-octane and cell concentrations in the resting cell biotransformations between 0.1 and 1.3 grams of cell dry weight (CDW) per liter.

In experiments to investigate the pH dependency of the specific activities of *E. coli* JM101 (pSPZ3), samples of cells were incubated for 5 minutes with 0.5 mM of pseudocumene,

DMB-alcohol, or DMB-aldehyde in 50 mM potassium phosphate buffer containing 1% (vol/vol) glucose at different pH, 30°C, and a cell concentration of about 0.5 (g of CDW) L<sup>-1</sup>. The assays were carried out twice independently. Initial specific activities were calculated as average activities based on the sum of all products formed in five minutes of reaction. One unit (U) is defined as the activity that forms 1 μmol of total products in 1 min. Specific activity was expressed as activity per g CDW [U · (g CDW)<sup>-1</sup>].

The kinetic parameters  $q_{\max,2\text{back}}$  and  $K_{m,\text{Ald,back}}$  ( $=K_{s,\text{Ald,back}}$ ) for the dehydrogenase type DMB-aldehyde reduction to DMB-alcohol catalyzed by *E. coli* JM101 without plasmid were determined in reactions carried out for 5 and 10 min with DMB-aldehyde concentrations ranging from 0.04 to 4 mM and a biocatalyst concentration of 1.28 (g of CDW) L<sup>-1</sup>. Specific activities were calculated based on the amount of DMB-alcohol formed.

The apparent maximal reaction velocities,  $q_{\max,2}$ , and substrate uptake constants,  $K_{s,\text{Ald}}$ , for DMB-alcohol oxidation at different inhibiting DMB-aldehyde concentrations (0, 0.1, 0.5, and 1 mM) catalyzed by *E. coli* JM101 (pSPZ3) were determined in reactions carried out for 5 min with DMB-alcohol concentrations ranging from 0.04 to 1 mM and a biocatalyst concentration of 0.097 (g of CDW) L<sup>-1</sup>. Such a low biocatalyst concentration was chosen in order to minimize the formation of a product mixture and to avoid significant substrate depletion. Specific activities were calculated based on the amount of products formed. Apparent  $q_{\max,2}$  and  $K_{s,\text{Ald}}$  values were calculated using the program Leonora designed to analyze enzyme kinetic data and described by Cornish-Bowden (Cornish-Bowden, 1995). The term “apparent” refers to the fact that these kinetic values were determined for whole-cells and in the presence of varying inhibitor (DMB-aldehyde) concentrations. As in the modeling, the substrate uptake constants  $K_s$  were assumed to be actually  $K_m$  values. Apparent inhibition constants,  $K_{i,\text{Ald},2}$ , were calculated according to the following correlation for competitive inhibition:

$$K_{m,\text{Ald}}^* = K_{m,\text{Ald}} \cdot \left(1 + \frac{C_{\text{Ald}}^{\text{aq}}}{K_{i,\text{Ald},2}}\right) \quad [\text{mmol L}_{\text{aq}}^{-1}] \quad (20)$$

In equation 20,  $K_{m,\text{Ald}}^*$  and  $K_{m,\text{Ald}}$  represent the apparent  $K_{s,\text{Ald}}$  values at the DMB-aldehyde concentration  $C_{\text{Ald}}^{\text{aq}}$  and in the absence of DMB-aldehyde, respectively.

**Process simulation.** The system of mathematical equations was programmed within Matlab version 6.1 (The Mathworks, Natick, MA), using the Simulink Block Library version 3.

## RESULTS AND DISCUSSION

In prior studies we demonstrated that recombinant *E. coli* containing XMO catalyze the multistep oxygenation of pseudocumene and toluene to corresponding benzylic alcohols, aldehydes, and acids (Chapter 2). Moreover, we reported that the two-liquid phase concept allowed the exploitation of the complex kinetics of this multistep oxygenation for the accumulation of one specific oxidation product from xylenes, e.g., 3,4-dimethylbenzaldehyde from pseudocumene (Chapters 3 and 4). We now discuss general biotransformation aspects as a basis for our mathematical model, which describes biotransformation experiments performed at varying pH, scale, and substrate concentrations and builds on kinetic analyses. In part, the respective experimental results have been presented earlier (Chapters 3, 4, and 5). Following that section, we present and discuss the modeling and simulation results for four representative biotransformations (referred to as biotransformations I, II, III, and IV throughout this chapter) with characteristic process parameters summarized in Table 6.3.

### BASIC CONSIDERATIONS

#### Solvent-cell mass transfer

Volumetric productivities attained in two-liquid phase systems can be, in contrast to aqueous single-phase systems, limited by the transport of substrates from an apolar phase to the cells residing in the aqueous phase. In our system, the maximal pseudocumene solvent-cell transfer rates amounted to 50 and 44 mmol per liter of aqueous medium per hour on a 2-L scale (at  $C_X = 17.6$  (g of CDW)  $L^{-1}$  and  $C_{Ps}^{org} = 244$  mM) and a 30-L scale (at  $C_X = 14.3$  (g of CDW)  $L^{-1}$  and  $C_{Ps}^{org} = 255$  mM), respectively. The independency on scale and the general dependency on cell and organic substrate concentrations as well as on pH (Chapters 4 and 5) indicate that a potential absolute maximum of the volumetric solvent-cell transfer rate for pseudocumene was not reached. This is in agreement with results obtained by Schmid et al., who investigated a two-liquid phase system with hexadecene as organic carrier solvent and, e.g., octane as growth substrate for *P. putida* GPo1 (Schmid, et al., 1998c). Despite the very high partition coefficient of  $6.7 \cdot 10^5$  for octane and its very low water solubility of 5  $\mu M$ , they found octane solvent-cell transfer rates of up to 30 mmol  $L_{aq}^{-1} h^{-1}$  at growth limiting organic octane concentrations below 3% (vol/vol). Furthermore, their results suggested that growth was



**Table 6.3. Process characteristics of representative biotransformations.\***

Parameter	Unit	Biotransformation			
		I <sup>a</sup>	II <sup>b</sup>	III <sup>b</sup>	IV <sup>b</sup>
Initial [pseudocumene] <sub>org</sub>	mmol L <sub>org</sub> <sup>-1</sup>	315	500	400	355
Working volume	L <sub>tot</sub>	2	2	30	30
pH		7.1	7.4	7.4	7.1→7.4
Growth rate <sup>c</sup>	h <sup>-1</sup>	0.35	0.24	0.25	0.34
Maximal CDW reached	(g of CDW) L <sub>aq</sub> <sup>-1</sup>	30	18	15.5	20
Final [DMB-aldehyde] <sub>org</sub>	mmol L <sub>org</sub> <sup>-1</sup>	220	330	254	274
Product share in all reactants <sup>d</sup>	%	92	80	76	97
Maximal specific pseudocumene oxidation rate	U (g of CDW) <sup>-1</sup>	27	61	65	51
Maximal specific DMB-aldehyde formation rate	U (g of CDW) <sup>-1</sup>	16	43	36	30
Maximal volumetric DMB-aldehyde formation rate	U L <sub>aq</sub> <sup>-1</sup>	390	710	440	500
Average volumetric DMB-aldehyde formation rate	U L <sub>aq</sub> <sup>-1</sup>	244	416	293	325

\* All experiments were carried out with BEHP as organic carrier solvent and at a phase ratio of 0.5. Initial pseudocumene concentration, scale, and pH varied. For details see Chapters 4 and 5. CDW: cell dry weight. Subscripts: org: organic phase; aq: aqueous phase; tot: total volume.

<sup>a</sup> Adapted from Chapter 4.

<sup>b</sup> Adapted from Chapter 5.

<sup>c</sup> Approximation for the exponential growth phase.

<sup>d</sup> In the organic phase at the end of the biotransformation.

kinetically limited by a reduced octane uptake capacity of the cells at low octane concentrations in the apolar phase (Moser, 1981; Atherton, 1994) and not by an absolute maximum of the volumetric substrate mass transfer from the organic phase to the cells. Our results indicate that the same is true for pseudocumene bioconversion by *E. coli* JM101 (pSPZ3).

### Substrate uptake mechanism

For a reasonable modeling of whole-cell based bioconversions of apolar substrates such as pseudocumene, the type of substrate uptake mechanism is important. Three different bacterial uptake mechanisms for apolar hydrocarbons have been described, including uptake from the aqueous phase, uptake of solubilized substrates, and uptake via direct cellular contact with organic phase droplets (Schmid, 1997).

Uptake of substrates dissolved in the aqueous phase was reported for *n*-alkanes with chain lengths shorter than nonane (Cameotra and Singh, 1990; Schmid, et al., 1998c), cyclic hydrocarbons (Köhler, et al., 1994; Sikkema, et al., 1995), and toluene, which is similar to pseudocumene but less hydrophobic (higher water solubility) (Woodley, et al., 1991). Different observations indicate that pseudocumene may not exclusively be taken up from the aqueous phase: The aqueous phase toxicity limit for pseudocumene in a two-liquid phase system is significantly lower than in an aqueous one-phase system and the product formation pattern does not only depend on the aqueous substrate concentration (Chapter 4). Furthermore, experimental pseudocumene oxidation rates at pH 7.1 tended to exceed maximal theoretical reaction rates calculated using the Lineweaver-Burk equation and aqueous pseudocumene concentrations derived from the partition coefficient and organic pseudocumene concentrations (Chapter 4). Note that the kinetic parameters used in the Lineweaver-Burk equation have been determined in an aqueous single-phase system. In biotransformations performed at pH 7.4 instead of 7.1, significantly higher bioconversion rates were achieved (Chapter 5). As shown in Figure 6.2, pseudocumene oxidation rates measured in such two-liquid phase biotransformations on laboratory (Fig. 6.2A) as well as technical scale (Fig. 6.2B) clearly exceed the theoretical maxima. Thus, we conclude that uptake of pseudocumene dissolved in the aqueous phase cannot account for the total pseudocumene uptake by the cells in the BEHP-based two-liquid phase system.

Hydrocarbon assimilating bacteria are known to excrete surface-active compounds when grown in two-liquid phase cultures (de Smet, et al., 1983; Desai and Banat, 1997; Schmid, et al., 1998b). Specific surfactants were reported to be necessary for the efficient uptake of long-chain alkanes by various *Pseudomonas* and *Candida* species (Reddy, et al., 1982; Hardegger, et al., 1994; Sekelsky and Shreve, 1999; Noordman, et al., 2002). To our knowledge, such a specific excretion of biosurfactants is not known for *E. coli*. Nevertheless, solubilizing effects caused by cell lysis products and/or surface-active outer membrane compounds (polysaccharides, phospholipids, proteins), which have been observed in growing *E. coli* cultures (Hoekstra, et al., 1976; Gankema, et al., 1980), could explain the low aqueous

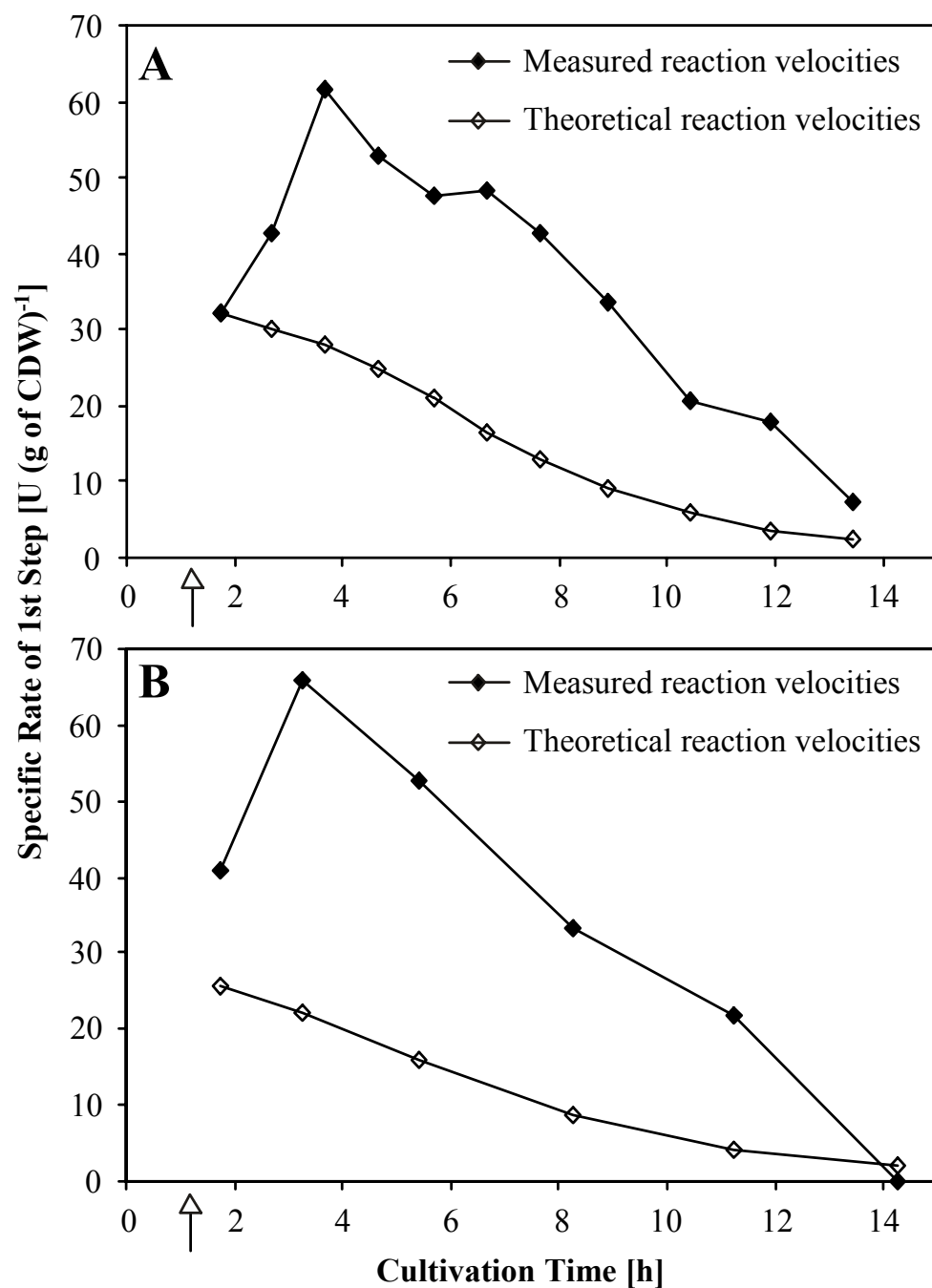


**Figure 6.2. Comparison of measured reaction velocities of pseudocumene oxidation and theoretical values corresponding to maximally possible reaction velocities** calculated via Lineweaver-Burk equation and aqueous pseudocumene concentrations derived from the partition coefficient. Panels A and B show the results for biotransformations II and III performed at pH 7.4 on a 2-L and a 30-L scale, respectively (Table 6.3). The experimental two-liquid phase biotransformations are based on *E. coli* JM101 (pSPZ3) growing in fed-batch mode as biocatalyst and BEHP as organic carrier solvent present at a phase ratio of 0.5 and containing, beside the substrate pseudocumene, 1% (vol/vol) *n*-octane for induction. Addition of the organic phase occurred after 1-1.33 h of fed-batch cultivation (open arrow). Experimental details have been described in Chapter 5.

toxicity limit for pseudocumene, the product formation pattern, and the high experimental pseudocumene oxidation rates in the two-liquid phase system under investigation. However, aqueous pseudocumene concentrations significantly higher than the theoretical values were not measured (Chapter 4). Thus, substrate solubilization can be ruled out as major mechanism for pseudocumene uptake.

Substrate uptake directly from the organic phase via cell-droplet interaction was assumed for substrates with low water solubilities, e.g., for long chain alkanes (Rosenberg and Rosenberg, 1981; Neufeld, et al., 1983; Goswami and Singh, 1991; Schmid, et al., 1998c), menthyl acetate (Westgate, et al., 1995), and trichlorophenol (Ascón-Cabrera and Lebeault, 1995). In our experiments, uptake via cell-droplet interactions would explain the observations that, in the two-liquid phase system, the cells sense significantly more pseudocumene than present in the aqueous phase and that the product formation pattern does not directly depend on aqueous substrate concentrations. Such an uptake mechanism does not depend on mass transfer from the organic to the aqueous phase and would explain the relatively high pseudocumene oxidation rates in our experiments.

Thus, we conclude that the product formation rate is dependent on the amount of pseudocumene present in the organic phase and suggest that pseudocumene uptake occurs at least in part directly from the organic phase. This was included in the model by introducing two rates for the first reaction step, one for the reaction in the aqueous phase and one for pseudocumene uptake from the organic phase and DMB-alcohol release into the aqueous phase.

### **pH dependency – metabolic inhibition**

The pH significantly influenced the reaction and growth rates as can be seen considering the process parameters shown in Table 6.3. When the modeling is performed according to model 1 for the rate equations of the biotransformation (equations 16.1 and 16.2; see Modeling Aspects section), appropriate modeling results for all the different biotransformations considered can only be obtained by changing the kinetic parameters, thus accelerating the individual reaction steps at higher pH. Introduction of an influence of the pH on pseudocumene uptake from the organic phase and on the non competitive inhibitions of DMB-alcohol oxidation by pseudocumene and DMB-aldehyde delivered acceptable modeling results (Fig. 6.3). Here, non competitive inhibition by DMB-aldehyde allowed better simulation results than competitive inhibition. At pH 7.4, the correct prediction of the biotransformation dynamics at different volumetric scales necessitated further adaptations of

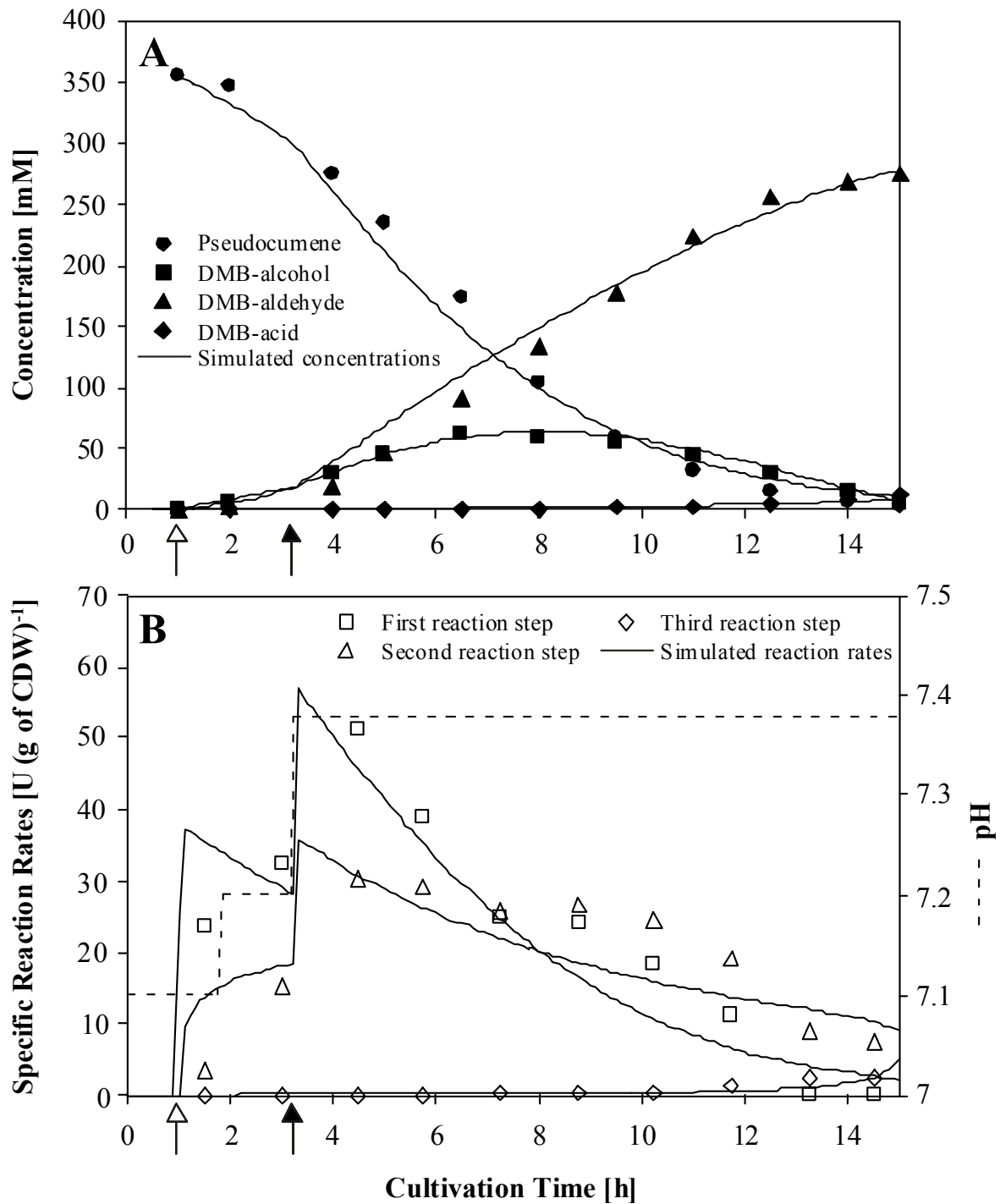


**Figure 6.3. Modeling results concerning the bioconversion in biotransformation IV using model 1 for the rate equations.** Symbols show experimentally measured values and solid lines the simulated course of reactant concentrations (A) and specific reaction rates (B). Panel B additionally shows the course of the experimental pH. The experimental two-liquid phase biotransformation on a technical scale (30 L working volume) included two pH-shifts and was performed as described for Figure 6.2 and in Chapter 5. The open arrow indicates organic phase addition. The closed arrow shows the time point of the change of the modeling parameters as a consequence of the pH shift and according to Table 6.4. The values for all other modeling parameters concerning bioconversion (except for  $M_i$ , which is not included in model 1 for the rate equations) and growth are listed in Tables 6.2 and 6.1, respectively.

**Table 6.4. Kinetic modeling parameters varied with pH and scale using model 1 for the rate equations of the bioconversion.\***

Parameter	Unit	Conditions		
		pH 7.1, both scales	pH 7.4, 2-L scale	pH 7.4, 30-L scale
$K_{m,Ps,org}$	$\text{mmol L}_{org}^{-1}$	4500	2400	1750
$K_{i,Ps,2}$	$\text{mmol L}_{aq}^{-1}$	0.0016	0.012	0.008
$K_{i,Ald,2}$	$\text{mmol L}_{aq}^{-1}$	0.045	0.19	0.09

\* Both inhibition constants, for pseudocumene and DMB-aldehyde as inhibitors, apply to non competitive inhibitions of the second reaction step. For the rest of the bioconversion related modeling parameters except for  $M_i$ , which is not considered in model 1, the parameters given in Table 6.2 were applied. The growth parameters used are listed in Table 6.1.

these kinetic parameters. The modeling parameters at varying pH and scale are summarized in Table 6.4. As an example, the simulation results for the 30-L scale biotransformation IV, including two pH shifts, are shown in Figure 6.3. At the time point of the second pH shift at 3.22 h of fed-batch cultivation, the parameters indicated in Table 6.4 were changed in one step being aware of the rather continuous than immediate response to such pH shifts. Similarly to the non-immediate induction, this inaccuracy was accepted for the modeling and resulted in a slight overestimation of the reaction rates in the beginning of the biotransformation. Good predictions of the reactant concentrations and specific reaction rates were achieved with a slight underestimation of the reaction rates towards the end of the biotransformation (Fig. 6.3). Good agreements of simulations with the experimental results also were obtained for all biotransformations presented in Chapters 3, 4, and 5. This supports the validity of the basic concept of the model formulation. However, it is improbable that pH and scale simultaneously influence substrate uptake and two inhibitions as assumed for the modeling based on model 1 for the rate equations.

In order to investigate the pH-dependent variance in specific biocatalyst activity, we performed short-term resting cell experiments (5 min of reaction) at varying pH: Exponentially growing cells were harvested, resuspended, and equilibrated in glucose containing potassium phosphate buffer (as described in the Materials and Methods section). Except for pH values below 7, these experiments revealed only a small dependence of the specific rates of the three monooxygenation steps on pH, whereas a significant difference

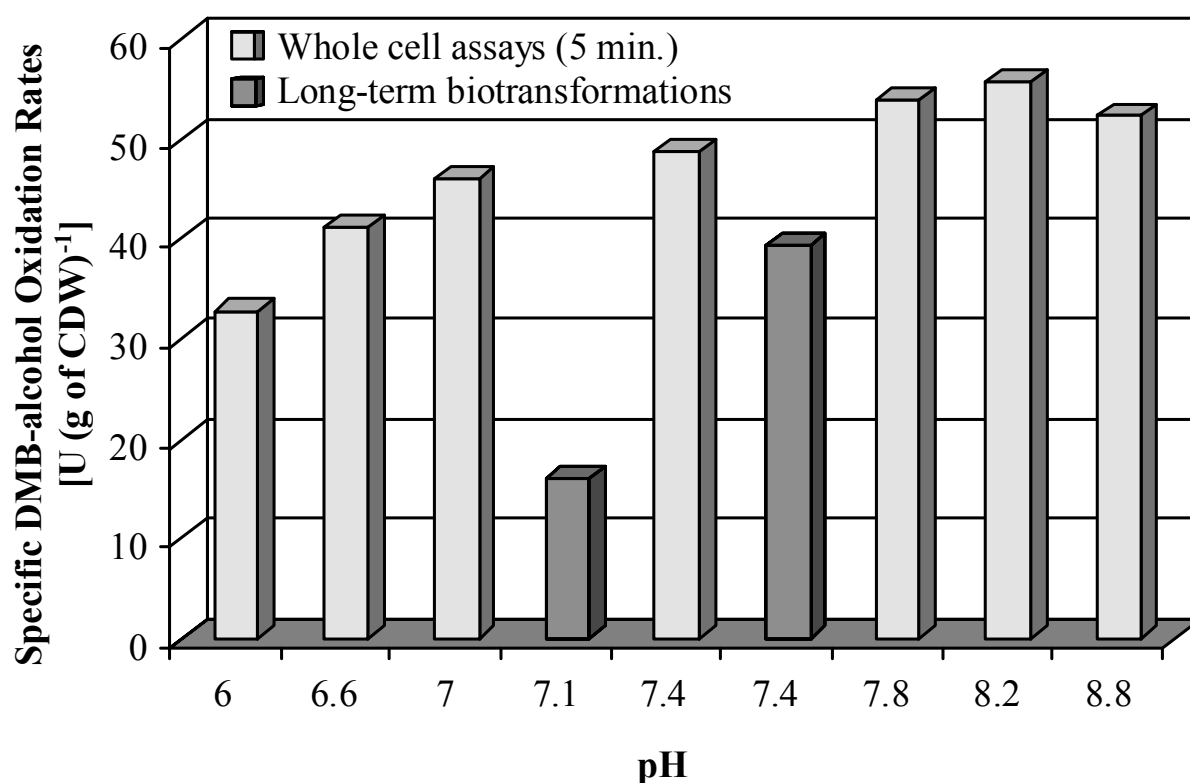


**Figure 6.4.** Comparison of specific DMB-alcohol oxidation rates at varying pH achieved in short-term (5 minutes) whole-cell activity assays with resting cells and in long-term two-liquid phase biotransformations with growing cells. Experimental details are described in the Materials and Methods section.

even between pH 7.1 and 7.4 was observed in long-term biotransformation experiments with cells growing in fed-batch mode. Figure 6.4 shows this phenomenon for DMB-alcohol oxidation, which is not substrate limited in two-liquid phase biotransformations. Long-term stability of specific activities necessitated the use of metabolically active growing cells allowing efficient NADH regeneration and was achieved by fed-batch cultivation (Chapter 4). Still, the higher specific activities in short-term resting cell biotransformations as compared to long-term biotransformations (Fig. 6.4) may be explained by a better availability of the cofactor due to the minor NADH depletion in only 5 min of reaction and the lack of other NADH consuming oxidation steps such as pseudocumene oxygenation. Thus, the clear effect of the pH in long-term biotransformations and the lack of such an effect in short-term bioconversions points to an influence of the pH on NADH availability in growing cells. In growing cells, biotransformation and oxidative phosphorylation, in which NADH is consumed for energy (ATP) generation, compete for NADH. Both may be inhibited by high

biotransformation rates causing metabolic stress and NADH shortage, especially at high overall reaction rates (Park and Schmid, unpublished results). The significant effect of the pH in such biotransformations (Fig. 6.4) may be explained by an influence of the pH on the competition of XMO and oxidative phosphorylation for NADH. Increasing the pH might promote the flow of reduction equivalents (NADH) to XMO at the expense of the flow to the oxidative phosphorylation and thus cause additional stress for the cells and interfere with cell growth. This is reasonable since the pH influences the proton gradient and thus the protonmotive force over the cytoplasmic membrane (Slonczewski, et al., 1981; Zilberstein, et al., 1984) where the enzyme systems competing for NADH, namely XMO and the enzymes involved in oxidative phosphorylation, are located. In fact, growth is influenced by the higher biotransformation rate. Biomass yield and growth rate are lower at higher biotransformation rates (Chapter 5). In order to evaluate such an influence of the pH on the competition for NADH, we introduced an inhibition of the biooxidation rates by the total NADH consuming biotransformation activity in model 2 for the rate equations of the biotransformation (equation 17). The extent of this so-called metabolic inhibition was assumed to vary with pH. Such a “feedback-inhibition” of the biotransformation rates opened the possibility to maintain  $K_{m,Ps,org}$ ,  $K_{i,Ps,2}$ , and  $K_{i,Ald,2}$  constant at different conditions.

## MODELING AND SIMULATION RESULTS

Growth parameters and the biotransformation parameters  $K_{i,b,n}$ ,  $K_{m,Ps,org}$ , and  $M_i$  were fitted to be as consistent as possible for the different biotransformations including experiments with and without yeast extract, with varying initial pseudocumene concentrations, at pH 7.1 and 7.4, and on 2- and 30-L scale (Chapters 3, 4, and 5). The simulation results for four representative biotransformations (Table 6.3) are shown in Figures 6.5 and 6.6 and are discussed in more detail regarding cell growth, biotransformation pattern, the inhibition of the second oxidation step by DMB-aldehyde, and organic-aqueous mass transfer.

### Cell growth

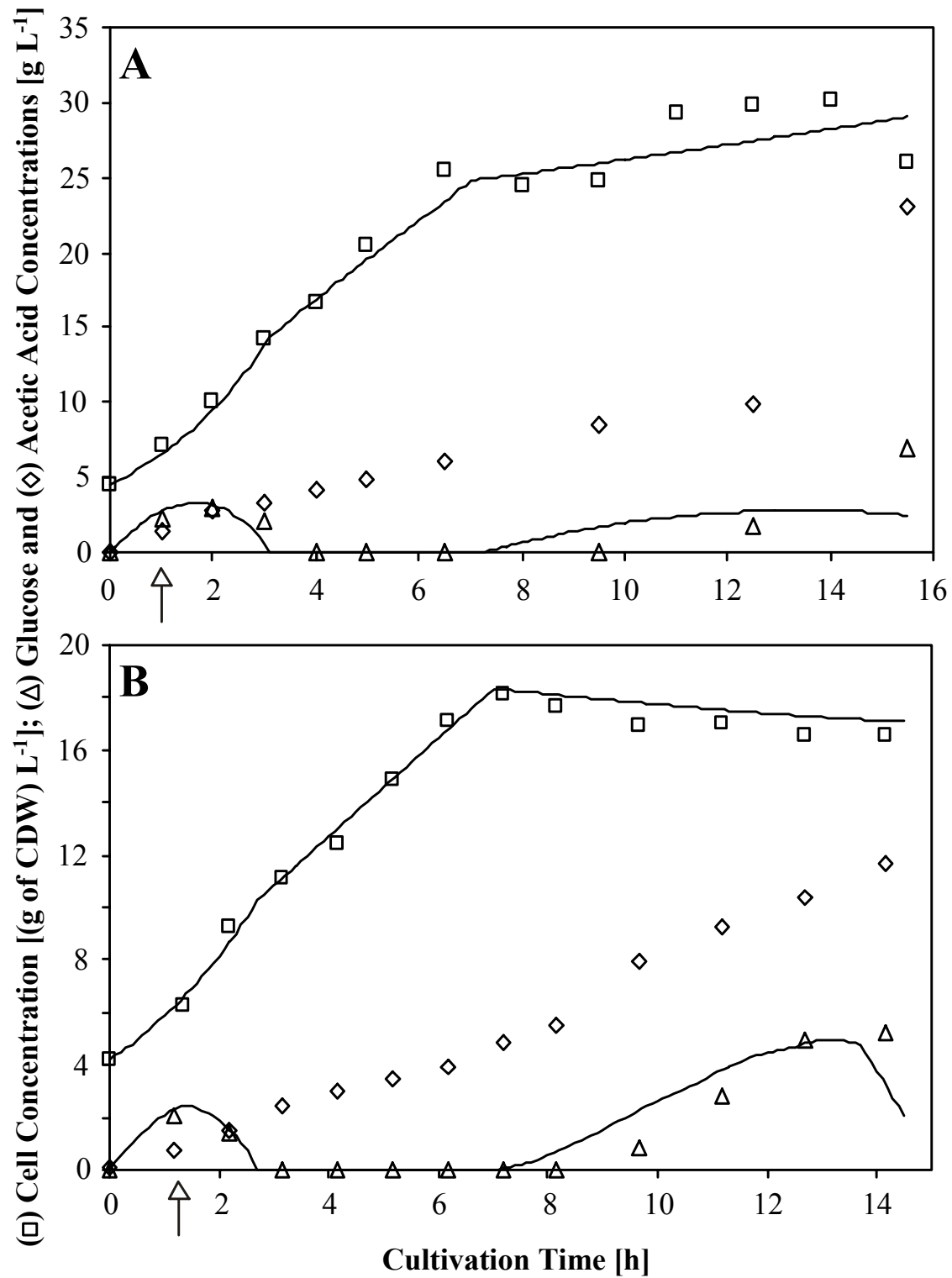
The main goal of the modeling was to investigate the bioconversion characteristics of a whole-cell multistep biooxidation in a two liquid-phase system on a theoretical level. The direct dependence of the volumetric bioconversion rates on biomass (biocatalyst) concentrations (Chapter 4) necessitates the correct prediction of cell concentrations. Table 6.1 shows a summary of the parameters used to simulate cell growth during the



biotransformations. As mentioned in the Modeling Aspects section, the presence of yeast extract as additional source of carbon and energy in the feeding solution was considered by increasing the yields and decreasing the maintenance requirements, which allowed a consistent modeling of such biotransformations. Four representative simulations of growth and glucose concentrations in biotransformations without yeast extract in the feeding solution are shown in Figure 6.5. The pH influenced the growth behavior. At pH 7.4 as compared to pH 7.1,  $Y_{X/Glc}^{max}$  and  $\mu_{max}$  changed to lower and  $m_{Glc}$  to higher values (Table 6.1). At higher pH, apparently, more glucose was needed for growth and maintenance. These results are in accordance with an influence of the pH on the competition for NADH between XMO and oxidative phosphorylation, favoring NADH flux to XMO at higher pH and causing additional metabolic stress for the cells, as assumed in model 2 for the rate equations of the bioconversion.

For the 2-L scale biotransformations at pH 7.1 and 7.4 (Fig. 6.5, A and B, respectively), exponential as well as glucose-limited growth were well predicted by the model. However, after about 7 h of fed-batch cultivation and 6 h of biotransformation, cell growth slowed down and stopped, which was not predicted by the model. Such transitions to the stationary phase may be caused, in addition to various effects observed in high cell density fed-batch cultures such as the occurrence of a nondividing cell population and cell lysis (Andersson, et al., 1996), by metabolic stress due to *xyIM*A expression, integration of XylM into the membrane, formation of reactive oxygen species, consumption of reduction equivalents (NADH) by XMO, and/or toxic effects of the reactants (Nieboer, et al., 1993; Chen, et al., 1995; Chen, et al., 1996; Neubauer, et al., 2003; van Beilen, et al., 2003). These yet poorly defined influences on cell metabolism necessitated switches of  $\mu_{max}$  (decrease to 0.01-0.03 h<sup>-1</sup>) and of the maintenance coefficient (increase to 0.2-0.3 g g<sup>-1</sup> h<sup>-1</sup>).

On a technical scale of 30 L working volume, glucose was present throughout the biotransformations (Fig. 6.5, C and D). There, apart from changes of  $Y_{X/Glc}^{max}$ ,  $m_{Glc}$ , and  $\mu_{max}$  due to pH shifts and transition to the stationary phase, further parameter changes were necessary to predict correct cell and glucose concentrations. This points to a continuously changing growth behavior. In order to model cell growth in biotransformation III (Fig. 6.5C), two switches of  $\mu_{max}$  and  $m_{Glc}$  were assumed. After 4 h of cultivation,  $m_{Glc}$  was increased to 0.12 g g<sup>-1</sup> h<sup>-1</sup> and  $\mu_{max}$  was lowered to 0.1 h<sup>-1</sup>. The transition to the stationary phase, in which a significant reduction of the cell concentration occurred, was considered by decreasing  $\mu_{max}$  to a negative value (-0.04 h<sup>-1</sup>) and increasing  $m_{Glc}$  to 0.31 g g<sup>-1</sup> h<sup>-1</sup>. For biotransformation



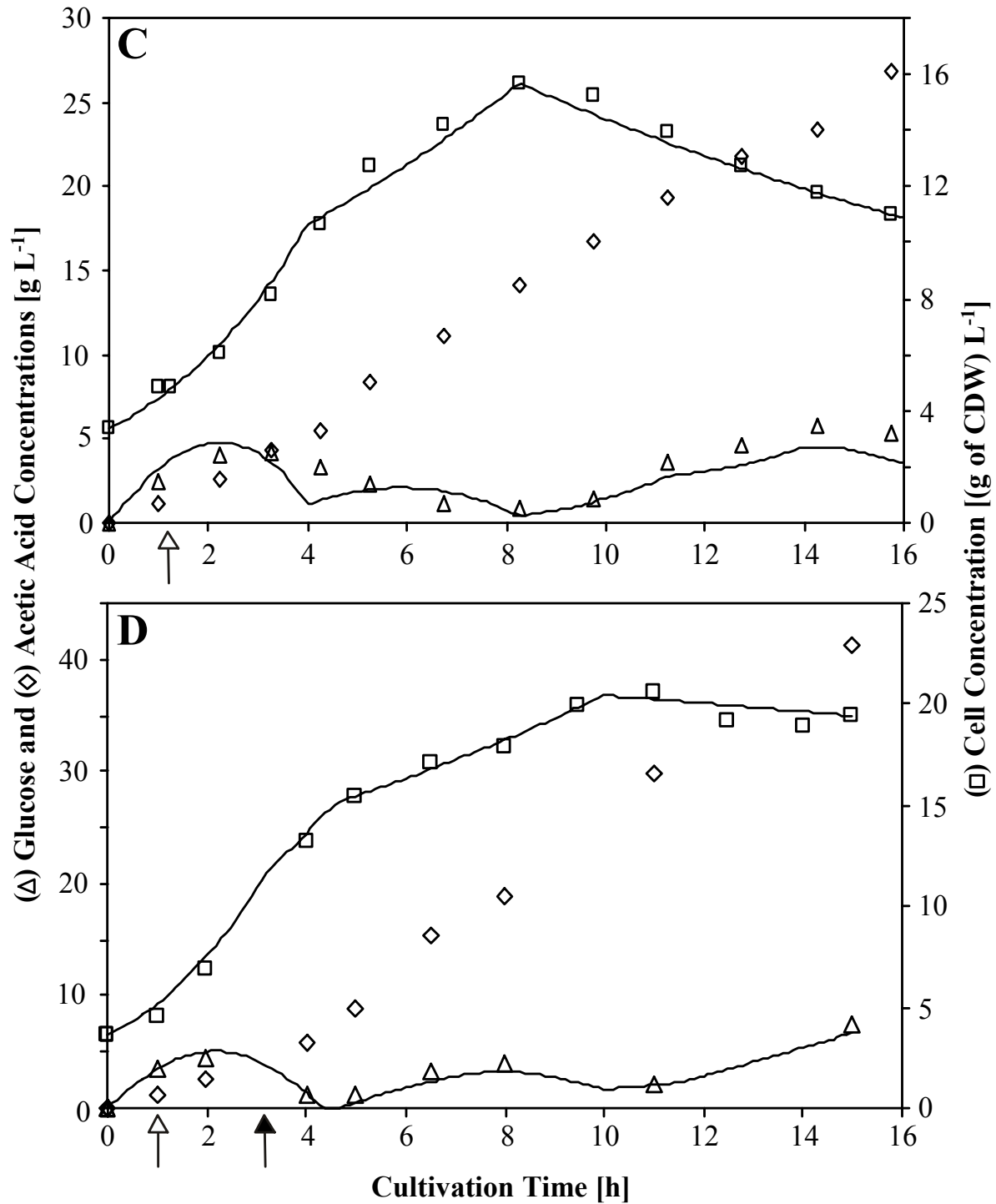


**Figure 6.5. Simulation of growth and glucose concentrations** during biotransformations I (A), II (B), III (C), and IV (D). Simulated cell and glucose concentrations did not substantially differ if model 1 or 2 for the rate equations of the bioconversion were used. Symbols show experimentally measured and solid lines simulated values. The experimental two-liquid phase biotransformations were performed as described for Figure 6.2 and in Chapters 4 and 5. Open arrows indicate organic phase addition. The closed arrow in panel D shows the time point of the change of the modeling parameters as a consequence of the pH shifts in biotransformation IV. Growth and bioconversion parameters used for the simulations are shown in Tables 6.1 and 6.2, respectively.

IV (Fig 6.5D), after 3.22 h of fed-batch cultivation (shift to pH 7.4),  $Y_{X/Glc}^{max}$ ,  $m_{Glc}$ , and  $\mu_{max}$  were changed to  $0.33 \text{ g g}^{-1}$ ,  $0.04 \text{ g g}^{-1} \text{ h}^{-1}$ , and  $0.2 \text{ h}^{-1}$ , respectively. After 4.7 h of cultivation,  $m_{Glc}$  was increased to  $0.15 \text{ g g}^{-1} \text{ h}^{-1}$  and  $\mu_{max}$  was lowered to  $0.067 \text{ h}^{-1}$ . Finally, the transition to the stationary phase was considered by decreasing  $\mu_{max}$  to  $0 \text{ h}^{-1}$  and increasing  $m_{Glc}$  to  $0.28 \text{ g g}^{-1} \text{ h}^{-1}$ . The generally lower  $\mu_{max}$  and  $Y_{X/Glc}^{max}$  at pH 7.4 on technical scale as compared to pH 7.4 on laboratory-scale may be explained by the higher acetic acid formation rate, which may be due to the presence of glucose throughout the biotransformations, resulting in growth inhibition and less efficient glucose utilization (Aristidou, et al., 1999). Furthermore, also initial  $\mu_{max}$  and  $Y_{X/Glc}^{max}$  were slightly lower at technical scale as compared to laboratory-scale (Table 6.1), which can be explained by a glucose gradient formation lowering cell yield and increasing acetic acid formation (Neubauer, et al., 1995; Bylund, et al., 1998).

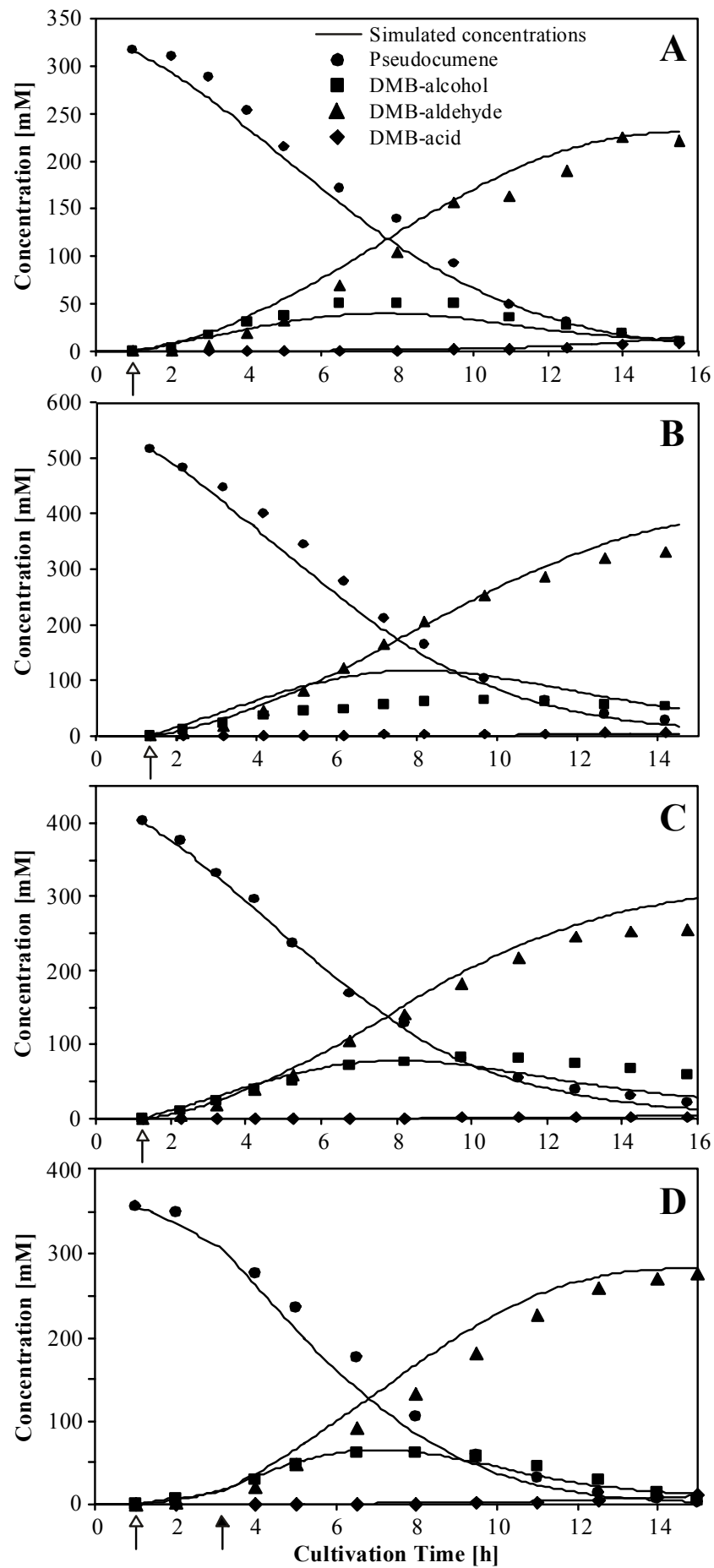
As mentioned in the Modeling Aspects section, only loose predictions of the oxygen concentration are possible due to the unknown interrelationship between recombinant oxygenase production, bioconversion, and metabolic stress. However, qualitatively, the predicted dissolved oxygen concentration kinetics correlate with the measured dissolved oxygen tension kinetics, when we consider that the discontinuous changes of the growth parameters in the model actually are continuous dynamic changes (results not shown). Quantitatively, the predicted oxygen concentrations at pH 7.4 and 7.1 tended to be too low and slightly too high, respectively, when compared with the measured oxygen tensions. At technical scale and pH 7.4 (biotransformation III) for instance, oxygen limitation could be prevented without oxygen admixture to the air stream. At the maximal power input of  $5 \text{ W L}^{-1}$  on this scale, a  $(k_L a)_{O_2}$  in the order of  $300\text{-}500 \text{ h}^{-1}$  would be expected (Schmid, 1997). However, a value of  $1300 \text{ h}^{-1}$  had to be chosen in order to prevent oxygen limitation in the simulation of biotransformation III and IV. In biotransformation IV with an initial pH of 7.1 followed by pH shifts, oxygen admixture was necessary to prevent oxygen limitation as predicted by the model including a  $(k_L a)_{O_2}$  in the order of  $300\text{-}500 \text{ h}^{-1}$ . These results again point to a significant influence of the pH on cell metabolism during biotransformation.

The modeling of cell growth necessitates yet undefined adaptations of growth parameters. It is thus still suboptimal and needs improvement in order to be applied for optimizing the growth conditions. Nevertheless, it meets the preliminary goal, the adequate simulation of biocatalyst concentrations, and allows the conclusion that biotransformation and pH have an impact on cell metabolism and thus growth.

### Product formation pattern and biotransformation rates

Figure 6.6 shows the simulations of pseudocumene bioconversion in biotransformations I – IV according to model 2 for the rate equations. The bioconversion parameters used for the simulations are given in Table 6.2 and allowed appropriate predictions of the biotransformation rates at pH 7.1 and 7.4 using a single set of kinetic parameters. The only parameter, which was changed with pH, was the metabolic inhibition coefficient  $M_i$  introduced in model 2 for the rate equations (equation 17).

With an  $M_i$  of  $18 \text{ U (g of CDW)}^{-1} = 1.08 \text{ mmol (g of CDW)}^{-1} \text{ h}^{-1}$  for biotransformation I at pH 7.1, reactant concentrations as well as biotransformation rates were simulated well with a minor deviation at the beginning due to the neglect of induction kinetics (Fig. 6.6, A and E). At pH 7.4, a significantly higher  $M_i$  of  $140 \text{ U (g of CDW)}^{-1} = 8.4 \text{ mmol (g of CDW)}^{-1} \text{ h}^{-1}$  resulted in good simulation results. For biotransformation II (Fig. 6.6, B and F), the transient DMB-alcohol accumulation was somewhat overestimated, which involved an underestimation of the specific DMB-alcohol oxidation rate. Towards the end of this biotransformation and of biotransformation III (Fig. 6.6, C and G), in which the transient DMB-alcohol accumulation was well predicted, the experimental reaction rates fell below the simulated rates, which may be due to the low metabolic activity of stationary-phase cells and thus to an impaired NADH regeneration. Such an increased loss of viability at pH 7.4 is affirmed by the higher impact of bioconversion on growth as discussed above and by the decreasing cell concentrations at the end of, e.g., biotransformation III (Fig. 6.5C). Thus, the reduced NADH regeneration capacity in the stationary phase as the transition to the stationary phase might be a consequence of the stress associated with the production and presence of heterologous proteins, especially of active membrane associated monooxygenases (Nieboer, et al., 1993; Chen, et al., 1995; Chen, et al., 1996; Neubauer, et al., 2003; van Beilen, et al., 2003) and with the high biotransformation rates causing high level production of toxic compounds and NADH shortage (Park and Schmid, unpublished results). As a consequence, a high pH as compared to a low pH seems to have a beneficial as well as an unfavorable effect on biotransformation efficiency. The beneficial effect is that higher specific activities of the biocatalyst can be reached during fed-batch growth. The adverse effect is the more pronounced stress for the host cells and the concomitant reduction of viability, which leads to lower biocatalyst concentrations and an earlier loss of biocatalyst activity.



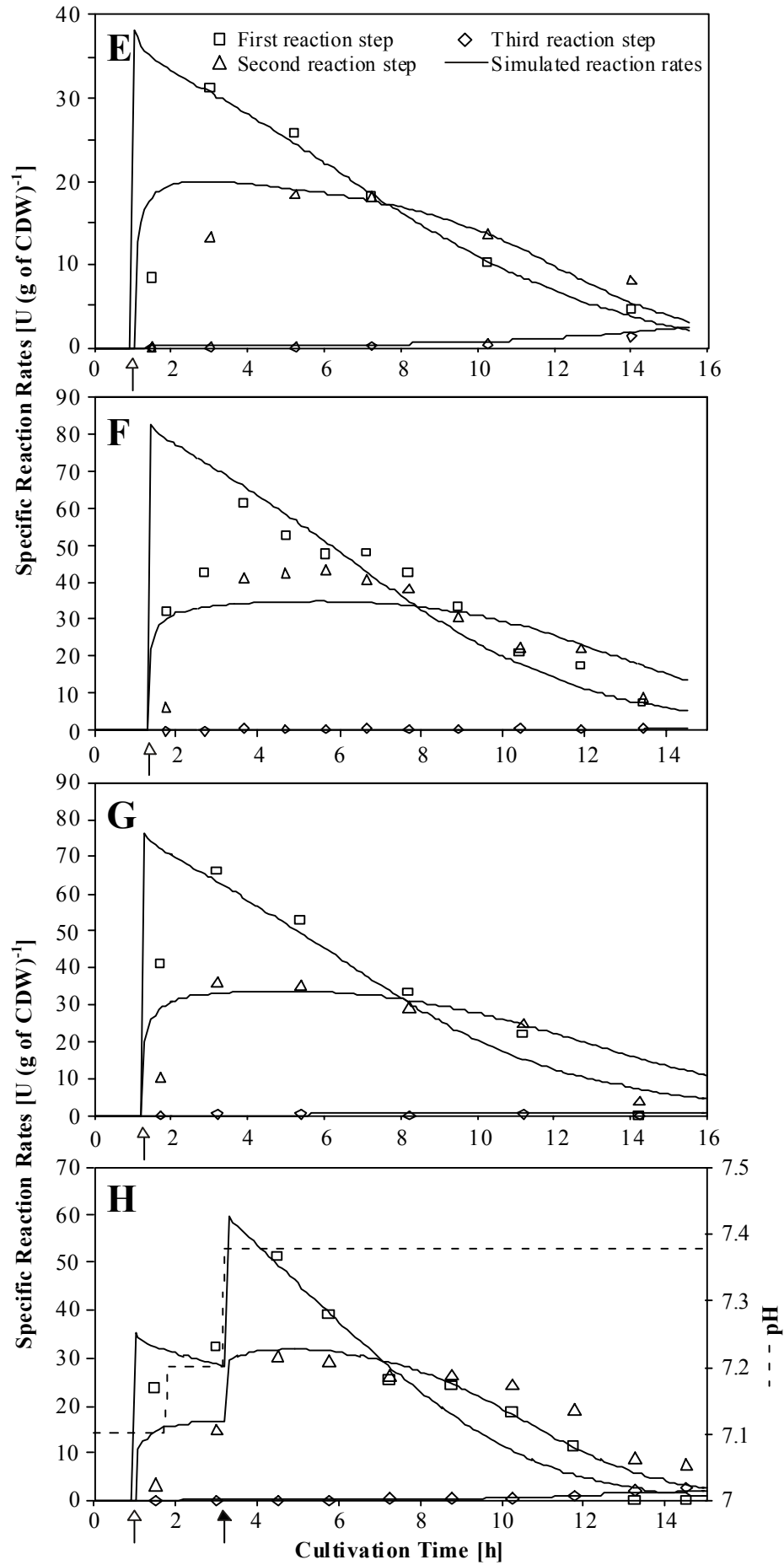


**Figure 6.6. Simulation results concerning the bioconversion** in biotransformations I (A, E), II (B, F), III (C, G), and IV (D, H). Symbols show experimentally measured values and solid lines the simulated course of reactant concentrations (A, B, C, D) and specific reaction rates (E, F, G, H). Panel H additionally shows the course of the experimental pH in biotransformation IV. The experimental two-liquid phase biotransformations were performed as described for Figure 2 and in Chapters 4 and 5. Open arrows indicate organic phase addition. Closed arrows indicate the change of the modeling parameters as a consequence of the pH shifts. Growth and bioconversion parameters used for the simulations are shown in Tables 6.1 and 6.2, respectively.

However, as indicated by biotransformation IV, the regulation of the pH during the process may allow profiting from beneficial effects while minimizing unfavorable effects. A single change of  $M_i$  after 3.22 h resulted in appropriate simulation of reactant concentrations and specific reaction rates in biotransformation IV (Fig. 6.6, D and H), although the response to the pH shifts is expected to be rather continuous than immediate. As compared to the simulation using model 1 for the rate equations (Fig. 6.3), the predicted course of the specific reaction rates was more accurate. Combined with the use of a single set of bioconversion parameters except for  $M_i$ , this demonstrates the superiority of model 2 over model 1 for the rate equations and supports a potential influence of the pH on the competition for NADH between XMO and the respiratory chain. This competition may be influenced by a pH-dependent variation of expression level, stability, or activity of XMO or of the enzymes involved in oxidative phosphorylation. A pH-dependency of XMO activity can be ruled out since the pH did not significantly influence the specific rate of DMB-alcohol oxidation in activity assays (Fig. 6.4) and since a pH optimum of 7 has been reported for partly purified XMO (Shaw and Harayama, 1995). A pH dependence of the expression level of NADH-dependent metabolic enzymes has been reported (Stancik, et al., 2002). However, the exact nature of the effect of the pH on biotransformation and cell growth remains to be investigated. This might lead to an improved model especially concerning cell growth. The high accuracy of the simulation results presented here illustrates the potential of the model for future process optimization.

### **Inhibition of DMB-alcohol oxidation by DMB-aldehyde**

All inhibitions exerted by pseudocumene and DMB-alcohol have been described in earlier studies (Chapters 2, 3, and 4). Here, reasonable simulation of DMB-alcohol oxidation necessitated the introduction of an additional inhibition by DMB-aldehyde into the model.



When model 1 for the rate equations was used for simulation, the best results were obtained by assuming a non competitive inhibition of the second reaction step by its product. In contrast, model 2 for the rate equations indicated a competitive type of inhibition. In order to prove the existence of such an inhibition and to gain insight in its characteristics, we experimentally analyzed the kinetics of the second oxygenation step in detail. We determined apparent maximal reaction velocities ( $q_{\max,2}$ ) and substrate uptake constants ( $K_{s,A1c}$ ) for *E. coli* JM101 (pSPZ3) at various initial DMB-aldehyde concentrations (Table 6.5). At all inhibitor concentrations, the cells showed Michaelis-Menten-like kinetics for DMB-aldehyde formation from DMB-alcohol. The corresponding Lineweaver-Burk plots are shown in Figure 6.7. The curves fitted according to the weighted parameters  $q_{\max,2}$  and  $K_{s,A1c}$  tend to intersect next to the y axis as expected from the low variance of the apparent  $q_{\max,2}$  and the high variance of the apparent  $K_{s,A1c}$  with inhibitor concentration (Table 6.5). This points to a competitive inhibition of the second step by its product as suggested by model 2 for the rate equations. However, mixed type inhibition with a strong contribution of competitive inhibition cannot completely be ruled out.

The apparent  $K_{i,A1d,2}$  values given in Table 6.5 were calculated according to equation 20 (see Materials and Methods) assuming competitive inhibition and normalizing  $q_{\max,2}$  at  $93 \text{ U (g of CDW)}^{-1} = 5.58 \text{ mmol (g of CDW)}^{-1} \text{ h}^{-1}$ . The variance of the apparent  $K_{i,A1d,2}$  with inhibitor concentrations may be due to various additional factors determining the kinetics of whole-cell biocatalysts as compared to isolated enzymes such as membrane permeability and cofactor availability. For the oxygenation of DMB-aldehyde to DMB-acid by *E. coli* JM101 (pSPZ3), we could not identify Michaelis-Menten like kinetics (Chapter 3). In further analyses, we observed a rather sigmoid than hyperbolic dependence of the reaction rate on the DMB-aldehyde concentration (results not shown) suggesting allosteric effects caused by DMB-aldehyde. Such effects might also influence DMB-alcohol oxidation thus partially overriding the inhibition by DMB-aldehyde at high DMB-aldehyde concentrations. Moreover, the kinetic analyses in aqueous single-phase systems showed that, at concentrations above the water solubility of DMB-aldehyde, increasing aldehyde amounts still caused increasing reaction rates, suggesting direct aldehyde uptake from organic-phase droplets (Chapter 3). Such interactions of DMB-aldehyde in the organic BEHP phase with the cells in the aqueous phase might explain the difference between the apparent inhibition constants determined in an aqueous single-phase system (Table 6.5) and the value for  $K_{i,A1d,2}$  ( $4 \mu\text{M}$ ) obtained by

**Table 6.5. Apparent<sup>a</sup>  $q_{\max,2}$ ,  $K_{s,\text{Alc}}$ , and  $K_{i,\text{Ald},2}$  values of *E. coli* JM101 (pSPZ3) for the second reaction step determined at different inhibitor (DMB-aldehyde) concentrations.**

DMB-aldehyde concentration [ $\mu\text{mol L}_{\text{aq}}^{-1}$ ]	Apparent <sup>a</sup> $q_{\max,2}$ [U (g of CDW) <sup>-1</sup> ]	Apparent <sup>a</sup> $K_{s,\text{Alc}}$ [ $\mu\text{mol L}_{\text{aq}}^{-1}$ ]	Apparent <sup>a</sup> $K_{i,\text{Ald},2}$ <sup>b</sup> [ $\mu\text{mol L}_{\text{aq}}^{-1}$ ]
0	93 ± 3	24 ± 3	
100	88 ± 4	51 ± 8	84
500	90 ± 2	83 ± 3	195
1000	74 ± 12	124 ± 36	171

CDW: cell dry weight.

<sup>a</sup> The term “apparent” refers to the fact that these kinetic values were determined for whole-cells and in the presence of varying inhibitor (DMB-aldehyde) concentrations.

<sup>b</sup> Apparent  $K_{i,\text{Ald},2}$  values were calculated according to equation 20 assuming competitive inhibition and normalizing  $q_{\max,2}$  at 93 U (g of CDW)<sup>-1</sup> (see Materials and Methods).

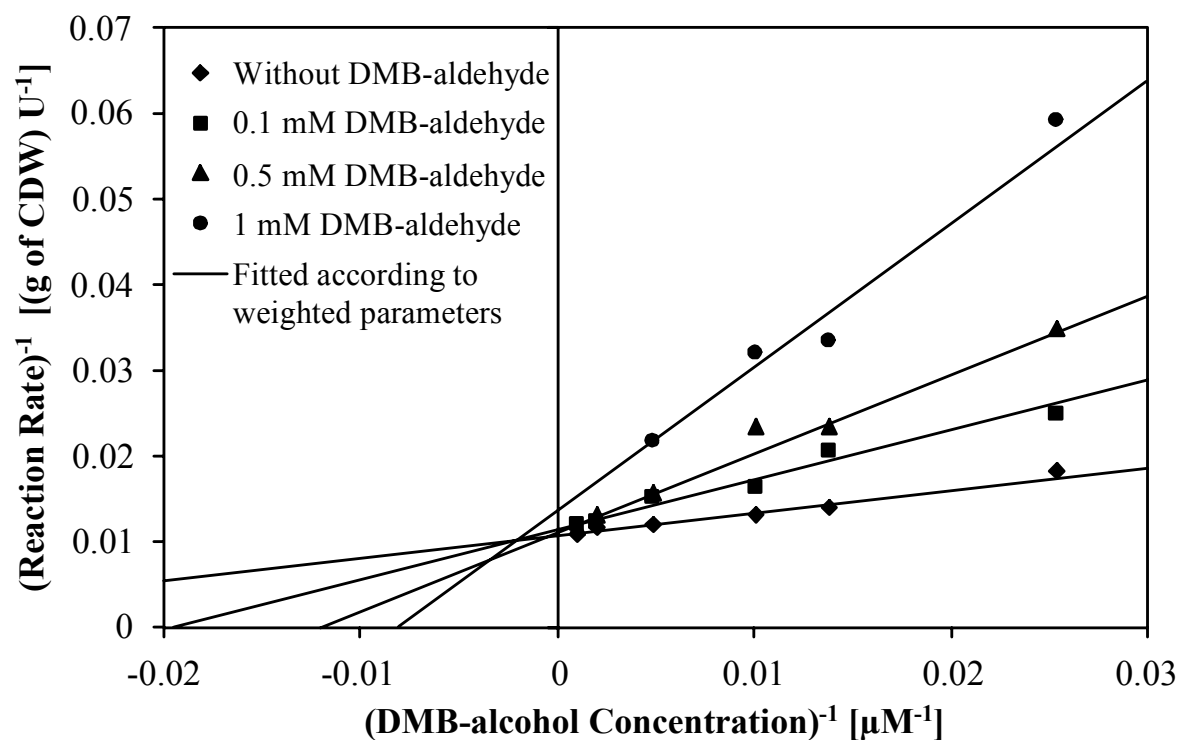


**Figure 6.7. Lineweaver-Burk plots for DMB-alcohol oxidation catalyzed by *E. coli* JM101 (pSPZ3) in the absence and in the presence of varying initial amounts of the product DMB-aldehyde.** Whole-cell assays to determine weighted apparent  $q_{\max,2}$  and  $K_{s,\text{Alc}}$  values were performed as described in the Materials and Methods section.

parameter fitting using the model for the two-liquid phase process. Such a direct uptake of DMB-aldehyde from the BEHP phase would influence the bioconversions of DMB-aldehyde, especially its reduction to DMB-alcohol by *E. coli* dehydrogenases.

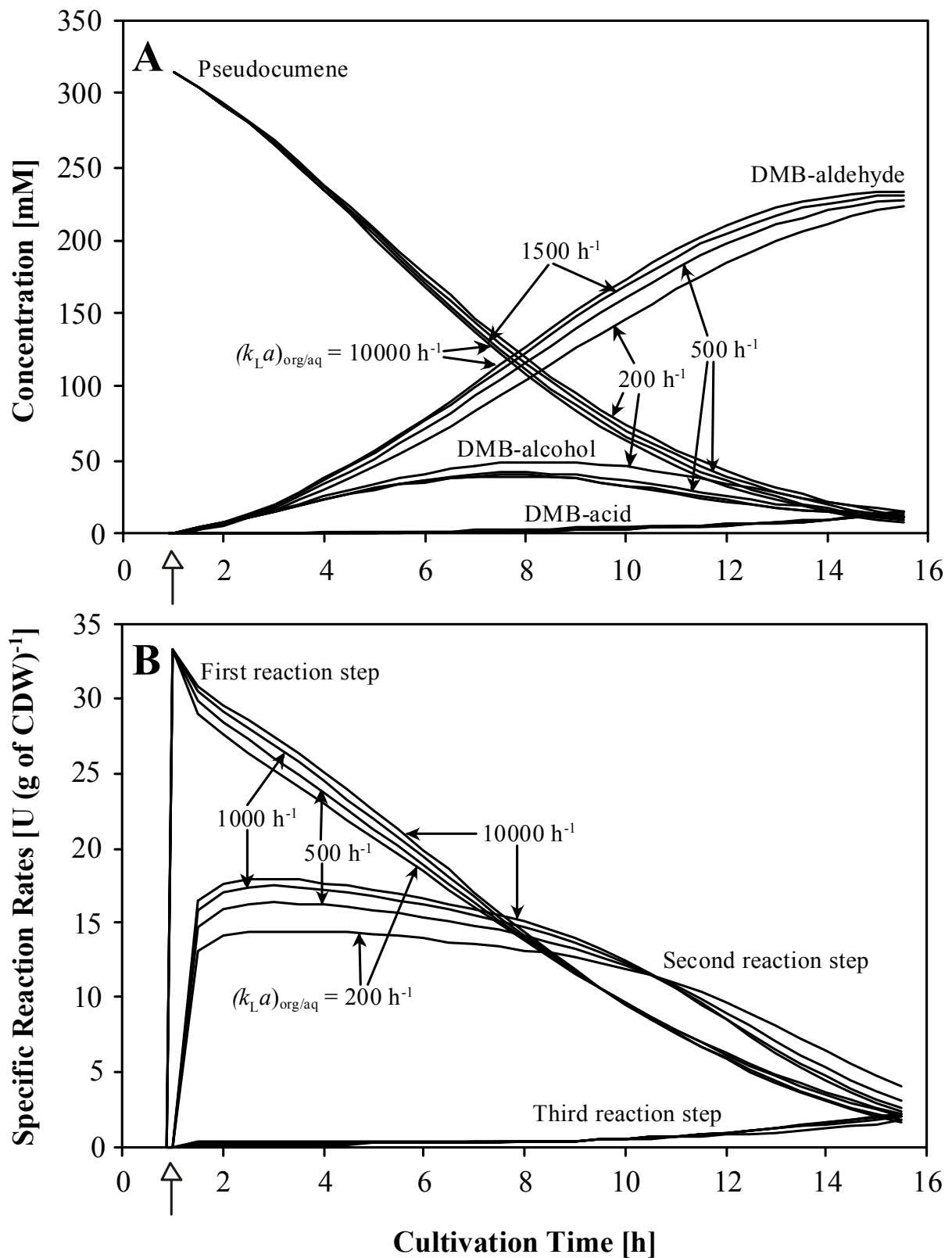
However, the experimental analysis of the kinetics of the second reaction step confirmed the inhibition by DMB-aldehyde predicted by the model. Model 2 for the rate equations even predicted a competitive type of inhibition, for which clear experimental evidence was found.

### Organic-Aqueous Mass Transfer

The mass transfer coefficient for the interexchange of reactants between the aqueous and the organic phase,  $(k_L a)_{\text{org/aq}}$ , was estimated to be 1300-1500 h<sup>-1</sup> on laboratory-scale (2 L) and 500 h<sup>-1</sup> on technical scale (30 L) (see modeling aspects). In order to examine the influence of  $(k_L a)_{\text{org/aq}}$  and of organic-aqueous mass transfer in general on the biotransformation pattern, we performed a sensitivity analysis for  $(k_L a)_{\text{org/aq}}$ . Panels A and B of Figure 6.8 show the simulation results for biotransformation I (2-L scale, pH 7.1), for which a  $(k_L a)_{\text{org/aq}}$  value of 1500 h<sup>-1</sup> has been used for the simulation shown in Panels A and E of Figure 6.6. Increasing this value had only a minor impact on biotransformation pattern and rates, which also applies to a decrease down to 500 h<sup>-1</sup>. Below, the simulated DMB-aldehyde accumulation is somewhat slower and the transient DMB-alcohol accumulation higher, which is due to a lower reaction rate for the second step.

The same was found for biotransformation IV on a 30-L scale including pH shifts (Fig. 6.8, C and D). Here, a  $(k_L a)_{\text{org/aq}}$  of 500 h<sup>-1</sup> has been used for the simulation shown in Panels D and H of Figure 6.6. The relatively low sensitivity of the first oxidation step to  $(k_L a)_{\text{org/aq}}$  can be ascribed to the contribution of direct pseudocumene uptake from the organic phase to the total substrate uptake. It cannot be excluded that such direct uptake also occurs for DMB-alcohol and DMB-aldehyde (see above). However, for these reactants the contribution of direct uptake would be low in the biotransformation system under investigation since their aqueous concentrations are considerably higher as compared to pseudocumene. This and the inhibitions of their oxygenations by other reactants, which in turn may also be influenced by direct interactions between cells and solvent droplets, hinder the identification of a potential direct uptake from the organic phase.

A modeling approach was also used to describe the interfacial mode of activity of hydroxynitrile lyase in a diisopropyl ether / aqueous buffer two-liquid phase system (Pereira, et al., 2002). This system was reported to show a linear dependence of the reaction rate on interfacial area and enzyme activity exclusively at the interface (Hickel, et al., 1999). The



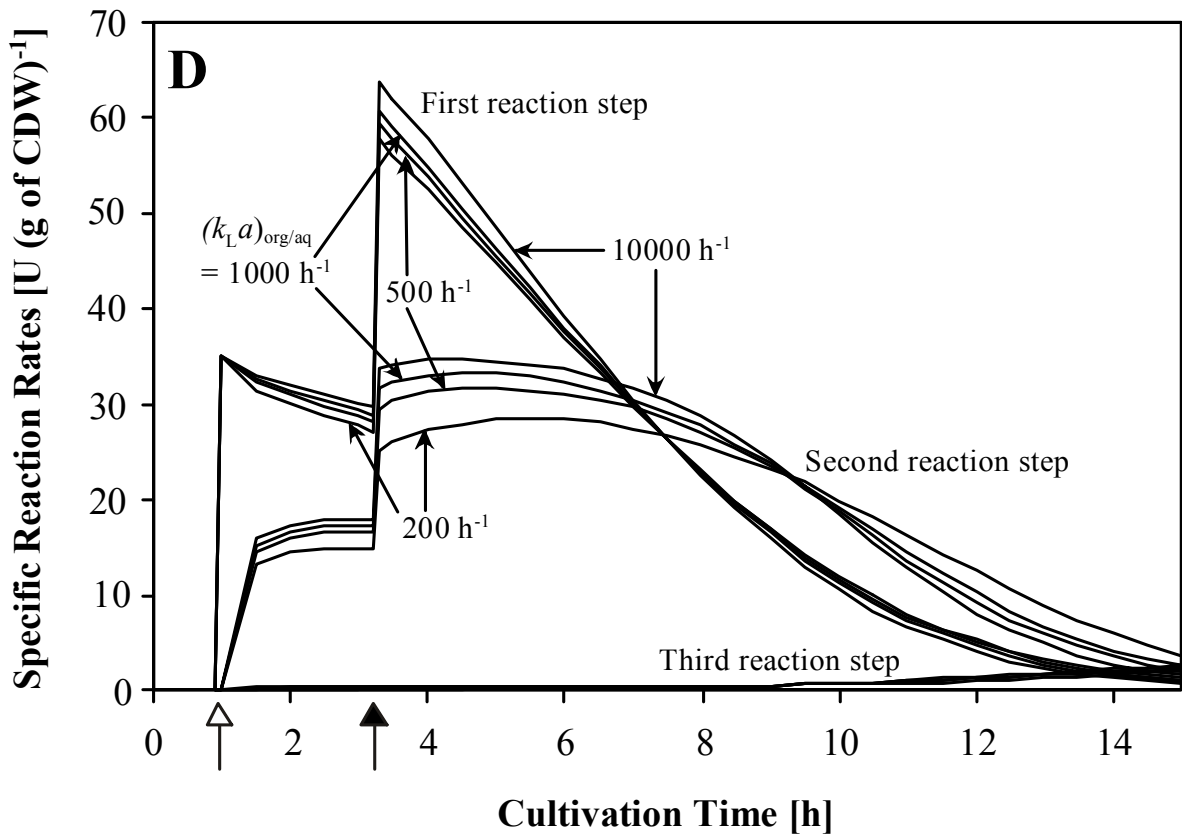
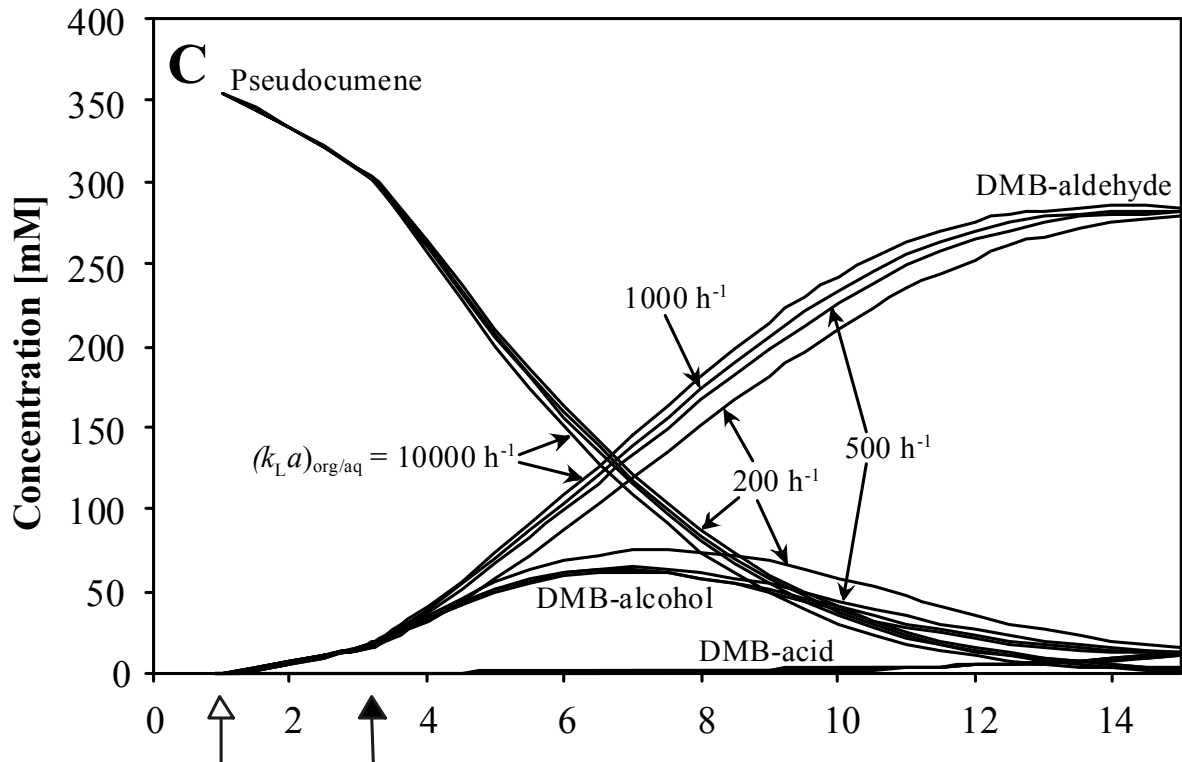


**Figure 6.8. Sensitivity analyses for the organic-aqueous mass transfer coefficient  $(k_{L,a})_{org/aq}$ .** The effect of varying  $(k_{L,a})_{org/aq}$  between 200 and 10000 h<sup>-1</sup> on the course of the reactant concentrations (A, C) and of the specific reaction rates (B, D) is shown for biotransformations I (A, B) and IV (C, D). Model 2 for the rate equations including metabolic inhibition was used for the simulation of the bioconversion. Open arrows indicate organic phase addition. Closed arrows indicate the switch of the modeling parameters as a consequence of the pH shifts in biotransformation IV. Except for  $(k_{L,a})_{org/aq}$ , the growth and bioconversion parameters shown in Tables 6.1 and 6.2 were used for the simulations.

model proposed a two-layer adsorption mechanism at the interface with a first layer consisting of unfolded enzymes with lower activity and a second layer consisting of native enzymes (Pereira, et al., 2002). Gerrits et al. exploited mass transfer limitation in a similar system with methyl *tert*-butyl ether as organic solvent to enhance the enantiomeric excess in the hydroxynitrile lyase based synthesis of chiral cyanohydrins (Gerrits, et al., 2001a; Gerrits, et al., 2001b). However, such a process for the production of (*R*)-mandelonitrile from benzaldehyde and hydrogen cyanide was consistently modeled without considering enzyme activity at the interface but assuming the reaction to occur in the bulk of the aqueous phase and by modeling substrate mass transfer from the organic to the aqueous phase (Willeman, et al., 2000; Willeman, et al., 2002a). A comparative evaluation of the mass transfer model and the adsorbed enzyme model showed that the two mechanisms often have qualitatively similar consequences and suggested that both models may be valid simultaneously (Straathof, 2003). Further developed versions of the mass transfer model, which is similar to the model developed in this study, facilitated reaction temperature optimization (Willeman, et al., 2002d) and allowed to compare batch, fed-batch, and continuous modes of operation (Willeman, et al., 2002c). Modeling indicated that continuous operation is not feasible and that the choice between batch and fed-batch operation depends on reactor and enzyme costs. It also facilitated the development of a process for the production of (*R*)-4-hydroxymandelonitrile from 4-hydroxybenzaldehyde and hydrogen cyanide (Willeman, et al., 2002b). Cruickshank et al. (2000) modeled phenol degradation by *P. putida* in a 2-undecanone based aqueous-organic two-liquid phase system and identified oxygen mass transfer as the main factor restricting the amount of phenol degradation over time, whereas phenol mass transfer was not limiting. This process model was used to optimize the phenol feeding strategy and included a cell entrainment factor in order to simulate the loss of active

cells to the organic phase and due to biofilm formation in the form of foam and wall growth (Collins and Daugulis, 1997).

In the process investigated in this study, we observed no significant cell loss, no cell-adsorption to the interphase (results not shown), and no significant dependence of the specific reaction rates on power input (scale) (Chapter 5). The developed model considers the reactions to occur in the bulk of the aqueous phase and additionally assumes direct pseudocumene uptake from the organic phase via collisions of cells and solvent droplets. The poor impact of the  $(k_{La})_{\text{org/aq}}$  on overall process performance indicates that, also on a technical scale, substrate-cell transfer is efficient and that, at the actual state of the process, other factors primarily affect the productivity of the whole-cell based two-liquid phase biotransformation of pseudocumene to DMB-aldehyde. Such factors may include intrinsic enzyme activity, enzyme stability, oxygen supply, and cofactor regeneration capacity, which is linked to cell viability. Studies on octane mass transfer in two-liquid phase cultures of *P. putida* GPo1 growing on octane contained in hexadecene as organic carrier solvent suggested that high solvent-cell transfer rates may also be achievable in biocatalytic two-liquid phase processes using recombinant strains for the production of a specific metabolic pathway intermediate, which is not further degraded (Schmid, et al., 1998a; Schmid, et al., 1998c). Together with the effective production of (*S*)-styrene oxide on pilot-scale by *E. coli* containing a recombinant styrene monooxygenase (Panke, et al., 2002), the efficient solvent-cell transfer attained for DMB-aldehyde production confirms this assessment.

## CONCLUSIONS

A process model has been developed to describe the multistep bioconversion of pseudocumene to DMB-aldehyde in a BEHP-based two-liquid phase system catalyzed by recombinant *E. coli* containing XMO and growing in fed-batch mode. The correlation between simulation and experimental results of biotransformations at varying conditions was high with respect to the course of the reactant concentrations and satisfying with respect to specific reaction rates. Simulation of cell growth meets the main goal to predict the biocatalyst concentration. However, the variation of the growth parameters during biotransformation is suboptimal, but allows the conclusion that bioconversion and pH have an impact on cell growth.

A comparison of the kinetics of the multistep oxygenation of pseudocumene in the aqueous single-phase system with the kinetics in the two-liquid phase system and process simulation indicated the occurrence of pseudocumene uptake directly from the organic phase. An increase of the pH from 7.1 to 7.4 has been found to increase biocatalyst activity at the expense of cell growth (Chapter 5) pointing to a pH-influenced competition for NADH between XMO and the respiratory chain. The introduction of a pH-dependent feedback inhibition of the NADH consuming bioconversions allowed good simulations of the multistep biooxidation of pseudocumene in experiments performed at varying pH, scale, and initial substrate concentration. This supported the assumed intracellular NADH shortage and the consequential pH-influenced competition for NADH. Furthermore, the modeling indicated competitive inhibition of the second oxidation step by DMB-aldehyde, which could be confirmed experimentally. A sensitivity analysis for  $(k_{La})_{\text{org/aq}}$  indicated that the organic-aqueous mass transfer does not affect the overall productivity of the process under the conditions applied and emphasized the efficient substrate-cell transfer in the BEHP-based two-liquid phase system.

The described model represents a first step towards the complete modeling of this biotransformation process. Ongoing research concentrates on the investigation of the interrelationship between bioconversion, cell growth, and acetic acid formation and thus is supposed to enable a more detailed modeling of bioconversion and especially of cell growth, also including acetic acid formation. The successful simulations presented in this study illustrate the potential of the model for future characterization and optimization of the present process and especially analogous processes using the same catalyst and concept for the production of different oxidation products. The model and results of this study will also provide valuable theoretical background for other two-liquid phase biooxidation processes based on growing cells.

## NOMENCLATURE

$C_a^{\text{aq}}$	concentration in aqueous phase [ $\text{mmol L}_{\text{aq}}^{-1}$ ]
$C_a^{\text{org}}$	concentration in organic phase [ $\text{mmol L}_{\text{org}}^{-1}$ ]
$C_{a,0}^{\text{org}}$	initial concentration in organic phase [ $\text{mmol L}_{\text{org}}^{-1}$ ]



$C_b^{\text{aq}}$	inhibitor concentration in aqueous phase [mmol L <sub>aq</sub> <sup>-1</sup> ]
$C_{\text{Glc}}^{\text{aq}}$	glucose concentration in aqueous phase [g L <sub>aq</sub> <sup>-1</sup> ]
$C_{\text{Glc},0}^{\text{aq}}$	initial glucose concentration in aqueous phase [g L <sub>aq</sub> <sup>-1</sup> ]
$C_{\text{Glc}}^{\text{feed}}$	glucose concentration in feeding solution [g L <sub>feed</sub> <sup>-1</sup> ]
$C_{\text{O}_2}^{\text{aq}}$	oxygen concentration in aqueous phase [mmol L <sub>aq</sub> <sup>-1</sup> ]
$C_{\text{O}_2,0}^{\text{aq}} = C_{\text{O}_2}^*$	aqueous oxygen concentration in equilibrium [mmol L <sub>aq</sub> <sup>-1</sup> ]
$C_X$	biomass concentration [(g of CDW) L <sub>aq</sub> <sup>-1</sup> or mMol L <sub>aq</sub> <sup>-1</sup> ]
$C_{X,0}$	initial biomass concentration [(g of CDW) L <sub>aq</sub> <sup>-1</sup> ]
$F$	aqueous glucose feed flow [L <sub>feed</sub> h <sup>-1</sup> ]
$F_{\text{sample}}$	sample flow [L h <sup>-1</sup> ]
$K_{m,a} (= K_{s,a})$	Michaelis (substrate uptake) constant for oxygenation of compound a [mmol L <sub>aq</sub> <sup>-1</sup> ]
$K_{m,\text{Ps,org}}$	Michaelis constant for pseudocumene uptake from organic phase [mmol L <sub>org</sub> <sup>-1</sup> ]
$K_{m,\text{Ald,back}}$	Michaelis constant for back reaction (dehydrogenation) of DMB-aldehyde to DMB-alcohol [mmol L <sub>aq</sub> <sup>-1</sup> ]
$K_{m,\text{Alc}}^*$	Michaelis constant for DMB-alcohol oxygenation in the presence of inhibiting DMB-aldehyde [mmol L <sub>aq</sub> <sup>-1</sup> ]
$K_{i,b,n}$	inhibition constant for compound b and reaction n [mmol L <sub>aq</sub> <sup>-1</sup> ]
$K_{p,a}$	partition coefficient for compound a [L <sub>aq</sub> L <sub>org</sub> <sup>-1</sup> ]
$K_{s,\text{Glc}}$	Saturation (Monod) constant for glucose [g L <sub>aq</sub> <sup>-1</sup> ]
$K_{s,\text{O}_2}$	Saturation (Monod) constant for oxygen [mmol L <sub>aq</sub> <sup>-1</sup> ]
$k_{\text{evap}}$	evaporation rate constant for pseudocumene [h <sup>-1</sup> ]
$(k_L a)_{\text{org/aq}}$	organic-aqueous mass transfer coefficient [h <sup>-1</sup> ]
$(k_L a)_{\text{O}_2}$	gas-aqueous mass transfer coefficient for oxygen [h <sup>-1</sup> ]
$M_i$	metabolic inhibition coefficient [mmol (g of CDW) <sup>-1</sup> h <sup>-1</sup> ]
$m_{\text{Glc}}$	maintenance coefficient for glucose [g (g of CDW) <sup>-1</sup> h <sup>-1</sup> or mMol mMol <sup>-1</sup> h <sup>-1</sup> ]
$m_{\text{O}_2}$	maintenance coefficient for oxygen [mmol (mMol biomass) <sup>-1</sup> h <sup>-1</sup> ]

$q_{\max,n}$	maximal rate for reaction n [ $\text{mmol (g of CDW)}^{-1} \text{ h}^{-1}$ ]
$r_n$	reaction rate for step n [ $\text{mmol L}_{\text{aq}}^{-1} \text{ h}^{-1}$ ]
$r_{\text{evap}}$	pseudocumene evaporation rate [ $\text{mmol L}_{\text{org}}^{-1} \text{ h}^{-1}$ ]
$r_{\text{p,NADH}}$	total NADH coupled bioconversion rate [ $\text{mmol L}_{\text{aq}}^{-1} \text{ h}^{-1}$ ]
$r_{\text{Glc}}$	glucose consumption rate [ $\text{g L}_{\text{aq}}^{-1} \text{ h}^{-1}$ ]
$r_{\text{O}_2}$	oxygen consumption rate [ $\text{mmol L}_{\text{aq}}^{-1} \text{ h}^{-1}$ ]
$r_X$	biomass formation rate [ $(\text{g of CDW}) \text{ L}_{\text{aq}}^{-1} \text{ h}^{-1}$ ]
$t$	time [h]
$t_0$	start of fed-batch cultivation [h]
$t_{\text{org}}$	time of organic phase addition [h]
$V^{\text{aq}}$	aqueous phase volume [ $\text{L}_{\text{aq}}$ ]
$V^{\text{org}}$	organic phase volume [ $\text{L}_{\text{org}}$ ]
$V_0^{\text{aq}}$	aqueous phase volume at $t_0$ [ $\text{L}_{\text{aq}}$ ]
$V_0^{\text{org}}$	organic phase volume at $t_{\text{org}}$ [ $\text{L}_{\text{org}}$ ]
$Y_{\text{P/Glc}}^{\text{max}}$	maximal yield of reaction steps on glucose [ $\text{mmol mCmol}^{-1}$ ]
$Y_{\text{P/O}_2}^{\text{max}}$	maximal yield of reaction steps on oxygen [ $\text{mmol mmol}^{-1}$ ]
$Y_{\text{X/Glc}}^{\text{max}}$	maximal yield of biomass on glucose [ $(\text{g of CDW}) \text{ g}^{-1}$ or $\text{mCmol mCmol}^{-1}$ ]
$Y_{\text{X/O}_2}^{\text{max}}$	maximal yield of biomass on oxygen [ $\text{mCmol mmol}^{-1}$ ]
$Y_{\text{O}_2/\text{Glc}}$	glucose dependent oxygen demand [ $\text{mmol mCmol}^{-1}$ ]
$\varphi_a$	organic-aqueous transfer rate of compound a [ $\text{mmol L}_{\text{aq}}^{-1} \text{ h}^{-1}$ ]
$\varphi_{\text{O}_2}$	oxygen transfer rate [ $\text{mmol L}_{\text{aq}}^{-1} \text{ h}^{-1}$ ]
$\mu_{\text{max}}$	maximum specific growth rate [ $\text{h}^{-1}$ ]

### Compounds a and b (inhibiting)

Ps	pseudocumene
Alc	3,4-dimethylbenzyl alcohol
Ald	3,4-dimethylbenzaldehyde
Acid	3,4-dimethylbenzoic acid

**Reaction step n**

1	$\text{Ps} \rightarrow \text{Alc}$
1org	$\text{Ps} \rightarrow \text{Alc}$ (Ps uptake from organic phase)
2	$\text{Alc} \rightarrow \text{Ald}$
2back	$\text{Ald} \rightarrow \text{Alc}$
3	$\text{Ald} \rightarrow \text{Acid}$



## CHAPTER 7

### **CONCLUSIONS AND OUTLOOK**

**Bruno Bühler**

## 7.1. MULTISTEP OXYGENATION CATALYZED BY XYLENE MONOOXYGENASE – BIOLOGICAL AND PRACTICAL IMPLICATIONS

As pointed out in Chapter 1 (section 1.4.2.3), oxygenases often catalyze multiple oxidations. This is a drawback in oxygenase-based biocatalysis when the product of the first oxygenation step, e.g., an alcohol, is the desired product. However, such an activity can also be beneficial, when the multistep oxidation can be controlled and thus allows the accumulation of a desired overoxidized product such as an aldehyde, ketone, or acid. With a focus on the application of enzymes of the upper xylene degradation pathway of *P. putida* mt-2 for the specific oxidation of xylenes to corresponding aldehydes, we investigated the potential of xylene monooxygenase (XMO) to catalyze multistep oxidations. Recombinant *E. coli* expressing the monooxygenase genes *xylM* and *xylA* were found to catalyze the consecutive oxidation of toluene and pseudocumene to corresponding alcohols, aldehydes, and acids (Chapter 2). For all three steps, the incorporation of one atom of molecular oxygen was demonstrated.

The second enzyme of the xylene degradation pathway, benzyl alcohol dehydrogenase (XylB) catalyzes a reaction with the thermodynamic equilibrium on the side of the benzyl alcohols and thus was found to lower benzaldehyde formation rates and to cause back formation of benzyl alcohols from benzaldehydes in recombinant *E. coli*. Consequently, the presence of XylB in a biocatalyst based on recombinant *E. coli* is not suitable for the biocatalytic production of benzaldehydes and a strategy based on *E. coli* containing only XMO was chosen.

In the wildtype, XylB may have two functions. It may prevent the intracellular accumulation of particularly reactive benzaldehydes. Moreover, in the case of high fluxes through the degradation pathways and low aldehyde concentrations, XylB may contribute to benzaldehyde formation via the NADH-producing and thus energetically more favorable dehydrogenation of benzyl alcohols. As described in Chapter 3, the multistep oxygenation catalyzed by *xylMA* expressing recombinant *E. coli* exhibits complex kinetics. Pseudocumene and toluene were shown to inhibit XMO-catalyzed alcohol and aldehyde oxygenations and corresponding alcohols were shown to inhibit XMO-catalyzed aldehyde oxygenations. At relatively high xylene concentrations, these inhibitions may promote aldehyde and acid formation via the energetically favorable dehydrogenations in the wildtype. The arrangement of NADH and substrate oxidation activities on two separate protein subunits may decelerate electron transfer and was proposed to minimize overoxidation (van Beilen, et al., 2003). Thus,

this may be another biological strategy to optimize the energetics of xylene degradation in the wildtype. Further studies including metabolic flux analysis are necessary to evaluate the exact role of the dual capability for alcohol and aldehyde oxidation during growth of *P. putida* mt-2 on xylenes.

## 7.2. PROCESS DEVELOPMENT FOR OXYGENASE CATALYSIS

The exploitation of the complex kinetics of the multistep reaction catalyzed by XMO for the specific accumulation of one oxidation product is discussed in Chapter 3 and was implemented for the production of 3,4-dimethylbenzaldehyde from pseudocumene as described in Chapter 4. A two-liquid phase system based on bis(2-ethylhexyl)phthalate as organic carrier solvent allowed to direct the multistep oxygenation of pseudocumene to the exclusive production of 3,4-dimethylbenzaldehyde. Process data of representative biotransformations at varying pH, scale, and initial pseudocumene concentration and with two different growth substrates are given in Table 7.1. Various issues generally associated with oxygenase- and/or multistep catalysis were addressed during process development and are summarized below.

### 7.2.1. PRODUCT DEGRADATION AND BIOCATALYST ACTIVITY - APPROACH: RECOMBINANT WHOLE-CELL BIOCATALYSIS

Aromatic aldehydes are further metabolized in *Pseudomonas* strains, also in the absence of the benzaldehyde dehydrogenase (XylC) of the xylene degradation pathway. Such product degradation was efficiently prevented by the use of *E. coli* as recombinant host strain.

Recombinant whole cells of *E. coli* JM101 allowed the efficient and stable expression of membrane bound XMO to specific oxygenation activities up to 252 U (g of CDW)<sup>-1</sup> in short-time activity assays based on resting cells (kinetic analyses, Chapter 3) and up to 100 U (g of CDW)<sup>-1</sup> under process conditions considering that a two-step oxygenation was catalyzed (Table 7.1, Chapter 5). Thus, the 100 U (g of CDW)<sup>-1</sup> reached on a laboratory as well as on a technical scale represent the respective sum of the two specific reaction rates for the two-step oxygenation of pseudocumene to 3,4-dimethylbenzyl alcohol and further to 3,4-dimethylbenzaldehyde. The expression system based on the *alk* regulatory system of *P. putida* GPo1 and present on plasmid pSPZ3, which has been constructed by Panke et al. (1999), proved to be very effective, also with respect to genetic stability. The plasmid as well as

**Table 7.1: Process data of representative biotransformations of pseudocumene to 3,4-dimethylbenzaldehyde.\***

Scale [L <sub>tot</sub> ]	pH	Growth substrate <sup>a</sup>	Initial pseudocumene concentration [g L <sub>org</sub> <sup>-1</sup> ]	Final product concentration [g L <sub>org</sub> <sup>-1</sup> ]	Molar yield [%]	Product share in all reactants <sup>b</sup> [%]	Maximal specific oxygenation rate <sup>c</sup> [U (g of CDW) <sup>-1</sup> ]	Maximal volume- tric activity <sub>ald</sub> [U L <sub>aq</sub> <sup>-1</sup> ]	Average pro- ductivity <sub>ald</sub> [g L <sub>tot</sub> <sup>-1</sup> h <sup>-1</sup> ]
2 <sup>d</sup>	7.1	glucose/ye	19.8	7.4	39	41	16	133	0.45
2 <sup>e</sup>	7.1	glucose/ye	101	15.8	14	13	50	200	0.6
2 <sup>e</sup>	7.1	glucose/ye	38.5	29	67	71	42	340	0.85
2 <sup>e</sup>	7.1	glucose/ye	19.6 + 2*4.9 <sup>g</sup>	18.8	58	60	16	167	0.37
2 <sup>e</sup>	7.1	glycerol	48.1	46.8	50	55	64	340	0.8
2 <sup>e</sup>	7.1	glucose	37.9	29.5	70	92	40	390	1
2 <sup>f</sup>	7.4	glucose	60.1	44.3	66	80	100	710	1.7
30 <sup>f</sup>	7.4	glucose	48.1	34.1	64	76	100	440	1.2
30 <sup>f</sup>	7.1→7.4	glucose	42.7	36.8	77	97	81	500	1.3

\*All experiments were carried out under the same conditions at varying pH and scale and with different growth substrates and media (organic carrier solvent, BEHP; phase ratio, 0.5; for details see respective Chapters. Subscripts: org, organic phase; aq, aqueous phase; tot, total volume; ald, referring to 3,4-dimethylbenzaldehyde formation.

<sup>a</sup> When the feeding solution was supplemented with yeast extract (ye), MS medium was used (Chapters 3 and 4). In all other cases RB medium was used (Chapters 4 and 5).

<sup>b</sup> Molar percentage of product with respect to the sum of all reactants in the organic phase at the end of the biotransformation.

<sup>c</sup> The specific oxygenation rates represent the sum of the two specific reaction rates for the two-step oxygenation of pseudocumene to 3,4-dimethylbenzyl alcohol and further to 3,4-dimethylbenzaldehyde.

<sup>d</sup> Adapted from Chapter 3.

<sup>e</sup> Adapted from Chapter 4.

<sup>f</sup> Adapted from Chapter 5.

<sup>g</sup> Pseudocumene was pulsed twice after 5 and 8 h of biotransformation (Chapter 4).



biocatalyst activity remained stable for 11 generations without selection pressure during two successive biotransformations, thus enabling the elimination of antibiotics from the bioprocess, which is useful from an economical and ecological point of view (Chapter 4). These results and the high volumetric activities during the process (Table 7.1) illustrate that reasonable oxygenation rates can be reached by recombinant whole-cell biocatalysis. This strategy also efficiently prevented product degradation.

### **7.2.2. BIOCATALYST STABILITY AND COFACTOR REGENERATION - APPROACH: FED-BATCH CULTIVATION**

High and stable productivities (Table 7.1) were reached by employing growing cells with a high metabolic activity providing enough energy for efficient cofactor regeneration and oxygenase synthesis. Cells were cultivated in fed-batch mode in a minimal medium optimized for *E. coli* (Riesenberg, et al., 1991) and *xylMA* expression. The medium contained glucose as the preferred carbon and energy source and high iron concentrations to support high and stable expression levels of the nonheme diiron enzyme XMO (Chapter 4). In the stationary phase, when metabolic activity and viability of the cells decreased, biocatalyst activities declined independently from the reactant concentrations.

The pH was found to have a significant effect on cell growth and specific biocatalyst activity (Table 7.1, Chapter 5). Increasing the pH from 7.1 to 7.4 caused a doubling of the specific biocatalyst activity and lowered the cell growth rate, the biomass yield on glucose, and the maximal cell (biocatalyst) concentration reached. The higher biocatalyst activity, obtained at the expense of cell growth, points to an intracellular NADH shortage leading to a pH-influenced competition for NADH between XMO and the respiratory chain. Chapter 6 describes the development of a mathematical model to further characterize and improve the process. Here, the introduction of a pH-dependent feedback inhibition of the NADH consuming bioconversions allowed good simulations of biotransformation experiments performed at varying pH, scale, and initial substrate concentration. This supported the assumed effect of intracellular NADH shortage and the pH-influenced competition for NADH.

Clearly, the results presented in this study show that the catalytic performance of oxygenase-based whole-cell biooxidation processes depends on the physiological state of the cells and that this catalytic performance can significantly be improved by both biocatalyst as well as biochemical process engineering.

Further investigation of the interrelationship between bioconversion, cell growth, and acetic acid formation is necessary. This and a more detailed process model may help in developing strategies towards a more efficient use of the cell machinery for oxygenase-based biocatalysis. Furthermore, uncoupling of oxygenase activity from cell growth would be of great interest. This would reduce oxygen and energy source requirements during the biotransformation and prevent the formation of biomass as “byproduct”.

### **7.2.3. TOXICITY AND LOW SOLUBILITY OF THE REACTANTS AND MULTISTEP BIOCATALYSIS - APPROACH: TWO-LIQUID PHASE CONCEPT**

Hydrocarbons and their oxidized products are often poorly water-soluble and toxic or inhibitory for the biocatalyst. In situ product removal, as described in section 1.4.4. of Chapter 1, is commonly used to overcome these hurdles.

In fact, the sparingly water-soluble substrate pseudocumene and its oxidation products are highly toxic for the biocatalyst *E. coli* JM101 (pSPZ3) as determined in Chapter 3. The use of a two-liquid phase system with bis(2-ethylhexyl)phthalate as organic carrier solvent afforded the addition of pseudocumene to high overall concentrations and efficiently prevented substrate and product toxicity. Furthermore, the use of this carrier solvent with its low flammability and low toxicity to *E. coli* (Chapter 3) and humans (Hasmall, et al., 2000) allowed the safe operation of stirred tank reactors at different scales with an organic phase volume fraction of 50%. Based on the kinetic data and the favorable partitioning behavior of the reactants in the two-liquid phase system, engineering of the initial pseudocumene concentration enabled exploiting the kinetically controlled multistep oxidation of pseudocumene for a process with 3,4-dimethylbenzaldehyde as the main product (Table 7.1, Chapter 4).

In this process, high substrate-cell transfer rates of up to 50 and 44 mmol per liter of aqueous medium were achieved on a 2-L and a 30-L scale, respectively (Chapters 5 and 6). A comparison of the kinetics of the multistep oxygenation of pseudocumene in the aqueous single-phase system with the kinetics in the two-liquid phase system and process simulation based on the model presented in Chapter 6 indicated the occurrence of direct substrate uptake from the organic phase via cell-droplet interactions. A sensitivity analysis for the organic-aqueous mass transfer coefficient showed that, above a value of 500 h<sup>-1</sup> for this coefficient, the organic-aqueous transfer is not critical for the process performance.

These results demonstrate that the two-liquid phase concept is an efficient tool to exploit the kinetics of multistep biotransformations. Furthermore, this concept was shown to allow high

substrate-cell transfer rates also for systems with high organic-aqueous partition coefficients for the substrate. Efficient substrate-cell mass transfer can be supported by direct substrate uptake from the organic phase, for which evidence was obtained in the system presented in this study.

A drawback of two-liquid phase cultivation is that stable emulsions can be formed, which complicates product isolation. In the process developed in this thesis, the tendency for the formation of a stable emulsion was reduced by eliminating yeast extract from the medium (Chapter 4) for a straightforward downstream processing consisting of phase separation by centrifugation followed by vacuum distillation of the product (Chapter 5). A strategy for a further simplification by eliminating the centrifugation step is the separation of the two phases by a membrane as described in section 1.4.4.3 of Chapter 1. This approach also allows uncoupling of the dilution or cycling rates of the separated organic and aqueous phases during continuous operation. Critical factors in the use of such membrane reactors are the often low rates for the mass transfer over the membrane, membrane fouling, and phase breakthrough due to membrane leakage.

### 7.3. INDUSTRIAL FEASIBILITY OF OXYGENASE CATALYSIS

Oxygenase-based two-liquid phase processes have thus far mostly been operated on a laboratory-scale. We scaled up the process to a 30-L scale in a bioreactor with an estimated power input of  $5 \text{ W L}^{-1}$ , which is close to values typically reached on industrial scales and thus allowed the evaluation of the industrial feasibility of biocatalytic hydrocarbon oxyfunctionalization (Chapter 5). On this technical scale we reached for the first time an average volumetric activity of  $330 \text{ U L}_{\text{aq}}^{-1}$  for a two-step oxygenation process. The maximum amounted to  $500 \text{ U L}_{\text{aq}}^{-1}$  (Table 7.1), which translates into a maximal overall oxygenation activity of  $1000 \text{ U L}_{\text{aq}}^{-1}$  or  $500 \text{ U L}_{\text{tot}}^{-1}$  (representing the sum of the reaction rates of both steps). The resulting production of 484 ml of 3,4-dimethylbenzaldehyde (purity: ~97%) from pseudocumene involved a mean productivity of  $31 \text{ g L}_{\text{tot}}^{-1} \text{ day}^{-1}$ , a final DMB-aldehyde concentration of  $37 \text{ g L}^{-1}$  in the organic phase, and an isolated product yield of 65% (conversion yield: 77%). These values meet the requirements for industrial oxidation processes as assessed by Straathof et al. (2002) and detailed in Chapter 5. This illustrates the practical feasibility of large-scale two-liquid phase processes and points to the high potential of biocatalytic hydrocarbon oxidation in organic synthesis.

This thesis and the present process show that the combined use of different concepts in the fields of biochemical engineering and modern DNA technology allows the application of oxygenases for complex reactions such as kinetically controlled multistep reactions. Future developments in these fields are thus considered to enable the development of many and varied industrial scale processes based on oxygenase catalysis.

## CHAPTER 8

## **REFERENCES**

- Abril M-A, Michan C, Timmis KN, Ramos JL. 1989. Regulator and enzyme specificities of the TOL plasmid-encoded upper pathway for degradation of aromatic hydrocarbons and expansion of the substrate range of the pathway. *J Bacteriol* 171:6782-6790.
- Adam W, Lazarus M, Saha-Möller CR, Weichold O, Hoch U, Häring D, Schreier P. 1999. Biotransformations with peroxidases. *Adv Biochem Eng Biotechnol* 63:73-108.
- Akiyoshi-Shibata M, Sakaki T, Ohyama Y, Noshiro N, Okuda K, Yabusaki Y. 1994. Further oxidation of hydroxycalcidiol by calcidiol 24-hydroxylase. A study with the mature enzyme expressed in *Escherichia coli*. *Eur J Biochem* 224:335-343.
- Andersson E, Hahn-Hägerdal B. 1990. Bioconversions in aqueous two-phase systems. *Enzyme Microb Technol* 12:242-254.
- Andersson L, Strandberg L, Enfors S-O. 1996. Cell segregation and lysis have profound effects on the growth of *Escherichia coli* in high cell density fed batch cultures. *Biotechnol Prog* 12:190-195.
- Appel D, Lutz-Wahl S, Fischer P, Schwaneberg U, Schmid RD. 2001. A P450BM-3 mutant hydroxylates alkanes, cycloalkanes, arenes and heteroarenes. *J Biotechnol* 88:167-171.
- Aristidou AA, San K-Y, Bennet GN. 1999. Metabolic flux analysis of *Escherichia coli* expressing the *Bacillus subtilis* acetolactate synthase in batch and continuous cultures. *Biotechnol Bioeng* 63:737-749.
- Arnold FH. 2001. Combinatorial and computational challenges for biocatalyst design. *Nature* 409:253-257.
- Arnold FH, May O, Drauz K, Bommarius A. 2000. Modified hydantoinase with improved enzymatic properties relative to unmodified hydantoinase is used in whole cell catalysis for the production of amino acids. WO 200058449.
- Ascón-Cabrera MA, Lebeault J-M. 1995. Cell hydrophobicity influencing the activity/stability of xenobiotic-degrading microorganisms in a continuous biphasic system. *J Ferm Bioeng* 80:270-275.
- Atherton JH. 1994. Mechanism in two-phase reaction systems: Coupled mass transfer and chemical reaction. In: Compton TG, Hancock G, editors. *Research in chemical kinetics*. Amsterdam: Elsevier. p 193-259.
- Atkinson B, Mavituna F. 1991. *Biochemical engineering and biotechnology handbook*. New York: Stockton Press.
- Austin RN, Chang H-K, Zylstra GJ, Groves JT. 2000. The non-heme diiron alkane monooxygenase of *Pseudomonas oleovorans* (AlkB) hydroxylates via a substrate radical intermediate. *J Am Chem Soc* 122:11747-11748.
- Azerad R. 2000. Regio- and stereoselective microbial hydroxylation of terpenoid compounds. In: Patel RN, editor. *Stereoselective Biocatalysis*. New York: Marcel Dekker. p 152-180.
- Bachmann R, Bastianelli E, Riese J, Schlenzka W. 2000. Using plants as plants. *McKinsey Quarterly* 93-99.
- Baptist JN, Gholson RK, Coon MJ. 1963. Hydrocarbon oxidation by a bacterial enzyme system. I. Products of octane oxidation. *Biochim Biophys Acta* 69:40-47.
- Bard M, Bruner DA, Pierson CA, Lees ND, Biermann B, Frye L, Koegel C, Barbuch R. 1996. Cloning and characterization of ERG25, the *Saccharomyces cerevisiae* gene encoding C-4 sterol methyl oxidase. *Proc Natl Acad Sci USA* 93:186-190.
- BASF. 2003. ChiPros™. [http://www.basf.de/en/produkte/chemikalien/interm/acidspec/chipros/?id=V00--82MMGA\\*\\*bsf000](http://www.basf.de/en/produkte/chemikalien/interm/acidspec/chipros/?id=V00--82MMGA**bsf000).
- Behrouzian B, Savile CK, Dawson B, Buist PH, Shanklin J. 2002. Exploring the hydroxylation-dehydrogenation connection: novel catalytic activity of castor stearyl-ACP D<sup>9</sup> desaturase. *J Am Chem Soc* 124:3277-3283.

- Bell LC, Guengerich FP. 1997. Oxidation kinetics of ethanol by human cytochrome P450 2E1. Rate-limiting product release accounts for effects of isotopic substitution and cytochrome *b*<sub>5</sub> on steady-state kinetics. *J Biol Chem* 272:29643-29651.
- Bell-Parikh LC, Guengerich FP. 1999. Kinetics of cytochrome P450 2E1-catalyzed oxidation of ethanol to acetic acid via acetaldehyde. *J Biol Chem* 274:23833-23840.
- Boddupalli SS, Pramanik BC, Slaughter CA, Estabrook RW, Peterson JA. 1992. Fatty acid monooxygenation by P450 BM-3: product identification and proposed mechanisms for the sequential hydroxylation reactions. *Arch Biochem Biophys* 292:20-28.
- Bolon DN, Voigt CA, Mayo SL. 2002. *De novo* design of biocatalysts. *Curr Opin Chem Biol* 6:125-129.
- Bommarius AS, Schwarm M, Drauz K. 2001. Comparison of different chemoenzymatic process routes to enantiomerically pure amino acids. *Chimia* 55:50-59.
- Bosetti A, van Beilen JB, Preusting H, Lageveen RG, Witholt B. 1992. Production of primary aliphatic alcohols with a recombinant *Pseudomonas* strain, encoding the alkane hydroxylase system. *Enzyme Microb Technol* 14:702-708.
- Bossert ID, Whited G, Gibson DT, Young LY. 1989. Anaerobic oxidation of *p*-cresol mediated by a partially purified methylhydroxylase from a denitrifying bacterium. *J Bacteriol* 171:2956-2962.
- Brazeau BJ, Austin RN, Tarr C, Groves JT, Lipscomb JD. 2001. Intermediate Q from soluble methane monooxygenase hydroxylates the mechanistic substrate probe norcarane: evidence for a stepwise reaction. *J Am Chem Soc* 123:11831-11837.
- Brazeau BJ, Lipscomb JD. 2000. Kinetics and activation thermodynamics of methane monooxygenase compound Q formation and reaction with substrates. *Biochemistry* 39:13503-13515.
- Broadwater JA, Whittle E, Shanklin J. 2002. Desaturation and hydroxylation. Residues 148 and 324 of *Arabidopsis* FAD2, in addition to substrate chain length, exert a major influence in partitioning of catalytic specificity. *J Biol Chem* 277:15613-15620.
- Broun P, Shanklin J, Whittle E, Somerville C. 1998. Catalytic plasticity of fatty acid modification enzymes underlying chemical diversity of plant lipids. *Science* 282:1315-1317.
- Bruce LJ, Daugulis A. 1991. Solvent selection strategies for extractive biocatalysis. *Biotechnol Prog* 7:116-124.
- Bruehne F, Wright E. 1985. Benzaldehyde. In: Gerhartz W, editor. *Ullmann's encyclopedia of industrial chemistry*. Weinheim, Germany: Wiley-VHC. p 463-474.
- Bruggink A. 1996. Biocatalysis and process integration in the synthesis of semisynthetic antibiotics. *Chimia* 50:431-432.
- Bruggink A, Roos EC, de Vroom E. 1998. Penicillin acylase in the industrial production of  $\beta$ -lactam antibiotics. *Org Proc Res Dev* 2:128-133.
- Burlage RS, Hooper SW, Saylor GS. 1989. The TOL (pWW0) catabolic plasmid. *Appl Environ Microbiol* 55:1323-1328.
- Burton SG, Cowan DA, Woodley JM. 2002. The search for the ideal biocatalyst. *Nat Biotechnol* 20:37-45.
- Bylund F, Collet E, Enfors S-O, Larsson G. 1998. Substrate gradient formation in the large-scale bioreactor lowers cell yield and increases by-product formation. *Bioproc Eng* 18:171-180.
- Cali JJ, Russell DW. 1991. Characterization of human sterol 27-hydroxylase. A mitochondrial cytochrome P-450 that catalyzes multiple oxidation reactions in bile acid biosynthesis. *J Biol Chem* 266:7774-7778.
- Cameotra SS, Singh HD. 1990. Uptake of volatile n-alkanes by *Pseudomonas* PG-1. *J Microb Biotechnol* 5:47-57.

- Canada KA, Iwashita S, Shim H, Wood TK. 2002. Directed evolution of toluene *ortho*-monooxygenase for enhanced 1-naphthol synthesis and chlorinated ethene degradation. *J Bacteriol* 184:344-349.
- Cánovas M, Maiquez J, de Diego T, Buendía B, Espinosa G, Iborra JL. 2003. Membrane cell retention system for continuous production of L-carnitine using *Proteus* sp. *J Membr Sci* 214:101-111.
- Carelli I, Chiarotto I, Cacchi S, Pace P, Amatore C, Jutand A, Meyer G. 1999. Electrosynthesis of aromatic aldehydes by palladium-catalyzed carbonylation of aryl iodides in the presence of formic acid. *Eur J Org Chem* 1999:1471-1473.
- Carmichael AB, Wong L-L. 2001. Protein engineering of *Bacillus megaterium* CYP102 - the oxidation of polycyclic aromatic hydrocarbons. *Eur J Biochem* 268:3117-3125.
- Carpenter EP, Hawkins AR, Frost JW, Brown KA. 1998. Structure of dehydroquinase synthase reveals an active site capable of multistep catalysis. *Nature* 394:299-302.
- Carragher JM, McClean WS, Woodley JM, Hack CJ. 2001. The use of oxygen uptake rate measurements to control the supply of toxic substrate: toluene hydroxylation by *Pseudomonas putida* UV4. *Enzyme Microb Technol* 28:183-188.
- Chakrabarty AM, Chou G, Gunsalus LG. 1973. Genetic regulation of octane dissimilation plasmid in *Pseudomonas*. *Proc Natl Acad Sci USA* 70:1137-1140.
- Chen Q, Janssen DB, Witholt B. 1995. Growth on octane alters the membrane lipid fatty acids of *Pseudomonas oleovorans* due to the induction of *alkB* and synthesis of octanol. *J Bacteriol* 177:6894-6901.
- Chen Q, Janssen DB, Witholt B. 1996. Physiological changes and *alk* gene instability in *Pseudomonas oleovorans* during induction and expression of *alk* genes. *J Bacteriol* 178:5508-5512.
- Cherry JR. 2000. Directed evolution of microbial oxidative enzymes. *Curr Opin Biotechnol* 11:250-254.
- Cherry JR, Lamsa MH, Schneider P, Vind J, Svendsen A, Jones A, Pedersen AH. 1999. Directed evolution of a fungal peroxidase. *Nat Biotechnol* 17:379-384.
- Cirino PC, Arnold FH. 2002. Protein engineering of oxygenases for biocatalysis. *Curr Opin Chem Biol* 6:130-135.
- Collins AM, Woodley JM, Liddell JM. 1995. Determination of reactor operation for the microbial hydroxylation of toluene in a two-liquid phase process. *J Ind Microbiol* 14:382-388.
- Collins AN, Sheldrake GN, Crosby J. 1997. *Chirality in Industry II*. New York: John Wiley and Sons.
- Collins LD, Daugulis AJ. 1997. Biodegradation of phenol at high initial concentrations in two-phase partitioning batch and fed-batch bioreactors. *Biotechnol Bioeng* 55:155-162.
- Coon MJ, Connery AH, Eastbrook RW, Gelboin V, Gillette JR, O'Brien PJ. 1980. *Microsomes, Drug Oxidation and Chemical Carcinogens*. New York: Academic Press.
- Cornish-Bowden A. 1995. *Analysis of enzyme kinetic data*. New York: Oxford University Press.
- Cruickshank SM, Daugulis AJ, McLellan PJ. 2000. Dynamic modeling and optimal fed-batch feeding strategies for a two-phase partitioning bioreactor. *Biotechnol Bioeng* 67:224-233.
- Dagley S. 1986. Biochemistry of aromatic hydrocarbon degradation in *Pseudomonads*. In: Sokatch JR, editor. *The Bacteria*. London: Academic Press. p 527-555.
- de Bont JAM. 1998. Solvent-tolerant bacteria in biocatalysis. *Trends Biotechnol* 16:493-499.
- de Carvalho CCCR, da Fonseca MMR. 2002. Influence of reactor configuration on the production of carvone from carveol by whole cells of *Rhodococcus erythropolis* DCL14. *J Mol Catal B Enzym* 19-20:377-387.



- de Smet M-J, Kingma J, Wynberg H, Witholt B. 1983. *Pseudomonas oleovorans* as a tool in bioconversions of hydrocarbons: growth, morphology and conversion characteristics in different two-phase systems. *Enzyme Microb Technol* 5:352-360.
- de Smet M-J, Witholt B, Wynberg H. 1981a. Practical approach to high-yield enzymatic stereospecific organic synthesis in multiphase systems. *J Org Chem* 46:3128-3131.
- de Smet M-J, Wynberg H, Witholt B. 1981b. Synthesis of 1,2-epoxyoctane by *Pseudomonas oleovorans* during growth in a two-phase system containing high concentrations of 1-octene. *Appl Environ Microbiol* 42:811-816.
- de Visser SP, Oligaro F, Harris N, Shaik S. 2001. Multi-state epoxidation of ethene by cytochrome P450: A quantum chemical study. *J Am Chem Soc* 123:3037-3047.
- Dean JA, Lange NA. 1985. Lange's Handbook of Chemistry. New York: McGraw-Hill, Inc.
- Desai JD, Banat IM. 1997. Microbial production of surfactants and their commercial potential. *Microbiol Mol Biol Rev* 61:47-64.
- Dingler C, Ladner W, Krei GA, Cooper B, Hauer B. 1996. Preparation of (*R*)-2-(4-hydroxyphenoxy)propionic acid by biotransformation. *Pestic Sci* 46:33-35.
- Doig SD, Avenell PJ, Bird PA, Gallati P, Lander KS, Lye GJ, Wohlgemuth R, Woodley JM. 2002a. Reactor operation and scale-up of whole cell Bayer-Villiger catalyzed lactone synthesis. *Biotechnol Prog* 18:1039-1046.
- Doig SD, Boam AT, Leak DI, Livingstone AG, Stuckey DC. 1998. A membrane bioreactor for biotransformations of hydrophobic molecules. *Biotechnol Bioeng* 58:587-594.
- Doig SD, Boam AT, Livingstone AG, Stuckey DC. 1999a. Epoxidation of 1,7-octadiene by *Pseudomonas oleovorans* in a membrane reactor. *Biotechnol Bioeng* 63:601-611.
- Doig SD, Boam AT, Livingstone AG, Stuckey DC. 1999b. Mass transfer of hydrophobic solutes in solvent swollen silicone rubber membranes. *J Membr Sci* 154:127-140.
- Doig SD, O'Sullivan LM, Patel S, Ward JM, Woodley JM. 2001. Large scale production of cyclohexanone monooxygenase from *Escherichia coli* TOP10 pQR239. *Enzyme Microb Technol* 28:265-274.
- Doig SD, Pickering SCR, Lye GJ, Woodley JM. 2002b. The use of microscale processing technologies for quantification of biocatalytic Baeyer-Villiger oxidation kinetics. *Biotechnol Bioeng* 80:42-49.
- Drauz K-H, Eils S, Schwarm M. 2002. Synthesis and production of enantiomerically pure amino acids. *Chim Oggi* 20:15-21.
- DSM. 2002a. DSM - Fine chemicals. <http://www3.dsm.com/dfc/>.
- DSM. 2002b. DSM: Cephalosporines and penicillins by biocatalysis. <http://www3.dsm.com/research/invention/innovative/%7Een/index.pl?f=healthcare.htm>.
- Duetz WA, Rüedi L, Hermann R, O'Connor K, Büchs J, Witholt B. 2000. Methods for intense aeration, growth, storage, and replication of bacterial strains in microtiterplates. *Appl Environ Microbiol* 66:2641-2646.
- Duetz WA, van Beilen JB, Witholt B. 2001. Using proteins in their natural environment: potential and limitations of microbial whole-cell hydroxylations in applied biocatalysis. *Curr Opin Biotechnol* 12:419-425.
- Duetz WA, Wind B, van Andel JG, Barnes MR, Williams PA, Rutgers M. 1998. Biodegradation kinetics of toluene, *m*-xylene, *p*-xylene and their intermediates through the upper TOL pathway of *Pseudomonas putida* (pWW0). *Microbiology* 144:1669-1675.
- Eichhorn E, Roduit J-P, Shaw N, Heinzmann K, Kiener A. 1997. Preparation of (*S*)-piperazine-2-carboxylic acid, (*R*)-piperazine-2-carboxylic acid, and (*S*)-piperidine-2-carboxylic acid by kinetic resolution of the corresponding racemic carboxamides with stereoselective amidases in whole bacterial cells. *Tetrahedron Asym* 8:2533-2536.

- Elango E, Radhakrishnan R, Froland WA, Wallar BJ, Earhart CA, Lipscomb JD, Ohlendorf DH. 1997. Crystal structure of the hydroxylase component of methane monooxygenase from *Methylosinus trichosporium* OB3b. *Protein Sci* 6:556-568.
- Ellis LBM, Hershberger CD, Bryan EM, Wackett LP. 2001. The University of Minnesota Biocatalysis/Biodegradation Database: Emphasizing Enzymes. *Nucleic Acids Research* 29:340-343.
- Faber K. 2000. *Biotransformations in Organic Chemistry*. Berlin, Germany: Springer.
- Falbe J, Regitz M. 1995. *CD Roempp Chemie Lexikon*. Stuttgart, Germany: Georg Thieme Verlag.
- Farinas ET, Butler T, Arnold FH. 2001a. Directed enzyme evolution. *Curr Opin Biotechnol* 12:545-551.
- Farinas ET, Schwaneberg U, Glieder A, Arnold FH. 2001b. Directed evolution of a cytochrome P450 monooxygenase for alkane oxidation. *Adv Synth Catal* 343:601-606.
- Favre-Bulle O, Schouten T, Kingma J, Witholt B. 1991. Bioconversion of *n*-octane to octanoic acid by a recombinant *Escherichia coli* cultured in a two-liquid phase bioreactor. *Bio/Technol* 9:367-371.
- Favre-Bulle O, Weenink E, Vos T, Preusting H, Witholt B. 1993. Continuous bioconversion of *n*-octane to octanoic acid by recombinant *Escherichia coli* (*alk*<sup>+</sup>) growing in a two-liquid-phase chemostat. *Biotechnol Bioeng* 41:263-272.
- Favre-Bulle O, Witholt B. 1992. Biooxidation of *n*-octane by a recombinant *Escherichia coli* in a two-liquid-phase system: effect of medium components on cell growth and alkane oxidation activity. *Enzyme Microb Technol* 14:931-937.
- Fessner W-D, Helaine V. 2001. Biocatalytic synthesis of hydroxylated natural products using aldolases and related enzymes. *Curr Opin Biotechnol* 12:574-586.
- Filatov M, Harris N, Shaik S. 1999. On the "rebound" mechanism of alkane hydroxylation by cytochrome P450: electronic structure of the intermediate and the electron transfer character in the rebound step. *Angew Chem Int Ed Engl* 38:3510-3512.
- Fischer RT, Stam SH, Johnson PR, Ko SS, Magolda RL, Gaylor JL, Trzaskos JM. 1989. Mechanistic studies of lanosterol 14 $\alpha$ -methyl demethylase: substrate requirements for the component reactions catalyzed by a single cytochrome P-450 isozyme. *J Lipid Res* 30:1621-1632.
- Flitsch SL, Aitken SJ, Chow CS-Y, Grogan G, Staines A. 1999. Biohydroxylation reactions catalyzed by enzymes and whole-cell systems. *Bioorg Chem* 27:81-90.
- Flitsch SL, Schmid A, Hollmann F, Bühler B, Grogan G, van Pée K-H. 2002. Oxidation reactions. In: Drauz K, Waldmann H, editors. *Enzyme Catalysis in Organic Synthesis*. Weinheim: Wiley-VCH. p 1065-1280.
- Fox BG, Froland WA, Dege JE, Lipscomb JD. 1989. Methane monooxygenase form *Methylosinus trichosporium* OB3b. *J Biol Chem* 264:10023-10033.
- Franklin FCH, Bagdasarian M, Bagdasarian MM, Timmis KN. 1981. Molecular and functional analysis of the TOL plasmid pWW0 from *Pseudomonas putida* and cloning of genes for the entire regulated aromatic ring *meta*-cleavage pathway. *Proc Natl Acad Sci USA* 78:7458-7462.
- Freeman A, Woodley JM, Lilly MD. 1993. *In situ* product removal as a tool for bioprocessing. *Bio/Technol* 11:1007-1012.
- Fu H, Newcomb M, Wong C-H. 1991. *Pseudomonas oleovorans* monooxygenase catalyzed asymmetric epoxidation of allyl alcohol derivatives and hydroxylation of a hypersensitive radical probe with the radical ring opening rate exceeding the oxygen rebound rate. *J Am Chem Soc* 113:5878-5880.
- Fujiyama S, Matsumoto S. 1984. Process for continuous production of alkylbenzaldehydes. US 4,460,794.

- Fujiyama S, Matsumoto S, Takamizawa Y. 1983. Process for formylating xylene mixture. US 4,368,336.
- Furuhashi K. 1984. Optimization of a medium for the production of 1,2-epoxytetradecane by *Nocardia corallina* B-276. *Appl Microbiol Biotechnol* 20:6-9.
- Furuhashi K. 1986. A fermentation process for the production of optically active epoxides. *Chem Econ Eng Rev* 18:21-26.
- Furuhashi K. 1992. Biological routes to optically active epoxides. In: Collins AN, Sheldrake GN, Crosby J. *Chirality in Industry*. John Wiley & Sons Ltd. p 167-186.
- Furuhashi K, Shintani M, Takagi M. 1986. Effects of solvents on the production of epoxides by *Nocardia corallina* B-276. *Appl Microbiol Biotechnol* 23:218-223.
- Furuhashi K, Taoka A, Uchida S, Karube I, Suzuki S. 1981. Production of 1,2-epoxyalkanes from 1-alkenes by *Nocardia corallina* B-276. *Eur J Appl Microbiol Biotechnol* 12:39-45.
- Gankema H, Wensink J, Guinee PAM, Jansen WH, Witholt B. 1980. Some characteristics of the outer membrane material released by growing enterotoxic *Escherichia coli*. *Infect Immun* 29:704-713.
- Gerrits JG, Marcus J, Birikaki L, van der Gen A. 2001a. Difficult substrates in the *R*-hydroxynitrile lyase catalyzed hydrocyanation reaction: applications of the mass transfer limitation principle in a two-phase system. *Tetrahedron Asym* 12:971-974.
- Gerrits PJ, Willeman WF, Straathof AJJ, Heijnen JJ, Brussee J, van der Gen A. 2001b. Mass transfer limitation as a tool to enhance the enantiomeric excess in the enzymatic synthesis of chiral cyanohydrins. *J Mol Catal B Enzym* 15:111-121.
- Gibson DT, Subramanian V. 1984. Microbial degradation of aromatic hydrocarbons. In: Gibson DT, editor. *Microbial degradation of organic compounds*. New York: Marcel Dekker, Inc. p 181-252.
- Giorno L, Drioli E. 2000. Biocatalytic membrane reactors: applications and perspectives. *Trends Biotechnol* 18:339-349.
- Glieder A, Farinas ET, Arnold FH. 2002. Laboratory evolution of a soluble, self-sufficient, highly active alkane hydroxylase. *Nat Biotechnol* 20:1135-1139.
- Goetz G, Iwan P, Hauer B, Breuer M, Pohl M. 2001. Continuous production of (*R*)-phenylacetylcarbinol in an Enzyme-Membrane Reactor using a potent mutant of pyruvate decarboxylase from *Zymomonas mobilis*. *Biotechnol Bioeng* 74:317-325.
- Goswami PC, Singh HD. 1991. Different modes of hydrocarbon uptake by two *Pseudomonas* species. *Biotechnol Bioeng* 37:1-11.
- Greated A, Lambertsen L, Williams PA, Thomas CM. 2002. Complete sequence of the IncP-9 TOL plasmid pWW0 from *Pseudomonas putida*. *Environ Microbiol* 4:856-871.
- Griffiths M. 2001. *The application of biotechnology to industrial sustainability*. Edited by Gram A, Treffenfeldt W, Lange U, McIntyre T, Wolf O. Paris: OECD.
- Grogan GJ, Holland HL. 2000. The biocatalytic reactions of *Beauveria* spp. *J Mol Catal B Enzym* 9:1-32.
- Groves JT, Han Y-Z. 1995. Models and mechanisms of cytochrome P-450 action. In: Ortiz de Montellano PR, editor. *Cytochrome P450 Structure, Mechanism, and Biochemistry*. New York: Plenum Press. p 3-48.
- Grund A, Shapiro J, Fennewald M, Bacha P, Leahy J, Markbreiter K, Nieder M, Toepfer M. 1975. Regulation of alkane oxidation in *Pseudomonas putida*. *J Bacteriol* 123:546-556.
- Guengerich FP. 1987. *Mammalian Cytochromes P450*. Boca Raton, FL: CRC Press.
- Guieysse B, Cirne MdDTG, Mattiasson B. 2001. Microbial degradation of phenanthrene and pyrene in a two-liquid phase-partitioning bioreactor. *Appl Microbiol Biotechnol* 56:796-802.

- Hack CJ, Woodley JM, Lilly MD, Liddell JM. 2000. Design of a control system for biotransformation of toxic substrates: toluene hydroxylation by *Pseudomonas putida* UV4. *Enzyme Microb Technol* 26:530-536.
- Hanahan D. 1983. Studies on transformation of *Escherichia coli* with plasmid. *J Mol Biol* 166:557-580.
- Harayama S, Kok M, Neidle EL. 1992. Functional and evolutionary relationships among diverse oxygenases. *Annu Rev Microbiol* 46:565-601.
- Harayama S, Lehrbach PR, Timmis KN. 1984. Transposon mutagenesis analysis of *meta*-cleavage pathway operon genes of the TOL plasmid of *Pseudomonas putida* mt-2. *J Bacteriol* 160:251-255.
- Harayama S, Leppik RA, Rekik M, Mermoud N, Lehrbach PR, Reineke W, Timmis KN. 1986. Gene order of the TOL catabolic plasmid upper pathway operon and oxidation of both toluene and benzyl alcohol by the *xyIA* product. *J Bacteriol* 167:455-461.
- Harayama S, Rekik M. 1989. Bacterial aromatic ring-cleavage enzymes are classified into two different gene families. *J Biol Chem* 264:15328-15333.
- Harayama S, Rekik M. 1990. The *meta* cleavage operon of TOL degradative plasmid pWW0 comprises 13 genes. *Mol Gen Genet* 221:113-120.
- Harayama S, Rekik M, Wubbolts M, Rose K, Leppik RA, Timmis KN. 1989. Characterization of five genes in the upper-pathway operon of TOL plasmid pWW0 from *Pseudomonas putida* and identification of the gene products. *J Bacteriol* 171:5048-5055.
- Harayama S, Timmis KN. 1987. Catabolism of aromatic hydrocarbons by *Pseudomonas*. In: Hopwood D, Chater K, editors. *Genetics of bacterial diversity*. London: Academic Press. p 151-174.
- Hardegger M, Koch AK, Ochsner UA, Fiechter A, Reiser J. 1994. Cloning and heterologous expression of a gene encoding an alkane-induced extracellular protein involved in alkane assimilation from *Pseudomonas aeruginosa*. *Appl Environ Microbiol* 60:3679-3687.
- Hartmann M, Ernst S. 2000. Selective oxidations of linear alkanes with molecular oxygen on molecular sieve catalysts - a breakthrough? *Angew Chem Int Ed Engl* 39:888-890.
- Hasmall SC, James NH, Macdonald N, Soames AR, Roberts RA. 2000. Species differences in response to diethylhexylphthalate: suppression of apoptosis, induction of DNA synthesis and peroxisome proliferator activated receptor alpha-mediated gene expression. *Arch Toxicol* 74:85-91.
- Hecht V, Vorlop J, Kalbitz H, Gerth K, Lehmann J. 1987. Vortex chamber for *in situ* recovery of the antibiotic myxovirescin A in continuous cultivation. *Biotechnol Bioeng* 29:222-227.
- Held M. 2000. Biocatalytic synthesis of 3-substituted catechols. Ph.D. thesis, Swiss Federal Institute of Technology, Zurich.
- Held M, Panke S, Kohler H-PE, Feiten H-J, Schmid A, Schmid A, Wubbolts MG, Witholt B. 1999a. Solid phase extraction for biocatalytic production of toxic compounds. *Bio World* 5/99:
- Held M, Schmid A, Kohler H-PE, Suske WA, Witholt B, Wubbolts MG. 1999b. An integrated process for the production of toxic catechols from toxic phenols based on a designer biocatalyst. *Biotechnol Bioeng* 62:641-648.
- Held M, Suske W, Schmid A, Engesser K-H, Kohler H-P, Witholt B, Wubbolts MG. 1998. Preparative scale production of 3-substituted catechols using a novel monooxygenase from *Pseudomonas azelaica* HBP 1. *J Mol Catal B Enzym* 5:87-93.

- Hermann T, Finkemeier M, Pfefferle W, Wersch G, Kramer R, Burkovski A. 2000. Two-dimensional electrophoretic analysis of *Corynebacterium glutamicum* membrane fraction and surface proteins. *Electrophoresis* 21:654-659.
- Hermann T, Pfefferle W, Baumann C, Busker E, Schaffer S, Bott M, Sahm H, Dusch N, Kalinowski J, Puhler A, Bendt AK, Kramer R, Burkovski A. 2001. Proteome analysis of *Corynebacterium glutamicum*. *Electrophoresis* 22:1712-1723.
- Hewitt CJ, Caron GN-V, Axelsson B, McFarlane CM, Nienow AW. 2000. Studies related to the scale-up of high-cell-density *E. coli* fed-batch fermentations using multiparameter flow cytometry: effect of a changing microenvironment with respect to glucose and dissolved oxygen concentration. *Biotechnol Bioeng* 70:381-390.
- Hewitt CJ, Caron GN-V, Nienow AW, McFarlane CM. 1999. The use of multi-parameter flow cytometry to compare the physiological response of *Escherichia coli* W3110 to glucose limitation during batch, fed-batch and continuous culture cultivations. *J Biotechnol* 75:251-264.
- Hickel A, Radke CJ, Blanch HW. 1999. Hydroxynitrile lyase at the diisopropyl ether/water interface: Evidence for interfacial enzyme activity. *Biotechnol Bioeng* 65:425-436.
- Higgins IJ, Best DJ, Hammond RC. 1980. New findings in methane-utilizing bacteria highlight their importance in the biosphere and their commercial potential. *Nature* 286:561-564.
- Hoekstra D, van der Laan JW, de Leij L, Witholt B. 1976. Release of outer membrane fragments from normally growing *Escherichia coli*. *Biochim Biophys Acta* 455:889-899.
- Holland HL. 1992. Organic synthesis with oxidative enzymes. New York: VCH Publishers.
- Holland HL. 1998. Hydroxylation and dihydroxylation. In: Kelly DR, editor. *Biotransformations 1*. Weinheim: Wiley-VCH. p 475-533.
- Holland HL. 1999. C-H activation. *Curr Opin Chem Biol* 3:22-27.
- Holland HL. 2000. Stereoselective hydroxylation reactions. In: Patel RN, editor. *Stereoselective Biocatalysis*. New York: Marcel Dekker. p 131-152.
- Holland HL, Weber HK. 2000. Enzymatic hydroxylation reactions. *Curr Opin Biotechnol* 11:547-553.
- Hollmann F, Lin PC, Witholt B, Schmid A. 2003. Stereospecific biocatalytic epoxidation: The first example of direct regeneration of a FAD dependent monooxygenase for catalysis. *J Am Chem Soc* 125:8209-8217.
- Hollmann F, Schmid A, Steckhan E. 2001. The first synthetic application of a monooxygenase employing indirect electrochemical NADH regeneration. *Angew Chem Int Ed Engl* 40:169-171.
- Holmberg-Betsholtz I, Lund E, Björkhem I, Wikvall K. 1993. Sterol 27-hydroxylase in bile acid biosynthesis. Mechanism of oxidation of 5 $\beta$ -cholestane-3 $\alpha$ ,7 $\alpha$ ,12 $\alpha$ ,27-tetrol into 3 $\alpha$ ,7 $\alpha$ ,12 $\alpha$ -trihydroxy-5 $\beta$ -cholestanoic acid. *J Biol Chem* 268:11079-11085.
- Hopper DJ, Jones MR, Causer MJ. 1985. Periplasmic location of *p*-cresol methylhydroxylase in *Pseudomonas putida*. *FEBS Letters* 182:485-488.
- Hou BK, Wackett LP, Ellis LBM. 2003. Microbial pathway prediction: a functional group approach. *J Chem Inf Comput Sci* 43:1051-1057.
- Hsu H-F, Que L, Jr., Shanklin J. 1999. XAS studies of membrane bound alkane w-hydroxylase: evidence for a histidine-rich ligand environment in the nonheme diiron site. *J of Inorg Biochem* 74:168.
- Hugo N, Armengaud J, Gaillard J, Timmis KN, Jouanneau Y. 1998. A novel [2Fe-2S] ferredoxin from *Pseudomonas putida* mt-2 promotes the reductive reactivation of catechol 2,3-dioxygenase. *J Biol Chem* 273:9622-3629.

- Hume R, Kelly RW, Taylor PL, Boyd GS. 1984. The catalytic cycle of cytochrome P-450<sub>sc</sub> and intermediates in the conversion of cholesterol to pregnenolone. *Eur J Biochem* 140:583-591.
- Hüsken LE, Beeftink HH, de Bont JAM, Wery J. 2001a. High-rate 3-methylcatechol production in *Pseudomonas putida* strains by means of a novel expression system. *Appl Microbiol Biotechnol* 55:571-577.
- Hüsken LE, Dalm DF, Tramper J, Wery J, de Bont JAM, Beeftink HH. 2001b. Integrated bioproduction and extraction of 3-methylcatechol. *J Biotechnol* 88:11-19.
- Hüsken LE, de Bont JAM, Beeftink HH, Tramper J, Wery J. 2002a. Optimisation of microbial 3-methylcatechol production as affected by culture conditions. *Biocatal Biotransf* 20:57-61.
- Hüsken LE, Oomes M, Schroën K, Tramper J, de Bont JAM, Beeftink HH. 2002b. Membrane-facilitated bioproduction of 3-methylcatechol in an octanol/water two-phase system. *J Biotechnol* 96:281-289.
- Imai T, Yamazaki T, Kominami S. 1998. Kinetic studies on bovine cytochrome P450<sub>11β</sub> catalyzing successive reactions from deoxycorticosterone to aldosterone. *Biochemistry* 37:8097-8104.
- Iwan P, Goetz G, Schmitz S, Hauer B, Breuer M, Pohl M. 2001. Studies on the continuous production of (*R*)-(-)-phenylacetylcarbinol in an enzyme-membrane reactor. *J Mol Catal B Enzym* 11:387-396.
- Iwata H, Fujita K, Kushida H, Suzuki A, Konno Y, Nakamura K, Fujino A, Kamataki T. 1998. High catalytic activity of human cytochrome P450 co-expressed with human NADPH-cytochrome P450 reductase in *Escherichia coli*. *Biochem Pharmacol* 55:1315-1325.
- Jin Y, Lipscomb JD. 2001. Desaturation reactions catalyzed by soluble methane monooxygenase. *J Biol Inorg Chem* 6:717-725.
- Johnson HA, Pelletier DA, Spormann AM. 2001. Isolation and characterization of anaerobic ethylbenzene dehydrogenase, a novel Mo-Fe-S enzyme. *J Bacteriol* 183:4536-4542.
- Jones JP, O'Hare EJ, Wong L-L. 2001. Oxidation of polychlorinated benzenes by genetically engineered CYP101 (cytochrome P450<sub>cam</sub>). *Eur J Biochem* 268:1460-1467.
- Junker F, Ramos JL. 1999. Involvement of the *cis/trans* Isomerase Cti in solvent resistance of *Pseudomonas putida* DOT-T1E. *J Bacteriol* 181:5693-5700.
- Kaptein B, Broxterman QB, Schoemaker HE, Rutjes FPJT, Veerman JJN, Kamphuis J, Peggion C, Formaggio F, Toniolo C. 2001. Enantiopure C<sup>a</sup>-tetrasubstituted α-amino acids. Chemoenzymatic synthesis and application to turn-forming peptides. *Tetrahedron* 57:6567-6577.
- Kasai Y, Inoue J, Harayama S. 2001. The TOL plasmid pWW0 *xyiN* gene product from *Pseudomonas putida* is involved in *m*-xylene uptake. *J Bacteriol* 183:6662-6666.
- Katopodis AG, Smith HA, Jr., May SW. 1988. New oxyfunctionalization capabilities for *w*-hydroxylases: asymmetric aliphatic sulfoxidation and branched ether demethylation. *J Am Chem Soc* 110:897-899.
- Katopodis AG, Wimalasena K, Lee J, May SW. 1984. Mechanistic studies on non-heme iron monooxygenase catalysis: epoxidation, aldehyde formation, and demethylation by the *w*-hydroxylation system of *Pseudomonas oleovorans*. *J Am Chem Soc* 106:7929-7935.
- Katsuki T, Sharpless KB. 1980. The first practical method for asymmetric epoxidation. *J Am Chem Soc* 102:5974-5976.
- Kaul R, Mattiason B. 1991. Extractive bioconversion in aqueous two-phase systems. In: Mattiason B, Holst O, editors. *Extractive bioconversions*. Monticello, NY: Marcel Dekker. p 173-188.

- Kawakami K, Nakahara T. 1994. Importance of solute partitioning in biphasic oxidation of benzyl alcohol by free and immobilized whole cells of *Pichia pastoris*. *Biotechnol Bioeng* 43:918-924.
- Keener WK, Arp DJ. 1994. Transformation of aromatic compounds by *Nitrosomonas europaea*. *Appl Environ Microbiol* 60:1914-1920.
- Kellis JTJ, Vickery LE. 1987. Purification and characterization of human placental aromatase cytochrome P-450. *J Biol Chem* 262:4413-4420.
- Kieboom J, Dennis JJ, de Bont JAM, Zylstra GJ. 1998. Identification and molecular characterization of an efflux pump involved in *Pseudomonas putida* S12 solvent tolerance. *J Biol Chem* 273:85-91.
- Kiener A. 1992. Enzymatic oxidation of methyl groups on aromatic heterocycles: a versatile method for the preparation of heteroaromatic carboxylic acids. *Angew Chem Int Ed Engl* 31:774-775.
- Kiener A. 1995. Biosynthesis of functionalized aromatic N-heterocycles. *Chemtech* 31-35.
- Klinman JP. 1996. Mechanisms whereby mononuclear copper proteins functionalize organic substrates. *Chem Rev* 96:2541-2561.
- Kniemeyer O, Heider J. 2001. Ethylbenzene dehydrogenase, a novel hydrocarbon-oxidizing molybdenum/iron-sulfur/heme enzyme. *J Biol Chem* 276:21381-21386.
- Köhler A, Schüttoff M, Bryniok D, Knackmuß H-J. 1994. Enhanced biodegradation of phenantrene in a biphasic culture system. *Biodegradation* 5:93-103.
- Kok M, Oldenhuis R, van der Linden MPG, Raatjes P, Kingma J, van Lelyveld PH, Witholt B. 1989. The *Pseudomonas oleovorans* alkane hydroxylase gene: sequence and expression. *J Biol Chem* 264:5435-5441.
- Kunz DA, Chapman PJ. 1981. Catabolism of pseudocumene and 3-ethyltoluene by *Pseudomonas putida* (*avarilla*) mt-2: evidence for new functions of the TOL (pWWO) plasmid. *J Bacteriol* 146:179-191.
- Kuo CL, Raner GM, Vaz ADN, Coon MJ. 1999. Discrete species of activated oxygen yield different cytochrome P450 heme adducts from aldehydes. *Biochemistry* 38:10511-10518.
- Laane C, Boeren S, Vos K, Veeger C. 1987. Rules for optimization of biocatalysis in organic solvents. *Biotechnol Bioeng* 30:81-87.
- Lange SJ, Que L, Jr. 1998. Oxygen activating nonheme iron enzymes. *Curr Opin Chem Biol* 2:159-172.
- Leadbetter ER, Foster JW. 1959. Incorporation of molecular oxygen in bacterial cells utilizing hydrocarbons for growth. *Nature* 184:1428-1429.
- Lee JM, Zhang SH, Saha S, Anna SS, Jiang C, Perkins J. 2001. RNA expression analysis using an antisense *Bacillus subtilis* genome array. *J Bacteriol* 183:7371-7380.
- Lee K. 1999. Benzene-induced uncoupling of naphthalene dioxygenase activity and enzyme inactivation by production of hydrogen peroxide. *J Bacteriol* 181:2719-2725.
- Lee K, Gibson DT. 1996. Toluene and ethylbenzene oxidation by purified naphthalene dioxygenase from *Pseudomonas* sp. strain NCIB 9816-4. *Appl Environ Microbiol* 62:3101-3106.
- Lee S-K, Lipscomb JD. 1999. Oxygen activation catalyzed by methane monooxygenase hydroxylase component: proton delivery during the O-O bond cleavage steps. *Biochemistry* 38:4423-4432.
- Lee S-K, Nesheim JC, Lipscomb JD. 1993. Transient intermediates of the methane monooxygenase catalytic cycle. *J Biol Chem* 268:21569-21577.
- Leon R, Fernandes P, Pinheiro HM, Cabral JMS. 1998. Whole-cell biocatalysis in organic media. *Enzyme Microb Technol* 23:483-500.

- León R, Prazeres DMF, Fernandes P, Molinari F, Cabral JMS. 2001. A multiphasic hollow fiber reactor for the whole-cell bioconversion of 2-methyl-1,3-propanediol to (*R*)-b-hydroxyisobutyric acid. *Biotechnol Prog* 17:468-473.
- Leonardo MR, Dailly Y, Clark DP. 1996. Role of NAD in regulating the *adhE* gene of *Escherichia coli*. *J Bacteriol* 178:6013-6018.
- Li Q-S, Ogawa J, Schmid RD, Shimizu S. 2001a. Engineering cytochrome P450 BM-3 for oxidation of polycyclic aromatic hydrocarbons. *Appl Environ Microbiol* 67:5735-5739.
- Li Q-S, Schwaneberg U, Fischer M, Schmitt J, Pleiss J, Lutz-Wahl S, Schmid RD. 2001b. Rational evolution of a medium chain-specific cytochrome P-450 BM-3 variant. *Biochim Biophys Acta Protein Struct Molec Enzym* 1545:114-121.
- Li Q-S, Schwaneberg U, Fischer P, Schmid RD. 2000. Directed evolution of the fatty-acid hydroxylase P450BM-3 into an indole-hydroxylating catalyst. *Chem Eur J* 6:1531-1536.
- Li Z, van Beilen JB, Duetz WA, Schmid A, de Raadt A, Griengl H, Witholt B. 2002. Oxidative biotransformations using oxygenases. *Curr Opin Chem Biol* 6:136-144.
- Liese A, Seelbach K, Wandrey C. 2000. *Industrial Biotransformations*. Weinheim: Wiley-VCH.
- Lilly MD. 1982. Two-liquid-phase biocatalytic reactions. *J Chem Tech Biotechnol* 32:162-169.
- Lilly MD, Woodley JM. 1996. A structured approach to design and operation of biotransformation processes. *J Ind Microbiol* 17:24-29.
- Lin Z, Thorsen T, Arnold FH. 1999. Functional expression of horseradish peroxidase in *E. coli* by directed evolution. *Biotechnol Prog* 15:467-471.
- Lindqvist Z, Huang W, Schneider G, Shanklin J. 1996. Crystal structure of delta9 stearoyl-acyl carrier protein desaturase from castor seed and its relationship to other di-iron proteins. *EMBO Journal* 15:4081-4092.
- Ling KHJ, Hanzlik RP. 1989. Deuterium isotope effects on toluene metabolism: product release as a rate-limiting step in cytochrome P-450 catalysis. *Biochem Biophys Res Com* 160:844-849.
- Liu W-H, Horng W-C, Tsai M-S. 1996. Bioconversion of cholesterol to cholest-4-en-3-one in aqueous/organic solvent two-phase reactors. *Enzyme Microb Technol* 18:184-189.
- Lombardi A, Summa CM, Geremia S, Randaccio L, Pavone V, DeGrado WF. 2000. Retrostructural analysis of metalloproteins: Application to the design of a minimal model for diiron proteins. *Proc Natl Acad Sci USA* 97:6298-6305.
- Lonza. 2003. Lonza: Biotransformations. <http://www.lonzabiotec.com/biotec/en/areas/0.html>.
- Lopez JL, Matson SL. 1997. A multiphase / extractive enzyme membrane reactor for production of diltiazem chiral intermediate. *J Membr Sci* 125:189-211.
- Luli GW, Strohl WR. 1990. Comparison of growth, acetate production, and acetate inhibition of *Escherichia coli* strains in batch and fed-batch fermentations. *Appl Environ Microbiol* 56:1004-1011.
- Luu PP, Yung CW, Sun AK, Wood TK. 1995. Monitoring trichloroethylene mineralization by *Pseudomonas cepacia* G4 PR1. *Appl Microbiol Biotechnol* 44:259-264.
- Lye GJ, Woodley JM. 1999. Application of *in situ* product-removal techniques to biocatalytic processes. *Trends Biotechnol* 17:395-402.
- Lynch RM, Woodley JM, Lilly MD. 1997. Process design for the oxidation of fluorobenzene to fluorocatechol by *Pseudomonas putida*. *J Biotechnol* 58:167-175.
- Manfredini R, Manfredini A. 1996. Design of industrial bioreactors. In: Larsson G, Förberg C, editors. *Bioreactor Engineering*. Salsjöbaden, Sweden: Working parties bioreactor performance, measurement, and control (EFB). p 49-92.



- Maruyama T, Iida H, Kakidani H. 2003. Oxidation of both termini of *p*- and *m*-xylene by *Escherichia coli* transformed with xylene monooxygenase gene. *J Mol Catal B Enzym* 21:211-219.
- Mathys RG, Ku OM, Witholt B. 1998a. Alkanol removal from the apolar phase of a two-liquid phase bioconversion system. Part 1: Comparison of a less volatile and a more volatile in-situ extraction solvent for the separation of 1-octanol by distillation. *J Chem Tech Biotechnol* 71:315-325.
- Mathys RG, Schmid A, Kut OM, Witholt B. 1998b. Alkanol removal from the apolar phase of a two-liquid phase bioconversion system. Part 2: Effect of the fermentation medium on batch distillation. *J Chem Tech Biotechnol* 71:326-334.
- Mathys RG, Schmid A, Witholt B. 1999. Integrated two-liquid phase bioconversion and product-recovery processes for the oxidation of alkanes: Process design and economic evaluation. *Biotechnol Bioeng* 64:459-477.
- Mavrovouniotis ML. 1990. Group Contributions for Estimating Standard Gibbs Energies of Formation of Biochemical Compounds in Aqueous Solution. *Biotechnol Bioeng* 36:1070-1082.
- Mavrovouniotis ML. 1991. Estimation of Standard Gibbs Energy Changes of Biotransformations. *J Biol Chem* 266:14440-14445.
- May O, Nguyen PT, Arnold FH. 2000. Inverting enantioselectivity by directed evolution of hydantoinase for improved production of L-methionine. *Nat Biotechnol* 18:317-320.
- May SW. 1999. Applications of oxidoreductases. *Curr Opin Biotechnol* 10:370-375.
- May SW, Katopodis AG. 1986. Oxygenation of alcohol and sulphide substrates by a prototypical non-haem iron monooxygenase: catalysis and biotechnological potential. *Enzyme Microb Technol* 8:17-21.
- May SW, Steltenkamp MS, Schwartz RD, McCoy CJ. 1976. Stereoselective formation of diepoxides by an enzyme system of *Pseudomonas oleovorans*. *J Am Chem Soc* 98:7856-7858.
- Mc Fall E, Newman EB. 1996. Amino acids as carbon sources. In: Neidhardt FC, editor. *Escherichia coli and Salmonella*. Washington, DC: ASM Press. p 358-379.
- Merkx M, Kopp DA, Sazinsky MH, Blazyk JL, Müller J, Lippard SJ. 2001. Dioxygen activation and methane hydroxylation by soluble methane monooxygenase: a tale of two irons and three proteins. *Angew Chem Int Ed Engl* 40:2782-2807.
- Mermod N, Harayama S, Timmis KN. 1986. New route to bacterial production of indigo. *Bio/Technol* 4:321-324.
- Messing J. 1979. A multipurpose cloning system based on single-stranded DNA bacteriophage M13. *Recomb DNA Tech Bull* 2:43-49.
- Meyer A, Held M, Schmid A, Kohler H-PE, Witholt B. 2003. Synthesis of 3-*tert*-butylcatechol by and engineered monooxygenase. *Biotechnol Bioeng* 81:518-524.
- Meyer A, Schmid A, Held M, Westphal AH, Röthlisberger M, Kohler H-PE, van Berkel WJH, Witholt B. 2002a. Changing the substrate reactivity of 2-hydroxybiphenyl 3-monooxygenase from *Pseudomonas azelaica* HBP1 by directed evolution. *J Biol Chem* 277:5575-5582.
- Meyer A, Würsten A, Schmid A, Kohler H-PE, Witholt B. 2002b. Hydroxylation of indole by laboratory evolved 2-hydroxybiphenyl 3-monooxygenase. *J Biol Chem* 277:34161-34167.
- Miles CS, Ost TWB, Noble MA, Munro AW, Chapman SK. 2000. Protein engineering of cytochrome P-450. *Biochim Biophys Acta* 1543:383-407.
- Moser A. 1981. *Bioprocess technology*. Wien: Springer-Verlag.

- Mosqueda G, Ramos JL. 2000. A set of genes encoding a second toluene efflux system in *Pseudomonas putida* DOT-T1E is linked to the *tod* genes for toluene metabolism. *J Bacteriol* 182:937-943.
- Munro AW, Leys DG, McLean KJ, Marshall KR, Ost TWB, Daff S, Miles CS, Chapman SK, Lysek DA, Moser CC, Page CC, Dutton PL. 2002. P450 BM3: the very model of a modern flavocytochrome. *Trends Biochem Sci* 27:250-257.
- Neubauer P, Häggström L, Enfors S-O. 1995. Influence of substrate oscillations on acetate formation and growth yield in *Escherichia coli* glucose limited fed-batch cultivations. *Biotechnol Bioeng* 47:139-146.
- Neubauer P, Lin HY, Mathiszik B. 2003. Metabolic load of recombinant protein production: inhibition of cellular capacities for glucose uptake and respiration after induction of a heterologous gene in *Escherichia coli*. *Biotechnol Bioeng* 83:53-64.
- Neufeld RJ, Zajic JE, Gerson DF. 1983. Growth characteristics and cell partitioning of *Acinetobacter* on hydrocarbon substrates. *J Ferm Technol* 61:315-321.
- Newcomb M, Hollenberg PF, Coon MJ. 2003. Multiple mechanisms and multiple oxidants in P450-catalyzed hydroxylations. *Arch Biochem Biophys* 409:72-79.
- Newcomb M, Shen R, Choi S-Y, Toy PH, Hollenberg PF, Vaz ADN, Coon MJ. 2000. Cytochrome P450-catalyzed hydroxylation of mechanistic probes that distinguish between radicals and cations. Evidence for cationic but not for radical intermediates. *J Am Chem Soc* 122:2677-2686.
- Nieboer M. 1996. Overproduction of a foreign membrane monooxygenase in *E. coli*: relation to membrane biogenesis. Ph.D. thesis, Rijksuniversiteit Groningen, Groningen.
- Nieboer M, Kingma J, Witholt B. 1993. The alkane oxidation system of *Pseudomonas oleovorans*: induction of the *alk* genes in *Escherichia coli* W3110(pGec47) affects membrane biogenesis and results in overexpression of alkane hydroxylase in a distinct cytoplasmic membrane subfraction. *Mol Microbiol* 8:1039-1051.
- Nikolova P, Ward OP. 1993. Whole cell biocatalysis in nonconventional media. *J Ind Microbiol* 12:76-86.
- Nishi T, Saito F, Nagahori H, Kataoka M, Morisawa Y. 1990. Synthesis and biological activities of renin inhibitors containing statine analogues. *Chem Pharm Bull* 38:103-109.
- Noble MA, Miles CS, Chapman SK, Lysek DA, MacKay AC, Reid GA, Hanzlik RP, Munro AW. 1999. Roles of key active-site residues in flavocytochrome P450 BM3. *Biochem J* 339:371-379.
- Noordman WH, Wachter JHJ, de Boer GJ, Janssen DB. 2002. The enhancement by surfactants of hexadecane degradation by *Pseudomonas aeruginosa* varies with substrate availability. *J Biotechnol* 94:195-212.
- Nordlund P, Sjöberg BM, Eklund H. 1990. Three-dimensional structure of the free radical protein of ribonucleotide reductase. *Nature* 345:593-598.
- Nöthe C, Hartmans S. 1994. Formation and degradation of styrene oxide stereoisomers by different microorganisms. *Biocatalysis* 10:219-225.
- Oligaro F, Harris N, Cohen S, Filatov M, de Visser SP, Shaik S. 2000. A model "rebound" mechanism of hydroxylation by cytochrome P450: stepwise and effectively concerted pathways, and their reactivity patterns. *J Am Chem Soc* 122:8977-8989.
- Onken U, Liefke E. 1989. Effect of total and partial pressure (oxygen and carbon dioxide) on aerobic microbial processes. *Adv Biochem Eng Biotechnol* 40:137-166.
- Ortiz de Montellano PR. 1995. *Cytochrome P450 Structure, Mechanism, and Biochemistry*. New York: Plenum Press.
- Ortiz de Montellano PR, Nishida C, Rodriguez-Crespo I, Gerber N. 1998. Nitric oxide synthase structure and electron transfer. *Drug Metab Dispos* 26:1185-1189.

- Ost TWB, Miles CS, Murdoch J, Cheung YF, Reid GA, Chapman SK, Munro AW. 2000. Rational re-design of the substrate binding site of flavocytochrome P450BM3. *FEBS Letters* 486:173-177.
- Panke S, Held M, Wubbolts MG, Witholt B, Schmid A. 2002. Pilot-scale production of (*S*)-styrene oxide from styrene by recombinant *Escherichia coli* synthesizing styrene monooxygenase. *Biotechnol Bioeng* 80:33-41.
- Panke S, de Lorenzo V, Kaiser A, Witholt B, Wubbolts MG. 1999a. Engineering of a stable whole-cell biocatalyst capable of (*S*)-styrene oxide formation for continuous two-liquid-phase applications. *Appl Environ Microbiol* 65:5619-5623.
- Panke S, Meyer A, Huber CM, Witholt B, Wubbolts MG. 1999b. An alkane responsive expression system for the production of fine chemicals. *Appl Environ Microbiol* 65:2324-2332.
- Panke S, Sánchez-Romero JM, de Lorenzo V. 1998a. Engineering quasi-natural *Pseudomonas putida* strains for metabolism of toluene through an *ortho*-cleavage degradation pathway. *Appl Environ Microbiol* 64:748-751.
- Panke S, Witholt B, Schmid A, Wubbolts MG. 1998b. Towards a biocatalyst for (*S*)-styrene oxide production: characterization of the styrene degradation pathway of *Pseudomonas* sp. strain VLB120. *Appl Environ Microbiol* 64:2032-2043.
- Panke S, Wubbolts M. 2002. Enzyme technology and bioprocess engineering. *Curr Opin Biotechnol* 13:111-116.
- Panke S, Wubbolts MG, Schmid A, Witholt B. 2000. Production of enantiopure styrene oxide by recombinant *Escherichia coli* synthesizing a two-component styrene monooxygenase. *Biotechnol Bioeng* 69:91-100.
- Parales RE, Bruce NC, Schmid A, Wackett LP. 2002. Biodegradation, Biotransformation, and Biocatalysis (B3). *Appl Environ Microbiol* 68:4699-4709.
- Parikh A, Gillam EMJ, Guengerich FP. 1997. Drug metabolism by *Escherichia coli* expressing human cytochromes P450. *Nat Biotechnol* 15:784-788.
- Patnaik R, Louie S, Gavrilovic V, Perry K, Stemmer WPC, Ryan CM, del Cardayré S. 2002. Genome shuffling of *Lactobacillus* for improved acid tolerance. *Nat Biotechnol* 20:707-712.
- Pereira LGC, Hickel A, Radke CJ, Blanch HW. 2002. A kinetic model for enzyme interfacial activity and stability: pa-hydroxynitrile lyase at the diisopropyl ether/water interface. *Biotechnol Bioeng* 78:595-605.
- Petersen M, Kiener A. 1999. Biocatalysis: Preparation and functionalization of N-heterocycles. *Green Chem* 99-106.
- Peterson JA, Basu D, Coon MJ. 1966. Enzymatic omega-oxidation. I. Electron carriers in fatty acid and hydrocarbon hydroxylation. *J Biol Chem* 241:5162-5164.
- Peters-Wendisch PG, Schiel B, Wendisch VF, Katsoulidis E, Sahn H, Eikmanns BJ. 2001. Pyruvate carboxylase is a major bottleneck for glutamate and lysine production by *Corynebacterium glutamicum*. *J Mol Microbiol Biotechnol* 3:295-300.
- Phumathon P, Stephens GM. 1999. Production of toluene *cis*-glycol using recombinant *Escherichia coli* strains in glucose-limited fed batch culture. *Enzyme Microb Technol* 25:810-819.
- Poulos TL, Cupp-Vickery J, Li H. 1995. Structural studies on prokaryotic cytochromes P450. In: Ortiz de Montellano PR, editor. *Cytochrome 450: Structure, Mechanism and Biochemistry*. New York, N.Y.: Plenum Press. p 125-150.
- Poulos TL, Raag R. 1992. Cytochrome P450cam: crystallography, oxygen activation, and electron transfer. *FASEB Journal* 6:674-679.

- Powell KA, Ramer SW, del Cardayré SB, Stemmer WPC, Tobin MB, Longchamp PF, Huisman GW. 2001. Directed evolution and biocatalysis. *Angew Chem Int Ed Engl* 40:3948-3959.
- Prescott AG, Lloyd MD. 2000. The iron(II) and 2-oxoacid-dependent dioxygenases and their role in metabolism. *Nat Prod Rep* 17:367-383.
- Preusting H, van Houten R, Hoefs A, van Langenberghe EK, Favre-Bulle O, Witholt B. 1993. High cell density cultivation of *Pseudomonas oleovorans*: growth and production of poly (3-hydroxyalkanoates) in two-liquid phase batch and fed-batch systems. *Biotechnol Bioeng* 41:550-556.
- Prichanont S, Leak DJ, Stuckey DC. 1998. Alkene monooxygenase-catalyzed whole cell epoxidation in a two-liquid phase system. *Enzyme Microb Technol* 22:471-479.
- Raag R, Li H, Jones BC, Poulos TL. 1993. Inhibitor-induced conformational change in cytochrome P-450<sub>cam</sub>. *Biochemistry* 32:4571-4578.
- Raag R, Poulos TL. 1989. Crystal structure of the carbon monoxide-substrate-cytochrome P-450<sub>cam</sub> ternary complex. *Biochemistry* 28:7586-7592.
- Rabus R, Kube M, Beck A, Widdel F, Reinhardt R. 2002. Genes involved in the anaerobic degradation of ethylbenzene in a denitrifying bacterium, strain EbN1. *Arch Microbiol* 178:506-516.
- Ramos JL, Duque E, Gallegos M-T, Godoy P, Ramos-González MI, Rojas A, Terán W, Segura A. 2002. Mechanisms of solvent tolerance in gram-negative bacteria. *Annu Rev Microbiol* 56:743-768.
- Ramos JL, Duque E, Godoy P, Segura A. 1998. Efflux pumps involved in toluene tolerance in *Pseudomonas putida* DOT-T1E. *J Bacteriol* 180:3323-3329.
- Ramos JL, Marqués S, Timmis KN. 1997. Transcriptional control of the *Pseudomonas* TOL plasmid catabolic operons is achieved through an interplay of host factors and plasmid-encoded regulators. *Annu Rev Microbiol* 51:341-373.
- Ramos JL, Timmis KN. 1987. Experimental evolution of catabolic pathways of bacteria. *Microbiol. Sci.* 4:228-237.
- Raner GM, Chiang EW, Vaz ADN, Coon JM. 1997. Mechanism-based inactivation of cytochrome P450 2B4 by aldehydes: relationship to aldehyde deformylation via a peroxyhemiacetal intermediate. *Biochemistry* 36:4895-4902.
- Rasor JP, Voss E. 2001. Enzyme-catalyzed processes in pharmaceutical industry. *Appl Catal A* 221:145-158.
- Rataj MJ, Kauth JE, Donnelly ME. 1991. Oxidation of deuterated compounds by high specific activity methane monooxygenase from *Methylosinus trichosporium*. Mechanistic implications. *J Biol Chem* 266:18684-18690.
- Ravichandran KG, Boddupalli SS, Hasermann CA, Peterson JA, Deisenhofer J. 1993. Crystal structure of hemoprotein domain of P450BM-3, a prototype for microsomal P450's. *Science* 261:731-736.
- Reddy PG, Singh HD, Roy PK, Baruah JN. 1982. Predominant role of hydrocarbon solubilization in the microbial uptake of hydrocarbons. *Biotechnol Bioeng* 24:1241-1269.
- Richardson TH, Jung F, Griffin KJ, Wester M, Raucy JL, Kemper B, Bornheim LM, Hassett C, Omiecinski CJ, Johnson EF. 1995. Universal approach to the expression of human and rabbit cytochrome P450s of the 2C subfamily in *Escherichia coli*. *Arch Biochem Biophys* 323:87-96.
- Riesenber D, Schulz V, Knorre WA, Pohl H-D, Korz D, Sanders EA, Ross A, Deckwer W-D. 1991. High cell density cultivation of *Escherichia coli* at controlled specific growth rate. *J Biotechnol* 20:17-28.

- Robertson JB, Spain JC, Haddock JD, Gibson DT. 1992. Oxidation of nitrotoluene by toluene dioxygenase: evidence for a monooxygenase reaction. *Appl Environ Microbiol* 58:2643-2648.
- Robinson GK, Stephens GM, Dalton H, Geary PJ. 1992. The production of catechols from benzene and toluene by *Pseudomonas putida* in glucose fed-batch culture. *Biocatalysis* 6:81-100.
- Rojas A, Duque E, Mosqueda G, Golden G, Hurtado A, Ramos JL, Segura A. 2001. Three efflux pumps are required to provide efficient tolerance to toluene in *Pseudomonas putida* DOT-T1E. *J Bacteriol* 183:3967-3973.
- Rosche B, Sandford V, Breuer M, Hauer B, Rogers P. 2001. Biotransformation of benzaldehyde into (*R*)-phenylacetylcarbinol by filamentous fungi or their extracts. *Appl Microbiol Biotechnol* 57:309-315.
- Rosenberg M, Rosenberg E. 1981. Role of adherence in growth of *Acinetobacter calcoaceticus* RAG-1 on hexadecane. *J Bacteriol* 148:51-57.
- Rosenzweig AC, Frederick CA, Lippard SJ, Nordlund P. 1993. Crystal structure of a bacterial non-haem iron hydroxylase that catalyses the biological oxidation of methane. *Nature* 366:537-543.
- Rothen SA, Sauer M, Sonnleitner B, Witholt B. 1998. Biotransformation of octane by *E. coli* HB101[pGEC47] on defined medium: octanoate production and product inhibition. *Biotechnol Bioeng* 58:356-365.
- Royce PCN, Thornhill NF. 1991. Estimation of dissolved carbon dioxide concentrations in aerobic fermentations. *AIChEJ* 37:1680-1686.
- Ruettinger RT, Griffith GR, Coon MJ. 1977. Characterization of the w-hydroxylase of *Pseudomonas oleovorans* as a non-heme iron protein. *Arch Biochem Biophys* 183:528-537.
- Ruettinger RT, Olson ST, Boyer RF, Coon MJ. 1974. Identification of the w-hydroxylase of *Pseudomonas oleovorans* as a nonheme iron protein requiring phospholipid for catalytic activity. *Biochem Biophys Res Com* 57:1011-1017.
- Russell JB, Cook GM. 1995. Energetics of bacterial growth: Balance of anabolic and catabolic reactions. *Microbiol Rev* 59:48-62.
- Ryle MJ, Hausinger RP. 2002. Non-heme iron oxygenases. *Curr Opin Chem Biol* 6:193-201.
- Salter GJ, Kell DB. 1995. Solvent selection for whole cell biotransformations in organic media. *Crit Rev Biotechnol* 15:139-177.
- Sambrook J, Fritsch EF, Maniatis T. 1989. *Molecular cloning: a laboratory manual*. Cold Spring Harbor, NY: Cold Spring Harbor Laboratory Press.
- Schlichting I, Berendzen J, Chu K, Stock AM, Maves SA, Benson DE, Sweet RM, Ringe D, Petsko GA, Sligar SG. 2000. The catalytic pathway of cytochrome P450<sub>cam</sub> at atomic resolution. *Science* 287:1615-1622.
- Schmid A. 1997. Two-liquid phase bioprocess development; interfacial mass transfer rates and explosion safety. Ph.D. thesis, Swiss Federal Institute of Technology, Zurich.
- Schmid A, Dordick JS, Hauer B, Kiener A, Wubbolts M, Witholt B. 2001. Industrial biocatalysis today and tomorrow. *Nature* 409:258-268.
- Schmid A, Hollmann F, Park JB, Bühler B. 2002. The use of enzymes in the chemical industry in Europe. *Curr Opin Biotechnol* 13:359-366.
- Schmid A, Kollmer A, Mathys RG, Witholt B. 1998a. Developments toward large-scale bacterial bioprocesses in the presence of bulk amounts of organic solvents. *Extremophiles* 2:249-256.
- Schmid A, Kollmer A, Sonnleitner B, Witholt B. 1999. Development of equipment and procedures for the safe operation of aerobic bacterial bioprocesses in the presence of bulk amounts of flammable organic solvents. *Bioproc Eng* 20:91-100.

- Schmid A, Kollmer A, Witholt B. 1998b. Effects of biosurfactant and emulsification on two-liquid phase *Pseudomonas oleovorans* cultures and cell-free emulsions containing n-decane. *Enzyme Microb Technol* 22:487-493.
- Schmid A, Sonnleitner B, Witholt B. 1998c. Medium chain length alkane solvent-cell transfer rates in two-liquid phase, *Pseudomonas oleovorans* cultures. *Biotechnol Bioeng* 60:10-23.
- Schneider S. 1998. Cytochrome P450<sub>BM3</sub> monooxygenase: Development of a whole cell biocatalyst for the regio- and stereoselective oxidation of long chain fatty acids. Ph.D. thesis, Swiss Federal Institute of Technology, Zurich.
- Schneider S, Wubbolts MG, Oesterhelt G, Sanglard D, Witholt B. 1999. Controlled regioselectivity of fatty acid oxidation by whole cells producing cytochrome P450<sub>BM-3</sub> monooxygenase under varied dissolved oxygen concentrations. *Biotechnol Bioeng* 64:333-341.
- Schneider S, Wubbolts MG, Sanglard D, Witholt B. 1998. Biocatalyst engineering by assembly of fatty acid transport and oxidation activities for in vivo application of cytochrome P-450(BM-3) monooxygenase. *Appl Environ Microbiol* 64:3784-3790.
- Schofield CJ, Zhang Z. 1999. Structural and mechanistic studies on 2-oxoglutarate-dependent oxygenases and related enzymes. *Curr Opin Struct Biol* 9:722-731.
- Schroen CGPH, Nierstrasz VA, Moody HM, Hoogschagen MJ, Kroon PJ, Bosma R, Beeftink HH, Janssen AEM, Tramper J. 2001. Modeling of the enzymatic kinetic synthesis of cephalixin - influence of substrate concentration and temperature. *Biotechnol Bioeng* 73:171-178.
- Schulze B, Broxterman R, Shoemaker H, Boesten W. 1998. Review of biocatalysis in the production of chiral fine chemicals. *Spec. Chem.* 18:244-246.
- Schwaneberg U, Appel D, Schmitt J, Schmid RD. 2000. P450 in biotechnology: zinc driven omega-hydroxylation of *p*-nitrophenoxydodecanoic acid using P450 BM-3 F87A as a catalyst. *J Biotechnol* 84:249-257.
- Schwartz RD, McCoy J. 1977. Epoxidation of 1,7-octadiene by *Pseudomonas oleovorans*: fermentation in the presence of cyclohexane. *Appl Environ Microbiol* 34:47-49.
- Sekelsky AM, Shreve GS. 1999. Kinetic model of biosurfactant-enhanced hexadecane biodegradation by *Pseudomonas aeruginosa*. *Biotechnol Bioeng* 63:401-409.
- Shanklin J, Achim C, Schmidt H, Fox BG, Münck E. 1997. Mössbauer studies of alkane  $\omega$ -hydroxylase: evidence for a diiron cluster in an integral-membrane enzyme. *Proc Natl Acad Sci USA* 94:2981-2986.
- Shanklin J, Whittle E. 1999. Integral membrane diiron proteins: a distinct and widespread group of enzymes with diverse catalytic plasticity. *J Inorg Biochem* 74:50.
- Shanklin J, Whittle E, Fox BG. 1994. Eight histidine residues are catalytically essential in a membrane-associated iron enzyme, stearyl-CoA desaturase, and are conserved in alkane hydroxylase and xylene monooxygenase. *Biochemistry* 33:12787-12794.
- Shannon MJR, Unterman R. 1993. Evaluating bioremediation: distinguishing fact from fiction. *Annu Rev Microbiol* 47:715-38.
- Shaw JP, Harayama S. 1990. Purification and characterisation of TOL plasmid-encoded benzyl alcohol dehydrogenase and benzaldehyde dehydrogenase of *Pseudomonas putida*. *Eur J Biochem* 191:705-714.
- Shaw JP, Harayama S. 1992. Purification and characterisation of the NADH:acceptor reductase component of xylene monooxygenase encoded by the TOL plasmid pWW0 of *Pseudomonas putida* mt-2. *Eur J Biochem* 209:51-61.
- Shaw JP, Harayama S. 1995. Characterization *in vitro* of the hydroxylase component of xylene monooxygenase, the first enzyme of the TOL-plasmid-encoded pathway for the mineralization of toluenes and xylenes. *J Ferm Bioeng* 79:195-199.

- Shaw JP, Rekik M, Schwager F, Harayama S. 1993. Kinetic studies on benzyl alcohol dehydrogenase encoded by TOL plasmid pWW0. *J Biol Chem* 268:10842-10850.
- Shaw JP, Schwager F, Harayama S. 1992. Substrate-specificity of benzyl alcohol dehydrogenase and benzaldehyde dehydrogenase encoded by TOL plasmid pWW0, metabolic and mechanistic implications. *Biochem J* 283:789-794.
- Shet MS, Fisher CW, Estabrook RW. 1997. The Function of recombinant cytochrome P450s in intact *Escherichia coli* cells: The 17 $\alpha$ -hydroxylation of progesterone and pregnenolone by P450c17. *Arch Biochem Biophys* 339:218-225.
- Shet MS, Fisher CW, Holmans PL, Estabrook RW. 1996. The omega-hydroxylation of lauric acid: oxidation of 12-hydroxylauric acid to dodecanedioic acid by a purified recombinant fusion protein containing P450 4A1 and NADPH-P450 reductase. *Arch Biochem Biophys* 330:199-208.
- Shu L, Nesheim JC, Kauffmann K, Münck E, Lipscomb JD, Que L, Jr. 1997. An Fe<sup>IV</sup>O<sub>2</sub> diamond core structure for the key intermediate Q of methane monooxygenase. *Science* 275:515-518.
- Sikkema J, de Bont JAM, Poolman B. 1995. Mechanisms of membrane toxicity of hydrocarbons. *Microbiol Rev* 59:201-222.
- Slonczewski JL, Rosen BP, Alger JR, Macnab RM. 1981. pH homeostasis in *Escherichia coli*: Measurement by <sup>31</sup>P nuclear magnetic resonance of methylphosphonate and phosphate. *Proc Natl Acad Sci USA* 78:6271-6275.
- Smith MEB, Lloyd MC, Derrien N, Lloyd RC, Taylor SJC, Chaplin DA, Casy G, Mc Cague R. 2001. An efficient route to all eight stereoisomers of a tri-functionalized cyclopentane scaffold for drug discovery. *Tetrahedron Asym* 12:703-705.
- Smits THM, Ballada SB, Witholt B, van Beilen JB. 2002. Functional analysis of alkane hydroxylases from Gram-negative and Gram-positive bacteria. *J Bacteriol* 184:1733-1742.
- Smits THM, Röthlisberger M, Witholt B, van Beilen JB. 1999. Molecular screening for alkane hydroxylase genes in Gram-negative and Gram-positive strains. *Environ Microbiol* 1:307-317.
- Solomon EI, Brunold TC, Davis MI, Kemsley JN, Lee S-K, Lehnert N, Neese F, Skulan AJ, Yang Y-S, Zhou J. 2000. Geometric and electronic structure/function correlations in non-heme iron enzymes. *Chem Rev* 100:235-349.
- Solomon EI, Sundaram UM, Machonkin TE. 1996. Multicopper oxidases and oxygenases. *Chem Rev* 96:2563-2605.
- Sono M, Roach MP, Coulter ED, Dawson JH. 1996. Heme-containing oxygenases. *Chem Rev* 96:2841-2887.
- Spain JC, Zylstra GJ, Blake CK, Gibson DT. 1989. Monohydroxylation of phenol and 2,5-dichlorophenol by toluene dioxygenase in *Pseudomonas putida* F1. *Appl Environ Microbiol* 55:2648-2652.
- Staijen IE, Marcionelli R, Witholt B. 1999. The P<sub>alkBFGHJKL</sub> promoter is under carbon catabolite repression control in *Pseudomonas oleovorans* but not in *Escherichia coli* *alk*<sup>+</sup> recombinants. *J Bacteriol* 181:1610-1616.
- Staijen IE, van Beilen JB, Witholt B. 2000. Expression, stability and performance of the three-component alkane mono-oxygenase of *Pseudomonas oleovorans* in *Escherichia coli*. *Eur J Biochem* 267:1957-1965.
- Staijen IE, Witholt B. 1998. Synthesis of alkane hydroxylase of *Pseudomonas oleovorans* increases the iron requirement of *alk*<sup>+</sup> bacterial strains. *Biotechnol Bioeng* 57:228-237.
- Stancik LM, Stancik DM, Schmidt B, Barnhart DM, Yoncheva YN, Slonczewski JL. 2002. pH-dependent expression of periplasmic proteins and amino acid catabolism in *Escherichia coli*. *J Bacteriol* 184:4246-4258.

- Straathof AJJ. 2003. Enzymatic catalysis via liquid-liquid interfaces. *Biotechnol Bioeng* 83:371-375.
- Straathof AJJ, Panke S, Schmid A. 2002. The production of fine chemicals by biotransformations. *Curr Opin Biotechnol* 13:548-556.
- Suske WA, Held M, Schmid A, Fleischmann T, Wubbolts MG, Kohler H-PE. 1997. Purification and characterization of 2-hydroxybiphenyl 3-monooxygenase, a novel NADH-dependent, FAD-containing aromatic hydroxylase from *Pseudomonas azeleica* HBP1. *J Biol Chem* 272:24257-24265.
- Suzuki M, Hayakawa T, Shaw JP, Rekik M, Harayama S. 1991. Primary structure of xylene monooxygenase: similarities to and differences from the alkane hydroxylation system. *J Bacteriol* 173:1690-1695.
- Taylor SV, Kast P, Hilvert D. 2001. Investigating and engineering enzymes by genetic selection. *Angew Chem Int Ed Engl* 40:3310-3335.
- Thayer AM. 2001. Biocatalysis. *Chem Eng News* 79:27-34.
- Thomas JM, Raja R, Sankar G, Bell RG. 1999. Molecular-sieve catalysts for the selective oxidation of linear alkanes by molecular oxygen. *Nature* 398:227-230.
- Thomas JM, Raja R, Sankar G, Bell RG. 2001. Molecular sieve catalysts for the regioselective and shape-selective oxyfunctionalization of alkanes in air. *Acc Chem Res* 34:191-200.
- Tsai JT, Wahbi LP, Dervakos GA, Stephens GM. 1996. Production of toluene-*cis*-glycol by a recombinant *Escherichia coli* in a two-liquid phase culture system. *Biotechnol Lett* 18:241-244.
- Turner NJ, Winterman JR, Mc Cague R, Parratt JS, Taylor SJC. 1995. Synthesis of homochiral L-(*S*)-*tert*-leucine via a lipase catalyzed dynamic resolution process. *Tetrahedron Lett* 36:1113-1116.
- Ueng Y-F, Kuwabara T, Chun Y-J, Guengerich FP. 1997. Cooperativity in oxidations catalyzed by cytochrome P450 3A4. *Biochemistry* 36:370-381.
- Ullah AJH, Murray RI, Bhattacharyya PK, Wagner GC, Gunsalus IC. 1990. Protein components of a cytochrome P-450 linalool 8-methyl hydroxylase. *J Biol Chem* 265:1345-1351.
- Urlacher V, Schmid RD. 2002. Biotransformations using prokaryotic P450 monooxygenases. *Curr Opin Biotechnol* 13:557-564.
- Vaidya AM, Bell G, Halling PJ. 1992. Aqueous-organic membrane bioreactors. Part I. A guide to membrane selection. *J Membr Sci* 71:139-149.
- Vaidya AM, Bell G, Halling PJ. 1994. Aqueous-organic membrane bioreactors. Part II. Breakthrough pressure measurement. *J Membr Sci* 97:13-26.
- Vaidya AM, Halling PJ, Bell G. 1993. Novel reactor for aqueous-organic 2-phase biocatalysis - a packed-bed hollow-fiber membrane bioreactor. *Biotechnol Tech* 7:441-446.
- van Beilen JB, Duetz WA, Schmid A, Witholt B. 2003. Practical issues in the application of oxygenases. *Trends Biotechnol* 21:170-177.
- van Beilen JB, Kingma J, Witholt B. 1994a. Substrate specificity of the alkane hydroxylase system of *Pseudomonas oleovorans* GPo1. *Enzyme Microb Technol* 16:904-911.
- van Beilen JB, Panke S, Lucchini S, Franchini AG, Röthlisberger M, Witholt B. 2001. Analysis of *Pseudomonas putida* alkane-degradation gene clusters and flanking insertion sequences: evolution and regulation of the *alk* genes. *Microbiology* 147:1621-1630.
- van Beilen JB, Penninga D, Witholt B. 1992. Topology of the membrane-bound alkane hydroxylase of *Pseudomonas oleovorans*. *J Biol Chem* 267:9149-9201.



- van Beilen JB, Smits THM, Whyte LG, Schorcht S, Röthlisberger M, Plaggemeier T, Engesser K-H, Witholt B. 2002. Alkane hydroxylase homologues in Gram-positive strains. *Environ Microbiol* 4:676-682.
- van Beilen JB, Wubbolts MG, Witholt B. 1994b. Genetics of alkane oxidation by *Pseudomonas oleovorans*. *Biodegradation* 5:161-174.
- van de Sandt EJAX, de Vroom E. 2000. Innovations in cephalosporin and penicillin production: Painting the antibiotics industry green. *Chim Oggi* 18:72-75.
- van de Velde F, Lourenco ND, Bakker M, van Rantwijk F, Sheldon RA. 2000. Improved operational stability of peroxidases by coimmobilization with glucose oxidase. *Biotechnol Bioeng* 69:286-291.
- van de Velde F, van Rantwijk F, Sheldon RA. 2001. Improving the catalytic performance of peroxidases in organic synthesis. *Trends Biotechnol* 19:73-80.
- van den Heuvel RHH, Fraaije MW, Mattevi A, Laane C, van Berkel WJH. 2001a. Vanillyl-alcohol oxidase, a tasteful biocatalyst. *J Mol Catal B Enzym* 11:185-188.
- van den Heuvel RHH, Laane C, van Berkel WJH. 2001b. Exploring the biocatalytic potential of vanillyl-alcohol oxidase by site-directed mutagenesis. *Adv Synth Catal* 343:515-520.
- van der Meer JR, de Vos WM, Harayama S, Zehnder AJB. 1992. Molecular mechanisms of genetic adaptation to xenobiotic compounds. *Microbiol Rev* 56:677-694.
- van Deurzen MPJ, Seelbach K, van Rantwijk F, Kragl U, Sheldon RA. 1997a. Chloroperoxidase: Use of a hydrogen peroxide-stat for controlling reactions and improving enzyme performance. *Biocatal Biotransf* 15:1-16.
- van Deurzen MPJ, van Rantwijk F, Sheldon RA. 1997b. Selective oxidations catalyzed by peroxidases. *Tetrahedron* 53:13183-13220.
- van Rantwijk F, Sheldon RA. 2000. Selective oxygen transfer catalyzed by heme peroxidases: synthetic and mechanistic aspects. *Curr Opin Biotechnol* 11:554-564.
- Vaz ADN, Coon MJ. 1994. On the mechanism of the action of cytochrome P450: evaluation of hydrogen abstraction in oxygen-dependent alcohol oxidation. *Biochemistry* 33:6442-6449.
- Vaz ADN, McGinnity DF, Coon MJ. 1998. Epoxidation of olefins by cytochrome P450: evidence from site-specific mutagenesis for hydroperoxo-iron as an electrophilic oxidant. *Proc Natl Acad Sci USA* 95:3555-3560.
- Voser W. 1982. Isolation of hydrophilic fermentation products by adsorption chromatography. *J Chem Tech Biotechnol* 32:109-118.
- Wahbi LP, Gokhale D, Minter S, Stephens GM. 1996. Construction and use of recombinant *Escherichia coli* strains for the synthesis of toluene *cis*-glycol. *Enzyme Microb Technol* 19:297-306.
- Wahler D, Reymond JL. 2001a. High-throughput screening for biocatalysts. *Curr Opin Biotechnol* 12:535-544.
- Wahler D, Reymond JL. 2001b. Novel methods for biocatalyst screening. *Curr Opin Chem Biol* 5:152-158.
- Wallar BJ, Lipscomb JD. 1996. Dioxygen activation by enzymes containing binuclear non-heme iron clusters. *Chem Rev* 96:2625-2657.
- Wallar BJ, Lipscomb JD. 2001. Methane monooxygenase component B mutants alter the kinetics of steps throughout the catalytic cycle. *Biochemistry* 40:2220-2233.
- Wandrey C, Liese A, Kihumbu D. 2000. Industrial biocatalysis: past, present, and future. *Org Proc Res Dev* 4:286-290.
- Wery J, Mendes da Silva DI, de Bont JAM. 2000. A genetically modified solvent-tolerant bacterium for optimized production of a toxic fine chemical. *Appl Microbiol Biotechnol* 54:180-185.

- Westgate S, Bell G, Halling PJ. 1995. Kinetics of uptake of organic liquid substrates by microbial cells: a method to distinguish interfacial contact and mass transfer-mechanisms. *Biotechnol Lett* 17:1013-1018.
- White RE, McCarthy M-B. 1986. Active site mechanics of liver microsomal cytochrome P-450. *Arch Biochem Biophys* 246:19-32.
- Whyte LG, Smits THM, Labbé D, Witholt B, Greer CW, van Beilen JB. 2002. Gene cloning and characterization of multiple alkane hydroxylase systems in *Rhodococcus* strains Q15 and NRRL B-16531. *Appl Environ Microbiol* 68:5933-5942.
- Willaert R, Smets A, de Vuyst L. 1999. Mass transfer limitations in diffusion-limited isotropic hollow fiber bioreactors. *Biotechnol Tech* 13:317-323.
- Willeman WF, Gerrits JP, Hanefeld U, Brussee J, Straathof AJJ, van der Gen A, Heijnen JJ. 2002a. Development of a process model to describe the synthesis of (*R*)-mandelonitrile by *Prunus amygdalus* hydroxynitrile lyase in an aqueous-organic biphasic reactor. *Biotechnol Bioeng* 77:239-247.
- Willeman WF, Hanefeld U, Straathof AJJ, Heijnen JJ. 2000. Estimation of kinetic parameters by progress curve analysis for the synthesis of (*R*)-mandelonitrile by *Prunus amygdalus* hydroxynitrile lyase. *Enzyme Microb Technol* 27:423-433.
- Willeman WF, Neuhofer R, Wirth I, Pöchlauer P, Straathof AJJ, Heijnen JJ. 2002b. Development of (*R*)-4-hydroxymandelonitrile synthesis in an aqueous-organic biphasic stirred tank batch reactor. *Biotechnol Bioeng* 79:154-164.
- Willeman WF, Straathof AJJ, Heijnen JJ. 2002c. Comparison of a batch, fed-batch and continuously operated stirred-tank reactor for the enzymatic synthesis of (*R*)-mandelonitrile by using a process model. *Bioproc Biosys Eng* 24:281-287.
- Willeman WF, Straathof AJJ, Heijnen JJ. 2002d. Reaction temperature optimization procedure for the synthesis of (*R*)-mandelonitrile by *Prunus amygdalus* hydroxynitrile lyase using a process model approach. *Enzyme Microb Technol* 30:200-208.
- Williams PA, Murray K. 1974. Metabolism of benzoate and the methylbenzoates by *Pseudomonas putida* (*avarilla*) mt-2: evidence for the existence of a TOL plasmid. *J Bacteriol* 120:416-423.
- Williams PA, Shaw LM, Pitt CW, Vrecl M. 1997. *xyIUW*, two genes at the start of the upper pathway operon of TOL plasmid pWW0, appear to play no essential part in determining its catabolic potential. *Microbiology* 143:101-107.
- Wimalasena K, Alliston KR. 1999. Mode of substrate interaction and energetics of carbon-oxygen bond formation of the dopamine b-monoxygenase reaction. *Biochemistry* 38:14916-14926.
- Witholt B, de Smet M-J, Kingma J, van Beilen JB, Lageveen RG, Eggink G. 1990. Bioconversions of aliphatic compounds by *Pseudomonas oleovorans* in multiphase bioreactors: background and economic potential. *Trends Biotechnol* 8:46-52.
- Witholt B, Favre-Bulle O, Lageveen R, Kingma J, van Beilen JB, Marvin H, Preusting H. 1992. Synthesis of apolar organic compounds by *Pseudomonas* spp. and *Escherichia coli* in two-liquid-phase fermentations. In: Galli E, Silver S, Witholt B, editors. *Pseudomonas: molecular biology and biotechnology*. Washington, DC: ASM Press. p 301-314.
- Wittcoff HA, Reuben BG. 1996. *Industrial organic chemicals*. New York: John Wiley & Sons.
- Wolf LB, Sonke T, Tjen KCMF, Kaptein B, Broxterman QB, Schoemaker HE, Rutjes FPJT. 2001. A biocatalytic route to enantiomerically pure unsaturated  $\alpha$ -H- $\alpha$ -amino acids. *Adv Synth Catal* 343:662-674.
- Wöltinger J, Drauz K, Bommarius AS. 2001. The membrane reactor in the fine chemicals industry. *Appl Catal A* 221:171-185.

- Wong JW, Watson J, H. A., Bouressa JF, Burns MP, Cawley JJ, Doro AE, Guzek DB, Hintz MA, McCormick EL, Scully DA, Siderewicz JM, Taylor WJ, Truesdell SJ, Wax RG. 2002. Biocatalytic oxidation of 2-methylquinoxaline to 2-quinoxalinecarboxylic acid. *Org Proc Res Dev* 6:477-481.
- Woodley JM. 1990. Stirred tank power input data for the scale-up of two-liquid phase biotransformations. In: Copping LG, editor. *Opportunities in Biotransformations*. London: Elsevier. p 63-66.
- Woodley JM, Brazier AJ, Lilly MD. 1991. Lewis cell studies to determine reactor design data for two-liquid phase bacterial and enzymatic reactions. *Biotechnol Bioeng* 37:133-140.
- Woodley JM, Lilly MD. 1990. Extractive biocatalysis: the use of two-liquid phase biocatalytic reactors to assist product recovery. *Chem Eng Sci* 45:2391-2396.
- Worsey MJ, Williams PA. 1975. Metabolism of toluene and xylenes by *Pseudomonas putida* (*avarilla*) mt-2: evidence for a new function of the TOL plasmid. *J Bacteriol* 124:7-13.
- Wubbolts M. 1994. Xylene and alkane mono-oxygenases from *Pseudomonas putida*. Ph.D. thesis, Rijksuniversiteit Groningen, Groningen.
- Wubbolts MG, Favre-Bulle O, Witholt B. 1996a. Biosynthesis of synthons in two-liquid-phase media. *Biotechnol Bioeng* 52:301-308.
- Wubbolts MG, Hoven J, Melgert B, Witholt B. 1994a. Efficient production of optically active styrene epoxides in two-liquid phase cultures. *Enzyme Microb Technol* 16:887-893.
- Wubbolts MG, Panke S, van Beilen JB, Witholt B. 1996b. Enantioselective oxidation by non-heme iron monooxygenases from *Pseudomonas*. *Chimia* 50:453-455.
- Wubbolts MG, Reuvekamp P, Witholt B. 1994b. TOL plasmid-specified xylene oxygenase is a wide substrate range monooxygenase capable of olefin epoxidation. *Enzyme Microb Technol* 16:608-615.
- Yamazaki T, Ohno T, Sakaki T, Akiyoshi-Shibata M, Yabusaki Y, Imai T, Kominami S. 1998. Kinetic analysis of successive reactions catalyzed by bovine cytochrome P450 17<sub>α,lyase</sub>. *Biochemistry* 37:2800-2806.
- Yano JK, Blasco F, Li H, Schmid RD, Henne A, Poulos TL. 2003. Preliminary characterization and crystal structure of a thermostable cytochrome P450 from *Thermus thermophilus*. *J Biol Chem* 278:608-616.
- Yano JK, Koo LS, Schuller DJ, Li H, Ortiz de Montellano PR, Poulos TL. 2000. Crystal structure of a thermophilic cytochrome P450 from the archaeon *Sulfolobus solfataricus*. *J Biol Chem* 275:31086-31092.
- Youshko MI, van Langen LM, de Vroom E, van Rantwijk F, Sheldon RA, Svedas VK. 2001. Highly efficient synthesis of ampicillin in an aqueous solution-precipitate system: repetitive addition of substrates in a semi-continuous process. *Biotechnol Bioeng* 73:426-430.
- Yun C-H, Song M, Ahn T, Kim H. 1996. Conformational change of cytochrome P450 1A2 induced by sodium chloride. *J Biol Chem* 271:31312-31316.
- Yuste L, Canosa I, Rojo F. 1998. Carbon-source-dependent expression of the *PalkB* promoter from the *Pseudomonas oleovorans* alkane degradation pathway. *J Bacteriol* 180:5218-5226.
- Zaks A. 2001. Industrial biocatalysis. *Curr Opin Chem Biol* 5:130-136.
- Zelder O, Hauer B. 2000. Environmentally directed mutations and their impact on industrial biotransformation and fermentation processes. *Curr Opin Microbiol* 3:248-251.
- Zhao H, Chockalingam K, Chen Z. 2002. Directed evolution of enzymes and pathways for industrial biocatalysis. *Curr Opin Biotechnol* 13:104-110.
- Zilberstein D, Agmon V, Schuldiner S, Padan E. 1984. *Escherichia coli* intracellular pH, membrane potential, and cell growth. *J Bacteriol* 158:246-252.



## **CURRICULUM VITAE**

**PERSONAL DATA**

Name: Bruno Albert Bühler  
Born: December 26, 1973 in Davos, Switzerland  
Domicile: Davos Platz  
Nationality: Swiss  
Family Status: Single

**EDUCATION**

1980-1993 School Education in Davos, Switzerland  
1980–1986 Primarschule Davos  
1986-1993 Schweizerische Alpine Mittelschule Davos  
*Matura Typus B*

1993 Military Service

1993-1998 University Education  
Eidgenössische Technische Hochschule Zürich (ETHZ)  
*Diploma of Natural Sciences*

1998-2003 Ph.D. studies under supervision of Prof. Dr. B. Witholt and Dr. A. Schmid  
Eidgenössische Technische Hochschule Zürich (ETHZ)  
Institute of Biotechnology

## PUBLICATIONS

- Bühler B, Bollhalder I, Hauer B, Witholt B, Schmid A. 2003. Chemical biotechnology for the specific oxyfunctionalization of hydrocarbons on a technical scale. *Biotechnol Bioeng* 82:833-842.
- Bühler B, Bollhalder I, Hauer B, Witholt B, Schmid A. 2003. Use of the two-liquid phase concept to exploit kinetically controlled multistep biocatalysis. *Biotechnol Bioeng* 81:683-694.
- Schmid A, Hollmann F, Park JB, Bühler B. 2002. The use of enzymes in the chemical industry in Europe. *Curr Opin Biotechnol* 13:359-366.
- Hollmann F, Bühler B, Schmid A. 2002. Oxidation of alcohols, phenols, aldehydes, acids and C-N bonds. In: Drauz K, Waldmann H, editors. *Enzyme Catalysis in Organic Synthesis*. Weinheim, Germany: Wiley-VCH. p 1108-1202, 1245-1261.
- Bühler B, Witholt B, Hauer B, Schmid A. 2002. Characterization and application of xylene monooxygenase for multistep biocatalysis. *Appl Environ Microbiol*. 68:560-568.
- Bühler B, Schmid A, Hauer B, and Witholt B. 2000. Xylene monooxygenase catalyzes the multistep oxygenation of toluene and pseudocumene to corresponding alcohols, aldehydes, and acids in *Escherichia coli* JM101. *J Biol Chem* 275:10085-10092.
- Prieto MA, Bühler B, Jung K, Witholt B, and Kessler B. 1999. PhaF, a Polyhydroxyalkanoate-granule-associated protein of *Pseudomonas oleovorans* GPo1 involved in the regulatory expression system for *pha* genes. *J Bacteriol* 181:858-868.

## PATENTS

- Schmid A, Hauer B, Witholt B, Bühler B. 1999. Microbiological method for producing aromatic aldehydes and/or carboxylic acids. WO 01/31047 A2.
- Schmid A, Hauer B, Witholt B, Bühler B. 2001. Verfahren zur Oxidation aromatischer Verbindungen. DE-10117359.8. PCT/EP02/03803.

